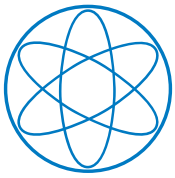

Running Neutrino Masses and Flavor Symmetries

Michael Andreas Schmidt

Max-Planck-Institut für Kernphysik
Saupfercheckweg 1
D-69117 Heidelberg

E-Mail: michael.schmidt@mpi-hd.mpg.de

Technische Universität München
Physik Department
Institut für Theoretische Physik T30d

Running Neutrino Masses and Flavor Symmetries

Dipl.-Phys. Univ. Michael Andreas Schmidt

Vollständiger Abdruck der von der Fakultät für Physik der Technischen Universität München zur Erlangung des akademischen Grades eines

Doktors der Naturwissenschaften (Dr. rer. nat.)

genehmigten Dissertation.

Vorsitzender:		Univ.-Prof. Dr. Reiner Krücken
Prüfer der Dissertation:	1.	Prof. Dr. Manfred Lindner, Ruprecht-Karls-Universität Heidelberg
	2.	Univ.-Prof. Dr. Andrzej J. Buras

Die Dissertation wurde am 10. Juni 2008 bei der Technischen Universität München eingereicht und durch die Fakultät für Physik am 30. Juni 2008 angenommen.

Running Neutrino Masses and Flavor Symmetries

Abstract

The flavor structure of neutral fermion masses is completely different from charged fermion masses. The cascade seesaw framework allows to implement a cancellation mechanism, which leads to a weak hierarchy of neutrinos despite the large hierarchy in the charged fermion masses. We present one realization by the gauge group E_6 and two in the framework of SO(10) based on discrete flavor symmetries T_7 and $\Sigma(81)$. Higher-dimensional operators as well as the flavon potential are discussed. Furthermore, since renormalization group (RG) effects can become very important in neutrino physics, especially in view of upcoming precision experiments, we have investigated several models. The $L_\mu - L_\tau$ flavor symmetry in the standard seesaw scenario leads to quasi-degenerate neutrinos and therefore to large RG corrections. The quantum corrections to quark-lepton-complementarity (QLC) relations are extensively discussed. In the minimal supersymmetric standard model (MSSM), the effect is almost always positive. In the standard model (SM), there are sizable RG corrections due to the threshold effects which are either positive for $\Delta\varphi \approx 0^\circ$ or negative for $\Delta\varphi \approx 180^\circ$. They have been studied in the leading log (LL) approximation and mainly lead to a rescaling of right-handed (RH) neutrino masses. The results are generalized beyond LL and the conditions for the applicability are derived. Finally, the results are applied to the cascade seesaw mechanism and the cancellation mechanism. The RG equations of the mixing parameters in the triplet seesaw are derived in terms of basis-independent quantities. The main results are the independence of Majorana phases and the proportionality to the mass squared difference in the strongly hierarchical case which differs from the standard seesaw mechanism.

Kurzfassung

Die Familienstruktur der neutralen Fermionen unterscheidet sich völlig von den geladenen Fermionmassen. Das kaskadierte Seesaw Szenario erlaubt die Konstruktion eines Auslöschungsmechanismus, der zu einer schwachen Hierarchie der Neutrinos führt trotz der starken Hierarchie der geladenen Fermionen. Wir präsentieren eine Realisierung durch die Eichgruppe E_6 und zwei im Kontext von SO(10), die auf einer diskreten Familiensymmetrie T_7 bzw. $\Sigma(81)$ basieren. Höher-dimensionale Operatoren und das Flavonpotential werden diskutiert. Da Renormierungsgruppen(RG)-Effekte in der Neutrinophysik sehr wichtig werden können, insbesondere im Blick auf die kommenden Präzisionsexperimente, wurden mehrere Modelle untersucht. Die $L_\mu - L_\tau$ Symmetrie im Standard Seesaw Modell führt zu quasi-degenerierten Neutrinos und somit zu großen RG Effekten. Die Quantenkorrekturen zu den Quark-Lepton Komplementarität Relationen werden ausführlich diskutiert. Im Minimalen Supersymmetrischen Modell (MSSM) sind die Korrekturen fast immer positiv. Im Standard Modell (SM), gibt es größere RG Korrekturen aufgrund von Schwelleneffekten, die positiv für $\Delta\varphi \approx 0^\circ$ bzw. negativ für $\Delta\varphi \approx 180^\circ$ sind. Sie werden in der führenden Logarithmus Näherung besprochen und führen hauptsächlich zu einer Reskalierung der rechtshändigen (RH) Neutrinomassen. Die Ergebnisse werden über die LL Näherung hinaus verallgemeinert und Bedingungen der Anwendbarkeit werden hergeleitet. Schließlich werden die Ergebnisse beim kaskadierten Seesaw Mechanismus und dem Auslöschungsmechanismus angewandt. Die RG Gleichungen der Mischungsparameter im Triplett Seesaw Mechanismus werden hergeleitet und basisunabhängig ausgedrückt. Die Hauptergebnisse sind die Unabhängigkeit von den Majoranaphasen und die Proportionalität der Massenquadratdifferenzen im stark hierarchischen Fall im Gegensatz zum Standard Seesaw Mechanismus.

Contents

Chapter 1

Introduction

The quantization of charge and the unification of the gauge couplings of all three forces in the minimal supersymmetric standard model (MSSM) at $\Lambda_{\rm GUT} = 2{\cdot}10^{16}\,\text{GeV}$ strongly suggest a further unification of all forces into a (supersymmetric (SUSY)) grand unified (GU) gauge group [1, 2]. Especially, models which unify all SM particles in one irreducible representation like SO(10) [3, 4] and E_6 [5–9] are appealing.
The flavor sector also shows regularities: (i) All charged fermion masses show a strong normal hierarchy. (ii) The mixing angles in the quark sector are small and in the lepton sector, there is maximal 2-3 mixing and possibly vanishing 1-3 mixing. (iii) The neutrino mass matrix is compatible with the exchange of the second and third row/column which suggests a $\mu - \tau$ exchange symmetry. Furthermore, there are some peculiar relations: (i) The light quark masses are related to the Cabibbo angle

$$\tan\vartheta_{12} \approx \sqrt{\frac{m_d}{m_s}} \tag{1.1}$$

which is known as Gatto-Sartori-Tonin (GST) relation[1] [11]. (ii) The quark mixing angles ϑ_{ij} and the lepton mixing angles θ_{ij}, which parameterize the Cabibbo-Kobayashi-Maskawa (CKM) and Maki-Nakagawa-Sakata (MNS) mixing matrix, respectively, add up to maximal mixing

$$\theta_{12} + \vartheta_{12} \approx \frac{\pi}{4}, \qquad \theta_{23} + \vartheta_{23} \approx \frac{\pi}{4}\,. \tag{1.2}$$

They are known as quark lepton complementarity (QLC) relations [12–14] because of the complementarity of θ_{ij} and ϑ_{ij} to maximal mixing. They suggest a further unification of quarks and leptons. Therefore the QLC relations are presumably due to a symmetry close to the unification scale. (iii) Moreover, to a very high precision (10^{-5}), the charged lepton masses fulfill

$$m_e + m_\mu + m_\tau = \frac{2}{3}\left(\sqrt{m_e} + \sqrt{m_\mu} + \sqrt{m_\tau}\right)^2\,, \tag{1.3}$$

which was found by Koide [15]. It indicates that the first generation is as important as the third one, which is in contradiction to the approach to generate the masses of the third generation at tree level and the light generations by non-renormalizable operators. Here, all flavors should be considered as equally important.
All these structures and relations of the experimental data indicate, that the masses and mixing angles are not accidental but determined by a flavor symmetry. There already exist several attempts to explain theses patterns by continuous (e.g. Abelian [16–24] and non-Abelian [25–29]) or discrete

[1] It can be explained by a symmetric mass matrix with vanishing 1-1 element [10], e.g. within SO(10).

(e.g. A_4 [30]) symmetries. However, the study of flavor symmetries has revealed, that they have to be broken, explicitly or spontaneously, above the electroweak scale since the low-energy data does not allow for an exact symmetry.
In view of these hints towards a GU theory (GUT) as well as a flavor symmetry, it is tempting to combine a GU gauge group and a flavor symmetry. However, this involves some difficulties, since the mass hierarchies in the charged and in the neutral fermions are completely different. In addition, it is not obvious how large mixing angles in the lepton sector can be reconciled with small mixing angles in the quark sector. This is taken into account in many low-energy models by assigning different representations to different particle species. But, this is not possible in GUTs which unify all SM particles within one representation. Some models aim to combine a flavor symmetry with a GUT [31–33], which use the standard seesaw mechanism [34–38]

$$m_\nu \propto -Y_\nu^T M_{NN}^{-1} Y_\nu \ ,$$

where RH neutrinos N with mass M_{NN} are integrated out (or a variant thereof [39–43]) to explain the difference between charged Dirac fermion mass matrices and the light Majorana neutrino mass matrix m_ν. However, in GUTs like SO(10) and E_6, the neutrino Yukawa couplings Y_ν are related to the up-type quark Yukawa couplings Y_u, which leads to a squared hierarchy in the light neutrino mass matrix. Therefore, it is essential to cancel this hierarchy. This can be achieved in the double seesaw (DS) framework [44, 45], where the effective light neutrino mass matrix is obtained by the successive application of the standard seesaw formula

$$m_\nu \propto Y_\nu^T Y_{SN}^{-1} M_{SS} Y_{SN}^{T\,-1} Y_\nu \ .$$

When the Yukawa couplings of the additional singlets S_i to the RH neutrinos Y_{SN} are proportional to Y_ν, the hierarchy automatically drops out [46, 47]. Furthermore, the effective light neutrino mass matrix is mainly given by the Majorana mass matrix M_{SS} of the additional singlets which is not related to the usual Yukawa couplings and, hence, can have a weaker hierarchy. Therefore, a special neutrino symmetry can be implemented, e.g. the $\mu - \tau$ symmetry [48–51].
Moreover, as GU gauge symmetries are generally broken at a high energy scale, they predict masses and mixing angles at this scale. However, gauge couplings as well as masses and mixing angles are not constant, but depend on the energy scale of the considered process through quantum corrections to the tree-level (classical) theory. This can be understood by thinking of the vacuum as a polarizable medium[2], e.g. the electric charge is screened by the dipoles in the polarizable medium which effectively reduces its strength at low energies. At high energies or short distances, the charge is probed closer to the center, which leads to a less screened, hence larger charge. This energy scale dependence is described by the renormalization group (RG). Thus, in order to compare predictions of GUTs which are valid at a high energy scale with the low-energy experimental data, RG corrections have to be considered. It turns out, that they can be sizable in the neutrino sector. They are especially large for quasi-degenerate neutrinos in the MSSM with large $\tan\beta$ [52–59] as well as above and between the seesaw scales due to large Y_ν [52, 60–69]. The running between mass thresholds is crucial in non-SUSY theories, because there are several contributions to the neutrino mass matrix which are renormalized differently. This generally leads to large corrections to the mixing parameters. But even small corrections are important, since the precision of neutrino masses and mixing angles has been increased by several neutrino oscillation experiments [70–76] and will be improved further. In the next-generation experiments, the mixing parameters will be measured on a 10 % level [77], θ_{12} will be known even more precisely, i.e. RG effects become comparable to the

[2]The Heisenberg uncertainty allows the creation of particle-antiparticle pairs which can be considered as dipoles.

precision of the experiment even for a hierarchical spectrum [69]. Moreover, the above mentioned low-energy relations Eqs. (1.1, 1.2, 1.3) are subject to quantum corrections, since it turns out that none of them is RG invariant. Especially the QLC relations are subject to potentially large corrections due to the strong running of θ_{12}. The Koide and the GST relation are expected to receive only small corrections, because masses usually show a flavor-independent rescaling. Large corrections to a low-energy relation disfavor an explanation by a symmetry and leave it as a mere numerical coincidence.

This thesis is structured in the following way. The basic concepts of the RG and effective field theories (EFTs) are introduced in Chapter 2. In Chapter 3, several aspects of model building are outlined. At first, the experimental status of neutrino mixing parameters is presented as well as different variants of the seesaw mechanism. GUTs and flavor symmetries are introduced and the QLC relations are discussed. In Chapter 4, a cancellation mechanism within the cascade seesaw mechanism is presented and realizations by a GUT symmetry as well as flavor symmetries are discussed. As thresholds can lead to large effects, we study the corrections due to mass thresholds in the standard seesaw framework in Chapter 5. The RG effects in the $L_\mu - L_\tau$ symmetric model as well as the phenomenologically motivated QLC scenario are discussed in terms of mixing parameters in Chapter 6. Furthermore, RG equations of the mixing parameters are derived in the triplet seesaw scenario. Finally, we conclude in Chapter 7.

Our conventions are shown in App. A. Technical details of GUTs and flavor symmetries are summarized in App. B. Lastly, the necessary RG formulas are collected in App. C. Part of this thesis has been already published in [78–81] or will be published [82].

Chapter 2

Renormalization Group

This chapter summarizes basic knowledge about the RG, EFTs and the decoupling of particles. In Sec. 2.1 the Wilsonian approach to the RG is presented using the example of ϕ^4-theory. The Callan-Symanzik equation which underlies all RG calculation techniques is derived in Sec. 2.2. As decoupling of particles is not automatic in mass-independent renormalization schemes, EFTs are outlined in Sec. 2.3. We discuss the decoupling of particles in Sec. 2.4.

2.1 Basic Picture – Wilson Renormalization Group

Before we derive specific results using RG techniques, we want to summarize the most important facts about RG evolution which we need in the following discussion.
The renormalization group can be understand most easily in the picture of Wilson (See e.g. [83].) with a momentum cutoff as regulator of the theory. However, it can be extended to other regularization techniques like dimensional regularization [84–86]. The starting point is the Euclidean Feynman path integral [1]

$$Z[J] = \int \mathcal{D}\phi \, e^{-\int[\mathscr{L}+J\phi]} = \prod_k \int \mathrm{d}\phi(k) \, e^{-\int[\mathscr{L}+J\phi]} \, . \tag{2.1}$$

A sharp [2] UV cutoff Λ can be imposed by restricting the integration variables $\phi(k)$ by $|k| \leq \Lambda$ and setting $\phi(k) = 0$ for $k > \Lambda$. This immediately leads to the question how the quantum fluctuations at very short distances or very large momenta influence the path integral and therefore the physical observables, more precisely, what is the dependence of the path integral on the cutoff Λ. In order to analyze this dependence, we first integrate out all momentum modes $b\Lambda < |k| \leq \Lambda$

$$\begin{aligned} Z[J] &= \int [\mathcal{D}\phi]_\Lambda \, e^{-\int[\mathscr{L}(\phi)+J\phi]} \\ &= \int [\mathcal{D}\phi]_{b\Lambda} \int [\mathcal{D}\hat{\phi}]_{[b\Lambda,\Lambda]} \, e^{-\int\left[\mathscr{L}(\phi_{b\Lambda}+\hat{\phi})+J\left(\phi_{b\Lambda}+\hat{\phi}\right)\right]} \\ &= \int [\mathcal{D}\phi]_{b\Lambda} \, e^{-\int[\mathscr{L}(\phi_{b\Lambda})+J\phi_{b\Lambda}]} \int [\mathcal{D}\hat{\phi}]_{[b\Lambda,\Lambda]} \, e^{-\int\left[\mathscr{L}(\phi_{b\Lambda}+\hat{\phi})-\mathscr{L}(\phi_{b\Lambda})+J\hat{\phi}\right]} \end{aligned} \tag{2.2}$$

[1] Since the metric is not positive semi-definite in Minkowskian space, it is difficult to impose a cutoff on momenta.
[2] In the exact RG, which is a generalization of the simple picture by Wilson, the cutoff is a smooth functional $F[\phi(k)]$.

where we used the notation

$$\phi_\Lambda(k) = \phi(k)\Theta(\Lambda - |k|) \tag{2.3a}$$

$$\hat{\phi}(k) = \phi(k)\Theta(\Lambda - |k|)\Theta(|k| - \Lambda') \tag{2.3b}$$

$$[\mathcal{D}\phi]_{[b\Lambda,\,\Lambda]} = \prod_{b\Lambda<|k|\leq\Lambda} \mathrm{d}\phi(k) \tag{2.3c}$$

$$[\mathcal{D}\phi]_\Lambda = [\mathcal{D}\phi]_{[0,\Lambda]} \,. \tag{2.3d}$$

This leads to an effective Lagrangian $\mathscr{L}_{\text{eff}}$ in

$$Z[J] = \int [\mathcal{D}\phi\prime]_{\Lambda'} e^{-\int[\mathscr{L}_{\text{eff}}(\phi_{\Lambda'})+J\phi_{\Lambda'}]} \,. \tag{2.4}$$

This effective Lagrangian $\mathscr{L}_{\text{eff}}$ can be related to the full Lagrangian $\mathscr{L}$ by rescaling all momenta and distances by

$$k \to k' = k/b \,, \qquad x \to x' = bx \,, \qquad \partial_\mu \to \partial'_\mu = \partial_\mu / b \,. \tag{2.5}$$

In order to be more explicit, we consider the ϕ^4 theory

$$\mathscr{L} = \frac{1}{2}\left(\partial_\mu\phi\right)^2 - \frac{m^2}{2}\phi^2 - \frac{\lambda}{4!}\phi^4 \tag{2.6}$$

which results in the effective Lagrangian

$$\mathscr{L}_{\text{eff}} = \frac{1}{2}\left(1+\delta Z_\phi\right)\left(\partial_\mu\phi\right)^2 - \frac{m^2+\delta m^2}{2}\phi^2 - \frac{\lambda+\delta\lambda}{4!}\phi^4 + \sum_{N,M} C_{N,M}\left(\partial_\mu^M \phi^N\right) \tag{2.7}$$

after a functional integration over the high momentum degrees of freedom $b\Lambda < k \leq \Lambda$ has been performed. This can be done be calculating the relevant Feynman diagrams. Note, that new local operators with N fields and M derivatives show up. The rescaling of the action results in

$$\int \mathrm{d}^d x'\, b^{-d} \left[\frac{1}{2}\left(1+\delta Z_\phi\right) b^2 \left(\partial_\mu\phi\right)^2 - \frac{m^2+\delta m^2}{2}\phi^2 - \frac{\lambda+\delta\lambda}{4!}\phi^4 + \sum_{N,M} C_{N,M} b^M \left(\partial_\mu^M \phi^N\right)\right] \tag{2.8}$$

which can be related to the original action by rescaling the fields ϕ:

$$\phi' = \left[b^{2-d}\left(1+\delta Z_\phi\right)\right]^{1/2} \phi \tag{2.9a}$$

$$m'^2 = \left(m^2+\delta m^2\right)\left(1+\delta Z_\phi\right)^{-1} b^{d-2} \tag{2.9b}$$

$$\lambda' = \left(\lambda+\delta\lambda\right)\left(1+\delta Z_\phi\right)^{-1} b^{d-4} \,. \tag{2.9c}$$

Hence, the integration over the high momentum degrees of freedom leads to a rescaling of the couplings and defines a flow (one parameter curve in parameter space) of the couplings or equivalently a flow of the Lagrangian. The successive integration over high momentum degrees of freedom is sometimes denoted as summing up large logarithms, since the corrections $\delta\lambda$,... become large for decreasing b.

The different operators of the Lagrangian can be classified by their behavior close to a fixed point of the flow ($\phi' = \phi$, $m'^2 = m^2$, ...). There are three different classes of operators:

- relevant operators grow, when they are approaching the fixed point;

- irrelevant ones decrease by approaching the fixed point;
- the behavior of marginal operators depends on higher order corrections.

The free theory

$$\mathscr{L}_0 = \frac{1}{2}\left(\partial_\mu \phi\right)^2 \tag{2.10}$$

is a fixed point, since at leading order

$$\lambda' = \lambda b^{d-4} \,, \qquad m'^2 = m^2 b^{d-2} \tag{2.11}$$

Therefore m^2 is relevant in $d = 4$ dimensions and λ is marginal. The next-to-leading order correction to λ in $d = 4$

$$\lambda' = \lambda - \frac{3\lambda^2}{16\pi^2} \ln \frac{1}{b} \tag{2.12}$$

leads to a decrease of λ while the high momentum degrees of freedom are integrated out step by step. Conversely, since

$$\lambda \xrightarrow{\Lambda \to \infty} \infty \,, \tag{2.13}$$

ϕ^4-theory does not exist for $\lambda \neq 0$ when the cutoff is removed, which is denoted as triviality. In general, an operator with N fields and M derivatives close to the free field fixed point transforms as

$$C'_{N,M} = b^{d-N(d/2-1)+M} C_{N,M} \,. \tag{2.14}$$

Hence, operators are relevant if

$$d \leq N\left(d/2 - 1\right) + M \,. \tag{2.15}$$

2.2 Callan-Symanzik Equation

The Wilsonian approach to the RG which has been discussed in the previous section is based on a rescaling of all momenta. In this section, we describe the derivation of the Callan-Symanzik equation which originates from the rescaling of all mass parameters. Since the RG scale μ in dimensional regularization or the cutoff scale Λ in a momentum cutoff scheme are auxiliary variables and physical results of a theory are independent of the regularization and renormalization procedure used, this independence can be used to derive a partial differential equation (PDE) which all Greens functions must satisfy. In the following derivation we restrict ourselves to dimensional regularization. A theory is uniquely described by its bare Greens functions

$$G_B^{(n)}(\{x_i\}, \lambda_j) = \langle \Omega | \mathcal{T} \phi_B(x_1) \ldots \phi_B(x_n) | \Omega \rangle \tag{2.16}$$

and it it independent of the used renormalization scheme. Therefore, we require the bare Greens functions to be independent of the renormalization scale μ.

$$\mu \frac{\mathrm{d}}{\mathrm{d}\mu} G_B^{(n)} = 0 \,. \tag{2.17}$$

Hence, the renormalized Greens functions

$$G^{(n)}(\{x_i\}, \lambda_i) = Z^{-n/2} G_B^{(n)}(\{x_i\}, \lambda_i) \tag{2.18}$$

obey

$$0 = \left[\mu\frac{\mathrm{d}}{\mathrm{d}\mu} + \frac{n}{2}\mu\frac{\mathrm{d}\ln Z}{\mathrm{d}\mu}\right] G^{(n)}(\{x_i\},\lambda_j) = \left[\mu\frac{\partial}{\partial\mu} + \mu\frac{\partial\lambda_k}{\partial\mu}\frac{\partial}{\partial\lambda_k} + \frac{n}{2}\mu\frac{\mathrm{d}\ln Z}{\mathrm{d}\mu}\right] G^{(n)}(\{x_i\},\lambda_j)\ . \quad (2.19)$$

This equation is called Callan-Symanzik equation [87, 88] which is usually shown in the form

$$0 = \left[\mu\frac{\partial}{\partial\mu} + \beta_k\frac{\partial}{\partial\lambda_k} + \frac{n}{2}\gamma\right] G^{(n)}(\{x_i\},\lambda_j)\ . \quad (2.20)$$

It is a quasi linear PDE which can be solved by the method of characteristic curves. This transforms the PDE into a system of ordinary differential equations

$$\beta_k(\mu) \equiv \mu\frac{\partial\lambda_k}{\partial\mu}, \qquad \gamma(\mu) \equiv \mu\frac{\mathrm{d}\ln Z}{\mathrm{d}\mu}\ , \quad (2.21)$$

which are called β-functions in the case of β_k and anomalous dimensions in the case of γ. Note that the β-functions and the anomalous dimension γ are independent of $\{x_i\}$, i.e. they are independent of the Greens functions $G^{(n)}$. The β-function of any operator Q can be derived similarly by requiring the independence of the renormalization scale μ of the bare operator Q_B. A formula for the resulting β-function can be found in [89–91]. The RG evolution of couplings has been experimentally shown. The electromagnetic fine-structure constant $\alpha_{\mathrm{em}} = \frac{e^2}{4\pi}$ has been measured in the OPAL experiment [92] at an energy of 181.94 GeV and at very low energies in quantum Hall experiments [93]

$$\alpha_{\mathrm{em}}^{-1}(181.94\,\mathrm{GeV}) = 126.2^{+3.5}_{-3.2}\ , \qquad \alpha_{\mathrm{em}}^{-1}(0\,\mathrm{GeV}) = 137.035999679(94)\ . \quad (2.22)$$

Another evidence for RG evolution is the strong coupling constant which becomes non-perturbative at the QCD scale $\Lambda_{\mathrm{QCD}} \sim 300\,\mathrm{MeV}$ and evolves asymptotically to zero at higher energies which was first shown by Gross, Politzer and Wilczek [94]. The β-function of a gauge coupling in an arbitrary Yang-Mills theory with gauge group G, gauge coupling g and an arbitrary number of representations (reps) is at 1 loop order

$$\beta_g^{1\mathrm{loop}} = -\frac{g^3}{16\pi^2}\left[\frac{11}{3}l(Ad) - \frac{2}{3}\sum_{F\in\{\text{Weyl reps}\}} l(F) - \frac{1}{6}\sum_{S\in\{\text{real scalar reps}\}} l(S)\right]\ , \quad (2.23)$$

where $l(R)$ denotes the Dynkin index of representation R and Ad is the adjoint representation, which summarizes the contribution of gauge vector bosons. In a supersymmetric theory, the gauge coupling β-function in terms of superfields is given by

$$\beta_g^{1\mathrm{loop}} = -\frac{g^3}{16\pi^2}\left[3\,l(Ad) - \frac{4}{3}\sum_{C\in\{\text{chiral superfield}\}} l(C)\right]\ . \quad (2.24)$$

2.3 Effective Field Theories

As we have already pointed out, all couplings or equivalently the effective action depend on the external momenta of the process. As mass-independent schemes do not implicitly decouple particles, since the renormalization scale does not know about particle masses, the decoupling has to be done by hand, i.e. at each mass threshold, particles are integrated out which leads to an EFT. EFTs are a

powerful tool to extract the relevant physical degrees of freedom at a given energy scale from a theory. The dominant contribution to processes at a given energy scale is due to particles which can become on-shell, especially those particles whose mass is close to the relevant energy scale. Particles, which cannot become on-shell, are treated effectively. They are integrated out. This can be understood in various equivalent ways. In Feynman diagrams, it results in deleting all propagator lines of heavy particles. In the Feynman path integral it amounts to integrating over the heavy degrees of freedom which cannot become on-shell. Finally, on the level of the action, these heavy particles fulfill their classical equation of motion and can be removed from the action by inserting the equation of motion into the action. Hence, in the EFT, we neglect all quantum fluctuations of the heavy particle and treat it classically. The full theory is expanded in a dimensionful parameter Λ^{-1} up to some power Λ^{-N}

$$\mathscr{L}_{\text{eff}} = \sum_{n=0}^{N} \mathscr{L}^{(n)} , \qquad N \geq 0 \tag{2.25}$$

where $\mathscr{L}^{(n+1)}$ is suppressed compared to $\mathscr{L}^{(n)}$ by Λ^{-1}. Hence an EFT can be arbitrarily precise by the inclusion of sufficiently many inverse powers of Λ. This systematic expansion is controlled by the "Power Counting" in Λ^{-1} of the effective theory.

EFTs are especially useful in calculations of the effective potential with many mass scales. For simplicity consider a theory of two massive particles with masses m_1 and m_2. Since in mass-independent renormalization schemes like $\overline{\text{MS}}$ combined with dimensional regularization, large logarithms of the mass ratio $\frac{m_1}{m_2}$ show up. They indicate that the loop expansion does not work properly, because powers of the same logarithm show up at higher loop orders, e.g. the logarithm $\ln \frac{m_1}{m_2}$ at 1 loop order appears at 2 loop order as $\left(\ln \frac{m_1}{m_2}\right)^2$. In an EFT, all particles which cannot become on-shell are already decoupled and particles which are much lighter than the renormalization scale can be treated as massless which essentially leaves only one mass scale in the effective potential. Therefore, the renormalization scale can be chosen such that all logarithms are small [95, 96]. In principle, there can be many mass scales, as it is shown in Fig. 2.1. At each mass threshold, the particle is integrated out and the effective theory is matched to the underlying theory. Concluding, we summarize the procedure to calculate the effective action at a given energy scale using an EFT:

- Identify the relevant degrees of freedom.
- Integrate out particles which cannot become on-shell.
- Identify the expansion parameter, like the mass of the RH neutrino in the standard seesaw mechanism.
- Match the couplings of the effective theory to the underlying theory at n loop order[3].
- Evolve all couplings at $n+1$ loop order to the next mass threshold and integrate out the next particle.
- ... as long as the relevant energy scale is reached.

[3]If the RG running is calculated at $n+1$ loop order, the matching has to be done at n loop order, since the logarithm of the running compensates for the suppression factor from the loop integral.

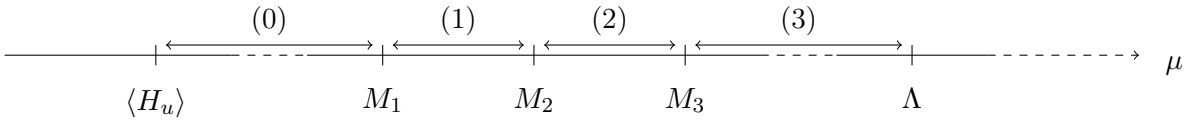

Figure 2.1: The thresholds due to masses M_i of RH neutrinos and the intervals of RG running. $\langle H_u \rangle$ denotes the VEV of the electroweak Higgs doublet coupling to neutrinos.

2.4 Decoupling

The power counting of the EFT ensures that Greens functions of both theories are equal at least up to the order $\mathcal{O}((\frac{p}{\Lambda})^N)$ where N denotes the maximal order in Λ^{-1} taken into account in the EFT and p is the largest external momentum of the process. Therefore, heavy particles are unobservable until close to their threshold where they have been integrated out. The couplings of the EFT have no a-priori value, but they have to be matched to the underlying theory if it is known or to experimental data. Symanzik [97] and later Appelquist and Carazzone [98] showed that particles with a large mass M decouple from the low-energy effective theory in the limit $M \to \infty$ and the resulting EFT is renormalizable. However, there are some exceptions to the decoupling theorem. The most prominent one is 4-Fermi theory which describes weak interactions at low energies. In the renormalizable part of the theory β-decay is forbidden by symmetries in contrast to the experimentally visible decays. It is still a good EFT, since there is power counting. However, dimension 6 (D6) operators are essential and therefore it is non-renormalizable. In general, an EFT has more symmetries than the full theory. Another example is the effective theory of Majorana neutrinos where ratios of the neutrino mass matrix elements are invariant under rescaling of the neutrino mass matrix [99]. A further exception are chiral theories where the mass is generated by the Higgs mechanism, e.g. the top quark in the SM is the heaviest particle and at low energies it can be integrated out. However, after electroweak symmetry breaking, the top Yukawa coupling y_t is proportional to the top mass. Hence in the limit $m_t \to \infty$, the top Yukawa coupling diverges and the top strongly couples. Thus it does not decouple from the low-energy effective theory. The gauge hierarchy problem can also be understood as non-decoupling of heavy degrees of freedom. It is summarized in the two questions why are there large hierarchies and why are they stable with respect to the RG. Fundamental scalars, like the SM Higgs boson receive quadratic corrections from all other particles in the theory which they couple to. Hence, when the SM is embedded into a GUT, there are also corrections which are proportional to Λ^2_{GUT} from GUT scale particles. Therefore heavy particles do not decouple from a theory which involves fundamental scalars as long as the RG corrections are not cancelled like quadratic divergences in SUSY theories where scalar masses receive only logarithmic corrections like fermions.

Chapter 3

Aspects of Model Building

In Sec. 3.1 the experimental data of neutrino experiments is presented and different mechanisms to generate neutrino masses are outlined. The discussion is focused on variants of the seesaw mechanism which show up in unified models. Some aspects of unified models are presented in Sec. 3.2. Sec. 3.3 outlines several flavor symmetries which aim to explain neutrino masses as well as leptonic mixing parameters. Finally, we discuss the QLC relations in Sec. 3.4.

3.1 Neutrino Masses

3.1.1 Experimental Data

After the first evidence of atmospheric neutrino oscillations in 1998 by SuperKamiokande [70] which was independently confirmed by K2K [73], there have been numerous successful experiments which increased the precision of neutrino masses and leptonic mixing parameters. SNO [72] proved that the neutrino deficit of solar neutrinos measured in the Homestake experiment [100] is due to neutrino oscillations. KamLand [74] independently confirmed the solar parameters by measuring the flux of anti-neutrinos coming from nuclear reactors. Recently, MINOS [75] improved the precision on the atmospheric mixing parameters and KamLand [101] on the solar parameters. Last year, MiniBoone [102] ruled out the explanation of a sterile neutrino for the LSND measurement [103]. So far, there is only an upper bound on the third mixing angle θ_{13} by the CHOOZ experiment [71]. In the next-generation experiments, the mixing parameters will be measured on a 10 % level [77] or even better in the case of θ_{12}. The current best fit values of neutrino masses and leptonic mixing angles are summarized in Tab. 3.1 in the standard parameterization. They will be further improved in the coming years by Borexino which measured for the first time the Berilium–7 line of the solar neutrino spectrum [76], SuperKamiokande, Double CHOOZ, T2K, NoVa, MINOS and other experiments. There exist upper bounds on the absolute neutrino mass from

- the MAINZ [104] experiment which has set a model-independent upper bound on the neutrino mass $m(\nu_e) = \sqrt{\sum_i |U_{ei}|^2 m_i^2} \leq 2.3\,\text{eV}(@\,95\%\,C.L.)$ by measuring the end point of the tritium β-spectrum, which determines the neutrino mass kinematically;

- the Heidelberg-Moscow experiment [105] which searched for neutrinoless double beta ($0\nu2\beta$) decay in Germanium detectors. It sets the current upper limit on $\langle m_{ee}\rangle \leq 0.35\,\text{eV}(@\,90\%\,C.L.)$. Part of the group [106] claims the discovery of $0\nu2\beta$ with an effective neutrino mass scale of $\langle m_{ee}\rangle = 0.11 - 0.56\,\text{eV}(@95\%\,C.L.)$;

parameter	$\Delta m^2_{21}[10^{-5}\,\mathrm{eV}^2]$	$\Delta m^2_{31}[10^{-3}\,\mathrm{eV}^2]$	$\sin^2\theta_{12}$	$\sin^2\theta_{13}$	$\sin^2\theta_{23}$
best fit	7.6	2.4	0.32	0.007	0.50
3σ	$7.1 - 8.3$	$2.0 - 2.8$	$0.26 - 0.40$	≤ 0.050	$0.34 - 0.67$

Table 3.1: Current measured neutrino mass squared differences $\Delta m^2_{ij} = m^2_i - m^2_j$ and leptonic mixing angles in standard parameterization [112]. Note that the current best fit value of the 1-3 mixing is non-zero. However, it is still compatible with a vanishing 1-3 mixing.

- astrophysical observations on the sum of neutrino masses by measuring the energy density of relativistic particles in the universe. The WMAP [107] data alone places an upper limit $\sum_i m_i < 1.3\,\mathrm{eV}(@\,95\%\,C.L.)$. The inclusion of distance measuring information of baryon acoustic oscillations and supernova data further improves the upper bound to $\sum_i m_i < 0.61\,\mathrm{eV}(@95\%\,C.L.)$, since neutrino-like particles erase structures on small scales.

In the coming years there will be a number of experiments to address the unsolved issues. To name a few

- Double CHOOZ [108] will set a bound on the 1-3 mixing angle $\sin 2\theta_{13} \leq 0.02{-}0.03(@90\%\,C.L.)$;
- KATRIN [109] is going to improve the upper bound on $m(\nu_e) \leq 0.35\,\mathrm{eV}$;
- GERDA [110] and other experiments are searching for $0\nu2\beta$ decay and are going to place a bound on m_{ee}. GERDA aims to have a sensitivity on $\langle m_{ee}\rangle$ of $0.09 - 0.29$ in 2009. The discovery of $0\nu2\beta$ decays would show that lepton flavor violating processes exist. This implies that neutrinos are Majorana particles;
- the PLANCK satellite [111] and weak lensing experiments will decrease the astrophysical bound on the sum of neutrino masses to $\sum_i m_i \lesssim \mathcal{O}(0.2)\,\mathrm{eV}$.

The standard parameterization of the MNS (leptonic mixing) matrix is presented in App. A.1. Since the solar mass squared difference is much smaller than the atmospheric one, it is sometimes useful to expand in the ratio

$$\zeta = \frac{\Delta m^2_{21}}{\Delta m^2_{32}}\,, \tag{3.1}$$

where $\Delta m^2_{ij} = m^2_i - m^2_j$. Finally, we present two special cases of the MNS matrix.

Bimaximal Mixing

Bimaximal mixing is produced by the mass matrix [113–117]

$$m_\nu^{\mathrm{bimax}} = \begin{pmatrix} D-C & B & -B \\ . & D & C \\ . & . & D \end{pmatrix} \tag{3.2}$$

in flavor basis, i.e. where the charged lepton Yukawa couplings are diagonal. B, C, D are arbitrary parameters which are related to the masses by

$$B = \frac{m_2 - m_1}{2\sqrt{2}}\,, \qquad C = -\frac{m_1}{4} - \frac{m_2}{4} + \frac{m_3}{2}\,, \qquad D = \frac{m_1}{4} + \frac{m_2}{4} + \frac{m_3}{2}\,. \tag{3.3}$$

It is diagonalized by two maximal rotations $U_{ij}(\pi/4)$ in the $i-j$ plane

$$U_{\rm bm} = U_{23}(\pi/4)U_{12}(\pi/4) = \frac{1}{2}\begin{pmatrix} \sqrt{2} & \sqrt{2} & 0 \\ -1 & 1 & \sqrt{2} \\ 1 & -1 & \sqrt{2} \end{pmatrix} . \tag{3.4}$$

Although bimaximal mixing is excluded at low energies by solar neutrino oscillation experiments, it is still a viable mass texture at high energies, since the RG running can drive bimaximal mixing to the LMA solution [64, 69, 81] which is shown in Sec. 6.4.4.

Tri-bimaximal Mixing

The tri-bimaximal mixing texture was proposed by Harrison, Perkins and Scott (HPS) [118–121]. It is inspired by the experimental data which suggest $U_{e3} = 0$, $|U_{\mu 3}|^2 = 1/2$ and $|U_{e2}|^2 = 1/3$. This leads to the MNS matrix

$$U_{\rm MNS} = \begin{pmatrix} \sqrt{\frac{2}{3}} & \frac{1}{\sqrt{3}} & 0 \\ -\frac{1}{\sqrt{6}} & \frac{1}{\sqrt{3}} & \frac{1}{\sqrt{2}} \\ -\frac{1}{\sqrt{6}} & \frac{1}{\sqrt{3}} & -\frac{1}{\sqrt{2}} \end{pmatrix} = \frac{1}{\sqrt{6}}\begin{pmatrix} 1 & 1 & 1 \\ 1 & \omega^2 & \omega \\ 1 & \omega & \omega^2 \end{pmatrix}\begin{pmatrix} 1 & 0 & 0 \\ . & 1 & -1 \\ . & . & 1 \end{pmatrix} , \tag{3.5}$$

where $\omega = e^{{\rm i}2\pi/3}$ which leads to $1+\omega+\omega^2 = 0$. The resulting mass matrix in flavor basis is

$$m_\nu^{\rm tbm} = \begin{pmatrix} C+D-B & B & B \\ . & D & C \\ . & . & D \end{pmatrix} , \tag{3.6}$$

where B, C, D are arbitrary parameters which are related to the masses by

$$B = \frac{m_2 - m_1}{3} , \qquad C = \frac{m_1}{6} + \frac{m_2}{3} - \frac{m_3}{2} , \qquad D = \frac{m_1}{6} + \frac{m_2}{3} + \frac{m_3}{2} . \tag{3.7}$$

The mass matrix can also be written in the suggestive form

$$m_\nu^{\rm tbm} = \frac{m_3}{2}\begin{pmatrix} 0 & 0 & 0 \\ . & 1 & -1 \\ . & . & 1 \end{pmatrix} + \frac{m_2}{3}\begin{pmatrix} 1 & 1 & 1 \\ . & 1 & 1 \\ . & . & 1 \end{pmatrix} + \frac{m_1}{6}\begin{pmatrix} 4 & -2 & -2 \\ . & 1 & 1 \\ . & . & 1 \end{pmatrix} . \tag{3.8}$$

3.1.2 Neutrino Mass Models

In this section, we summarize the most important facts about neutrino masses and possibilities to generate small neutrino masses with the focus on the different variants of the seesaw mechanism, which are used in the following chapters. As the nature of neutrino masses is not known yet, Dirac as well as Majorana neutrinos are possible. Indeed, there are several models which explain the smallness of Dirac neutrino masses by a suppression with respect to the GUT scale or other extra heavy degrees of freedom, e.g. [122, 123]. In models with extra dimensions, the smallness can be explained by a small overlap of the corresponding zero-mode profiles along extra dimensions (See, e.g., [124]) or in the case of large extra dimensions by the volume suppression factor, if the RH neutrino is chosen to propagate in the bulk. Another possibility are mechanisms which generate small neutrino masses radiatively, which ensures that there is a suppression factor of $1/(8\pi)^2$ coming from the loop and small couplings on the other side. Two examples for radiative generation of neutrino masses are the Zee model [125] which generates the mass term at 1 loop level and the Babu model [126]. There,

the neutrino mass is generated at the 2 loop level. Even gravitational interactions can generate neutrino masses [127], although they can only lead to a subdominant contribution, since they are suppressed by the Planck scale. In the following, we restrict ourselves to the seesaw mechanism and just refer to [47, 128, 129] for recent overviews of alternatives. The seesaw mechanism naturally shows up in GUTs since there are heavy particles which couple to neutrinos. There are essentially three different variants, the standard (type I) [34–38], triplet (type II) [39–41] and the fermionic triplet (type III) [42, 43] seesaw mechanism. The cascade seesaw mechanism can be viewed as a special case of the standard seesaw mechanism with more additional singlets (RH neutrinos) and a special structure of the neutral fermion mass matrix. Since in the following chapters, we concentrate on the standard, cascade and triplet seesaw mechanism, we give some more details on them and just note about the fermionic triplet seesaw mechanism, that it leads to the same decoupling formula (up to a group theoretical factor) as in the standard seesaw case.

Effective Theory

At low energies the Majorana neutrino mass can be described by an effective dimension 5 (D5) operator which is, in fact, the only D5 operator compatible with $\mathrm{SU}(3)_C \times \mathrm{SU}(2)_L \times \mathrm{U}(1)_Y$ and the SM field content [130]. The concrete term in the Lagrangian is

$$-\mathscr{L}_\kappa = \frac{1}{4}\kappa_{fg}\overline{\ell^f_{La}}\epsilon_{ab}H^b_u(\ell^g_{Lc})^{\mathcal{C}}\epsilon_{cd}H^d_u\,, \tag{3.9}$$

where ℓ_L denotes the lepton doublet and $\mathcal{C}$ is the charge conjugation matrix with respect to the Lorentz group. After the SM Higgs field H_u acquires its VEV, the D5 operator leads to a neutrino mass term

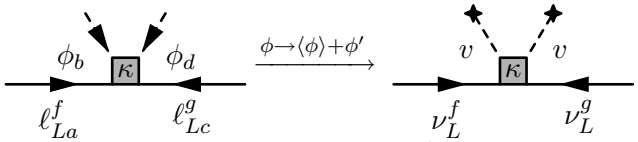

$$-\frac{1}{4}\kappa_{fg}\overline{\ell^f_{La}}\epsilon_{ab}H^b_u\cdot(\ell^g_{Lc})^{\mathcal{C}}\epsilon_{cd}H^d_u \xrightarrow{\phi\to\langle\phi\rangle+\phi'} -\frac{v^2}{4}\kappa_{fg}\overline{\nu^f_L}(\nu^g_L)^{\mathcal{C}}\,. \tag{3.10}$$

Standard (Type I) Seesaw

The standard (type I) seesaw mechanism [34–38] provides a natural explanation of the smallness of neutrino mass. It can also be the origin of the difference of the quark and lepton mixings. The smallness of neutrino masses is explained by the introduction of RH neutrinos N which lead to additional Yukawa couplings Y_ν and mass terms M_{NN} in the Lagrangian

$$-\mathscr{L}_N = (Y_\nu)_{fg}\,\overline{N}^f\ell^g_L H_u{}^{\mathcal{C}} + \frac{1}{2}\,(M_{NN})_{fg}\,N^{f\,T}\mathcal{C}N^g + \text{h.c.}\,. \tag{3.11}$$

The corresponding mass matrix of uncharged particles is

$$\mathcal{M} = \begin{pmatrix} 0 & m_D^T \\ m_D & M_{NN} \end{pmatrix}\,, \tag{3.12}$$

where $m_D = Y_\nu\,\langle H_u\rangle$ denotes the Dirac neutrino mass matrix and M_{NN} is the Majorana mass matrix of the RH neutrinos. The Majorana mass scale is assumed to be much larger than the Dirac mass scale, since the RH neutrinos are total singlets which are not constrained by any gauge symmetry. At low energies, the RH neutrinos are decoupled and physics is described by an effective

theory, where the neutrino mass matrix of the light neutrinos is given by the D5 operator. The effective D5 operator is determined by matching the full theory and the effective theory.

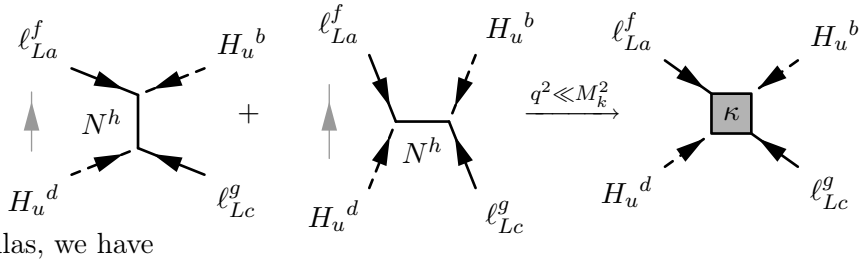

(3.13)

In terms of formulas, we have

$$\begin{aligned}\left[-i\left(Y_\nu^T\right)_{fh}\epsilon_{ab}\mathrm{P}_L\right]\frac{i\not{q}+iM_h}{q^2-M_h^2+\mathrm{i}\varepsilon}\left[-i\left(Y_\nu\right)_{hg}\left(\epsilon^T\right)_{dc}\mathrm{P}_L\right]\\ +\left[-i\left(Y_\nu^T\right)_{fh}\epsilon_{ad}\mathrm{P}_L\right]\frac{i\not{q}+iM_h}{q^2-M_h^2+\mathrm{i}\varepsilon}\left[-i\left(Y_\nu\right)_{hg}\left(\epsilon^T\right)_{bc}\mathrm{P}_L\right]\\ \xrightarrow{q^2\ll M_h^2} i\left(Y_\nu^T\right)_{fh}M_h^{-1}\left(Y_\nu\right)_{hg}\left(\epsilon_{ab}\epsilon_{cd}+\epsilon_{ad}\epsilon_{cb}\right)\mathrm{P}_L\ ,\end{aligned} \tag{3.14}$$

where M_k denotes the Majorana mass of the RH neutrino N_k. Thus the matching condition is given by

$$\kappa^{\mathrm{EFT}} = \kappa + 2\,Y_\nu^T M_{NN}^{-1} Y_\nu \tag{3.15}$$

To be more precise, the RH neutrinos are in general non-degenerate in mass and they are integrated out one after the other, such that there are different effective theories as shown in Fig. 2.1.

Cascade Seesaw

The cascade seesaw scenario is similar to the standard seesaw scenario. The main difference is that there are more SM singlets. It can be motivated from string theory, since some string theory models predict many ($\mathcal{O}(100)$) singlets (See e.g. [131]).

$$-\mathscr{L} = \left(Y_\nu\right)_{fg} N^f \overline{\ell}^g H_u + \left(Y_{SN}\right)_{fg}\overline{S}^f N^g \Delta + \left(Y_{S\nu}\right)_{fg}\overline{S}^f \ell^g \Delta' + \frac{1}{2}\left(M_{SS}\right)_{fg}\overline{S}^{f\,T}\mathcal{C}S^g\ . \tag{3.16}$$

In the SM, Δ is a Higgs singlet and Δ' a electroweak Higgs doublet. In SO(10), Δ and Δ' are $\underline{\overline{\mathbf{16}}}$ Higgs representations. However, some singlets do not have a direct mass term which results in the following mass matrix of uncharged particles

$$\mathcal{M} = \begin{pmatrix} 0 & m_D^T & m_{S\nu}^T \\ m_D & 0 & M_{SN}^T \\ m_{S\nu} & M_{SN} & M_{SS} \end{pmatrix} \tag{3.17}$$

in the basis $\begin{pmatrix} \nu & N & S \end{pmatrix}^T$, where $m_{S\nu} = Y_{S\nu}\langle\Delta'\rangle$ and $M_{SN} = Y_{SN}\langle\Delta\rangle$ originate from the Yukawa couplings of the additional singlets. For definiteness, the SM singlets without direct Majorana mass term are denoted RH neutrinos N and the massive SM singlets are called additional singlets S. The decoupling of the additional singlets leads to the effective mass matrix

$$\begin{pmatrix} -m_{S\nu}^T M_{SS}^{-1} m_{S\nu} & m_D^T - m_{S\nu}^T M_{SS}^{-1} M_{SN} \\ . & -M_{SN}^T M_{SS}^{-1} M_{SN} \end{pmatrix}\ . \tag{3.18}$$

Hence the RH neutrino masses are given by the standard seesaw formula

$$M_{NN} \approx -M_{SN}^T M_{SS}^{-1} M_{SN}\ . \tag{3.19}$$

The decoupling of the RH neutrinos leads to the effective neutrino mass matrix at low energies

$$m_\nu \approx m_\nu^{DS} + m_\nu^{LS} \,, \tag{3.20}$$

which consists of two contributions. They are called DS contribution [44, 45]

$$m_\nu^{DS} = m_D^T \left(M_{SN}^{-1} M_{SS} M_{SN}^{-1T} \right) m_D \tag{3.21}$$

and linear seesaw (LS) contribution [132]

$$m_\nu^{LS} = -\left[m_D^T \left(M_{SN}^{-1} m_{S\nu} \right) + \left(M_{SN}^{-1} m_{S\nu} \right)^T m_D \right] \,. \tag{3.22}$$

The standard seesaw contribution m_ν^{T1} which shows up in the 1-1 element of Eq. (3.18) exactly vanishes. Note, that the DS contribution is proportional to the direct mass term of the additional singlets in contrast to the standard seesaw mechanism. There are two common setups. Either the additional singlet masses are very large, such that the suppression of the neutrino mass scale comes from the ratio $(m_D/M_{SN})^2$. In this scenario, it is usually assumed, that the singlets are related to Planck scale physics and the scale M_{SN} is related to the GUT scale, which nicely leads to a neutrino mass scale of the right order of magnitude. In the other approach, the direct singlet mass term is assumed to be very small, since the vanishing of M_{SS} enhances the symmetry of the Lagrangian. In the limit $M_{SS} \to 0$, lepton number becomes a symmetry of the theory. Therefore, small singlet masses are natural by 't Hoofts argument [133], which states that a parameter can be naturally small, if its vanishing increases the symmetry. In this setup, a low scale seesaw mechanism is discussed, i.e. the scale $M_{SN} \sim \mathcal{O}(10 - 100\,\mathrm{TeV})$ and $M_{SS} \sim \mathcal{O}(\,\mathrm{keV})$. The LS term is independent of the direct mass term and it is usually discussed in the GUT context at large energy scales.

Triplet (Type II) Seesaw

In the triplet (type II) seesaw mechanism [39–41], the SM is extended by a charged Higgs triplet $\Delta \sim (\underline{\mathbf{3}}, 1)_{\mathrm{SU}(2)\times\mathrm{U}(1)}$:

$$\Delta = \frac{\sigma^i}{\sqrt{2}} \Delta_i = \begin{pmatrix} \Delta^+/\sqrt{2} & \Delta^{++} \\ \Delta^0 & -\Delta^+/\sqrt{2} \end{pmatrix} \tag{3.23}$$

in contrast to the standard seesaw mechanism where fermions are added. The SM Lagrangian is extended by additional Yukawa couplings as well as Higgs couplings

$$\begin{aligned} \mathscr{L}_\Delta =& \mathrm{tr}\left[(D_\mu \Delta)^\dagger D^\mu \Delta \right] - M_\Delta^2 \mathrm{tr}\left(\Delta^\dagger \Delta \right) - \frac{\Lambda_1}{2} \left(\mathrm{tr} \Delta^\dagger \Delta \right)^2 - \frac{\Lambda_2}{2} \left[\left(\mathrm{tr} \Delta^\dagger \Delta \right)^2 - \mathrm{tr}\left(\Delta^\dagger \Delta \Delta^\dagger \Delta \right) \right] \\ & - \Lambda_4 H_u^\dagger H_u \mathrm{tr}\left(\Delta^\dagger \Delta \right) - \Lambda_5 H_u^\dagger \left[\Delta^\dagger, \Delta \right] H_u - \left[\frac{\Lambda_6}{\sqrt{2}} H_u^T i\sigma_2 \Delta^\dagger H_u + \mathrm{h.c.} \right] \\ & - \left[\frac{1}{\sqrt{2}} \left(Y_\Delta \right)_{fg} \ell_L^{Tf} \mathcal{C} i\sigma_2 \Delta \ell_L^g + \mathrm{h.c.} \right] \,. \end{aligned} \tag{3.24}$$

The covariant derivative of the Higgs triplet is given by

$$D_\mu \Delta = \partial_\mu \Delta + \mathrm{i}\sqrt{\frac{3}{5}} g_1 B_\mu \Delta + \mathrm{i} g_2 \left[W_\mu, \Delta \right] \,. \tag{3.25}$$

Note, that the complex Higgs triplet couples to the SM Higgs doublet as well as the leptonic doublet which leads to a neutrino mass term after the triplet acquires a VEV or equivalently decouples. After

decoupling, the matching yields a contribution to the effective D5 operator

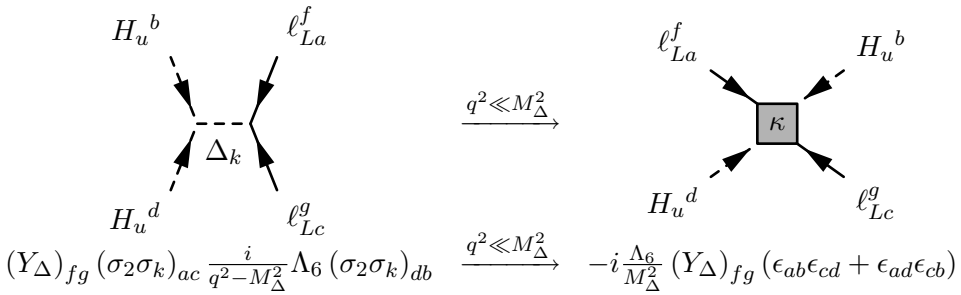

(3.26)

which results in

$$\kappa^{\mathrm{EFT}} = \kappa - 2\frac{Y_\Delta \Lambda_6}{M^2_\Delta}\,. \tag{3.27}$$

The decoupling of the Higgs triplet also gives a contribution to the SM model Higgs self–coupling because there is a coupling between the SM Higgs doublet and the Higgs triplet given in Eq. (3.24)

$$\lambda^{\mathrm{EFT}} = \lambda + 2\frac{|\Lambda_6|^2}{M^2_\Delta}\,. \tag{3.28}$$

In the MSSM, in addition to the Higgs triplet $\mathbb{\Delta} \sim (\underline{\mathbf{3}}, 1)$, a second Higgs triplet $\overline{\mathbb{\Delta}} \sim (\underline{\mathbf{3}}, -1)$ with opposite hypercharge is needed to generate a D5 mass term for neutrinos. Furthermore, $\overline{\mathbb{\Delta}}$ ensures that the model is anomaly-free. Note, however, that only $\mathbb{\Delta}$ couples to the left–handed leptons. The additional terms in the superpotential are given by

$$W_\Delta = M_\Delta \mathrm{Tr}(\overline{\mathbb{\Delta}}\mathbb{\Delta}) + \frac{(Y_\Delta)_{fg}}{\sqrt{2}}\mathbb{l}^{fT} i\sigma_2 \mathbb{\Delta} \mathbb{l}^g + \frac{\Lambda_u}{\sqrt{2}}\mathbb{h}^{(2)T} i\sigma_2 \overline{\mathbb{\Delta}}\mathbb{h}^{(2)} + \frac{\Lambda_d}{\sqrt{2}}\mathbb{h}^{(1)T} i\sigma_2 \mathbb{\Delta}\mathbb{h}^{(1)}\,, \tag{3.29}$$

where $\mathbb{l}$ denotes the left-handed doublet and $\mathbb{h}^{(i)}$ denotes the Higgs doublets. We use the same notation as in [134]. Analogously to the SM, we add an effective neutrino mass operator κ. The decoupling of the Higgs triplet generates an effective dimension 4 term κ^{EFT} in the superpotential, whereas the tree-level matching condition reads

$$\kappa^{\mathrm{EFT}} = \kappa - 2\frac{Y_\Delta \Lambda_u}{M_\Delta}\,. \tag{3.30}$$

3.2 Unified Theories

Unification of forces is a common concept in physics. One well-established example is the electromagnetic force which describes electric and magnetic interactions at the same time. Today, it is appealing to think about the unification of the forces in the SM, the strong $\mathrm{SU}(3)_C$, the weak $\mathrm{SU}(2)_L$ and the hypercharge $\mathrm{U}(1)_Y$ to one force in analogy to the electromagnetic force. The two main hints which point towards a further unification are

- the quantization of hypercharge, which satisfy the anomaly constraint
- and that the gauge couplings unify at the same energy scale of $2 \cdot 10^{16}\,\mathrm{GeV}$ in the MSSM.

The most prominent examples of grand unified theories [1, 2] are SU(5) [2] and SO(10) [3, 4] which unify all three forces. SO(10) also unifies all SM matter particles and additionally a RH neutrino into one irreducible representation. Furthermore the anomaly-free group E_6 [5–9] is discussed, since it is

an exceptional Lie group and a subgroup of E_8 which is motivated by heteorotic string theory. From a low-energy perspective, it contains SO(10) and the trinification group $\mathrm{SU}(3)^3 \times Z_3$ [6, 135, 136], where Z_3 is a discrete symmetry which relates the gauge couplings of the three SU(3) factors.
Besides GUTs, there is the possibility of partial unification, e.g. in left-right symmetric models. In the minimal left-right symmetric model $\mathrm{SU}(2)_L \times \mathrm{SU}(2)_R \times \mathrm{U}(1)_{B-L} \times \mathrm{SU}(3)_C$ [40, 137–139], the Pati-Salam (PS) group $\mathrm{SU}(2)_L \times \mathrm{SU}(2)_R \times \mathrm{SU}(4)_{PS}$ which further unifies color and the $B - L$ quantum number[1] [140] or the already mentioned trinification group $\mathrm{SU}(3)^3 \times Z_3$.
Although the GUT scale is large and possibly not accessible to direct detection experiments from todays knowledge, there are bounds on GU models. Models with simple GU groups lead necessarily to proton decay [35]. Therefore proton decay measurements put strong bounds on GUTs. The current model-independent lower bound [93] on the proton life-time is

$$\tau_p > 2.1 \cdot 10^{29} \,\text{years} \,, \quad \text{CL } 90\% \,. \tag{3.31}$$

Under the assumption that the dominant decay mode is among the investigated ones, the bound can be improved to

$$\tau_p > 10^{31} \text{ to } 10^{33} \text{ years} \,. \tag{3.32}$$

Proton decay has already excluded minimal SUSY SU(5) [141–143]. Product groups, like the left-right symmetric models, are not as sensitive to proton decay. The main contributions to proton decay are the exchange of X and Y bosons in SU(5) and groups which contain SU(5). They lead to effective D6 operators like $uu\bar{d}e^+$ and $ud\bar{u}e^+$. In SUSY GUTs there are further D5 operators due to the exchange of colored triplet Higgsinos of the form $QQQL/M_H$. This operator can be suppressed by a large mass of the colored triplet Higgsino M_H. However, the $\underline{\mathbf{5}}$ and $\overline{\underline{\mathbf{5}}}$ Higgs particles in SU(5) contain both an electroweak Higgs doublet as well as a colored triplet Higgs. Therefore, a GU model has to provide a mechanism to split the masses of the doublet and the triplet which is denoted by Doublet-Triplet-Splitting (DTS). This can be achieved by the missing partner mechanism [144–146] in SU(5) by a mismatch in the number of electroweak doublets and colored triplets, such that all colored triplets become massive but some electroweak doublets do not obtain a direct mass term. In SUSY, there is the sliding singlet mechanism [147–150]. Although it does not work in SU(5) phenomenologically, but only in rank 5 and large gauge groups, we present it in SU(5) notation. It requires an additional SM singlet as well as an adjoint Higgs representation. The superpotential contains the term

$$W \supset \overline{\underline{\mathbf{5}}} \, (\underline{\mathbf{45}} + \underline{\mathbf{1}}) \, \underline{\mathbf{5}} \,. \tag{3.33}$$

If the adjoint acquires a vacuum expectation value (VEV) $\langle \underline{\mathbf{45}} \rangle = v_{\underline{\mathbf{45}}} \mathrm{diag}\left(-\frac{1}{3}, -\frac{1}{3}, -\frac{1}{3}, -\frac{1}{2}, -\frac{1}{2}\right)$, SU(5) is broken down to the SM. F-term flatness requires

$$\left\langle \overline{\underline{\mathbf{5}}} \right\rangle \left(\langle \underline{\mathbf{45}} \rangle + \langle \underline{\mathbf{1}} \rangle \right) = \left(\langle \underline{\mathbf{45}} \rangle + \langle \underline{\mathbf{1}} \rangle \right) \langle \underline{\mathbf{5}} \rangle = 0 \,. \tag{3.34}$$

Therefore, the F-term flatness with respect to H_u and H_d leads to $\langle \underline{\mathbf{1}} \rangle = -\frac{1}{2} v_{\underline{\mathbf{45}}}$ which results in $\langle \underline{\mathbf{45}} \rangle + \langle \underline{\mathbf{1}} \rangle = v_{\underline{\mathbf{45}}} \mathrm{diag}\,(-5/6, -5/6, -5/6, 0, 0)$. Hence, the electroweak doublets remain massless whereas the colored triplets acquire a vector-like mass of order $v_{\underline{\mathbf{45}}}$.
Besides proton decay, flavor changing neutral currents (FCNCs) in the quark sector as well as the lepton sector provide strong bounds to GUTs, especially SUSY GUTs which are favored due to the gauge coupling unification in the MSSM. At the Paul-Scherrer Institute (PSI) in Villigen, the MEG experiment [151] searches for the process $\mu \to e\gamma$ which is forbidden in the SM (without RH neutrinos). It will improve the present upper limit of $1.2 \cdot 10^{-11}$ on the branching ratio by the

[1] B denotes the baryon number and L lepton number.

MEGA experiment [152] to 10^{-13}. Of course, there are also other processes like $\tau \to e\gamma$ and $\tau \to \mu\gamma$. However, the experimental sensitivity is not as good as in $\mu \to e\gamma$. Another interesting process is $\mu \to e$ conversion in Ti, which has the potential to exclude many SUSY GU models discussed by Albright and Chen [153]. However, they did not impose the flavor symmetry on the soft masses, but imposed mSUGRA initial conditions. FCNCs in the quark sector are also able to constrain and even exclude GU models as it has been done in [154] by the combination of several FCNCs. Due to the uncertainty in the hadronic matrix elements, the calculations are difficult and there is a large theoretical uncertainty compared to leptonic processes.
Another sign for GU models are $N - \overline{N}$ oscillations. However, theoretical predictions for the experimental bound on the oscillation time $\tau_{N-\overline{N}} \geq 0.86 \cdot 10^8$sec [155] can be easily satisfied by a shifting the $B - L$ breaking scale, since this process violates $B - L$.
The RG evolution in the MSSM leads to the unification of the third generation Yukawa couplings for specific values of $\tan\beta$. However, the second and the first generation do not unify. Evolving the Yukawa couplings from the electroweak scale to Λ_{GUT} leads to

$$m_d \approx 3m_e \,, \qquad m_s \approx \frac{1}{3}m_\mu \quad \text{and} \quad m_b \approx m_\tau \tag{3.35}$$

which can be explained by a specific arrangement of Clebsch-Gordan coefficients [156, 157].
Different types of the seesaw mechanism naturally show up in unified theories. In the PS model, as soon as the RH neutrinos acquire a Majorana mass term, there is a type I+II seesaw mechanism, since there will generally be a contribution to the left-handed neutrinos as well. The type of seesaw mechanism which is implemented in SU(5) depends on the particle content. Additional fermionic singlets lead to the standard seesaw mechanism. A $\underline{\mathbf{15}}$ Higgs representation, however, leads to a triplet seesaw mechanism. The fermionic triplet seesaw will be operating, if there is a fermionic adjoint representation. In SO(10), RH neutrinos acquire a Majorana mass term by the coupling to a $\overline{\underline{\mathbf{126}}}$ representation and consequently lead to a type I+II seesaw mechanism. It can be a $\overline{\underline{\mathbf{126}}}$ Higgs particle or two $\overline{\underline{\mathbf{16}}}$ Higgs particles which form effectively a $\overline{\underline{\mathbf{126}}}$ representation in the symmetric part of their tensor product. Additional fermions in the adjoint representation lead to a fermionic triplet seesaw.
Since SO(10) and E_6 are used in Chapter 4, we briefly review basic properties of these groups. Technical details about Lie groups can be found in App. B.1

3.2.1 SO(10)

SO(10) is a Lie group of rank 5. Hence, the rank has to be lowered by 1 to obtain the SM which has rank 4. SO(10) has several advantages in model building:

- it is free of anomalies (See. App. B.3.);
- it unifies all SM particles and additionally a RH neutrino in one $\underline{\mathbf{16}}$ spinor representation;
- $B - L$ is a gauge symmetry, which allows to explain baryogenesis via leptogenesis by its breaking. Since R parity is a discrete subgroup of $\mathrm{U}(1)_{B-L}$, it is automatically a symmetry at high energies in SUSY theories;
- in some models R parity is automatically conserved, which ensures that there are no dimension 4 operators which lead to proton decay [158, 159].

It can be broken to the SM in two different ways, either via the PS group or $\mathrm{SU}(5) \times \mathrm{U}(1)_X$. The breaking via PS leads to the hypercharge $Y = 2\,T_{3R} + (B - L)$ and the breaking via SU(5) × U(1)

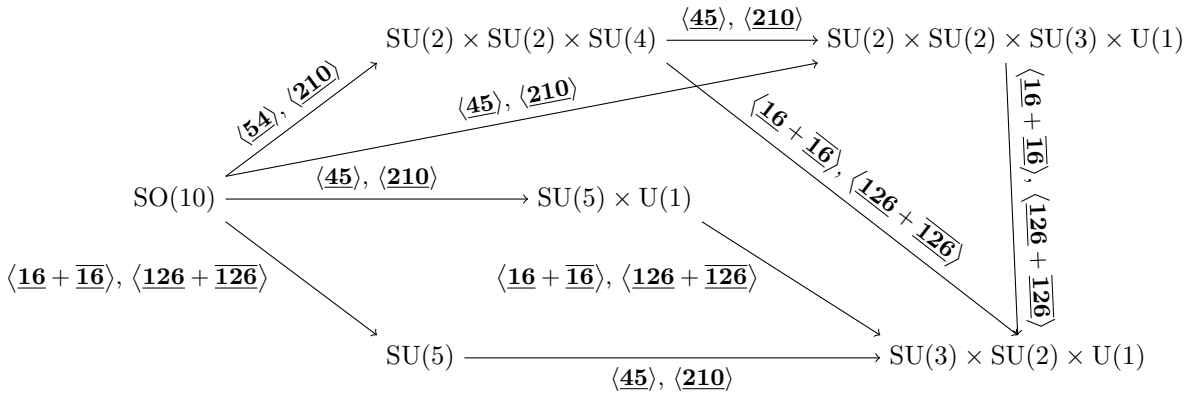

Figure 3.1: Different ways of breaking SO(10) to the SM.

leads to $Y/2 = \alpha z + \beta x$ where z and x are the charges with respect to $\mathrm{U}(1)_Z$ and $\mathrm{U}(1)_X$ in

$$\begin{aligned} \mathrm{SO}(10) &\to \mathrm{SU}(5) \times \mathrm{U}(1)_X \\ &\to \mathrm{SU}(3) \times \mathrm{SU}(2) \times \mathrm{U}(1)_Z \times \mathrm{U}(1)_X \\ &\to \mathrm{SU}(3) \times \mathrm{SU}(2) \times \mathrm{U}(1)_Y \ . \end{aligned} \tag{3.36}$$

The hypercharge in the SM shows that there are two different possibilities to choose α and β, either $(\alpha, \beta) = (1/6, 0)$ or $(\alpha, \beta) = (-1/5, 1/5)$. These combinations lead to $Y/2 = z/6$ for the breaking via SU(5) and $Y/2 = \frac{1}{5}(z - x)$ for the breaking via flipped SU(5) [145, 146, 160], which is $\mathrm{SU}(5) \times \mathrm{U}(1)_X$. In flipped SU(5), the up-type and down-type quarks are exchanged $u^{(c)} \leftrightarrow d^{(c)}$ as well as the neutrinos and the charged leptons $\nu^{(c)} \leftrightarrow e^{(c)}$. There is also a variant of SO(10) which is accompanied by an additional U(1) factor. It is called flipped SO(10) [161]. The arrangement of SM particles in its multiplets differs from ordinary SO(10), similarly to flipped SU(5). The breaking sequences and the necessary representations are depicted in Fig. 3.1. The Higgs potential which leads to this breaking has only been studied in the simplest cases [162–166]. Bounds on the different mass scales (e.g. the scale related to proton decay) in the breaking sequences have been studied in [167]. It is found that the proton decay scale in SO(10) is larger than in SU(5).
As it has already been mentioned, all SM fermions and in addition a SM singlet, i.e. a RH neutrino, fit into one $\underline{\mathbf{16}}$ of SO(10) which explains charge quantization of the SM particles and intimately links all particles of one family. There is no additional exotic matter, as it is in other groups. As the tensor product

$$\underline{\mathbf{16}} \otimes \underline{\mathbf{16}} = \underline{\mathbf{10}}_S \oplus \underline{\mathbf{120}}_A \oplus \underline{\mathbf{126}}_S \tag{3.37}$$

decomposes into a sum of three irreducible representations, it is possible to accommodate different mass matrices for the different SM particles at the renormalizable level depending on the specific VEV structure of the SO(10) Higgs representations. The SM mass matrices are completely determined by the SO(10) structure. The Higgs representations $\underline{\mathbf{10}}$ and $\overline{\underline{\mathbf{126}}}$ lead to symmetric mass matrices which fulfill $m_u \sim m_D$ and $m_d \sim m_e^T$, where m_u and m_d are the up-type and down-type quark mass matrices, respectively, m_D is the Dirac neutrino mass matrix and m_e is the mass matrix of charged leptons. The relation $m_u \sim m_D$ is broken by the introduction of $\underline{\mathbf{120}}$, also since $\underline{\mathbf{120}}$ is contained in the antisymmetric part of the tensor product, the contribution to the mass matrices from $\underline{\mathbf{120}}$ is antisymmetric. The Georgi-Jarlskog factor can be obtained by the Higgs representations $\underline{\mathbf{120}}$ and $\overline{\underline{\mathbf{126}}}$. In terms of SU(5), $\overline{\underline{\mathbf{45}}}$ of SU(5) has to acquire a VEV and in terms of the PS model, ($\underline{\mathbf{2}}$, $\underline{\mathbf{2}}$, $\underline{\mathbf{15}}$) has to acquire a VEV to obtain the factor 3 between quarks and leptons in Eq.

(3.35). There also exists a DTS mechanism which uses the mismatch of doublets and triplets in the $\underline{\mathbf{126}}$ Higgs representation [168], such that all colored triplets become massive while two Higgs doublets do not have a direct mass term and consequently remain light. However, the mass of colored triplet Higgs has to be about an order of magnitude larger than the GUT scale to account for the non-observation of proton decay.
Most models are SUSY, because gauge coupling unification is possible in the MSSM. Renormalizable SO(10) models usually include a $\underline{\mathbf{10}}$ and $\underline{\overline{\mathbf{126}}}$ Higgs representation (See, e.g., [158, 169, 170]) to account for Majorana neutrino masses. However, recently, it has been shown [171, 172], that a phenomenologically viable renormalizable model probably needs all three Higgs representations $\underline{\mathbf{10}}$, $\underline{\mathbf{120}}$ and $\underline{\overline{\mathbf{126}}}$. But, such a large Higgs sector leads to a very strong running of the gauge coupling. In the case of a SUSY model containing $\underline{\mathbf{10}}$, $\underline{\mathbf{120}}$, $\underline{\overline{\mathbf{126}}}$, the β-function of the gauge coupling becomes according to Eq. (2.24)

$$\beta_g = \frac{25}{3\pi^2} g^3 \tag{3.38}$$

and $\alpha = \frac{g^2}{4\pi}$ enters the non-perturbative regime after less than one order of magnitude of running[2]. Hence, a more fundamental theory is needed.
Alternatively, masses can be generated by non-renormalizable interactions with low-dimensional irreducible Higgs representations only, i.e. $\underline{\mathbf{10}}$, $\underline{\mathbf{16}}$, $\underline{\overline{\mathbf{16}}}$, $\underline{\mathbf{45}}$ and $\underline{\mathbf{54}}$. This implies the existence of a more fundamental theory which explains non-renormalizable operators, e.g. heteorotic string theory which only predicts small representations [173]. There are several models which implement this idea. Let us mention two models which have been studied in detail: Babu, Pati and Wilczek [174] suggested a model which uses an Abelian U(1) flavor symmetry and in addition to the SM matter fields $\underline{\mathbf{16}}_i$, there are a $\underline{\mathbf{10}}$, a $\underline{\mathbf{45}}$ and one vector-like $\underline{\mathbf{16}} \oplus \underline{\overline{\mathbf{16}}}$ Higgs representations. Albright and Barr [175–177] proposed a model which has a $\mathrm{U}(1) \times Z_4 \times Z_4$ family symmetry to forbid unwanted couplings and besides the SM matter fields, two vector-like $\underline{\mathbf{16}} \oplus \underline{\overline{\mathbf{16}}}$, two vector-like $\underline{\mathbf{10}}$ and six additional singlet matter fields and four $\underline{\mathbf{10}}$, two vector-like $\underline{\mathbf{16}} \oplus \underline{\overline{\mathbf{16}}}$, one $\underline{\mathbf{45}}$ and five singlet Higgs representations. The extended particle content in the Albright-Barr model is used to explain the generation of all non-renormalizable operators by decoupling heavy vector-like particles.
Generally in these models, the third generation becomes massive at tree level and the remaining masses are generated at the non-renormalizable level. Here, we briefly summarize the most important contributions to the mass matrices in the above mentioned models, since we refer to them in Chapter 4:

- the coupling $\underline{\mathbf{16}}_i\, \underline{\mathbf{16}}_j\, \underline{\mathbf{10}}$ leads to symmetric mass matrices $m_u = m_d = m_e = m_D$ and usually generates the masses of the third generation;
- the coupling $\underline{\mathbf{16}}_i\, \underline{\mathbf{16}}_j\, \underline{\overline{\mathbf{16}}}\, \underline{\overline{\mathbf{16}}}$ acts like the coupling $\underline{\mathbf{16}}_i\, \underline{\mathbf{16}}_j\, \underline{\overline{\mathbf{126}}}$ in a renormalizable SO(10) model. The RH neutrino Majorana mass matrix is generated by this term;
- the coupling $\underline{\mathbf{16}}_i\, \underline{\mathbf{16}}_j\, \underline{\mathbf{10}}\, \underline{\mathbf{45}}$ generates a difference between leptons and quarks. It leads to the Georgi-Jarlskog factor if $\underline{\mathbf{45}}$ acquires a VEV in $B - L$ direction;
- the coupling $\underline{\mathbf{16}}_i\, \underline{\mathbf{16}}_j\, \underline{\mathbf{16}}\, \underline{\mathbf{16}}'$ contributes only to down-type quarks and charged leptons $m_e = m_d^T$ which leads to non-trivial CKM mixing and a lopsided structure of those mass matrices;
- equivalently, the coupling $\underline{\mathbf{16}}_i\, \underline{\mathbf{16}}_j\, \underline{\overline{\mathbf{16}}}\, \underline{\overline{\mathbf{16}}}'$ contributes to the up-type quark and neutrino Dirac mass matrices only.

[2] If all particles have a mass of the GUT scale, $\alpha(\Lambda = 6.4 \cdot 10^{16}\,\mathrm{GeV}) \approx 1$.

Most non-renormalizable SO(10) models are accompanied by an Abelian flavor symmetry U(1) [174–179] to forbid couplings or relate couplings by a non-Abelian flavor symmetry. There are models based on SU(2) [180, 181] and SU(3) [182–184].
There exist two variants of the DTS mechanism which make use of the mismatch of electroweak doublets and colored triplets in the $\underline{\mathbf{45}}$ Higgs representation. Dimopoulos and Wilczek [185] proposed a mechanism which achieves the mass splitting by a VEV in the $B - L$ direction

$$\langle \underline{\mathbf{45}} \rangle = \mathrm{i}\tau_2 \otimes \mathrm{diag}\,(a,\, a,\, a,\, 0,\, 0) \tag{3.39}$$

and Chacko and Mohapatra [186] proposed another mechanism which leads to a complimentary VEV pattern

$$\langle \underline{\mathbf{45}} \rangle = \mathrm{i}\tau_2 \otimes \mathrm{diag}\,(0,\, 0,\, 0,\, b,\, b)\ . \tag{3.40}$$

More technical details can be found in App. B.1.1.

3.2.2 E_6

E_6 is a Lie group of rank 6 which can be broken to the SM in three different ways as depicted in Fig. 3.2. Like SO(10), it is free of anomalies. The SM matter is embedded into the fundamental

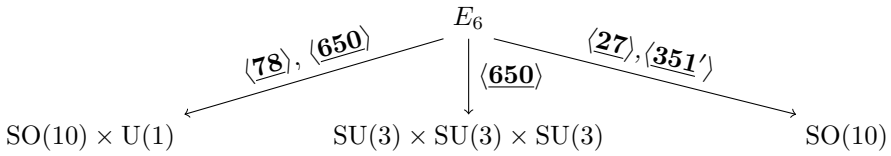

Figure 3.2: Breaking of E_6 to SO(10), flipped SO(10) and the trinification group. The breaking of SO(10) is shown in Fig. 3.1.

representation $\underline{\mathbf{27}}$ which contains in addition a RH neutrino, a $\underline{\mathbf{10}}$ of SO(10) matter multiplet and an additional SO(10) singlet which can be used in the cancellation mechanism being discussed in Chapter 4. The tensor product

$$\underline{\mathbf{27}} \otimes \underline{\mathbf{27}} = \overline{\underline{\mathbf{27}}} \oplus \overline{\underline{\mathbf{351}}}_A \oplus \overline{\underline{\mathbf{351}}}_S \tag{3.41}$$

decomposes in 3 summands where $\overline{\underline{\mathbf{27}}}$ and $\overline{\underline{\mathbf{351}}}_S$ are contained in the symmetric part and $\overline{\underline{\mathbf{351}}}_A$ in the antisymmetric one. A Majorana mass term of RH neutrinos is obtained from the coupling of $\underline{\mathbf{27}}$ to $\underline{\mathbf{351}}_S$. Since $\mathrm{U}(1)_{B-L}$ is a subgroup of E_6, the scale of the RH neutrino masses is related to $B - L$ breaking and the relation to baryogenesis via leptogenesis as well as the conservation of R-parity work similarly like in SO(10). The fundamental representation $\underline{\mathbf{27}}$ of E_6 does not allow a quartic coupling $\underline{\mathbf{27}}^4$. Therefore D5 proton decay operators are suppressed [187], i.e. the proton decay bound can be relaxed in E_6 models. The Georgi-Jarlskog factor can be obtained in the same way as in SO(10), since the relevant SO(10) representation is contained in the $\underline{\mathbf{351}}$ and $\underline{\mathbf{351}}'$ representation. As there are several models, we restrict ourselves and mention only two recent models which are worked out. In the model by Stech and Tavartkiladze [9], which we use to implement the cancellation mechanism in Sec. 4.4, they use a $\underline{\mathbf{27}}$ to incorporate the SM matter and 3 Higgs representations $\underline{\mathbf{27}}$, $\underline{\mathbf{351}}_A$ and $\underline{\mathbf{351}}_S$ to generate all fermion mass matrices. E_6 is broken to the SM via the trinification group $\mathrm{SU}(3)^3$. They do not consider the $\underline{\mathbf{650}}$ Higgs representation which is required to break E_6 to the trinification group. Note, that the gauge coupling of E_6 becomes non-perturbative almost immediately above the GU scale due to the large Higgs representations like in SO(10). The model was extended to include the flavor symmetry SO(3) [33]. The E_6 model by King,

Moretti and Nezorov [188] is inspired by string theory. However, they mainly consider the low-energy phenomenology of an extra non-anomalous $\mathrm{U}(1)'$ factor to the MSSM which is motivated from an E_6 GU model. E_6 is broken via the Hosotani mechanism [189], i.e. breaking via non-trivial boundary conditions in the compactification procedure, directly to $\mathrm{SU}(3)\times\mathrm{SU}(2)\times\mathrm{U}(1)_Y\times\mathrm{U}(1)_X\times\mathrm{U}(1)_Z$ and $\mathrm{U}(1)_X\times\mathrm{U}(1)_Z$ is broken in a second step to $\mathrm{U}(1)'$. The $\mathrm{U}(1)'$ is chosen such that RH neutrinos are uncharged and can acquire a large mass. It predicts many exotic particles at the TeV scale which can be tested by the large hadron collider (LHC). Indeed, there are three complete $\underline{\mathbf{27}}$ and one additional pair of electroweak Higgs doublets from an incomplete $\underline{\mathbf{27}}\oplus\overline{\underline{\mathbf{27}}}$ representation. However, gauge coupling unification is still possible, since the exotic matter comes in full SU(5) multiplets which affect all three gauge couplings in the same way. The μ-problem of the MSSM is solved, since the $\mu H_u H_d$ term is forbidden by the additional $\mathrm{U}(1)'$ symmetry. More technical details can be found in App. B.1.2.

3.3 Flavor Symmetries

Flavor symmetries can be classified in different categories according to whether they are

- global or local;
- Abelian or non-Abelian;
- continuous or discrete.

In the SM, the largest flavor group [3] is $\mathrm{U}(3)^5$, since there are five different particle species and three families. In SO(10), the maximal flavor group is U(3), since all SM fermions are contained in $\underline{\mathbf{16}}$. Hence, every flavor symmetry has to be a subgroup of $\mathrm{U}(3)^5$ in the case of the SM and U(3) within SO(10). As the masses and mixing parameters do not reveal a flavor symmetry at low energies, the flavor symmetry has to be broken spontaneously or explicitly above the electroweak scale. In the following, we firstly outline continuous flavor symmetries, before we summarize facts about discrete symmetries, which are needed in the following discussion. Technical details regarding group theory can be found in App. B.

3.3.1 Continuous Symmetries

Additional Abelian symmetry factors are common in string theory below the compactification scale. But, they can only explain hierarchies in mass matrices by the Froggatt-Nielsen mechanism and texture zeros. Exact relations between elements are not possible. Non-Abelian flavor symmetries, like SU(2), SO(3) and SU(3) relate different couplings. Barbieri et al. [25, 26] proposed $\mathrm{U}(2)\cong\mathrm{SU}(2)\times\mathrm{U}(1)$ as flavor group where SM fermions are assigned to the representation $\underline{\mathbf{2}}+\underline{\mathbf{1}}$, which only allows direct mass terms for the third family, especially the top quark. The symmetry is broken in two steps $\mathrm{SU}(2)\to\mathrm{U}(1)\to$ nothing. However, SU(2) cannot explain the number of generations, because the fundamental representation is two dimensional. As the fundamental representation of SO(3) and SU(3) are three-dimensional, they are ideal candidates to explain the number of generations. On the level of Lie algebras $\mathfrak{so}(3)\cong\mathfrak{su}(2)$, since SU(2) is the double covering of SO(3). Therefore, SO(3) models differ from SU(2) models by the used representations only. In SO(3) models, e.g. [27], only vectorial representations are used, but half integer spin representations are not used. SU(2) can be further embedded into SU(3). King and Ross [28, 29] introduced a model

[3] In almost all models, the flavor symmetry and the gauge symmetry are a direct product and commute. However, there are models, where gauge interactions and the flavor symmetry do not commute, e.g. [190].

based on SU(3) which is firstly broken to SU(2). They explain fermion masses by a set of flavon VEVs, i.e. VEVs of gauge singlets which transform under the flavor symmetry. Models based on the Abelian flavor symmetry U(1) and the non-Abelian group SU(3) might be anomalous and the anomaly constraints have to be fulfilled in a local flavor symmetry. Anomalies are outlined in App. B.3.
In the following two subsections, we briefly introduce the Froggatt-Nielsen mechanism and lepton flavor charge symmetries, since their knowledge is required in the following chapters.

Froggatt-Nielsen Mechanism

Froggatt and Nielsen [191] proposed a mechanism to explain the large hierarchies in the quark and charged lepton sector by the introduction of a U(1) symmetry, usually denoted by Froggatt-Nielsen symmetry. The U(1) charges Q_i of the particles F_i determine the suppression factor of each element m_{ij} in the mass matrix, i.e.

$$m_{ij} \sim \lambda^{Q_i+Q_j} \tag{3.42}$$

where λ is some small number. The mass of the heaviest particle is usually generated at tree level. The Froggatt-Nielsen mechanism is implemented in an EFT approach. At some high-energy scale, there are heavy vector-like fermions X which couple to massless fermions. After the heavy vector-like fermions are integrated out and the scalar fields θ in the Yukawa couplings acquire a VEV, they generate mass terms for the light fermions which are suppressed by $\lambda = \langle\theta\rangle / M_X$ where M_X is the mass of the vector-like fermions X. However, since the Yukawa couplings $XF_i\theta$ are arbitrary numbers of $\mathcal{O}(1)$, which are not related among each other, the Froggatt-Nielsen mechanism can only explain the hierarchy but not the value exactly. There are several models which implement the Froggatt-Nielsen mechanism. The additional U(1) factor can be anomalous, if the model relies of the cancellation of the anomalies by the Green-Schwarz mechanism [192]. However, there are also models which are non-anomalous, where the anomalies are cancelled by additional fermions.

Lepton Flavor Charge Symmetries

In this section, we consider continuous flavor symmetries of the neutrino mass matrix. One class of them are the lepton flavor charges L_e, L_μ and L_τ and combinations thereof. The charge assignment is given in Tab. 3.2. In total, there are 10 different linear combinations $c_eL_e + c_\mu L_\mu + c_\tau L_\tau$, $c_{e,\mu,\tau} = 0, \pm 1$ which can serve as a symmetry of the neutrino mass matrix. However, most of them are already phenomenologically excluded (L_μ, L_τ, $L_e - L_\mu$, $L_e - L_\tau$, $L_e + L_\mu - L_\tau$ and $L_e - L_\mu + L_\tau$), only 4 of them are viable (L_e, $L_\mu - L_\tau$, $L_e - L_\mu - L_\tau$ and $L_e + L_\mu + L_\tau$). The last one $L_e + L_\mu + L_\tau$ corresponds to total lepton number conservation which results in Dirac neutrinos but does not constrain masses and mixing angles. In the following, we concentrate on the lepton flavor charges which are compatible with Majorana neutrinos. In the Dirac neutrino case, the RG effect is rather small, since the neutrino Yukawa couplings are small. We briefly discuss the flavor symmetries L_e, $L_e - L_\mu - L_\tau$ and $L_\mu - L_\tau$.

The flavor symmetry $\boldsymbol{L_e}$ [16–18] restricts the form of the lepton Yukawa couplings and the effective neutrino mass matrix to

$$Y_e = \begin{pmatrix} y_e & 0 & 0 \\ 0 & Y_e^{(22)} & Y_e^{(23)} \\ 0 & Y_e^{(32)} & Y_e^{(33)} \end{pmatrix}, \qquad m_\nu = \begin{pmatrix} 0 & 0 & 0 \\ . & m_{\mu\mu} & m_{\mu\tau} \\ . & . & m_{\tau\tau} \end{pmatrix} \tag{3.43}$$

	$\ell_L^{(e)}$	$\ell_L^{(\mu)}$	$\ell_L^{(\tau)}$	e_1, N_1	e_2,N_2	e_3, N_3
L_e	1	0	0	-1	0	0
L_μ	0	1	0	0	-1	0
L_τ	0	0	1	0	0	-1

Table 3.2: Lepton flavor charge assignment. In some models (e.g. [17]), only the charge of the left-handed doublets are specified and the charges of the RH particles is chosen differently. We restrict ourselves to this charge assignment.

in flavor basis

$$Y_e = \begin{pmatrix} y_e & 0 & 0 \\ 0 & y_\mu & 0 \\ 0 & 0 & y_\tau \end{pmatrix}, \qquad m_\nu = \sqrt{|\Delta m^2_{32}|} \begin{pmatrix} 0 & 0 & 0 \\ . & a & b \\ . & . & d \end{pmatrix} \tag{3.44}$$

where a, b and d are parameters of $\mathcal{O}(1)$. a and d can be chosen real (after electroweak symmetry breaking). The neutrino mass matrix results in a normal mass hierarchy $m_1 \ll m_2 \leq m_3$. The neutrino masses are $m_1 = 0$, $m_{2,3} = \frac{1}{2}\left(a + d \pm \sqrt{(a-d)^2 + 4b^2}\right)$. The atmospheric mixing angle is close to maximal, i.e. $\tan\theta_{23} = \mathcal{O}(1)$. However, the solar mixing angle and θ_{13} vanish. Therefore, the symmetry has to be broken by additional contributions to the first row of the neutrino mass matrix. These breaking terms can originate from flavon fields of the U(1) symmetry [17], as it is done in the Froggatt-Nielsen mechanism [191].

$\boldsymbol{L_e - L_\mu - L_\tau}$ [19] restricts the flavor structure to

$$Y_e = \begin{pmatrix} y_e & 0 & 0 \\ 0 & Y_e^{(22)} & Y_e^{(23)} \\ 0 & Y_e^{(32)} & Y_e^{(33)} \end{pmatrix}, \qquad m_\nu = \begin{pmatrix} 0 & m_{e\mu} & m_{e\tau} \\ . & 0 & 0 \\ . & . & 0 \end{pmatrix} \tag{3.45}$$

in flavor basis

$$Y_e = \begin{pmatrix} y_e & 0 & 0 \\ 0 & y_\mu & 0 \\ 0 & 0 & y_\tau \end{pmatrix}, \qquad m_\nu = \sqrt{|\Delta m^2_{32}|} \begin{pmatrix} 0 & a & b \\ . & 0 & 0 \\ . & . & 0 \end{pmatrix} \tag{3.46}$$

where a and b are real (after electroweak symmetry breaking) coefficients of $\mathcal{O}(1)$, which result in an inverted mass hierarchy $\sqrt{a^2 + b^2} = m_2 = m_1 \gg m_3 = 0$. The atmospheric mixing angle is $\tan\theta_{23} = \frac{\sqrt{3}b^2}{\sqrt{2|a|^4 + |b|^4}}$ and θ_{13} vanishes. As the solar mass squared difference vanishes, the solar mixing angle is unphysical. Small corrections, which induce a solar mass squared difference, however, lead to an almost maximal solar angle.

$\boldsymbol{L_\mu - L_\tau}$ [20–24] restricts the flavor structure to

$$Y_e = \begin{pmatrix} y_e & 0 & 0 \\ 0 & y_\mu & 0 \\ 0 & 0 & y_\tau \end{pmatrix}, \qquad m_\nu = \sqrt{|\Delta m^2_{32}|} \begin{pmatrix} a & 0 & 0 \\ . & 0 & b \\ . & . & 0 \end{pmatrix} \tag{3.47}$$

where a and b are coefficients of $\mathcal{O}(1)$, which result in a quasi-degenerate mass spectrum $a = m_1 \simeq m_2 = m_3 = b$, where the atmospheric mixing angle is maximal and the solar angle and θ_{13} vanish. The mass matrix automatically obeys a $\mu - \tau$ exchange symmetry [48–51], i.e. , the mass matrix is

of the form

$$m_\mu = \begin{pmatrix} A & B & B \\ . & D & E \\ . & . & D \end{pmatrix} . \tag{3.48}$$

$L_\mu - L_\tau$ can be gauged, since it is anomaly-free [193, 194]. Moreover, it can be extended to include RH neutrinos with charges given in Tab. 3.2. As a consequence, the charged lepton Yukawa couplings are real and diagonal as in Eq. (3.47). The neutrino Yukawa couplings and the RH neutrino Majorana mass matrix are

$$m_D = v \begin{pmatrix} a & 0 & 0 \\ 0 & b & 0 \\ 0 & 0 & d \end{pmatrix} \text{ and } M_{NN} = M \begin{pmatrix} X\, e^{\mathrm{i}\phi} & 0 & 0 \\ \cdot & 0 & Y\, e^{\mathrm{i}\omega} \\ \cdot & \cdot & 0 \end{pmatrix} , \tag{3.49}$$

where $a, b, d, X, Y, \phi, \omega$ are real parameters. After integrating out the heavy RH neutrinos, the effective light neutrino mass matrix is given by

$$m_\nu = -\frac{v^2}{M} \begin{pmatrix} \frac{a^2\, e^{-\mathrm{i}\phi}}{X} & 0 & 0 \\ \cdot & 0 & \frac{b\, d\, e^{-\mathrm{i}\omega}}{Y} \\ \cdot & \cdot & 0 \end{pmatrix} , \tag{3.50}$$

which has the same form as the one in Eq. (3.47). Therefore, $L_\mu - L_\tau$ has to be broken [24] in order to generate a successful phenomenology. The non-vanishing mass squared difference Δm^2_{21} is given by

$$\Delta m^2_{21} = \frac{v^4}{M^2} \left| \frac{b^2 d^2}{Y^2} - \frac{a^4}{X^2} e^{\mathrm{i}(\phi-\omega)} \right| . \tag{3.51}$$

In the following, we break $L_\mu - L_\tau$ softly by additional small parameters in M_{NN}. The first and minimal approach is to add just one small entry to M_{NN}. For instance, we can add to the 1-2 element an entry $\epsilon\, e^{i\chi}$ with real $\epsilon \ll 1$. The resulting low energy mass matrix reads

$$m_\nu = \frac{v^2}{M} \begin{pmatrix} \frac{a^2\, e^{-i\phi}}{X} & 0 & \frac{-a\, d\, \epsilon\, e^{i(\chi-\omega-\phi)}}{X\, Y} \\ \cdot & 0 & \frac{b\, d\, e^{-i\omega}}{Y} \\ \cdot & \cdot & \frac{d^2\, \epsilon^2\, e^{i(2\chi-2\omega-\phi)}}{X\, Y^2} \end{pmatrix} . \tag{3.52}$$

It is interesting to note that there is no CP violation in oscillation experiments which can be immediately seen by the vanishing of J_{CP} (See App. A.) or at high energies. In order to have CP violation, we are therefore forced to add another perturbation to M_{NN}:

$$M_{NN} = M \begin{pmatrix} X\, e^{i\phi} & \epsilon_1\, e^{i\psi_1} & 0 \\ \cdot & \epsilon_2\, e^{i\psi_2} & Y\, e^{i\omega} \\ \cdot & \cdot & 0 \end{pmatrix} . \tag{3.53}$$

By rephasing all mass matrices, it can be shown that there is only one physical phase. Therefore, we choose $\phi = \omega = \psi_1 = 0$ and $\psi_2 = \psi$. This leads to the low energy effective mass matrix

$$m_\nu = -\frac{v^2}{M} \begin{pmatrix} \frac{a^2}{X} & 0 & \frac{-a\, d\, \epsilon_1}{X\, Y} \\ \cdot & 0 & \frac{b\, d}{Y} \\ \cdot & \cdot & \frac{-d^2 \left(X\, \epsilon_2\, e^{i\psi} - \epsilon_1^2 \right)}{X\, Y^2} \end{pmatrix} , \tag{3.54}$$

which has 2 texture zeros. This allows us to use the well-known predictions [195–198] for neutrino mass matrices with zeros in the 1-2 and 2-2 elements. In particular, only quasi–degenerate light neutrinos are compatible with such a matrix and in addition it is required that the 1-1 and the 2-3 elements are of leading order and similar magnitude [196]. This is however just the approximate form of a mass matrix conserving $L_\mu - L_\tau$.
After inserting the conditions of vanishing 1-2 and 2-2 elements in the definition of the general neutrino mass matrix in flavor basis, an expression for the ratio of neutrino masses is obtained. In the expansion in terms of the small parameter $\sin\theta_{13}$

$$\left|\frac{m_1}{m_3}\right| \simeq \tan^2\theta_{23} - \sin\theta_{13}\,\cos\delta\,\cot\theta_{12}\,\frac{\tan\theta_{23}}{\cos^2\theta_{23}}\ , \tag{3.55a}$$

$$\left|\frac{m_2}{m_3}\right| \simeq \tan^2\theta_{23} + \sin\theta_{13}\,\cos\delta\,\tan\theta_{12}\,\frac{\tan\theta_{23}}{\cos^2\theta_{23}} \tag{3.55b}$$

is obtained. As the atmospheric mixing angle is close to maximal and $\sin\theta_{13}$ is small, the light neutrinos are obviously quasi–degenerate. The ratio of the mass squared differences ζ which is defined in Eq. (3.1) is obtained from the ratio of masses

$$\zeta \simeq \left|4\,\sin\theta_{13}\,\cos\delta\,\frac{\tan\theta_{23}}{\cos 2\theta_{23}}\frac{\sin^2\theta_{23}}{\sin 2\theta_{12}}\right|\ . \tag{3.56}$$

As ζ is inversely proportional to the rather small quantity $\cos 2\theta_{23}$, it is necessary that $\sin\theta_{13}\,\cos\delta = \mathrm{Re}\,U_{e3} \ll \cos 2\theta_{23}$. Hence, the Dirac phase should be located around its maximal value $\pi/2$, i.e., CP violation is close to maximal. The larger $\sin\theta_{13}$ is, the smaller $\cos\delta$ has to be, i.e. the CP violation becomes close to maximal. Furthermore, the angle θ_{23} cannot become maximal in order to keep ζ small. From Eq. (3.55a) it can be deduced that the mass ordering for $\theta_{23} > \pi/4$ is inverted and otherwise normal. These predictions are almost independent of the precise value of θ_{12}, which can receive large renormalization corrections which we discuss in Sec. 6.2. The effective mass governing $0\nu2\beta$ decay shows again that maximal atmospheric neutrino mixing is forbidden

$$\langle m_{ee}\rangle = \frac{v^2}{M}\,\frac{a^2}{X} \simeq \tan^2\theta_{23}\sqrt{\frac{|\Delta m^2_{32}|}{|1-\tan^4\theta_{23}|}}\ . \tag{3.57}$$

Since the charged leptons display a hierarchy, it is natural to assume that also the eigenvalues of the Dirac mass matrix are hierarchical. Then it is required that also the heavy Majorana neutrinos display a hierarchy in the form of $Y \gg X$. Typical values of the parameters which in this case successfully reproduce the neutrino data are $Y = \mathcal{O}(1)$, $a = \mathcal{O}(0.01)$, $b \sim d = \mathcal{O}(0.1)$, $X = \mathcal{O}(0.001)$, $\epsilon_1 = \mathcal{O}(0.001)$ and $\epsilon_2 = \mathcal{O}(0.1)$. With these values, the eigenvalues of M_{NN} are approximatively given by $M\,X$ and $M\,(Y \pm \epsilon_2/2)$.

3.3.2 Discrete Symmetries

After continuous flavor symmetries are broken, there might be still discrete symmetries of the Lagrangian. There might be even discrete symmetries which are not embedded into a continuous symmetry. Compared to continuous flavor symmetries, they have the advantage, that they usually contain more small representations which can be used to construct models and the spontaneous breaking of a discrete symmetry does not lead to Goldstone or massive gauge bosons. Abelian discrete groups $\bigoplus_i Z_{N_i}$ contain only one dimensional representations and they can be used to forbid or suppress certain couplings. However, it is not possible to relate couplings similar to the continuous

Abelian group U(1). In the following, we briefly review the most important facts of $\mu-\tau$ symmetry and the way to obtain tri-bimaximal mixing from the group A_4, since we refer to both in the following sections.

$\mu - \tau$ exchange symmetry

The experimental data of the neutrino mass matrix is compatible with a $\mu - \tau$ exchange symmetry [48–51], i.e. neutrino masses can be described by the matrix

$$m_\nu = \begin{pmatrix} A & B & -B \\ . & D & C \\ . & . & D \end{pmatrix} \tag{3.58}$$

in flavor basis which is invariant under the exchange of the second and third row and column. The neutrino masses are given by

$$m_3 = C + D \,, \qquad m_{1,2} = \frac{1}{2}\left(A - C + D \pm \sqrt{8B^2 + (A + C - D)^2} \right) \,. \tag{3.59}$$

The $\mu-\tau$ exchange symmetry leads to maximal atmospheric mixing and vanishing 1-3 mixing. The solar mixing angle is determined by

$$\tan 2\theta_{12} = \frac{2\sqrt{2}B}{D - C - A} \,. \tag{3.60}$$

The bimaximal neutrino mass matrix is automatically $\mu-\tau$ symmetric. However, the $\mu-\tau$ exchange symmetry is not compatible with the charged lepton mass matrix, since $m_\mu \neq m_\tau$. Therefore, it is difficult to implement this symmetry. One possibility is by the Dirac screening mechanism which is described in Chapter 4 which completely cancels the flavor structure of the Dirac mass matrices in the DS mechanism. Therefore the neutrino mass matrix is not related to Yukawa couplings and its flavor structure is given by M_{SS} which is independent and can obey a $\mu - \tau$ symmetry.

A_4

The group A_4 is of order 12 and is the symmetry group of the regular tetrahedron. It is also isomorphic to the group of even permutations of 4 distinct elements. Ma [30] used it to describe the neutrino mass matrix and to explain the MNS matrix. It is the smallest group with a three dimensional representation. In addition, there are three one dimensional representations which are denoted by $\underline{\mathbf{1}}_\mathbf{1} \cong \underline{\mathbf{1}}$, $\underline{\mathbf{1}}_\mathbf{2} \cong \underline{\mathbf{1}}'$ and $\underline{\mathbf{1}}_\mathbf{3} \cong \underline{\mathbf{1}}''$. $\underline{\mathbf{1}}'$ and $\underline{\mathbf{1}}''$ are complex conjugated to each other while the other representations are real. It can be embedded into the group SO(3). The character table, generators and the Kronecker products are given in [30].
Phenomenologically, A_4 is interesting, since it can lead to tri-bimaximal mixing in the lepton sector [199]. Ma assigns the left-handed lepton doublets to $\underline{\mathbf{3}}$ and $(e_R, \mu_R, \tau_R)^T \sim \underline{\mathbf{1}} \oplus \underline{\mathbf{1}}' \oplus \underline{\mathbf{1}}''$. A_4 is broken by electroweak Higgs doublets $\phi \sim \underline{\mathbf{3}}$. After the Higgs doublets acquire all the same VEV $\langle \phi_i \rangle = v$ the charged lepton mass matrix becomes

$$m_e = \mathrm{diag}\,(m_e,\, m_\mu,\, m_\tau)\, U_e \,, \tag{3.61}$$

where $\omega = e^{\mathrm{i}2\pi/3}$ and $m_i = y_i v$. The charged lepton mass matrix is diagonalized by the so-called magic matrix

$$U_e = \frac{1}{\sqrt{3}} \begin{pmatrix} 1 & 1 & 1 \\ 1 & \omega & \omega^2 \\ 1 & \omega^2 & \omega \end{pmatrix} \,. \tag{3.62}$$

In addition, Higgs triplets are introduced which transform as $\xi \sim \underline{\mathbf{1}} \oplus \underline{\mathbf{1}}' \oplus \underline{\mathbf{1}}'' \oplus \underline{\mathbf{3}}$. The neutrinos acquire a mass via the triplet seesaw mechanism

$$m_\nu = \begin{pmatrix} a+b+c & 0 & 0 \\ . & 1+\omega b+\omega^2 c & d \\ . & . & a+\omega^2 b+\omega c \end{pmatrix} \tag{3.63}$$

with a, b, c coming from the A_4 singlets and $d = \langle \xi_4 \rangle$ from the first component of the A_4 triplet. The other components of the triplet do not acquire a VEV. The neutrino mass matrix is diagonalized by a maximal 2-3 rotation if the equality $b = c$ is assumed, which results in a tri-bimaximal mixing matrix, as it has been shown in Sec. 3.1.1.
Altarelli and Feruglio [200] derived tri-bimaximal mixing by flavons. A_4 is broken by two $\underline{\mathbf{3}}$ flavons in the directions $\langle \phi' \rangle = (v', 0, 0)$ and $\langle \phi \rangle = (v, v, v)$, which break A_4 to two different subgroups. In addition, there is a singlet ξ which obtains the VEV $\langle \xi \rangle = u$. ϕ couples to the charged leptons and leads to the mass matrix given in Eq. (3.61) ϕ' and ξ couple to the D5 operator which results in the mass matrix

$$m_\nu = \frac{\langle H_u \rangle^2}{\Lambda} \begin{pmatrix} a & 0 & 0 \\ . & a & d \\ . & . & a \end{pmatrix} \tag{3.64}$$

where

$$a \sim \frac{u}{\Lambda}\,, \qquad d \sim \frac{v'}{\Lambda}\,. \tag{3.65}$$

The separation between the two sectors, which allows the breaking to different subgroups, can be explained by an additional symmetry.

3.4 Quark Lepton Complementarity

Recently, it has been realized [12–14] that the sums of the 1-2 and 2-3 mixing angles add up to 45° within 1σ

$$\theta_{12} + \vartheta_{12} \approx \frac{\pi}{4}, \qquad \theta_{23} + \vartheta_{23} \approx \frac{\pi}{4}\,. \tag{1.2}$$

According to Eq. (1.2), which are called quark lepton complementarity (QLC) relations, the quark and lepton mixing angles are complementary to maximal mixing. If these relations are not accidental coincidences, they will imply a symmetry which connects quarks and leptons as well as some mechanism which produces maximal or bimaximal mixing. However, even in this context, deviations from the QLC relations can be expected due to symmetry breaking and RG effects.
There are several attempts [13, 201–205] to implement the QLC relations which mostly lead to approximate QLC relations by the interplay of several independent contributions. The simplest unified model which implements a quark-lepton symmetry in a straightforward way is the PS model [201,203]. The phenomenology of schemes which obey the QLC relations has been studied in several works [202, 205–211].
One general scheme for the QLC relations is that

$$\text{“lepton mixing} = \text{bimaximal mixing} - \text{CKM}'',$$

where the bimaximal mixing matrix is $U_{\rm bm} = U_{23}(\pi/4)U_{12}(\pi/4)$.
We assume that bimaximal mixing is generated by the neutrino mass matrix. That is, the same mechanism which is responsible for the smallness of neutrino mass also leads to the large lepton

mixing, and it is the seesaw mechanism that plays the role of the additional structure that generates bimaximal mixing. Therefore

$$U_{MNS} = U_e^\dagger U_\nu = V_{\rm CKM}^\dagger \Gamma_\alpha U_{\rm bm}, \tag{3.66}$$

where $\Gamma_\alpha \equiv {\rm diag}(e^{i\alpha_1}, e^{i\alpha_2}, e^{i\alpha_3})$ is a phase matrix that can appear, in general, in the diagonalization of the charged lepton or neutrino Dirac mass matrix. A quark-lepton symmetry leads to similar Dirac mass matrices in the lepton and quark sector which is the origin of the CKM rotations in the lepton sector. There are two appealing possibilities:

- In a certain ("symmetry") basis, where the theory of flavor is formulated, the neutrino mass matrix is of bimaximal form. So
$$U_\nu = U_{\rm bm} \ , \tag{3.67}$$
and the charged lepton mass matrix is diagonalized by the CKM rotation
$$U_e = V_{\rm CKM}. \tag{3.68}$$
However, as it has been noted in Sec. 3.2, the masses of charged leptons and down quarks are different at the GUT scale: in particular, $m_e/m_\mu = 0.0047$, whereas $m_d/m_s = 0.04 - 0.06$, and also $m_\mu \neq m_s$. Since $m_e \neq m_d$, the equality in Eq. (3.68) implies a certain structure of the mass matrices in which the mixing weakly depends on the eigenvalues.

- In the "symmetry" basis both bimaximal and CKM mixings come from the neutrino mass matrix, and the charged lepton mass matrix is diagonal, i.e. the symmetry basis coincides with the flavor basis. In this case the Dirac mass matrix of neutrinos is the origin of the CKM rotation, whereas the Majorana mass matrix of the RH neutrinos is responsible for bimaximal mixing. Since the eigenvalues of the Dirac neutrino mass matrix are unknown we can assume an exact equality of the mass matrices
$$m_u = m_D \ , \tag{3.69}$$
as a consequence of the quark-lepton symmetry. The equality in Eq. (3.69) propagates the CKM mixing from the quark to the lepton sector. In this case, however, the GST relation between ϑ_{12} and the ratio of m_d and m_s [11] turns out to be accidental. Moreover, it is to be explained why in the symmetry basis the charged lepton and down quark mass matrices are simultaneously diagonal in spite of their different mass eigenvalues.

These two cases have different theoretical implications, however the phenomenological consequences and the RG effects are the same. In the following, we assume the first scenario for definiteness, i.e. the effective light neutrino mass matrix, Eq. (3.15), should generate the bimaximal rotation:

$$m_\nu = m_{\rm bm} = \Gamma_\delta U_{\rm bm} \Gamma_{\varphi/2} m_\nu^{\rm diag} \Gamma_{\varphi/2} U_{\rm bm}^T \Gamma_\delta. \tag{3.70}$$

Here $\Gamma_\delta \equiv {\rm diag}(e^{{\rm i}\delta_1}, e^{{\rm i}\delta_2}, e^{{\rm i}\delta_3})$ is a phase matrix, $m_\nu^{\rm diag}$ is the diagonal matrix of the light neutrinos, and $\Gamma_{\varphi/2} \equiv {\rm diag}(e^{{\rm i}\varphi_1/2}, e^{{\rm i}\varphi_2/2}, 1)$ with φ_i being the Majorana phases of light neutrinos.
According to our assumption, the CKM rotation follows from the diagonalization of the charged lepton mass matrix and we parameterize it as

$$U_e = \Gamma_\phi V_{\rm CKM}(\vartheta_{ij}, \delta^q) \ . \tag{3.71}$$

Here the diagonal matrix of the phase factors on the RH side has been absorbed in the charged lepton field redefinition; $V_{\rm CKM}$ is the CKM matrix in the standard parameterization, ϑ_{ij} and δ^q are the CKM mixing angles and phase, and

$$\Gamma_\phi \equiv \mathrm{diag}(e^{\mathrm{i}\phi_1}, e^{\mathrm{i}\phi_2}, e^{\mathrm{i}\phi_3}) \; . \tag{3.72}$$

Thus, in general, there are three phase matrices, Γ_δ, Γ_φ and Γ_ϕ, relevant for relations between the mixing angles. Finally, from Eq. (3.71) and Eq. (3.70) we obtain

$$U_{MNS} = V^\dagger_{\rm CKM}(\vartheta_{ij}, \delta^q)\Gamma(\delta_l - \phi_l)U_{\rm bm}, \tag{3.73}$$

and therefore in Eq. (3.66) $\alpha_j = \delta_j - \phi_j$. The neutrino mass matrix in flavor basis equals

$$m^f_\nu = V^T_{\rm CKM} m_{\rm bm} V_{\rm CKM} \; . \tag{3.74}$$

From Eq. (3.15) and Eq. (3.70) we find an expression for the RH neutrino mass matrix analogous to [212]:

$$M_{NN} = \Gamma_\delta m_D^{\rm diag} U_{\rm bm} \Gamma_{\varphi/2} (m_\nu^{\rm diag})^{-1} \Gamma_{\varphi/2} U^T_{\rm bm} m_D^{\rm diag} \Gamma_\delta \; , \tag{3.75}$$

where $m_D^{\rm diag}$ denotes the diagonalized neutrino Dirac mass matrix m_D. We absorb the phase factor Γ_δ in M_{NN} and omit it in the following. Also the CP phases φ_i are included into the masses of the light neutrinos $\Gamma_{\varphi/2}(m_\nu^{\rm diag})^{-1}\Gamma_{\varphi/2} = (\tilde{m}_\nu^{\rm diag})^{-1}$. Hence, we obtain

$$M_{NN} = m_D^{\rm diag} U_{\rm bm} (\tilde{m}_\nu^{\rm diag})^{-1} U^T_{\rm bm} m_D^{\rm diag} \; , \tag{3.76}$$

which can be written explicitly in terms of neutrino masses and m_D

$$M_{NN} = \frac{1}{4} m_D^{\rm diag} \begin{pmatrix} 2A & \sqrt{2}B & -\sqrt{2}B \\ . & C+A & C-A \\ . & . & C+A \\ \end{pmatrix} m_D^{\rm diag}, \tag{3.77}$$

where

$$A \equiv \frac{1}{\tilde{m}_1} + \frac{1}{\tilde{m}_2}, \quad B \equiv \frac{1}{\tilde{m}_2} - \frac{1}{\tilde{m}_1}, \quad C \equiv \frac{2}{m_3} \; . \tag{3.78}$$

We can parameterize $m_D^{\rm diag}$ as

$$m_D^{\rm diag} = m_t \, \mathrm{diag}(\epsilon'^2, \epsilon, 1), \tag{3.79}$$

with m_t being the mass of the top quark and $\epsilon' \approx \epsilon \sim 3 \cdot 10^{-3}$. The RH neutrino masses are easily estimated using the smallness of ϵ and ϵ'

$$M_3 \approx \frac{m_t^2}{4}(A+C) \; , \quad M_2 \approx m_t^2 \epsilon^2 \frac{AC}{A+C} \; , \quad M_1 \approx m_t^2 \epsilon'^4 \frac{A^2 - B^2}{2A} \; . \tag{3.80}$$

Furthermore, the 1-2 and 2-3 mixing angles are of the order of ϵ, whereas the 1-3 mixing is of the order of ϵ^2.
In the case of a normal mass hierarchy, $m_1 \ll m_2 \ll m_3$, Eq. (3.80) lead to

$$M_3 \approx \frac{m_t^2}{4m_1}, \quad M_2 \approx \frac{2m_t^2\epsilon^2}{m_3}, \quad M_1 \approx \frac{2m_t^2\epsilon'^4}{m_2}, \tag{3.81}$$

in agreement with the results of [212]. Notice the permutation character of these expressions: the masses of the RH neutrinos M_1, M_2 and M_3 are determined by the light masses m_2, m_3 and m_1. With $m_1 \to 0$, apparently, $M_3 \to \infty$. For $\epsilon' = \epsilon \sim 3 \cdot 10^{-3}$ and $m_1 = 10^{-3}\,\mathrm{eV}$, the masses equal

$$M_3 = 9 \cdot 10^{15}\ \text{GeV}, \quad M_2 = 1 \cdot 10^{10}\ \text{GeV}, \quad M_1 = 5 \cdot 10^{5}\ \text{GeV}. \tag{3.82}$$

Thus, there is a "quadratic" hierarchy as expected to cancel the hierarchy in m_D.
In the case of an inverted mass hierarchy, $m_3 \ll m_1 \approx m_2 \equiv m_A$, and the same CP phases of ν_1 and ν_2 we obtain from Eq. (3.80)

$$M_3 \approx \frac{m_t^2}{2m_3}, \quad M_2 \approx \frac{2m_t^2\epsilon^2}{m_A}, \quad M_1 \approx \frac{m_t^2\epsilon'^4}{m_A}, \tag{3.83}$$

where $m_A \equiv \sqrt{|\Delta m^2_{31}|}$. This leads again to a strong mass hierarchy. Notice that now the mass of the lightest RH neutrino is determined by the atmospheric mass scale. Thus, apart from special regions in the parameter space that correspond to level crossings (See Sec. 6.3.5.) the QLC relations imply generically a very strong ("quadratic") mass hierarchy of the RH neutrinos and very small mixing: $\Theta_{ij} \sim \epsilon$. As we will see, this determines substantially the size of the RG effects.
Let us introduce the unitary matrix, U_N, which diagonalizes the RH neutrino mass matrix

$$U_N^T M_{NN} U_N = M_{NN}^{\text{diag}} \equiv \text{diag}\,(M_1,\, M_2,\, M_3)\,, \tag{3.84}$$

and the mixing matrix can be parameterized as

$$U_N = \Gamma_\Delta V(\Theta_{ij}, \Delta)\Gamma_{\xi/2}, \tag{3.85}$$

where Θ_{ij} and Δ are the angles and CP-phase of the RH neutrino mixing matrix. They are used in the discussion of the RG effects in Sec. 6.3.
We will not elaborate further on the origin of the particular structures of M_{NN} in Eq. (3.77), just noticing that it can be related to the cancellation mechanism which is discussed in Sec. 4.1.
Note, that the relation Eq. (1.2) is not realized precisely even for zero phases α_i since the rotation matrix related to the Cabibbo angle has to be permuted with $U_{23}(\pi/4)$ in Eq. (3.66) to reduce the mixing matrix to the standard parameterization form. From Eq. (3.66) we obtain the following expressions for the leptonic mixing angles:

$$U_{e2} \equiv \cos\theta_{13}\sin\theta_{12} = \sin(\frac{\pi}{4} - \vartheta_{12}) + \frac{1}{2}\sin\vartheta_{12}\left[\sqrt{2} - 1 - V_{cb}\cos(\alpha_3 - \alpha_1)\right] + \frac{1}{2}V_{ub}\cos(\alpha_3 - \alpha_1 - \delta^q). \tag{3.86}$$

This expression differs from the one derived in [14] by a factor $\cos\theta_{13}$ as well as by the last term, that turns out to be relevant at the level of accuracy we will consider here. The 1-3 mixing [14, 206–211]:

$$\sin\theta_{13} = -\frac{\sin\vartheta_{12}}{\sqrt{2}}(1 - V_{cb}\cos\alpha_3) - \frac{V_{ub}}{\sqrt{2}}\cos(\alpha_3 - \delta^q) \approx -\frac{\sin\vartheta_{12}}{\sqrt{2}} \tag{3.87}$$

or equivalently $|U_{e3}| = |\sin\theta_{13}|$ is large in this scenario and, hence, the Dirac CP phase δ is close to 180°. So, for the 1-2 mixing we find the relation

$$\sin\theta_{12} = \frac{|U_{e2}|}{\sqrt{1 - |U_{e3}|^2}} \approx U_{e2}(1 + \frac{1}{4}\sin^2\vartheta_{12}), \tag{3.88}$$

and U_{e2} is given in Eq. (3.86).
Note, that the QLC relation for the 1-2 mixing angles can also be written in the form

$$\arcsin(V_{us}) + \arcsin(U_{e2}) = \frac{\pi}{4} \tag{3.89}$$

which coincides in the limit $U_{e3} \to 0$ with Eq. (1.2). The expression for the 2-3 mixing reads

$$U_{\mu 3} = \cos\theta_{13}\sin\theta_{12} = \cos\vartheta_{12}\left[\sin(\pi/4 - \theta_{cb}) + \frac{V_{cb}}{\sqrt{2}}(1 - \cos\alpha_3)\right]. \tag{3.90}$$

Chapter 4

Cancellation Mechanism

As we have pointed out in Sec. 3.2, Yukawa couplings are related in unified theories, especially in left-right symmetric models, like G_{2231} and G_{224} $Y_\nu \sim Y_e$ and in SO(10) or E_6 $Y_\nu \sim Y_u$. Therefore, neutrino Yukawa couplings are strongly hierarchical, although the neutrino masses show a very modest hierarchy. In this chapter, we present a simple and elegant mechanism to cancel the strong hierarchy encoded in the neutrino Yukawa couplings. In Sec. 4.1, we explain the cancellation mechanism. In Sec. 4.2, we argue that the same formulas hold for singular mass matrices of the additional singlets. Finally, specific realizations are discussed in Sec. 4.3.

4.1 Description of the Mechanism

We work in the framework of the cascade seesaw mechanism which is described in Sec. 3.1.2. Defining

$$F = M_{SN}^{-1\,T} m_D \,, \tag{4.1}$$

we can rewrite the formulas of the DS contribution

$$m_\nu^{DS} = F^T M_{SS} F \tag{4.2}$$

and the LS contribution

$$m_\nu^{LS} = -\left[F^T m_{S\nu} + m_{S\nu}^T F\right] \tag{4.3}$$

in terms of F and the matrices M_{SS} and $m_{S\nu}$, which are not a priori related to the SM Yukawa couplings. If M_{SN}^T shows the same hierarchy as m_D, the hierarchies cancel and F becomes a non-hierarchical matrix. Turning the argument around, we impose the relation $M_{SN} = F^{-1\,T} m_D^T$, where the singular values of F are required to be quasi-degenerate. We call that complete cancellation. More generally, the cancellation can be incomplete or partial, i.e. F is still hierarchical, which shows up in the realization by the flavor symmetry T_7 (See Sec. 4.5.1).
The relative size of the two contributions

$$\frac{m_\nu^{LS}}{m_\nu^{DS}} \sim \frac{m_{S\nu} M_{SN}}{m_D M_{SS}} = \frac{m_{S\nu}}{M_{SS}} F^{-1} \tag{4.4}$$

depends on the relative hierarchy between $m_{S\nu}$, M_{SS} and F. One appealing possibility in the context of GUTs is $m_{S\nu}, m_D \sim \mathcal{O}(\Lambda_{\rm ew})$, $M_{SN} \sim \mathcal{O}(\Lambda_{\rm GUT})$ and $M_{SS} \sim \mathcal{O}(M_{Pl})$. Then the DS term dominates over the LS term by $m_\nu^{LS}/m_\nu^{DS} \sim \mathcal{O}(10^{-3})$. At the same time, the neutrino mass scale $m_\nu \lesssim$ eV is naturally explained by the hierarchies between m_D, $\Lambda_{\rm GUT}$ and M_{Pl}. However, since the singlets are not related to the GUT and their mass scale is also not fixed by any other

means besides the experimental data, it is arbitrary and could also be lower than $\Lambda_{\rm GUT}$. The LS term gains importance when the singlet mass scale is lowered from the Planck scale while all other mass scales are fixed. At the same time, the LS contribution leads to a complete cancellation of hierarchies. Let us comment on the special case that m_D and M_{SN}^T are proportional to each other, which leads to a complete cancellation of the flavor structure and

$$F \propto \mathbb{1} \Rightarrow m_D \propto M_{SN}^T \tag{4.5}$$

which is called Dirac screening [78]. In the remainder of this chapter, we concentrate on the scenario, where $m_{S\nu}, m_D \sim \mathcal{O}(\Lambda_{\rm ew})$, $M_{SN} \sim \mathcal{O}(\Lambda_{\rm GUT})$ and $\mathcal{O}(\Lambda_{\rm GUT}) \lesssim M_{SS} \lesssim \mathcal{O}(M_{Pl})$. Therefore we neglect the LS contribution in the following, such that the mass matrix of the uncharged fermions is given by

$$\mathcal{M} = \begin{pmatrix} 0 & Y_\nu^T \langle H_u \rangle & 0 \\ Y_\nu \langle H_u \rangle & 0 & Y_{SN}^T \langle \Delta \rangle_N \\ 0 & Y_{SN} \langle \Delta \rangle_N & M_{SS} \end{pmatrix} . \tag{4.6}$$

As we have already discussed in the introduction, the mass matrix M_{SS} of the singlets S_i might be generated above the GUT scale and it is not related to the quark mass matrices. Therefore it is possible that M_{SS} has a certain symmetry which is translated to light neutrinos (See, e.g., [12–14, 48–51, 118–121]) and not seen in the quark and charged lepton sector. In the case of Dirac screening, this symmetry propagates immediately to the light neutrino sector. In general, it is slightly perturbed by F.
For example, the QLC relation [12–14] can be realized within Dirac screening, since the mass matrix M_{SS} can be the origin of bimaximal mixing. Then the CKM type mixing follows from the charged lepton mass matrix which is related to the mass matrix of the down quarks, so that $U_e = V_{\rm CKM}$. In the lowest order (without radiative corrections) we find from Eq. (3.21)

$$m_\nu^f = \left[\frac{\langle H_u \rangle}{\langle \Delta \rangle_N}\right]^2 U_e^T M_{SS} U_e = \left[\frac{\langle H_u \rangle}{\langle \Delta \rangle_N}\right]^2 V_{\rm CKM}^T U_{\rm bm}^* M_{SS}^{diag} U_{\rm bm}^\dagger V_{\rm CKM} . \tag{4.7}$$

The leptonic mixing matrix equals $U_{MNS} = V_{\rm CKM}^\dagger U_{\rm bm}$. This realizes the so called "neutrino scenario" which leads to deviations from the exact QLC relations [14].

4.2 Singular M_{SS}

Let us consider the special case of the DS contribution of a singular M_{SS}, $\det M_{SS} = 0$, which can be a consequence of a certain symmetry in the singlet sector. Now one cannot immediately use Eq. (3.21) and the whole DS mass matrix should be considered. In what follows we show that the tree-level mass matrix of the light neutrinos is still proportional to M_{SS}, that is, Eq. (3.21) will hold even if M_{SS} is singular. For this we will compare the light neutrino mass spectra in the lowest approximation found from the whole DS matrix Eq. (4.6) and from the matrix m_ν after decoupling of the heavy degrees of freedom in Eq. (3.21).
According to Eq. (3.21) the condition $\det M_{SS} = 0$ implies (at least one) zero eigenvalue in the spectrum of the usual left-handed neutrinos. The same follows from the complete matrix. Indeed,

$$\det \mathcal{M} = -\left(\det m_D\right)^2 \det M_{SS} = 0,$$

and hence, a zero eigenvalue of M_{SS} leads to a massless eigenstate of $\mathcal{M}$. The non-zero eigenvalues of the matrix m_ν, ξ_i, coincide with eigenvalues of the full matrix $\mathcal{M}$ up to corrections of the order

$\langle H_u \rangle / \langle \Delta \rangle_N$. This can be seen by inserting ξ_i in the characteristic polynomial of the complete matrix $\chi_{\mathcal{M}}[\lambda]$. The result is of the order of $\mathcal{O}((\langle H_u \rangle / \langle \Delta \rangle_N)^8) \sim 0$ which proves the claim.
There are no other light states, because the expansion of the polynomial

$$\chi_{\mathcal{M}}[\lambda] \prod_i (\lambda - \xi_i)^{-1} ,$$

in eigenvalues of the order $\langle H_u \rangle$ does not yield any new solutions. All other eigenvalues are at least of the order $\mathcal{O}(\langle \Delta \rangle_N^2 / M_{SS})$.
A peculiarity of the spectrum of $\mathcal{M}$ is the appearance of one heavy Dirac particle, if the eigenstate of M_{SS} with zero mass, S, couples to only one right-handed neutrino N. This Dirac particle is formed by S and N.
The mass spectrum can be easily obtained if $M_{SS} = \mathrm{diag}\,(M_{S1},\ M_{S2},\ 0)$ in the basis where $Y_{SN} = \mathrm{diag}\,(y_1,\ y_2,\ y_3)$. Apart from one zero mass which corresponds mainly to ν_3, and two super heavy eigenvalues M_{S1} and M_{S2} for two singlets S, we find

$$m_1 = M_{S1} \frac{\langle H_u \rangle^2}{\langle \Delta \rangle_N^2}, \quad m_2 = M_{S2} \frac{\langle H_u \rangle^2}{\langle \Delta \rangle_N^2}, \quad M_1 = -\frac{y_1^2 \langle \Delta \rangle_N^2}{M_{S1}}, \quad M_2 = -\frac{y_1^2 \langle \Delta \rangle_N^2}{M_{S2}}, \quad M_{DS} = y_3 \langle \Delta \rangle_N ,$$

that is, two light neutrinos are predominantly given by $\nu_{1,2}$ with masses m_1 and m_2, two heavy neutrinos mostly consisting of $N_{1,2}$ with masses M_1 and M_2 and one heavy Dirac particle of the GUT scale mass M_{DS} which is formed by N_3 and S_3. The light eigenstates are mainly composed of the left-handed neutrinos and the mixing with other neutral leptons is of the order $\mathcal{O}(\langle H_u \rangle / \langle \Delta \rangle_N)$.
The coincidence of the spectrum of m_ν and the spectrum of light states of $\mathcal{M}$ is related essentially to the fact that the relation between m_ν and M_{SS} is linear, and the characteristic polynomial is linear in the eigenvalues for the non-degenerate case. The same conclusion holds for M_{SS} with two zero eigenvalues.

4.3 Realization of DS Matrix Structure

In the following, we outline different possible origins of the DS structure Eq. (4.6) and discuss how the condition Eq. (4.2) can be achieved.
The texture of Eq. (4.6) with zero 1-1, 1-3, and 2-2 blocks can be obtained by assigning lepton numbers, *e.g.*

$$L(\nu) = L(S) = 1, \quad L(N) = -1, \quad L(H_u) = 0, \quad L(\Delta) = 0 .$$

Therefore, the lepton numbers of the blocks in mass matrix of the neutral fermions Eq. (4.6) equal

$$L(\mathcal{M}) = \begin{pmatrix} 2 & 0 & 2 \\ 0 & -2 & 0 \\ 2 & 0 & 2 \end{pmatrix} . \tag{4.8}$$

Hence, the DS texture shows up if the introduced lepton number is only broken by the Majorana mass terms of the additional singlets S. It can be broken explicitly or spontaneously by the VEV of a new scalar field ρ which has lepton number $L(\rho) = -2$ and couples to S only: $S^T Y_S S \rho$. The interaction $\nu^T S \rho$ is forbidden by gauge symmetry. The possible non-renormalizable term

$$\frac{1}{M_{Pl}} \ell S H_u \rho$$

is suppressed, if the VEV $\langle\rho\rangle < M_{Pl}$. In the SUSY version, the term $NN\rho$ is absent due to holomorphy. Otherwise, an extended gauge symmetry can forbid the 2-2 entry in the non-SUSY version or if also the left superfield ρ^c exists.
Indeed, in left-right symmetric models N is part of an $SU(2)_R$ doublet and the 2-2 block has gauge charge $(\underline{\mathbf{1}}, \underline{\mathbf{3}})$. The 2-2 entry appears only if a RH Higgs triplet obtains a VEV. The whole texture Eq. (4.6) can be a consequence of gauge symmetry. Let us consider the $\mathrm{SU}(2)_L \times \mathrm{SU}(2)_R \times \mathrm{U}(1)_{B-L}$ symmetry [40, 137–140]. The transformation properties with respect to the $(\mathrm{SU}(2)_L, \mathrm{SU}(2)_R)$ gauge group of the mass matrix elements are

$$G(\mathcal{M}) = \begin{pmatrix} (\underline{\mathbf{3}}, \underline{\mathbf{1}}) & (\underline{\mathbf{2}}, \underline{\mathbf{2}}) & (\underline{\mathbf{2}}, \underline{\mathbf{1}}) \\ . & (\underline{\mathbf{1}}, \underline{\mathbf{3}}) & (\underline{\mathbf{1}}, \underline{\mathbf{2}}) \\ . & . & (\underline{\mathbf{1}}, \underline{\mathbf{1}}) \end{pmatrix} . \tag{4.9}$$

The required matrix structure is generated if a Higgs bidoublet with an electroweak VEV, a RH doublet with a GUT scale VEV and a direct Planck scale mass term of the singlets exist.
Within SO(10) [3, 4], ν and N are part of $\underline{\mathbf{16}}$ and S is a singlet. The required texture can be generated by the following Yukawa interactions:

$$Y_u \; \underline{\mathbf{16}}\, \underline{\mathbf{16}}\, H + Y_{SN} \; \underline{\mathbf{16}}\, S\, \Delta + M_{SS} S\, S, \tag{4.10}$$

where $H \sim \underline{\mathbf{10}}$, $\Delta \sim \overline{\underline{\mathbf{16}}}$ are Higgs multiplets. To generate the required matrix Eq. (4.6) H should acquire an electroweak scale VEV and Δ a GUT scale VEV in N (SU(5) singlet) direction.
However, the interactions Eq. (4.10) do not produce any mixing, and the Dirac masses of quarks and leptons are equal at the GUT scale. Thus, a realistic model has to contain additional contributions to the fermion masses which may, in general, destroy the cancellation. For instance, the introduction of a $\overline{\underline{\mathbf{126}}}$-plet of Higgs fields which acquire VEVs in the directions of the left-handed and RH triplets in terms of the minimal left-right symmetric model generates the 1-1 and 2-2 blocks. This leads to additional contributions to the neutrino mass matrix, which are not governed by the cancellation mechanism.
Apparently, none of those constructions directly lead to the cancellation relation Eq. (4.2). The relation between the Yukawa couplings Eq. (4.2) can appear due to

- a further unification of ν and S, which is discussed in Sec. 4.4;
- a non-Abelian[1] flavor symmetry. Two realizations within SO(10) are discussed in Sec. 4.5.

4.4 Realization of Cancellation Mechanism with GUT Symmetry

In Sec. 4.3, several possibilities are shown to implement the DS matrix structure, although none of these realizations automatically led to the condition Eq. (4.1) or even Eq. (4.5). Here, we demonstrate how the Dirac screening mechanism can be implemented within E_6 [5–8]. In this context, we obtain Dirac screening.
The neutral fermions ν, N and S are part of the fundamental representation $\underline{\mathbf{27}}$ of E_6. Note that there are two additional neutral leptons per generation: S' and S''. All three Higgs representations, $\underline{\mathbf{27}}$, the symmetric $\underline{\mathbf{351}}_S$ and the antisymmetric $\underline{\mathbf{351}}_A$, which can couple to the tensor product of two $\underline{\mathbf{27}}_i$, are introduced,

$$(Y_{27})_{ij} \;\; \underline{\mathbf{27}}_i\, \underline{\mathbf{27}}_j\, \underline{\mathbf{27}} + (Y_{351_S})_{ij} \;\; \underline{\mathbf{27}}_i\, \underline{\mathbf{27}}_j\, \underline{\mathbf{351}}_S + (Y_{351_A})_{ij} \;\; \underline{\mathbf{27}}_i\, \underline{\mathbf{27}}_j\, \underline{\mathbf{351}}_A \; , \tag{4.11}$$

[1] An Abelian flavor symmetry, like in the Froggatt-Nielsen approach [191], can only relate hierarchies of different couplings, which results in an approximate cancellation. In order to obtain an exact relation, a non-Abelian flavor symmetry is required.

to generate the screening structure, i.e. the matrix Eq. (4.6) with the proportionality Eq. (4.5). In terms of the maximal subgroup $\mathrm{SU}(3)_L \times \mathrm{SU}(3)_R \times \mathrm{SU}(3)_C \subset E_6$, the left-handed leptons transform as $L \sim \left(\underline{\overline{3}}, \underline{3}, \underline{1}\right)$. The $(\mathrm{SU}(3))^3$ assignment of the neutral leptons is

$$\nu \sim L_3^{\dot{2}}, \;\; N \sim L_2^{\dot{3}}, \;\; S \sim L_3^{\dot{3}}, \;\; S' \sim L_1^{\dot{1}}, \;\; S'' \sim L_2^{\dot{2}}. \tag{4.12}$$

See App. B.1.2 for the $\mathrm{SU}(3)^3$ index structure[2]. The neutral components of the Higgs multiplets H, H_A and H_S which can acquire VEVs belong to

$$\begin{aligned} H &\subset \left(\underline{\overline{3}}, \underline{3}, \underline{1}\right) \subset \underline{\mathbf{27}} \\ H_S &\subset \left(\underline{\overline{3}}, \underline{3}, \underline{1}\right) + \left(\underline{6}, \underline{\overline{6}}, \underline{1}\right) \subset \underline{\mathbf{351}}_S \\ H_A &\subset \left(\underline{\overline{3}}, \underline{3}, \underline{1}\right) + \left(\underline{\overline{3}}, \underline{\overline{6}}, \underline{1}\right) + \left(\underline{6}, \underline{3}, \underline{1}\right) \subset \underline{\mathbf{351}}_A \, . \end{aligned}$$

The Majorana mass term is generated by H_S [3] [9] while the Higgs multiplets H and H_A can generate only the Dirac structure. Note that it is not possible to get a Dirac mass term of $S = L_3^{\dot{3}}$ with $N = L_2^{\dot{3}}$, using a $\underline{\mathbf{27}}$ Higgs multiplet due to the antisymmetry in the SU(3) indices. However, all mass terms of the neutral leptons which are required for Dirac screening can be generated by the symmetric Higgs representation $\underline{\mathbf{351}}_S$. Indeed, the VEVs of $(H_S)^{\{23\}}_{\{\dot{2}\dot{3}\}}$ and $(H_S)^{\{33\}}_{\{\dot{2}\dot{3}\}}$ can be of order of the electroweak scale and of the $\mathrm{SU}(2)_R$ breaking scale, respectively. Furthermore, the Majorana mass of the additional singlets S can be generated by $(H_S)^{\{33\}}_{\{\dot{3}\dot{3}\}}$. However, a single $\underline{\mathbf{351}}_S$ leads to the same structure of M_{SS} and the Dirac mass matrices. An additional $\underline{\mathbf{351}}_S$ can lead to different structures.
The introduction of the antisymmetric $\underline{\mathbf{351}}_A$ Higgs representation is more promising, because otherwise it is difficult to explain why two $\underline{\mathbf{351}}_S$ couple differently. The antisymmetric $\underline{\mathbf{351}}_A$ Higgs multiplet generates all necessary Dirac matrices. It does not produce the Majorana masses of S which can be done using $\underline{\mathbf{351}}_S$ so that the structure of M_{SS} is different from that of all Dirac structures.
The following VEVs of the $\underline{\mathbf{351}}_A$ and $\underline{\mathbf{351}}_S$ components

$$\begin{aligned} \left\langle (H_A)^{\dot{1}}_1 \right\rangle &\simeq \mathcal{O}(\mathrm{SU}(2)_L \text{ breaking scale}) \\ \left\langle (H_A)^{\{33\}}_1 \right\rangle &\simeq \mathcal{O}(\mathrm{SU}(2)_R \text{ breaking scale}) \\ \left\langle (H_S)^{\{33\}}_{\{\dot{3}\dot{3}\}} \right\rangle \simeq \left\langle (H_A)^{\dot{3}}_3 \right\rangle &\simeq \mathcal{O}(\mathrm{SU}(3)_L \times \mathrm{SU}(3)_R \text{ breaking scale}) \end{aligned}$$

lead to the DS structure. Indeed, in the basis (ν, N, S, S', S'') the mass matrix

$$\begin{pmatrix} 0 & -Y_{351_A} \left\langle (H_A)^{\dot{1}}_1 \right\rangle & 0 & 0 & 0 \\ . & 0 & -Y_{351_A} \left\langle (H_A)^{\{33\}}_1 \right\rangle & 0 & 0 \\ . & . & Y_{351_S} \left\langle (H_S)^{\{33\}}_{\{\dot{3}\dot{3}\}} \right\rangle & Y_{351_A} \left\langle (H_A)^{\dot{1}}_1 \right\rangle & 0 \\ . & . & . & 0 & Y_{351_A} \left\langle (H_A)^{\dot{3}}_3 \right\rangle \\ . & . & . & . & 0 \end{pmatrix} \tag{4.13}$$

[2] Flavor indices are suppressed.

[3] The $\underline{\mathbf{27}}$ and $\underline{\mathbf{351}}_A$ cannot generate Majorana mass terms because the corresponding Yukawa interactions have to be antisymmetric in the SU(3) indices.

is generated with the required structure for ν, N and S. Moreover, there is a pseudo-Dirac particle formed by the additional singlets S' and S'' with a mass of the order of the $\mathrm{SU}(3)_L \times \mathrm{SU}(3)_R$ breaking scale.
Note that interactions with a $\underline{\mathbf{27}}$ Higgs multiplet can be used to generate sub-leading effects, correcting the masses of quarks and producing some deviation from complete screening if needed. Furthermore, VEVs of components contributing to the 1-3 and 2-2 block can only lead to entries which are at most of the order of the electroweak scale since they break $\mathrm{SU}(2)_L$.
Finally, we comment on a completely different possibility within SO(10). Since N and S are both SM singlets, they can be, in principle, exchanged. If S is part of $\underline{\mathbf{16}}$ and N is a singlet of SO(10), the required relation between the Yukawa couplings Eq. (4.2) is automatically reproduced. There is even a proportionality as needed by the Dirac screening mechanism in Eq. (4.5). The screening structure can be generated by the interactions

$$Y \underline{\mathbf{16}}\, \underline{\mathbf{1}}\, \underline{\overline{\mathbf{16}}} + Y_S\, \underline{\mathbf{16}}\, \underline{\mathbf{16}}\, \underline{\overline{\mathbf{126}}} + Y_q \underline{\mathbf{16}}\, \underline{\mathbf{16}}\, \underline{\mathbf{10}}\,, \tag{4.14}$$

if $\underline{\overline{\mathbf{16}}}$ obtains an electroweak VEV in the ν direction and a GUT scale VEV in the N direction, and $\underline{\overline{\mathbf{126}}}$ has a Planck scale VEV in the direction of the SU(5) singlet. The last term in Eq. (4.14) leads to Dirac masses of quarks and leptons and also to the Dirac mass term of ν and S. The mass matrix generated by Eq. (4.14) equals

$$\mathcal{M} = \begin{pmatrix} \sim 0 & Y^T \langle \underline{\overline{\mathbf{16}}} \rangle & Y_q^T \langle \underline{\mathbf{10}} \rangle \\ . & \sim 0 & Y^T \langle \underline{\overline{\mathbf{16}}} \rangle \\ . & . & Y_S \langle \underline{\overline{\mathbf{126}}} \rangle \end{pmatrix}. \tag{4.15}$$

The $\underline{\overline{\mathbf{126}}}$ Higgs multiplet can also contribute to the 1-1 and 2-2 blocks. However, now Y_ν and Y_{SN} are not related to the Dirac matrices of quarks, and the problem of cancellation does not exist from the beginning. Note, that there is also a strongly hierarchical LS contribution, but it is suppressed compared to the DS contribution.

4.5 Realization of Cancellation Mechanism with Flavor Symmetry

We explain a realization of the cancellation mechanism within SO(10) with a flavor symmetry. The SM fermions are unified with RH neutrinos N into three $\underline{\mathbf{16}}_i$-plets, $i = 1, 2, 3$. Furthermore, we consider three SO(10) singlet fermions S_i. In order to ensure that the gauge couplings are perturbative well above the GUT scale, we only choose low-dimensional Higgs representations: $H \sim \underline{\mathbf{10}}$, $\Delta \sim \underline{\overline{\mathbf{16}}}$ and $\underline{\mathbf{45}}$. The form of the uncharged fermion mass matrix is given in Eq. (3.17), whereas the zeros are due to the particle content, especially, since there is no $\underline{\overline{\mathbf{126}}}$-plet and we do not introduce non-renormalizable operators of the form $\underline{\mathbf{16}}_i\, \underline{\mathbf{16}}_j\, \Delta\, \Delta$ which is forbidden by symmetry. The coupling of H to the fermions generates the usual Dirac Yukawa couplings and Δ couples the singlets S_i and the $\underline{\mathbf{16}}$-plet. After the Higgs scalars acquire a VEV, they lead to mass matrices for the uncharged fermions. Since the top mass is of the electroweak scale and H also generates the up-type quark masses, $\langle H \rangle$ is of the order of the electroweak scale. The components of Δ can acquire two different VEVs, one SO(10)-breaking in the SU(5) singlet direction and the other in the direction of the electroweak doublet breaks the SM down to $\mathrm{SU}(3)_C \times \mathrm{U}(1)_{em}$. Therefore, we assume $\langle \Delta \rangle_N \sim \mathcal{O}(\Lambda_{\mathrm{GUT}})$ and $\langle \Delta \rangle_\nu \sim \mathcal{O}(\langle H \rangle)$.
In order to explain the number of three generations we assume the fermions $\underline{\mathbf{16}}$ to transform with respect to the flavor group G_F as representation $\underline{\mathbf{3}}$. Additionally, we choose the representation to be complex to forbid the coupling $\underline{\mathbf{16}}\, \underline{\mathbf{16}}\, H$. This excludes the discrete group A_4, since it has only a real three-dimensional representation.

In order to disentangle the gauge and the flavor sector, we assign all SO(10) Higgs fields to the trivial representation of G_F and introduce flavons which are additional scalar fields trivially transforming under the gauge group but non-trivially under G_F. The cancellation mechanism requires a relation between the VEVs of the different Higgs fields, which is not obviously achievable for the SO(10) Higgs multiplets H and Δ. However, it is easy to obtain this relation using flavons. Therefore, we require that the VEV relation is explained by flavon fields, which forces us to describe all fermion masses by non-renormalizable operators

$$\frac{\alpha_{fg}}{\Lambda}\underline{\mathbf{16}}_f\,\underline{\mathbf{16}}_g H\chi + \frac{\beta_{fg}}{\Lambda}S_f\,\underline{\mathbf{16}}_g\Delta\chi' + (M_{SS})_{fg}\,S_f S_g\,, \tag{4.16}$$

where χ and χ' are flavons. The VEV relation is achieved by $\chi' = \chi$ or $\chi' = \chi^*$. As all SM fermion masses originate from non-renormalizable operators $\underline{\mathbf{16}}\,\underline{\mathbf{16}}\,\underline{\mathbf{10}}\,\chi$, at least one coupling has to be large in order to explain the top mass. Hence the expansion parameter $\langle\chi\rangle/\Lambda$ is not small and multi-flavon insertions have to be taken into account.

The smallest [82] discrete groups which allow the realization of the cancellation mechanism are T_7 and $\Sigma(81)$ which have been discussed in high-energy physics literature for the first time by Luhn [213] and by Ma [214,215], respectively. In the following sections, the cancellation mechanisms is realized by these minimal groups. They explain the lowest order of fermion mixing, i.e. possibly lead to tri-bimaximal mixing in the lepton sector and no mixing in the quark sector. The hierarchy of up-type quark masses are explained only by the VEV hierarchy.

The required idea to cancel the hierarchy in the neutrino mass matrix in a unified context was first implemented by King and Malinsky [216,217] which considered the standard seesaw mechanism in a PS model and showed that a relation between different VEVs can in principle be to achieved in the flavon potential. Our model has the advantage that it can be implemented in SO(10) without introducing extra dimensions.

4.5.1 T_7 Realization

The group $T_7 \cong Z_7 \rtimes Z_3$ is of order 21 and it contains five irreducible representations which are denoted by $\underline{\mathbf{1_1}}$, $\underline{\mathbf{1_2}}$, $\underline{\mathbf{1_3}}$ and $\underline{\mathbf{3}}$, $\underline{\mathbf{3}}^\star$. The representations $\underline{\mathbf{1_2}}$ and $\underline{\mathbf{1_3}}$ as well as $\underline{\mathbf{3}}$ and $\underline{\mathbf{3}}^\star$ are complex conjugated to each other. It was discussed in [213] for the first time as a subgroup of $PSL(2,\mathbb{F}_7)$ which is a subgroup of SU(3). T_7 is also called Frobenius group. Its structure is similar to the previously introduced A_4. The main difference is, that T_7 has two complex three dimensional representations and not a real one like A_4. Indeed, it is the smallest non-Abelian discrete group with complex three dimensional representations. Therefore, the product $\underline{\mathbf{3}}\otimes\underline{\mathbf{3}}$ does not contain the trivial representation, but only three dimensional representations, i.e. an additional $\underline{\mathbf{3}}^*$ is needed to form an invariant. The character table, generators and Kronecker products are given in App. B.2.1. Due to its similarity to A_4, it can be used to generate tri-bimaximal mixing. In the following, we present a SUSY realization of the cancellation mechanism.

Lowest Order

As it has been pointed out above, the SM fermions $\underline{\mathbf{16}}_i$ are assigned to the three dimensional $\underline{\mathbf{3}}$ in order to explain the number of generations. The fermion masses are generated by the symmetric coupling to H which transforms trivially under T_7 and the flavon $\chi \sim \underline{\mathbf{3}}^\star$. The Kronecker product which is given in App. B.2.1 leads to a diagonal Dirac mass matrix where the hierarchy is determined by the VEVs of χ_i. The additional fermionic SO(10) singlets S_i are assigned to the representation $\underline{\mathbf{1_1}}\oplus\underline{\mathbf{1_2}}\oplus\underline{\mathbf{1_3}}$ which leads to a partial cancellation of the large mass hierarchy from the Dirac mass

Field	$\underline{\mathbf{16}}_i$	S_1	S_2	S_3	H	Δ	χ_i
$SO(10)$	$\underline{\mathbf{16}}$	$\underline{\mathbf{1}}$	$\underline{\mathbf{1}}$	$\underline{\mathbf{1}}$	$\underline{\mathbf{10}}$	$\underline{\overline{\mathbf{16}}}$	$\underline{\mathbf{1}}$
T_7	$\underline{\mathbf{3}}$	$\underline{\mathbf{1_1}}$	$\underline{\mathbf{1_2}}$	$\underline{\mathbf{1_3}}$	$\underline{\mathbf{1_1}}$	$\underline{\mathbf{1_1}}$	$\underline{\mathbf{3}}^\star$

Table 4.1: Minimal particle content in the SUSY T_7 model. $\underline{\mathbf{16}}_i$ and S_i are fermions, H and Δ are Higgs fields and χ_i are flavons.

matrix in the light effective neutrino mass matrix. The singlets S_i are coupled to the SM matter by Δ. This information is collected in Tab. 4.1. Hence, the resulting Yukawa couplings in the Lagrangian are

$$\begin{aligned}\mathcal{L}_Y = {} & \alpha\,(\underline{\mathbf{16}}_3\,H\,\underline{\mathbf{16}}_3\,\chi_1 + \underline{\mathbf{16}}_1\,H\,\underline{\mathbf{16}}_1\,\chi_2 + \underline{\mathbf{16}}_2\,H\,\underline{\mathbf{16}}_2\,\chi_3)/\Lambda \\ & + \beta_1\,\Delta\,S_1\,(\underline{\mathbf{16}}_1\,\chi_1 + \underline{\mathbf{16}}_2\,\chi_2 + \underline{\mathbf{16}}_3\,\chi_3)/\Lambda \\ & + \beta_2\,\Delta\,S_2\,(\underline{\mathbf{16}}_1\,\chi_1 + \omega\,\underline{\mathbf{16}}_2\,\chi_2 + \omega^2\,\underline{\mathbf{16}}_3\,\chi_3)/\Lambda \\ & + \beta_3\,\Delta\,S_3\,(\underline{\mathbf{16}}_1\,\chi_1 + \omega^2\,\underline{\mathbf{16}}_2\,\chi_2 + \omega\,\underline{\mathbf{16}}_3\,\chi_3)/\Lambda \\ & + A\,S_1\,S_1 + B\,(S_2\,S_3 + S_3\,S_2) + \text{h.c.}\end{aligned} \tag{4.17}$$

They generate the mass matrices matrices m_D, M_{SN} and M_{SS} of the form

$$\begin{aligned} m_D &= \frac{\alpha\,\langle H\rangle}{\Lambda}\begin{pmatrix}\langle\chi_2\rangle & 0 & 0\\ 0 & \langle\chi_3\rangle & 0\\ 0 & 0 & \langle\chi_1\rangle\end{pmatrix}, \\ M_{SN} &= \frac{\langle\Delta\rangle_N}{\Lambda}\begin{pmatrix}\beta_1\,\langle\chi_1\rangle & \beta_1\,\langle\chi_2\rangle & \beta_1\,\langle\chi_3\rangle\\ \beta_2\,\langle\chi_1\rangle & \omega\,\beta_2\,\langle\chi_2\rangle & \omega^2\,\beta_2\,\langle\chi_3\rangle\\ \beta_3\,\langle\chi_1\rangle & \omega^2\,\beta_3\,\langle\chi_2\rangle & \omega\,\beta_3\,\langle\chi_3\rangle\end{pmatrix} \\ &= \frac{\langle\Delta\rangle_N}{\Lambda}\begin{pmatrix}\beta_1 & 0 & 0\\ 0 & \beta_2 & 0\\ 0 & 0 & \beta_3\end{pmatrix}\begin{pmatrix}1 & 1 & 1\\ 1 & \omega & \omega^2\\ 1 & \omega^2 & \omega\end{pmatrix}\begin{pmatrix}\langle\chi_1\rangle & 0 & 0\\ 0 & \langle\chi_2\rangle & 0\\ 0 & 0 & \langle\chi_3\rangle\end{pmatrix}, \\ M_{SS} &= \begin{pmatrix}A & 0 & 0\\ 0 & 0 & B\\ 0 & B & 0\end{pmatrix}. \end{aligned} \tag{4.18}$$

Eq. (3.21) leads to the light effective neutrino mass matrix

$$m_\nu \approx \left(\frac{\alpha\,\langle H\rangle}{\langle\Delta\rangle_N}\right)^2 D_\chi\begin{pmatrix}\tilde{A}+2\tilde{B} & \tilde{A}-\tilde{B} & \tilde{A}-\tilde{B}\\ . & \tilde{A}+2\tilde{B} & \tilde{A}-\tilde{B}\\ . & . & \tilde{A}+2\tilde{B}\end{pmatrix} D_\chi, \tag{4.19}$$

where

$$D_\chi = \text{diag}\left(\frac{\langle\chi_2\rangle}{\langle\chi_1\rangle},\,\frac{\langle\chi_3\rangle}{\langle\chi_2\rangle},\,\frac{\langle\chi_1\rangle}{\langle\chi_3\rangle}\right), \quad \tilde{A} = \frac{A}{9\beta_1^2}, \quad \tilde{B} = \frac{B}{9\beta_2\beta_3}. \tag{4.20}$$

The VEVs $\langle\chi_i\rangle$ have to be chosen as

$$\frac{\langle\chi_2\rangle}{\langle\chi_1\rangle} \approx \epsilon^2, \qquad \frac{\langle\chi_3\rangle}{\langle\chi_1\rangle} \approx \epsilon \;\text{ with }\; \epsilon \approx 3\cdot 10^{-3} \tag{4.21}$$

in order to produce the up-type quark mass hierarchy. We outline a possibility to achieve this hierarchy. On the other hand, the large top quark mass requires that $\langle\chi_1\rangle$ is large, i.e. the ratio

$\frac{\langle\chi_1\rangle}{\Lambda} = \eta$ has to be of the order $\mathcal{O}(1)$. Hence Eq. (4.21) results in

$$m_\nu \approx \left(\frac{\alpha\,\langle H\rangle}{\langle\Delta\rangle_N\,\epsilon}\right)^2 \begin{pmatrix} (\tilde{A}+2\tilde{B})\,\epsilon^6 & (\tilde{A}-\tilde{B})\,\epsilon^3 & (\tilde{A}-\tilde{B})\,\epsilon^3 \\ . & \tilde{A}+2\tilde{B} & \tilde{A}-\tilde{B} \\ . & . & \tilde{A}+2\tilde{B} \end{pmatrix}. \tag{4.22}$$

Note the dominant 2-3 block, which leads to an (almost) maximal atmospheric mixing angle θ_{23}, unless $\tilde{A}$ and $\tilde{B}$ are equal. However, the elements in the first row and column are strongly suppressed and therefore the two other mixing angles are very small. Especially, the solar mixing angle has to be generated by additional contributions. The mass spectrum is normally ordered with an approximately vanishing m_1. For $3\,|\tilde{B}| < |2\tilde{A}+\tilde{B}|$ we find

$$m_2 = 3\left(\frac{\alpha\,\langle H\rangle}{\langle\Delta\rangle_N\,\epsilon}\right)^2 |\tilde{B}|\,, \qquad m_3 = \left(\frac{\alpha\,\langle H\rangle}{\langle\Delta\rangle_N\,\epsilon}\right)^2 |2\tilde{A}+\tilde{B}| \tag{4.23}$$

and therefore

$$\zeta \approx \frac{9\,|\tilde{B}|^2}{|2\tilde{A}+\tilde{B}|^2 - 9\,|\tilde{B}|^2}\,. \tag{4.24}$$

A small ζ is obtained by $|\tilde{B}| \ll |\tilde{A}|$. For a weak hierarchy in the additional singlet mass, i.e. $A \sim B$, a hierarchy in the couplings $\beta_1 \ll \beta_{2,3}$ fulfills this condition.
Otherwise in the case $|2\tilde{A}+\tilde{B}| < 3\,|\tilde{B}|$, the light neutrino masses are obtained by interchanging m_2 and m_3, which changes Δm^2_{21} and Δm^2_{32} accordingly. Hence the mixing angles θ_{12} and θ_{13} are also exchanged.
Note, the VEV hierarchy in the Dirac mass matrix enhances the neutrino mass $\epsilon^{-2} \approx \left(3\cdot 10^{-3}\right)^{-2} \approx 1.1\cdot 10^5$, as it can be seen in Eq. (4.22). Therefore, the bounds on the absolute neutrino mass scale $\mathcal{O}(\text{ eV}) \gtrsim m_\nu \sim \frac{\alpha^2\,\langle H\rangle^2\,\tilde{A}}{\langle\Delta\rangle_N^2}\frac{1}{\epsilon^2}$ requires a weaker or even an inverse hierarchy between the singlet masses (A,B) and $\langle\Delta\rangle_N$. Either $\langle\Delta\rangle_N$ is close to the Planck scale or the singlet masses (A,B) are of the order $\mathcal{O}(\Lambda_{\text{GUT}})$. The couplings β_i have to be as large as possible.
According to Sec. 3.1.2 a similar contribution enters the expression of the ratio of the LS over the DS contribution $\frac{\langle H\rangle}{\langle\Delta\rangle_\nu}\frac{\tilde{A},\tilde{B}}{\langle\Delta\rangle_N}$. Thus a suppression of the DS contribution leads to a relative enhancement of the LS contribution and the only way to suppress the LS vs the DS contribution is a small VEV ratio $\langle\Delta\rangle_\nu / \langle H\rangle \ll 10^{-2}$. In this minimal setup, the LS term is diagonal and cannot generate a solar mixing angle. However, the introduction of a second field Δ leads to a non-diagonal LS term.

Contributions from Higher-Dimensional Operators

As mentioned the large top quark mass requires the flavon VEV $\langle\chi_1\rangle$ to be of the order of $\mathcal{O}(\Lambda)$, i.e. $\eta = \langle\chi_1\rangle/\Lambda \sim \mathcal{O}(1)$. More precisely, we require $\eta \sim \mathcal{O}(\epsilon^{1/8}) \approx 0.48$. Therefore, a careful study of the higher-dimensional operators is indispensable, since they might destroy the leading order structure. It is necessary to consider at least all corrections up to order η^{17}, since the smallest element in the leading order contribution is of the order $\eta\epsilon^2 \sim \eta^{17}$. The group structure of T_7 allows to directly read off the transformation property of a given operator $O(\chi_i)$ from the transformation property with respect to the generator A. All relevant operators are presented in Tab. 4.2. Note, that the order of the operator in ϵ always has to be multiplied by η^n, where n denotes the number of flavons in the operator. Tab. B.8 in the appendix shows the relevant contributions at each order in n in the different representations. It can be derived from Tab. 4.2. All corrections from higher-dimensional operators to the mass matrices m_D, M_{SN} and M_{SS} are obtained by the help of these two tables. The higher-dimensional operators show a different structure compared to the

Structure	Transformation Properties under Generator A	Order in ϵ
χ_1^n	$\mathrm{e}^{-\frac{2\pi i}{7}n}\,\chi_1^n$	$\mathcal{O}(1)$
$\chi_1^{n-1}\,\chi_2$	$\mathrm{e}^{-\frac{2\pi i}{7}(n+1)}\,\chi_1^{n-1}\,\chi_2$	$\mathcal{O}(\epsilon^2)$
$\chi_1^{n-1}\,\chi_3$	$\mathrm{e}^{-\frac{2\pi i}{7}(n+3)}\,\chi_1^{n-1}\,\chi_3$	$\mathcal{O}(\epsilon)$
$\chi_1^{n-2}\,\chi_2\,\chi_3$	$\mathrm{e}^{-\frac{2\pi i}{7}(n+4)}\,\chi_1^{n-2}\,\chi_2\,\chi_3$	$\mathcal{O}(\epsilon^3)$
$\chi_1^{n-2}\,\chi_3^2$	$\mathrm{e}^{-\frac{2\pi i}{7}(n+6)}\,\chi_1^{n-2}\,\chi_3^2$	$\mathcal{O}(\epsilon^2)$
$\chi_1^{n-3}\,\chi_3^3$	$\mathrm{e}^{-\frac{2\pi i}{7}(n+9)}\,\chi_1^{n-3}\,\chi_3^3$	$\mathcal{O}(\epsilon^3)$

Table 4.2: List of products of χ_i which lead to contributions up to $\mathcal{O}(\epsilon^3)$ for $\langle\chi_1\rangle/\Lambda = \eta \sim \mathcal{O}(1)$, $\langle\chi_2\rangle/\langle\chi_1\rangle \approx \epsilon^2$ and $\langle\chi_3\rangle/\langle\chi_1\rangle \approx \epsilon^1$. Note that the factor η^n has to be included for the order n. The generator A uniquely determines the T_7-transformation properties of each operator.

Field	$\underline{\mathbf{16}}_i$	S_1	S_2	S_3	H	Δ	χ_i
T_7	$\underline{\mathbf{3}}$	$\underline{\mathbf{1}}_1$	$\underline{\mathbf{1}}_2$	$\underline{\mathbf{1}}_3$	$\underline{\mathbf{1}}_1$	$\underline{\mathbf{1}}_1$	$\underline{\mathbf{3}}^*$
Z_7	3	0	0	0	0	3	1

Table 4.3: The Z_7 charge assignment of all fields.

leading order one. Hence, they have to be properly constrained by an additional symmetry. An investigation of the different contributions reveals that an additional Z_7 symmetry is enough, since it forbids all higher-dimensional operators up to order η^7. The Z_7 charge assignment is presented in Tab. 4.3. Moreover, the covariants in Tab. 4.2 show a periodicity in seven because the phase factors are of the form $e^{\mathrm{i}2\pi n/7}$ with n being an integer and hence periodic in seven. The periodicity is due to the subgroup $Z_7 \subset T_7$. Then all non-vanishing matrix elements are corrected only by small contributions. However, vanishing matrix elements will be filled.

In the Dirac mass matrix, tiny off-diagonal elements of the order of $\mathcal{O}(\epsilon^3\eta^8)$ are generated. Thus quark mixing angles cannot be obtained in this way and have to be generated by higher-dimensional operators of the form $\underline{\mathbf{16}}_i\,\underline{\mathbf{16}}_j\,\underline{\mathbf{16}}\,\underline{\mathbf{16}}'\chi^n$ (See Sec. 3.2.1.) which contribute to the down quark as well as the charged lepton mass matrix. It is suppressed compared to the leading order by $\langle\underline{\mathbf{16}}\rangle_\nu\,/\,\langle H\rangle\,\langle\underline{\mathbf{16}}'\rangle_N\,/\Lambda$. The first row (and column) of the neutrino mass matrix also receives small corrections from higher-dimensional (Z_7 invariant) operators in the 1-2 and 1-3 elements of the order of $\mathcal{O}(\eta^7\epsilon^2)$. m_1 remains approximately massless and m_2 and m_3, as well as the atmospheric mixing angle receive corrections of $\mathcal{O}(\eta^7)$ relative to the leading order result. The corrections to the solar mixing angle and θ_{13} are of the order of $\mathcal{O}(\eta^7)$, which cannot account for a viable solar mixing angle.

In addition, RG corrections cannot generate a sizable solar mixing angle, since the neutrino masses show a strong normal hierarchy and the solar mixing angle is small. Even if we do not constrain the higher-dimensional operators by the additional Z_7 symmetry, but only require that we fine-tune some of the couplings such that the additional operators do not spoil the leading order result concerning the charged fermion mass hierarchy and the largeness of θ_{23} in the lepton sector, we cannot enhance the elements of the first row (and column) in the light neutrino mass matrix m_ν in order to generate a large solar mixing angle by higher dimensional operators. For this to see,

observe that the hierarchy is generated by m_D. Corrections to m_D which cancel the neutrino mass hierarchy are incompatible with the hierarchy in the quark mass spectrum. It can be checked that unitary rotations of m_D cannot generate a viable θ_{12} while preserving maximal atmospheric mixing. Therefore corrections to m_D do not lead to a viable phenomenology. Corrections to M_{SS} cannot change the hierarchy of the neutrino mass matrix as long as they are subdominant. By inversion of the DS formula, it can be shown, that M_{SS} has to be almost singular $(M_{SS})_{fg} \propto \beta_f \beta_g$ in order to fit the neutrino mass matrix. This results in a huge hierarchy of the singlet masses. Small corrections to M_{SN} cannot change the hierarchy in m_ν because it depends on the inverse of M_{SN}. A cancellation of order $\mathcal{O}(\epsilon^{3/2})$ between different contributions to the elements in the first column of M_{SN} weakens the large hierarchy in m_ν. It would require the coefficients of the next-to-leading order to be $\mathcal{O}(\eta^{-7})$ larger than the leading order. In summary, it is not possible to explain the solar mixing angle by the DS term alone and additional contributions are needed.

Contribution from the Linear Seesaw

Up to now, the LS term has been neglected. As the LS contribution coming from Δ alone is diagonal, we extend our setup by a second Δ which we denote $\Delta' \sim \overline{\underline{\mathbf{16}}}$. The additional Yukawa couplings are defined by

$$\begin{aligned}\mathcal{L}_{\Delta'} = &\beta_1' \, \Delta' \, S_1 \, (\underline{\mathbf{16}}_1 \, \chi_1 + \underline{\mathbf{16}}_2 \, \chi_2 + \underline{\mathbf{16}}_3 \, \chi_3)/\Lambda \\ &+ \beta_2' \, \Delta' \, S_2 \, (\underline{\mathbf{16}}_1 \, \chi_1 + \omega \, \underline{\mathbf{16}}_2 \, \chi_2 + \omega^2 \, \underline{\mathbf{16}}_3 \, \chi_3)/\Lambda \\ &+ \beta_3' \, \Delta' \, S_3 \, (\underline{\mathbf{16}}_1 \, \chi_1 + \omega^2 \, \underline{\mathbf{16}}_2 \, \chi_2 + \omega \, \underline{\mathbf{16}}_3 \, \chi_3)/\Lambda \, .\end{aligned} \tag{4.25}$$

Note, that it is always possible to find a linear combination of Δ and Δ' with a vanishing GUT scale VEV. Therefore we assume $\langle \Delta' \rangle_N = 0$ and the cancellation mechanism in the DS contribution is not affected. The leading order of the LS contribution is

$$m_\nu^{LS} = -\frac{\alpha \eta \, \langle H \rangle \, \langle \Delta' \rangle_\nu}{3 \epsilon \, \langle \Delta \rangle_N} \begin{pmatrix} 2 \left(3 \frac{\langle \Delta \rangle_\nu}{\langle \Delta' \rangle_\nu} + \sum\limits_{i=1}^{3} \tilde{\beta}_i \right) \epsilon^3 & \sum\limits_{i=1}^{3} \tilde{\beta}_i \omega^{1-i} & \sum\limits_{i=1}^{3} \tilde{\beta}_i \omega^{i-1} \\ . & \mathcal{O}(\epsilon^2) & \mathcal{O}(\epsilon) \\ . & . & \mathcal{O}(\epsilon) \end{pmatrix} , \tag{4.26}$$

where $\tilde{\beta}_i = \beta_i'/\beta_i$ and we assume $\langle \Delta \rangle_\nu \lesssim \langle \Delta' \rangle_\nu$ such that the main contribution is due to Δ'. In order to produce the solar mixing angle, the LS contribution has to be comparable to the DS contribution. The dominant terms of the neutrino mass matrix are

$$m_\nu \approx \left(\frac{\alpha \, \langle H \rangle}{\langle \Delta \rangle_N \, \epsilon} \right)^2 \begin{pmatrix} -2X \left(3 \frac{\langle \Delta \rangle_\nu}{\langle \Delta' \rangle_\nu} + \sum\limits_{i=1}^{3} \tilde{\beta}_i \right) \epsilon^3 & -X \sum\limits_{i=1}^{3} \tilde{\beta}_i \omega^{1-i} & -X \sum\limits_{i=1}^{3} \tilde{\beta}_i \omega^{i-1} \\ . & \tilde{A} + 2\tilde{B} & \tilde{A} - \tilde{B} \\ . & . & \tilde{A} + 2\tilde{B} \end{pmatrix} . \tag{4.27}$$

Hence, the remaining hierarchy is by an interplay between both contributions. The SO(10) Higgs VEVs can been adjusted such that

$$X = \frac{\langle \Delta \rangle_N \, \langle \Delta' \rangle_\nu \, \epsilon \eta}{3 \alpha \, \langle H \rangle} \tag{4.28}$$

leads to the correct hierarchy between the first row and the 2-3 block, i.e. the masses of the singlets S_i encoded in $\tilde{A}$, $\tilde{B}$ (See Eq. (4.20).) have to be smaller than $\langle \Delta \rangle_N$. The resulting mixing angles

are

$$\tan\theta_{12} \approx \frac{X|\tilde{\beta}_2 - \tilde{\beta}_3|}{\sqrt{6}\,|\tilde{B}|} \tag{4.29a}$$

$$\sin\theta_{13} \approx \frac{X|2\tilde{\beta}_1 - \tilde{\beta}_2 - \tilde{\beta}_3|}{\sqrt{2}\,|2\tilde{A} + \tilde{B}|} \tag{4.29b}$$

$$\theta_{23} \approx \frac{\pi}{4} \tag{4.29c}$$

under the assumptions that $|\tilde{B}| \ll |\tilde{A}|$ coming from the discussion of the lowest order and $X|\tilde{\beta}_i| \ll |\tilde{A}|$. Hence a large solar mixing angle and small θ_{13} can be accommodated. The masses are also corrected by the LS contribution, especially m_1 and m_2

$$m_1 \approx \left(\frac{\alpha\ \langle H\rangle}{\langle\Delta\rangle_N\ \epsilon}\right)^2 \left|3|\tilde{B}|\tan^2\theta_{12} - |2\tilde{A} + \tilde{B}|\sin^2\theta_{13}\right| \tag{4.30a}$$

$$m_2 \approx 3\left(\frac{\alpha\ \langle H\rangle}{\langle\Delta\rangle_N\ \epsilon}\right)^2 |\tilde{B}|\left|1 - \tan^2\theta_{12}\right| \tag{4.30b}$$

$$m_3 \approx \left(\frac{\alpha\ \langle H\rangle}{\langle\Delta\rangle_N\ \epsilon}\right)^2 |2\tilde{A} + \tilde{B}|\left|1 + \sin^2\theta_{13}\right| \tag{4.30c}$$

as well as the mass squared differences and their ratio ζ which are given by

$$\Delta m^2_{21} \approx \left(\frac{\alpha\ \langle H\rangle}{\langle\Delta\rangle_N\ \epsilon}\right)^4 9|\tilde{B}|^2(1 - 2\tan^2\theta_{12}) \tag{4.31a}$$

$$\Delta m^2_{32} \approx \left(\frac{\alpha\ \langle H\rangle}{\langle\Delta\rangle_N\ \epsilon}\right)^4 \left(|2\tilde{A} + \tilde{B}|^2 - 9|\tilde{B}|^2\left(1 - \tan^2\theta_{12}\right)^2\right) \tag{4.31b}$$

$$\zeta \approx \frac{1 - 2\tan^2\theta_{12}}{\left|\frac{2\tilde{A}+\tilde{B}}{3\tilde{B}}\right|^2 - 1 + 2\tan^2\theta_{12} - \tan^4\theta_{12}} \tag{4.31c}$$

in the limit of vanishing θ_{13}. This limit corresponds to a $\mu - \tau$ symmetric mass texture [48–51]. Hence, the LS term leads to large changes in the 1-2 sector, but mainly preserves the 2-3 sector. Thus maximal atmospheric mixing is still a prediction of the T_7 realization and the other mixing angles and masses can be fitted to the experimental data. Additionally, higher-dimensional operators to the LS term are controlled by the Z_7 symmetry, as it was discussed for the DS term.

Flavon Potential

The VEV hierarchy which is assumed in Eq. (4.21) has to be explained by the minimization of the flavon potential. As we assume that the SUSY breaking scale is much lower, we do not consider soft SUSY breaking terms. Additionally, since the SO(10) Higgs representations transform trivially under T_7 and the flavons trivially under SO(10), the flavons and SO(10) Higgs fields are disentangled up to RG corrections as well as the flavor-breaking scale Λ and the GUT scale Λ_{GUT} can be separated. Therefore, the flavon potential can be discussed separately. Firstly, we consider the renormalizable part of the flavon superpotential without any additional symmetry

$$W = \kappa\chi_1\chi_2\chi_3\ . \tag{4.32}$$

The F-terms of the flavon fields χ_i have to vanish which results in the set of equations

$$\frac{\partial W}{\partial \chi_1} = \kappa \chi_2 \chi_3 \ , \quad \text{and cyclic} \ . \tag{4.33}$$

Eq. (4.33) is solved if the VEVs of two of the three flavons vanish. Assuming $\langle \chi_1 \rangle \neq 0$ explains the leading order structure of the VEV hierarchy.
However, the phenomenology of the fermion mass matrices requires the introduction of an additional Z_7 symmetry to forbid dangerous contributions. We assume that the additional Z_7 symmetry also exists in the flavon potential. The renormalizable part of the superpotential is then forbidden and the lowest order is described by

$$W = \frac{a_1}{\Lambda^4} \left(\chi_1^7 + \chi_2^7 + \chi_3^7\right) + \frac{a_2}{\Lambda^4} \left(\chi_1^2 \chi_2^4 \chi_3 + \chi_1^4 \chi_2 \chi_3^2 + \chi_1 \chi_2^2 \chi_3^4\right) , \tag{4.34}$$

but these terms do not allow for the configuration $\langle \chi_1 \rangle \neq 0$ and $\langle \chi_{2,3} \rangle = 0$. Hence, we conclude that Z_7 should be broken in the flavon superpotential or there have to exist other fields apart from the flavons χ_i. One possibility to reconcile the VEV structure and the Z_7 symmetry is to introduce a driving field $\phi \sim (\underline{\mathbf{3}}^*, 5)$ analogous to [218] and an additional $\mathrm{U}(1)_R$ symmetry which is an extension of R-parity. The superpotential has charge +2, the driving field has charge +2, fermions have charge +1 and flavons and Higgs scalars are uncharged under $\mathrm{U}(1)_R$ symmetry. Hence, the driving field only appears linear in the superpotential and does not couple to fermions. The flavon superpotential is given by

$$W = \kappa \phi \chi^2 \ . \tag{4.35}$$

The F-term of the driving field ϕ leads to the same condition as Eq. (4.33) and, hence, is solved if the VEVs of two of the three flavons vanish.

4.5.2 Σ(81) Realization

The discrete group $\Sigma(81)$ is of order 81 and has nine one-dimensional representations $\underline{\mathbf{1_i}}$ and eight three-dimensional representations $\underline{\mathbf{3_i}}$. The first six of the three dimensional representations are faithful, i.e. all group elements are represented by distinct elements of the representation. Like in T_7 all representations besides the trivial one are complex. It has been firstly discussed in physics literature by Ma in [214, 215]. In contrast to T_7, $\Sigma(81)$ is not a subgroup of SU(3) but of U(3). Note, that the realization in the context of $\Sigma(81)$ has to be non-SUSY[4] because the Clebsch-Gordan coefficients in App. B.2.2 require the complex conjugated flavon field coupling to the SM matter $\underline{\mathbf{16}}_i$ in the coupling of the singlets S_i to $\underline{\mathbf{16}}_j$ in order to produce the magic matrix. It turns out that $\Sigma(81)$ leads to a complete cancellation of the mass hierarchy.

Lowest Order

Analogously to T_7, the three generations of fermions $\underline{\mathbf{16}}_i$ are assigned to a three-dimensional representation, more precisely to one of the six faithful representations. Without loss of generality we choose $\underline{\mathbf{3_1}}$. The flavon $\chi_i \sim \underline{\mathbf{3_2}}$, i.e. the complex conjugate representation of $\underline{\mathbf{3_1}}$ and the SO(10) Higgs fields H and Δ transform trivially under $\Sigma(81)$, which leads to a diagonal Dirac mass matrix. The three additional singlets S_i are assigned to three inequivalent singlets, $S_i \sim \underline{\mathbf{1_1}} \oplus \underline{\mathbf{1_2}} \oplus \underline{\mathbf{1_3}}$ like in T_7. The particle content is summarized in Tab. 4.4. It results in the same matrix structures of

[4] Due to this gauge coupling unification might not be maintained without additional fields.

Field	$\underline{\mathbf{16}}_i$	S_1	S_2	S_3	H	Δ	χ_i
$SO(10)$	$\underline{\mathbf{16}}$	$\underline{\mathbf{1}}$	$\underline{\mathbf{1}}$	$\underline{\mathbf{1}}$	$\underline{\mathbf{10}}$	$\underline{\overline{\mathbf{16}}}$	$\underline{\mathbf{1}}$
$\Sigma(81)$	$\underline{\mathbf{3_1}}$	$\underline{\mathbf{1_1}}$	$\underline{\mathbf{1_2}}$	$\underline{\mathbf{1_3}}$	$\underline{\mathbf{1_1}}$	$\underline{\mathbf{1_1}}$	$\underline{\mathbf{3_2}}$

Table 4.4: Particle assignment in $\Sigma(81)$ model. $\underline{\mathbf{16}}_i$ and S_i are fermions, H and Δ are Higgs fields and χ_i are flavons. Note that $\underline{\mathbf{3_2}}$ is equivalent to $\underline{\mathbf{3}}_\mathbf{1}^*$.

M_{SN} and M_{SS}, see Eq. (4.18). The Dirac mass matrix m_D, however, is of the form:

$$m_D = \frac{\alpha \langle H \rangle}{\Lambda} \begin{pmatrix} \langle \chi_1 \rangle^\star & 0 & 0 \\ 0 & \langle \chi_2 \rangle^\star & 0 \\ 0 & 0 & \langle \chi_3 \rangle^\star \end{pmatrix} , \tag{4.36}$$

i.e. the flavon VEVs are complex conjugated and permuted compared to Eq. (4.18). Like in T_7, the up-quark mass hierarchy is generated by the flavon VEVs

$$\frac{\langle \chi_1 \rangle}{\langle \chi_3 \rangle} \approx \epsilon^2, \quad \frac{\langle \chi_2 \rangle}{\langle \chi_3 \rangle} \approx \epsilon \;\text{ and }\; \eta = \frac{\langle \chi_3 \rangle}{\Lambda} \sim \mathcal{O}(1) \;\text{ with }\; \epsilon \approx 3 \cdot 10^{-3} . \tag{4.37}$$

The effective neutrino mass matrix is given by

$$m_\nu \approx \left(\frac{\alpha \langle H \rangle}{\langle \Delta \rangle_N} \right)^2 \begin{pmatrix} \tilde{A} + 2\tilde{B} & \tilde{A} - \tilde{B} & \tilde{A} - \tilde{B} \\ . & \tilde{A} + 2\tilde{B} & \tilde{A} - \tilde{B} \\ . & . & \tilde{A} + 2\tilde{B} \end{pmatrix} \tag{4.38}$$

(after a phase redefinition), where $\tilde{A}$ and $\tilde{B}$ are defined in Eq. (4.20). Note, the missing factors D_χ compared to the light neutrino mass matrix in the realization by T_7. Therefore, the hierarchy of the up-quark masses is completely erased in m_ν without any further assumptions on $\langle \chi_i \rangle$ or any of the couplings.
The masses obtained from Eq. (4.38) equal

$$m_1 = 3 \left| \frac{\alpha \langle H \rangle}{\langle \Delta \rangle_N} \right|^2 |\tilde{A}|, \quad m_2 = m_3 = 3 \left| \frac{\alpha \langle H \rangle}{\langle \Delta \rangle_N} \right|^2 |\tilde{B}| , \tag{4.39}$$

and the mass squared differences amount to

$$\Delta m_{21}^2 = 9 \left| \frac{\alpha \langle H \rangle}{\langle \Delta \rangle_N} \right|^4 (|\tilde{B}|^2 - |\tilde{A}|^2) , \qquad \Delta m_{32}^2 = 0 . \tag{4.40}$$

The result is unsatisfactory, since the atmospheric mass squared difference vanishes. A difference is generated by higher-dimensional corrections which is pointed out in the next section. Obviously, m_ν of Eq. (4.38) is diagonalized by the tri-bimaximal mixing matrix. Nevertheless the maximal atmospheric mixing angle is unphysical because of the degeneracy of m_2 and m_3. It is interesting to note that the matrix given in Eq. (4.38) is the most general one which is S_3 invariant [219].
Finally, we want to comment on the LS contribution, since it improved the phenomenology in the T_7 realization. In the minimal scenario, it is diagonal and mainly the 3-3 element of m_ν is changed. The introduction of Δ' dominantly results in corrections to the third row and column. Therefore, in both cases, it is not possible to generate a viable atmospheric mass squared difference while preserving maximal atmospheric mixing.

Order in ϵ	Operator Structure	No. of Operators
$\mathcal{O}(1)$	$\chi_3^m\,(\chi_3^\star)^{n-m}\ (m=0,...,n)$	$n+1$
$\mathcal{O}(\epsilon^2)$	$\chi_3^m\,(\chi_3^\star)^{n-1-m}\,\chi_1^{(\star)}\ (m=0,...,n-1)$	$2\,n$
$\mathcal{O}(\epsilon)$	$\chi_3^m\,(\chi_3^\star)^{n-1-m}\,\chi_2^{(\star)}\ (m=0,...,n-1)$	$2\,n$
$\mathcal{O}(\epsilon^3)$	$\chi_3^m\,(\chi_3^\star)^{n-2-m}\,\chi_1\,\chi_2\ (m=0,...,n-2)$ $\chi_3^m\,(\chi_3^\star)^{n-2-m}\,\chi_1^\star\,\chi_2\ (m=0,...,n-2)$ $\chi_3^m\,(\chi_3^\star)^{n-2-m}\,\chi_1\,\chi_2^\star\ (m=0,...,n-2)$ $\chi_3^m\,(\chi_3^\star)^{n-2-m}\,\chi_1^\star\,\chi_2^\star\ (m=0,...,n-2)$	$4\,(n-1)$
$\mathcal{O}(\epsilon^2)$	$\chi_3^m\,(\chi_3^\star)^{n-2-m}\,\chi_2^2\ (m=0,...,n-2)$ $\chi_3^m\,(\chi_3^\star)^{n-2-m}\,\chi_2\,\chi_2^\star\ (m=0,...,n-2)$ $\chi_3^m\,(\chi_3^\star)^{n-2-m}\,(\chi_2^\star)^2\ (m=0,...,n-2)$	$3\,(n-1)$
$\mathcal{O}(\epsilon^3)$	$\chi_3^m\,(\chi_3^\star)^{n-3-m}\,\chi_2^3\ (m=0,...,n-3)$ $\chi_3^m\,(\chi_3^\star)^{n-3-m}\,\chi_2^2\,\chi_2^\star\ (m=0,...,n-3)$ $\chi_3^m\,(\chi_3^\star)^{n-3-m}\,\chi_2\,(\chi_2^\star)^2\ (m=0,...,n-3)$ $\chi_3^m\,(\chi_3^\star)^{n-3-m}\,(\chi_2^\star)^3\ (m=0,...,n-3)$	$4\,(n-2)$

Table 4.5: List of products of χ_i and $\chi_i^\star$ which lead to contributions up to $\mathcal{O}(\epsilon^3)$. Note that for the order n the power η^n has to be taken into account. Since we have to deal with fields χ_i and their complex conjugates $\chi_i^\star$, the number of possible operators is increased compared to T_7 and depends on the order n.

Contributions from Higher-Dimensional Operators

Similarly to the realization with T_7, the large top quark mass requires to take into account higher-dimensional operators which are potentially dangerous. The necessary flavon VEV hierarchies are given in Eq. (4.37). We again assume $\eta \sim \mathcal{O}(\epsilon^{1/8}) \approx 0.48$. The number of different higher-dimensional operators is larger compared to the realization by T_7, since complex-conjugate fields are allowed in the operators because the realization is not supersymmetric. Therefore, the general structure of the higher-dimensional operators is given by $\chi_i^{n_1}\chi_j^{\star\,n_2}/\Lambda^n$ with $n_1+n_2=n$. As the smallest non-vanishing element at leading order is of the order of $\eta\epsilon^2$, at least all operators up to order η^{17} have to be considered. The relevant monomials in the fields χ_i and $\chi_i^\star$ are displayed in Tab. 4.5. Similarly to T_7, it is possible to determine the transformation properties of a given operator under $\Sigma(81)$ by its transformation properties with respect to the generators which is summarized in Tab. B.12. With the help of these tables, the corrections to each element of m_D, M_{SN} and M_{SS} can be derived. They are not corrected by arbitrary powers in ϵ but the corrections are at most of the equal power in ϵ than the leading order result for non-vanishing matrix elements. Vanishing ones are filled by higher-dimensional corrections. For m_D, they are less or equal to the elements on the corresponding elements on the diagonal which can be seen in Eq. (4.41). The vanishing elements in M_{SS} are filled by contributions of $\mathcal{O}(\eta^2)$ which can lead to a phenomenologically viable neutrino mass matrix.

Higher-dimensional operators lead to off-diagonal entries in the Yukawa couplings which can generate quark mixing angles. The dominant contributions are

$$m_D \sim \begin{pmatrix} \mathcal{O}(\epsilon^2\eta) & \mathcal{O}(\epsilon^3\eta^2) & \mathcal{O}(\epsilon^2\eta^2) \\ . & \mathcal{O}(\epsilon\eta) & \mathcal{O}(\epsilon\eta^2) \\ . & . & \mathcal{O}(\eta) \end{pmatrix} . \tag{4.41}$$

Although the generated quark mixing angles are larger compared to T_7

$$(\vartheta_{12},\, \vartheta_{13},\, \vartheta_{23}) \sim \big(\mathcal{O}(\epsilon^2\eta),\, \mathcal{O}(\epsilon^2\eta),\, \mathcal{O}(\epsilon\eta)\big) \tag{4.42}$$

but still too small. Therefore we also have to rely on higher-dimensional operators of the form $\underline{\mathbf{16}}_i\, \underline{\mathbf{16}}_j\, \underline{\mathbf{16}}\, \underline{\mathbf{16}}'\chi^n\chi^{\star\, m}$ as it was pointed out in Sec. 4.5.1.
In the following, we discuss the corrections of higher-dimensional operators to the neutrino mass matrix. Analytic formulas of the neutrino masses and leptonic mixing angles are difficult to obtain, because the neutrino mass matrix elements are all of the same order, if there are no further restrictions on the couplings. Therefore, we just note some aspects which can be seen easily and prove that a viable neutrino mass matrix can be obtained by a numerical example. The atmospheric mass squared difference Δm^2_{32} is of the order of η and does not depend on corrections coming from M_{SS}. Since the atmospheric mixing angle is (almost) maximal, $(m_\nu)_{23} \gg \delta m_{32} = (m_\nu)_{33} - (m_\nu)_{22}$. Therefore, $\tilde{A} - \tilde{B}$ has to be large compared to the corrections to $\left(\frac{\langle\Delta\rangle_N}{\alpha\,\langle H\rangle}\right)^2 \delta m_{32} \sim \mathcal{O}(\eta)$. As the smallness of the solar mass squared difference requires $|\tilde{A}| \sim |\tilde{B}|$ which can be seen in Eq. (4.40) the relative phase between $\tilde{A}$ and $\tilde{B}$ has to be around π to fulfill the phenomenological constraints. Hence

$$\tilde{B} = -\tilde{A} + \mathcal{O}(\eta^4)\ ,$$

can lead to the ratio of mass squared differences $\zeta \sim \mathcal{O}(\eta^3)$.
Let us present one numerical example, that demonstrates the possibility to fit the experimental data. The relevant mass matrices are

$$m_D = \begin{pmatrix} 1.1589\cdot 10^{-6} & 0 & 8.6454\cdot 10^{-7} \\ . & 1.0051\cdot 10^{-3} & 3.4268\cdot 10^{-4} \\ . & . & 0.63863 \end{pmatrix} \langle H_u\rangle\ , \tag{4.43}$$

$$M_{SN} = \begin{pmatrix} 7.4031\cdot 10^{-6} & 4.6288\cdot 10^{-6} & 3.2038\cdot 10^{-6} \\ 3.0486\cdot 10^{-3} & 1.9009\cdot 10^{-3}\,\omega & 1.4336\cdot 10^{-3}\,\omega^2 \\ 1.2503 & 0.91423\,\omega^2 & 0.71852\,\omega \end{pmatrix} \langle\Delta\rangle_N\ , \tag{4.44}$$

$$M_{SS} = \begin{pmatrix} 1 & 1.7689\cdot 10^{-2}\,\omega^2 & 3.8688\cdot 10^{-2}\,\omega \\ . & 1.1516\cdot 10^{-2}\,\omega & -0.7475 \\ . & . & 2.3890\cdot 10^{-2}\,\omega^2 \end{pmatrix} M_{Pl} \tag{4.45}$$

with $\langle\Delta\rangle_N = \Lambda_{\mathrm{GUT}}$, which result in the effective neutrino mass matrix

$$m_\nu \approx \begin{pmatrix} 1.1809\cdot e^{\mathrm{i}\,0.019} & 1.7675\cdot e^{\mathrm{i}\,3.12} & 1.5297\cdot e^{-\mathrm{i}\,3.08} \\ . & 2.5403\cdot e^{-\mathrm{i}\,0.031} & 3.4549\cdot e^{\mathrm{i}\,3.11} \\ . & . & 1.8254 \end{pmatrix} \cdot 10^{-2}\,\mathrm{eV}\ . \tag{4.46}$$

The 3σ bounds of the measured parameters [220] given in the standard parameterization [93]:

$$\Delta m^2_{21} = 7.9\,10^{-5}\,\mathrm{eV}^2\ ,\quad \Delta m^2_{32} = 2.5\,10^{-3}\,\mathrm{eV}^2\ ,\quad \theta_{12} = 33.0^\circ\ ,$$
$$\theta_{13} = 4.5^\circ\ ,\quad \theta_{23} = 49.5^\circ\ ,\quad \delta = 137^\circ\ ,\quad \varphi_1 = 313^\circ\ ,\quad \varphi_2 = 162^\circ$$

are fulfilled. This set of parameters is fully compatible with the experimental data and therefore it is possible to produce a phenomenologically viable neutrino mass matrix in this model by the inclusion of higher-dimensional operators. RG corrections are discussed in Sec. 5.3.5.

Flavon Potential

The renormalizable part of the flavon potential is given by

$$V_\chi(\chi_j) = M^2 \sum_i |\chi_i|^2 + \left[\kappa e^{\mathrm{i}\alpha} \sum_i \chi_i^3 + \text{h.c.}\right] + \lambda_1 \sum_i |\chi_i|^4 + \lambda_2 \sum_{i\neq j} |\chi_i|^2 |\chi_j|^2 \,, \tag{4.47}$$

where λ_i, κ and α are real coefficients. In order to analyze it, we parameterize χ_i in polar coordinates, i.e. $\chi_i = X_i e^{\mathrm{i}\xi_i}$. Then

$$V_\chi(X_j, \xi_j) = M^2 \sum_i X_i^2 + \lambda_1 \sum_i X_i^4 + \lambda_2 \sum_{i\neq k} X_i^2 X_k^2 + 2\kappa \sum_i X_i^3 \cos(\alpha + 3\xi_i) \,. \tag{4.48}$$

The extremization conditions for the VEVs $\langle X_1\rangle$ and $\langle \xi_1\rangle$ read

$$\frac{\partial V_\chi}{\partial X_1} = 2X_1 \left(M^2 + 2\lambda_1 X_1^2 + \lambda_2 X_2^2 + \lambda_2 X_3^2 + 3\kappa X_1 \cos(\alpha + 3\xi_1)\right) = 0 \tag{4.49a}$$

$$\frac{\partial V_\chi}{\partial \xi_1} = -6\kappa X_1^3 \sin(\alpha + 3\xi_1) = 0 \,. \tag{4.49b}$$

The corresponding equations for $\langle X_{2,3}\rangle$ and $\langle \xi_{2,3}\rangle$ are obtained by a cyclic permutation. Eq. (4.49b) is solved by either a vanishing VEV $\langle X_i\rangle$ or the relation $3\langle\xi_i\rangle + \alpha = n\pi,\ n \in \mathbb{Z}$ between the phase of $\langle\chi\rangle$ and the phase α of the cubic term.
Hence there is a solution which results in the required VEV configuration at leading order. If we set $\langle X_1\rangle = \langle X_2\rangle = 0$, $\langle X_3\rangle \neq 0$ and require that the extremum is actually a minimum of the potential, we will obtain the following solutions

$$\langle X_3\rangle = \frac{3\kappa + \sqrt{9\kappa^2 - 8M^2\lambda_1}}{4\lambda_1} \,, \quad \langle\xi_1\rangle = \langle\xi_2\rangle = 0 \,, \quad \langle\xi_3\rangle = -\frac{\alpha \pm \pi}{3} \tag{4.50}$$

together with the consistency condition $9\kappa^2 > 8M^2\lambda_1$.
Higher-dimensional operators modify this result. Here we systematically discuss their effect by using power counting in Λ^{-1}. In polar coordinates the D5 part of the flavon potential is given by

$$\begin{aligned} V_\chi^{(5)} = {} & \frac{2\,b_1}{\Lambda} \sum_i X_i^5 \cos(\beta_1 + 3\xi_i) \\ & + \frac{2}{\Lambda}\left(b_2 X_1^3 X_2^2 \cos(\beta_2 + 3\xi_1) + b_3 X_1^3 X_3^2 \cos(\beta_3 + 3\xi_1) + \text{cyclic}\right) \,, \end{aligned} \tag{4.51}$$

where b_i and β_i are real coefficients. $\langle X_1\rangle$ and $\langle X_2\rangle$ still vanish. There are only corrections to $\langle X_3\rangle$ and $\langle\xi_3\rangle$ of the order $\mathcal{O}(\Lambda^{-1})$. More generally, this holds at higher orders in Λ^{-1} too, since the leading order in Λ^{-1} of Eq. (4.49a) is proportional to $\langle X_1\rangle$ or $\langle X_2\rangle$, respectively

$$\frac{\partial V_\chi}{\partial X_1} \stackrel{\text{LO}}{=} \left(2M^2 + 2\lambda_2 X_3^2\right) X_1 = 0 \,, \tag{4.52}$$

which forces $\langle X_1\rangle$ and $\langle X_2\rangle$ to vanish in order to ensure the vanishing of $\frac{\partial V}{\partial X_{1,2}}$.
Concluding, the leading order structure of the VEVs can be explained. Additional flavon fields have to be introduced to generate non-vanishing VEVs for $\langle X_{2,3}\rangle$.

Chapter 5

Threshold Corrections

In this chapter, we discuss threshold corrections in the standard seesaw framework and its extension, the cascade seesaw model. In Sec. 5.1, the RG effect between thresholds in the standard seesaw framework is studied. The result is applied to the cascade seesaw mechanism in Sec. 5.2. The stability of the cancellation mechanism with respect to the RG is investigated in Sec. 5.3 using the results from Sec. 5.2.

5.1 Thresholds in the Standard (Type I) Seesaw Model

In this section we will consider effects of the radiative corrections [60, 61, 221, 222] in the standard seesaw model with non-degenerate RH neutrino masses. Our main goal is to understand the corrections between the mass thresholds of the RH neutrinos, since the dominant RG effect is due to this region for non-degenerate mass thresholds.
Here we will consider the RG effects below a certain scale Λ:

$$M_i \ll \Lambda, \tag{5.1}$$

where M_i are the masses of RH neutrinos (See Fig. 2.1.).
Let us stress that the mass spectrum of the RH neutrinos can be strongly hierarchical. Therefore effects of the RG running between different mass thresholds are crucial [9, 62, 63, 69, 223]. We introduce the effective operator $\overset{(n)}{O}_M$ which generates neutrino masses in the basis (ν, N)

$$\mathscr{L} = -(\nu^T, N^T)\, \overset{(n)}{O}_M\, (\nu^T, N^T)^T\, . \tag{5.2}$$

The superscript (n) designates the number of RH neutrinos which are not decoupled at a given energy scale, that is, RH neutrinos in the effective theory. This superscript will denote also a range of RG running with a given number of RH neutrinos. In addition, we use the notation $\overset{(n-m)}{Z} \equiv \overset{(n)}{Z}\overset{(n+1)}{Z} \cdots \overset{(m-1)}{Z}\overset{(m)}{Z}$.
Below the scale Λ the effective operator $\overset{(3)}{O}_M$ can be written as

$$\overset{(3)}{O}_M\,(\Lambda) = \begin{pmatrix} 0 & \overset{(3)}{Y}{}_\nu^T\, H_u \\ \overset{(3)}{Y}_\nu\, H_u & \overset{(3)}{M}_{NN} \end{pmatrix} \tag{5.3}$$

where $\overset{(3)}{M}_{NN}$ is the RH neutrino mass matrix $M_{NN}(\Lambda)$ and $\overset{(3)}{Y}_\nu$ is the neutrino Yukawa coupling matrix $Y_\nu(\Lambda)$ at the scale Λ.

The effect of the RG evolution can be split in effects coming from the renormalization of the wave functions and the vertex corrections. It turns out, that the RG corrections can be factorized in the LL approximation. So, in general, the renormalization of Y_ν, M_{NN} and κ is given by

$$Y_\nu \xrightarrow{\text{RG}} Z_N^T Y_\nu Z_{\text{ext}} \tag{5.4a}$$

$$M_{NN} \xrightarrow{\text{RG}} Z_N^T M_{NN} Z_N \tag{5.4b}$$

$$\kappa \xrightarrow{\text{RG}} Z_{\text{ext}}^T \kappa Z_{\text{ext}} Z_\kappa \ . \tag{5.4c}$$

Here Z_{ext} combines the renormalization effect of the left-handed doublets ℓ, the Higgs doublet H_u, and the vertex correction to Y_ν. Z_N denotes the wave function renormalization effect of the RH neutrinos N. In order to simplify the presentation, we define the wave function renormalization so that the usual powers of $1/2$ are absent. Eq. (5.4c) describes the renormalization of the effective D5 operator which appears after decoupling (integration out) of the corresponding RH neutrino. Apart from renormalization of the wave functions and vertices which exist in the SM model this operator has additional vertex corrections given by the diagrams in Fig. 5.1. The RG effect due to these diagrams denoted by $\overset{(n)}{Z}_\kappa$ plays a crucial role in the discussion of the stability of the cancellation mechanism[1]. These D5 operator corrections are absent in the SUSY version of theory due to the non-renormalization theorem [224, 225].

(a) Higgs self-coupling (b) Gauge interactions

Figure 5.1: The D5 operator vertex corrections. Shown are additional divergent diagrams in the effective theory.

The RG evolution of the charged leptons can be treated separately. As they are integrated out below the electroweak scale, we do not have to consider thresholds and their RG evolution from Λ down to the electroweak scale is simply obtained by integrating the β-function which is given in Sec. 6.1. However, as it has been mentioned in Sec. 6.1, the main RG effect on the MNS matrix is due to neutrinos because of their weak mass hierarchy. Therefore, in the following discussion, we work in the flavor basis and concentrate on the neutrino mass matrix.

We describe the RG effects in the effective theory, where the heavy RH neutrinos are decoupled successively[2] [9,62,63,69,223] as depicted in Fig. 2.1. In each step (interval between mass thresholds) we first calculate the RG correction to the matrices. We diagonalize the resulting matrices at the lower end of the interval, *i.e.*, at $\mu = M_i$ and then decouple N_i, $(i = 3, 2, 1)$. We will denote the

[1] As the additional corrections are flavor blind, these factors are ordinary numbers.

[2] The running between mass thresholds of RH neutrinos has been treated analytically in the approximation of strongly hierarchical and diagonal Yukawa matrix [9]. Here we present a general consideration required for our approach.

renormalization factors in the LL approximation by $\overset{(n)}{Z} = 1 + \overset{(n)}{\delta Z}$. This notation is also used for the parameters of the effective theory. The renormalization factors in the extended (by RH neutrinos) SM and the MSSM are given in App. C.2.
Let us describe the main steps of the renormalization procedure.

1. The RG evolution between Λ and M_3 yields the operator $\overset{(3)}{O}_M$ at M_3

$$\overset{(3)}{O}_M\,(M_3) = \begin{pmatrix} 0 & \overset{(3)}{Z}{}^T_{\rm ext}\overset{(3)}{Y}{}^T_\nu\, H_u\, \overset{(3)}{Z}_N \\ . & \overset{(3)}{Z}{}^T_N \overset{(3)}{M}_{NN} \overset{(3)}{Z}_N \end{pmatrix} . \tag{5.5}$$

   Performing a rotation of the RH neutrinos $N = \overset{(3)}{U}_N\, N'$ we reduce the renormalized RH neutrino mass matrix to the form

$$\overset{(3)}{U}{}^T_N \overset{(3)}{Z}{}^T_N \overset{(3)}{M}_{NN} \overset{(3)}{Z}_N \overset{(3)}{U}_N = \begin{pmatrix} \overset{(2)}{M}_{NN} & 0 \\ 0 & M_3 \end{pmatrix} , \tag{5.6}$$

   where $\overset{(2)}{M}_{NN}$ is a 2×2 (in general non-diagonal) mass matrix. Let us split the 3×3 Dirac type Yukawa coupling matrix in Eq. (5.5) after this rotation into two parts as

$$\overset{(3)}{Z}{}^T_{\rm ext}\overset{(3)}{Y}{}^T_\nu \overset{(3)}{Z}_N \overset{(3)}{U}_N \equiv \begin{pmatrix} \overset{(2)}{Y}{}^T_\nu, & y_3^T \end{pmatrix} , \tag{5.7}$$

   where y_3 is the 3rd row of the Yukawa couplings matrix, i.e. the couplings between ν_i and N_3, and $\overset{(2)}{Y}_\nu$ is the remaining 3×2 submatrix. Then in the rotated basis the operator Eq. (5.5) can be written as

$$\overset{(3)}{O}_M\,(M_3) = \begin{pmatrix} 0 & \overset{(2)}{Y}{}^T_\nu\, H_u & y_3^T H_u \\ . & \overset{(2)}{M}_{NN} & 0 \\ & 0 & M_3 \end{pmatrix} . \tag{5.8}$$

   Below the scale M_3 the neutrino N_3 is integrated out and from Eq. (5.8) we obtain

$$\overset{(2)}{O}_M\,(M_3) = \begin{pmatrix} -y_3^T M_3^{-1} y_3 H_u^2 & \overset{(2)}{Y}{}^T_\nu\, H_u \\ . & \overset{(2)}{M}_{NN} \end{pmatrix} . \tag{5.9}$$

   Notice that the D5 operator is formed in the 1-1 block due to the decoupling of N_3.

2. The discussion of the RG running is analogous in the interval $M_2 - M_3$. We can write the operator O_M at the scale M_2 (threshold of N_2) as

$$\overset{(2)}{O}_M\,(M_2) = \begin{pmatrix} -\overset{(2)}{Z}{}^T_{\rm ext}\overset{(2)}{Z}_\kappa\, y_3^T M_3^{-1} y_3 H_u^2\, \overset{(2)}{Z}_{\rm ext} & \overset{(2)}{Z}{}^T_{\rm ext}\overset{(2)}{Y}{}^T_\nu\, H_u\, \overset{(2)}{Z}_N \\ . & \overset{(2)}{Z}{}^T_N \overset{(2)}{M} \overset{(2)}{Z}_N \end{pmatrix} . \tag{5.10}$$

Here we have included the corrections $\overset{(2)}{Z}_\kappa$ to the D5 operator.

By applying the rotation $N' = \overset{(2)}{U}_N N''$ the renormalized mass matrix of the RH neutrinos is diagonalized:

$$\overset{(2)}{U}{}_N^T \overset{(2)}{Z}{}_N^T \overset{(2)}{M} \overset{(2)}{Z}_N \overset{(2)}{U}_N \equiv \begin{pmatrix} \overset{(1)}{M}_{NN} & 0 \\ 0 & M_2 \end{pmatrix}. \tag{5.11}$$

The renormalized Yukawa matrix is then split as

$$\overset{(2)}{Z}{}_{\rm ext}^T \overset{(2)}{Y}{}_\nu^T \overset{(2)}{Z}_N \overset{(2)}{U}_N \equiv \begin{pmatrix} \overset{(1)}{Y}{}_\nu^T, & y_2^T \end{pmatrix}, \tag{5.12}$$

where $\overset{(1)}{Y}_\nu$ and y_2 are two component rows. Decoupling the second neutrino N_2 we obtain

$$\overset{(1)}{O}_M(M_2) = \begin{pmatrix} -\overset{(2)}{Z}{}_{\rm ext}^T \overset{(2)}{Z}_\kappa\, y_3^T M_3^{-1} y_3 H_u^2 & \overset{(2)}{Z}_{\rm ext} & -y_2^T M_2^{-1} y_2 H_u^2 & \overset{(1)}{Y}{}_\nu^T H_u \\ & . & & \overset{(1)}{M}_{NN} \end{pmatrix}. \tag{5.13}$$

3. Running the matrix down to the lowest seesaw scale M_1 and integrating out N_1 yields

$$\begin{aligned} \overset{(0)}{O}_M(M_1) = &- \overset{(1-2)}{Z}{}_{\rm ext}^T \overset{(1-2)}{Z}_\kappa\, y_3^T M_3^{-1} y_3 H_u^2 \overset{(1-2)}{Z}_{\rm ext} \\ &- \overset{(1)}{Z}{}_{\rm ext}^T \left[\overset{(1)}{Z}_\kappa\, y_2^T M_2^{-1} y_2 + \overset{(1)}{Y}{}_\nu^T \overset{(1)}{M}{}_{NN}^{-1} \overset{(1)}{Y}_\nu \right] H_u^2 \overset{(1)}{Z}_{\rm ext} \ . \end{aligned} \tag{5.14}$$

4. Finally, evolving $\overset{(0)}{O}_M(M_1)$ down to the EW scale, we obtain (after H_u develops a VEV) the mass matrix of the light neutrinos

$$m_\nu = -\langle H_u \rangle^2 \overset{(0-3)}{Z}{}_{\rm ext}^T \overset{(3)}{Y}{}_\nu^T \overset{(3)}{Z}_N \overset{(3)}{U}_N \begin{pmatrix} K_{12} & 0 \\ 0 & \frac{\overset{(0-2)}{Z}_\kappa}{M_3} \end{pmatrix} \overset{(3)}{U}{}_N^T \overset{(3)}{Z}{}_N^T \overset{(3)}{Y}_\nu \overset{(0-3)}{Z}_{\rm ext} \ , \tag{5.15}$$

with

$$K_{12} \equiv \overset{(2)}{Z}_N \overset{(2)}{U}_N \begin{pmatrix} \frac{\overset{(0)}{Z}_\kappa}{\overset{(1)}{M}_{NN}} & 0 \\ 0 & \frac{\overset{(0-1)}{Z}_\kappa}{M_2} \end{pmatrix} \overset{(2)}{U}{}_N^T \overset{(2)}{Z}{}_N^T \ . \tag{5.16}$$

This expression can be presented in a simpler and more transparent way. Using the definitions of the matrices $\overset{(2)}{U}_N$ and $\overset{(3)}{U}_N$ in Eqs. (5.11, 5.6) we can rewrite m_ν as

$$m_\nu = -\langle H_u \rangle^2 Z_{\rm ext}^T \left[\overset{(3)}{Y}{}_\nu^T X_N \overset{(3)}{M}{}_{NN}^{-1} \overset{(3)}{Y}_\nu \right] Z_{\rm ext} \ , \tag{5.17}$$

where

$$X_N \equiv \overset{(3)}{Z}_N \overset{(3)}{U}_N \overset{(2)}{Z'}_N \overset{(2)}{U'}_N \; Z_\kappa \; \overset{(2)}{U'^{\dagger}_N} \overset{(2)}{Z'^{-1}_N} \overset{(3)}{U^{\dagger}_N} \overset{(3)}{Z^{-1}_N} \tag{5.18}$$

describes the RG effects due to the running between the thresholds. Here

$$\overset{(2)}{Z'_N} \equiv \begin{pmatrix} \overset{(2)}{Z_N} & 0 \\ 0 & 1 \end{pmatrix}, \quad \overset{(2)}{U'_N} \equiv \begin{pmatrix} \overset{(2)}{U_N} & 0 \\ 0 & 1 \end{pmatrix}, \tag{5.19}$$

and

$$Z_\kappa \equiv \mathrm{diag} \begin{pmatrix} \overset{(0)}{Z_\kappa}, & \overset{(0-1)}{Z_\kappa}, & \overset{(0-2)}{Z_\kappa} \end{pmatrix} \tag{5.20}$$

is the matrix of the effective D5 operator corrections (Fig. 5.1). Note, that

$$X_N \; \overset{(3)}{M^{-1}_{NN}} = \overset{(3)}{M^{-1}_{NN}} \; X^T_N \tag{5.21}$$

which can be seen in two different ways, either by looking at the step from Eq. (5.15) to Eq. (5.17) or simply by the property that the effective neutrino mass matrix is symmetric which cannot be changed by the RG evolution.

5.1.1 Effects of Vertex Corrections

In order to study D5 operator corrections in the (non-SUSY) SM in more details we introduce the matrix V_N which diagonalizes the RH neutrino mass matrix at Λ:

$$V^T_N \; \overset{(3)}{M_{NN}} \; V_N = D_N \equiv \mathrm{diag}(M_1, M_2, M_3). \tag{5.22}$$

In the lowest order approximation: $\overset{(2)}{Z_N} = \overset{(3)}{Z_N} = 1$, and according to Eq. (5.6) and Eq. (5.11) we obtain

$$V_N = \overset{(3)}{U_N} \overset{(2)}{U'_N} \, . \tag{5.23}$$

Therefore the matrix X_N Eq. (5.18) can be rewritten in the form

$$X_N = V_N Z_\kappa V^{\dagger}_N = I + V_N \delta Z_\kappa V^{\dagger}_N, \tag{5.24}$$

where

$$\delta Z_\kappa \equiv Z_\kappa - I. \tag{5.25}$$

Plugging this expression in for X_N in Eq. (5.17) we find

$$\begin{aligned} m_\nu &\approx - \langle H_u \rangle^2 \, Z^T_{\mathrm{ext}} \left[\overset{(3)}{Y^T_\nu} \; V_N Z_\kappa D^{-1}_N V^T_N \; \overset{(3)}{Y_\nu} \right] Z_{\mathrm{ext}} \\ &= - \langle H_u \rangle^2 \, Z^T_{\mathrm{ext}} \left[\overset{(3)}{Y^T_\nu} \left(M^{-1}_{NN} + V_N \delta Z_\kappa D^{-1}_N V^T_N \right) \overset{(3)}{Y_\nu} \right] Z_{\mathrm{ext}} \\ &= - \langle H_u \rangle^2 \, Z^T_{\mathrm{ext}} \left[\overset{(3)}{Y^T_\nu} \; M'^{-1}_{NN} \; \overset{(3)}{Y_\nu} \right] Z_{\mathrm{ext}} \end{aligned} \tag{5.26}$$

where

$$M'_{NN} \equiv V_N^* \mathrm{diag}\left(M_1 \overset{(0)}{Z_\kappa^{-1}}, M_2 \overset{(0-1)}{Z_\kappa^{-1}}, M_3 \overset{(0-2)}{Z_\kappa^{-1}}\right) V_N^\dagger \,. \tag{5.27}$$

According to this expression the effects of the D5 operator corrections are reduced to renormalization of the (running) masses of the RH neutrinos (at the largest RH neutrino mass).

5.1.2 Generalizations

This result can be easily generalized in two different ways.

More RH neutrinos

Eq. (5.17) depends only implicitly on the number of RH neutrinos. Therefore, we can easily generalize our results to the case of an arbitrary number n of RH neutrinos. The effective neutrino mass matrix becomes

$$m_\nu = -\langle H_u \rangle^2 Z_{\mathrm{ext}}^T \left[\overset{(n)}{Y_\nu^T} X_N \overset{(n)}{M_{NN}^{-1}} \overset{(n)}{Y_\nu}\right] Z_{\mathrm{ext}} \,. \tag{5.28}$$

The RG effect between the thresholds is summarized in

$$X_N \equiv \left(\prod_{i=2}^{n} \overset{(i)}{Z'_N} \overset{(i)}{U'_N}\right) Z_\kappa \left(\prod_{i=2}^{n} \overset{(i)}{U'^\dagger_N} \overset{(i)}{Z'^{-1}_N}\right) \,, \tag{5.29}$$

where

$$\overset{(i)}{Z'_N} \equiv \begin{pmatrix} \overset{(i)}{Z_N} & 0 \\ 0 & \mathbb{1}_{n-i} \end{pmatrix}, \quad \overset{(i)}{U'_N} \equiv \begin{pmatrix} \overset{(i)}{U_N} & 0 \\ 0 & \mathbb{1}_{n-i} \end{pmatrix}, \tag{5.30}$$

and

$$Z_\kappa \equiv \mathrm{diag}\left(\overset{(0)}{Z_\kappa}, \overset{(0-1)}{Z_\kappa}, \ldots, \overset{(0-(n-1))}{Z_\kappa}\right) \,. \tag{5.31}$$

Hence, the main result still holds and the RG evolution between the seesaw scales leads at the leading order to a rescaling of the RH neutrino masses which can be seen in

$$m_\nu \approx -\langle H_u \rangle^2 Z_{\mathrm{ext}}^T \left[\overset{(n)}{Y_\nu^T} V_N Z_\kappa D_N^{-1} V_N^T \overset{(n)}{Y_\nu}\right] Z_{\mathrm{ext}} \,, \tag{5.32}$$

where

$$V_N^T \overset{(n)}{M_N} V_N = D_N \equiv \mathrm{diag}(M_1, M_2, \ldots, M_n). \tag{5.33}$$

Beyond LL Approximation

Beyond the LL approximation, the calculation becomes more involved. There are several difficulties:

- The renormalization factors do not commute any longer like they do in the LL approximation.
- The effective D5 neutrino mass operator receives additional non-diagonal corrections. Thus κ has to be renormalized additively by

$$\kappa \xrightarrow{\mathrm{RG}} Z_L^T \left[\kappa + \delta\kappa\right] Z_L Z_\phi^2 \,, \tag{5.34}$$

because the renormalization cannot be factorized (See Fig. 5.2(a).) due to diagrams like in Fig. 5.2(b). As these two loop contributions are of the order of $\frac{y_\tau^4}{(4\pi)^4}$, they are about four orders of magnitude smaller than the one loop contributions and can be neglected in a first approximation.

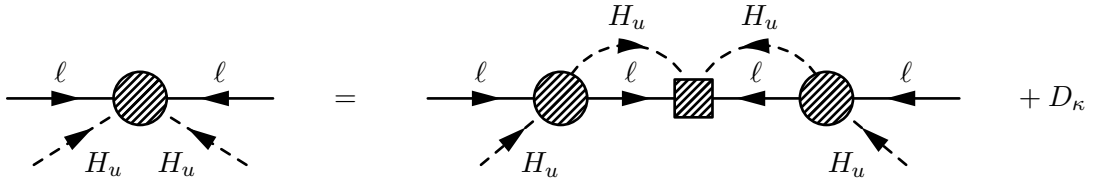

(a) The vertex corrections to the effective neutrino mass matrix do not factorize. There are additional non–factorizable divergent diagrams D_κ which emerge in the effective theory and correspond to a UV finite diagram in the full theory.

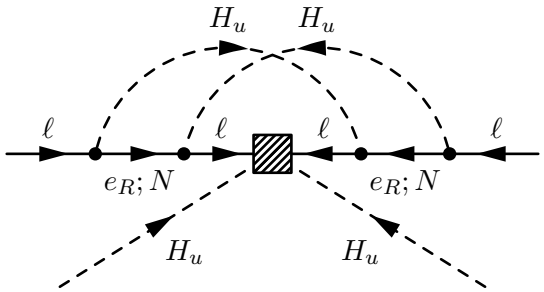

(b) Example of a two loop diagram which destroys the factorization of the vertex corrections to the effective neutrino mass matrix.

Figure 5.2: Renormalization of the effective neutrino mass operator.

- Finally, finite threshold corrections have to be taken into account, because the threshold effects to n loop order are of the same order as the RG effects to $n+1$ loop order. They factorize like the renormalization effects, since they emerge from the same diagrams. These effects might also destroy the structure, as the effective neutrino mass operator receives an additional contribution compared to $-Y_\nu^T M_{NN}^{-1} Y_\nu$.

However, the form of the renormalization of Y_ν and M_{NN} remains the same. The vertex correction to Y_ν factorizes to all orders because N is a singlet and the only coupling of N to other particles is the neutrino Yukawa coupling as it is shown in Fig. 5.3(b). Furthermore, there are no vertex corrections to the mass of chiral fields to all orders due to chirality. Especially, there are no vertex corrections to the mass of the RH neutrinos. Fig. 5.3(a) shows the general wave function renormalization of a chiral field N. For definiteness, we choose a RH field. The blob has a certain γ–structure Γ which can be expanded in a basis of the γ–algebra

$$\Gamma = a^L P_L + a^R P_R + b_\mu^L P_L \gamma^\mu + b_\mu^R P_R \gamma^\mu + c_{\mu\nu}\sigma^{\mu\nu} \ . \tag{5.35}$$

The chirality of the field N ensures that the correction is proportional to $P_L \Gamma P_R = b_\mu^L \gamma^\mu P_R$. Hence, there is no vertex correction to the mass.
Concluding, the simple formulas which have been derived do not hold beyond LL approximation in the SM. In the MSSM, however, the formula can be easily generalized up to arbitrary loop order, because the only obstacle is the non–commutativity of the wave function renormalization factors.

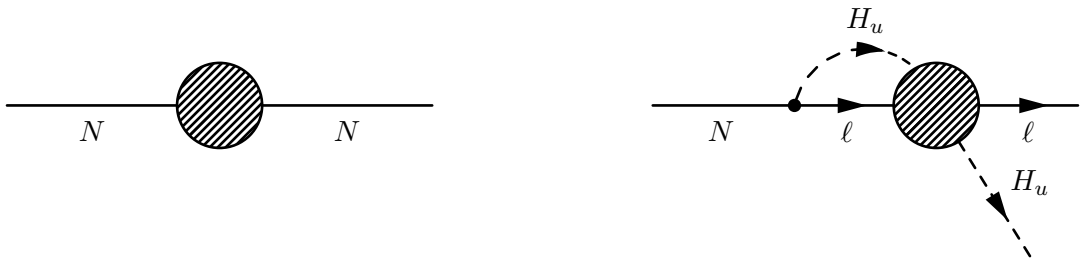

(a) The renormalization of a chiral field.

(b) The vertex corrections to the neutrino Yukawa couplings factorize.

Figure 5.3: Vertex Renormalization.

Generally, the result also holds for the decoupling of other heavy particles if the following three conditions are fulfilled:

- its mass term does not receive vertex corrections;
- the vertex corrections of its couplings to light particles factorize in the way shown in Fig. 5.3(a);
- vertex corrections to the effective operator κ are scalars or more precisely can be factorized in the form $Z_\kappa^{T\,1/2}\kappa Z_\kappa^{1/2}$.

5.2 Thresholds in the Cascade Seesaw

The renormalization of the cascade seesaw mechanism is similar to the standard seesaw mechanism, since it can be understood as a successive application of the standard seesaw mechanism. Therefore, the results of Sec. 5.1 can be applied. However, the additional massive singlets may be so heavy that additional particles coming from GUT representations have to be considered in the discussion of the renormalization. Hence, we have to make some assumptions about the high energy theory in order to discuss the RG effects. We assume that either the additional massive singlets S as well as the RH neutrinos N are total singlets of the gauge group, which is often the case in low energy theories or

- all additional singlets S are heavier than the RH neutrinos N in Eq. (3.1.2), i.e. the eigenvalues of M_{SS} are strictly larger than the eigenvalues of $-M_{SN}^T M_{SS}^{-1} M_{SN}$;
- the additional singlets S are total singlets, at least below the scale of their largest mass;
- the RH neutrinos N are total singlets, at least below the scale of their largest mass.

Then, the scales can be clearly separated and the renormalization of the singlets S and the RH neutrinos N can be treated separately. In the context of SO(10) where we are going to apply our results in Sec. 4.5, the requirements are fulfilled when all additional singlets are heavier than the LR-breaking scale and all RH neutrinos masses are below the LR-breaking scale. This ensures that the formulas of Sec. 5.1 are applicable, because all requirements which are stated at the end of Sec. 5.1 are fulfilled.

We introduce the effective operator $O_M(\Lambda)$ at scale Λ which generates the masses of all uncharged fermions

$$O_M(\Lambda) = \begin{pmatrix} \nu \\ N \\ S \end{pmatrix} \begin{pmatrix} 0 & Y_\nu^T H_u & Y_{S\nu}^T \Delta' \\ . & 0 & Y_{SN}^T \Delta \\ . & . & M_{SS} \end{pmatrix} \begin{pmatrix} \nu & N & S \end{pmatrix} . \tag{5.36}$$

The Yukawa couplings are related to the mass matrices in Eq. (3.17) by $m_D = Y_\nu \langle H_u \rangle$, $m_{S\nu} = Y_{S\nu} \langle \Delta' \rangle_\nu$ and $M_{SN} = Y_{SN} \langle \Delta \rangle_N$, where H_u, Δ and Δ' are Higgs fields. We assume, that Δ obtains a GUT scale VEV and H_u, Δ' acquire an electroweak scale VEV. The application of Eq. (5.17) results in the effective mass operator $O_M(\Lambda')$

$$O(\Lambda') = Z_{\text{ext},S}^T \begin{pmatrix} -Y_{S\nu}^T X_S M_{SS}^{-1} Y_{S\nu} \Delta'^2 & Y_\nu^T H_u - Y_{S\nu}^T X_S M_{SS}^{-1} Y_{SN} \Delta \Delta' \\ . & -Y_{SN}^T X_S M_{SS}^{-1} Y_{SN} \Delta'^2 \end{pmatrix} Z_{\text{ext},S} \tag{5.37}$$

after all additional singlets have been integrated out, where X_S subsumes the renormalization of the singlet mass matrix and $Z_{\text{ext},S}$ denotes the external renormalization factor between Λ and Λ'. The exact form can be easily obtained by Eq. (5.18) and the knowledge of the underlying theory. At the scale $\langle \Delta \rangle_N$, the RH neutrinos become massive by spontaneous symmetry breaking and a subsequent application of Eq. (5.17) results in the following contributions to the effective neutrino mass matrix

$$m_\nu^{DS} = Z_{\text{ext}}^T m_D^T X'_N M_{SN}^{-1} M_{SS} X_S M_{SN}^{T\,-1} m_D Z_{\text{ext}} \tag{5.38a}$$

$$m_\nu^{LS} = -Z_{\text{ext}}^T \left[\left(m_{S\nu}^T X_S M_{SS}^{-1} M_{SN} X'_N M_{SN}^{-1} M_{SS} X_S^{-1} M_{SN}^{T\,-1} m_D \right) + (\dots)^T \right] Z_{\text{ext}} \tag{5.38b}$$

$$m_\nu^{T1} = Z_{\text{ext}}^T m_{S\nu}^T X_S M_{SS}^{-1} \left(1 - M_{SN} X'_N M_{SN}^{-1} \right) m_{S\nu} Z_{\text{ext}} \, , \tag{5.38c}$$

where $X'_N = Z_{\text{ext},S} X_N Z_{\text{ext},S}^{-1}$, X_N equals Eq. (5.18) and $Z_{\text{ext}} = Z_{\text{ext},S} Z_{\text{ext},N}$ denotes the external renormalization factor between Λ and $\langle H_u \rangle$. Note, that the DS contribution receives at leading order a contribution from the RG effect due to the singlet thresholds as well as the thresholds of the RH neutrinos, the LS contribution receives only a correction from the threshold of the RH neutrinos at leading order and the standard seesaw contribution m_ν^{T1} which vanishes in the cascade seesaw formula, receives a correction from RH neutrino thresholds. However, it is negligible in most cases because it is suppressed by the large mass scale of the additional singlets. The expressions can be further expanded keeping only the leading order which results in the following corrections to the different contributions

$$\delta m_\nu^{DS} = Z_{\text{ext}}^T \left[m_D^T \delta X'_N M_{SN}^{-1} M_{SS} M_{SN}^{T\,-1} m_D + m_D^T M_{SN}^{-1} M_{SS} \delta X_S M_{SN}^{T\,-1} m_D \right] Z_{\text{ext}} \tag{5.39a}$$

$$\delta m_\nu^{LS} = -Z_{\text{ext}}^T \left[\left(m_{S\nu}^T M_{SS}^{-1} M_{SN} \delta X'_N M_{SN}^{-1} M_{SS} M_{SN}^{T\,-1} m_D \right) + (\dots)^T \right] Z_{\text{ext}} \tag{5.39b}$$

$$\delta m_\nu^{T1} = Z_{\text{ext}}^T m_{S\nu}^T M_{SS}^{-1} M_{SN} \delta X'_N M_{SN}^{-1} m_{S\nu} Z_{\text{ext}} \, , \tag{5.39c}$$

where $\delta X'_N \equiv X'_N - 1$ and $\delta X_S \equiv X_S - 1$.
In the case, in which the masses of the additional singlets are below the scale $\langle \Delta \rangle_N \sim \mathcal{O}(\Lambda_{\text{GUT}})$, there are basically no threshold corrections, since the RH neutrinos and the additional singlets form pseudo Dirac particles with a mass of the order $\mathcal{O}(M_{SN} \pm M_{SS})$. The thresholds corrections are proportional to $\ln\left(1 - M_{SS} / \langle \Delta \rangle_N\right) \ll \mathcal{O}(1)$.

5.3 RG Stability of the Cancellation Mechanism

In Sec. 5.2, the RG corrections to the light neutrino mass matrix have been considered. Here, we apply the result to the cancellation mechanism, especially the DS contribution. If Eq. (4.1) is

satisfied, the DS contributions shown in Eq. (5.38a) to the neutrino mass becomes

$$m_\nu \approx m_\nu^{DS} = Z_{\rm ext}^T m_D^T X'_N M_{SN}^{-1} M_{SS} X_S F Z_{\rm ext} \tag{5.40}$$

which is approximately given by

$$m_\nu \approx Z_{\rm ext}^T \left[F^T M_{SS} F + F^T M_{SS} \delta X_S F + m_D^T \delta X'_N M_{SN}^{-1} M_{SS} F \right] Z_{\rm ext} \, . \tag{5.41}$$

Since the RG effect due to the mass thresholds of the singlets can be subsumed in a redefinition of M_{SS}, which is described by a rescaling of the singlet masses, we concentrate on the RG effect due to the RH neutrinos. In the special case of Dirac screening, i.e. $F \propto \mathbb{1}$, the RG corrections to the neutrino mass matrix amount to

$$m_\nu \approx \frac{\langle H_u \rangle^2}{\langle \Delta \rangle_N^2} Z_{\rm ext}^T \left[M_{SS} + Y_\nu^T \delta X'_N Y_\nu^{-1} M_{SS} \right] Z_{\rm ext} \tag{5.42}$$

neglecting threshold corrections of the additional singlets S. Dirac screening is reproduced and the dependence of m_ν on the Yukawa (Dirac) couplings disappears if $X_N = I$. The expression Eq. (5.42) coincides with that in Eq. (4.2) up to external renormalization. In turn, according to Eq. (5.18) the equality $X_N = I$ holds provided that $Z_\kappa = I$, that is, when the D5 operator corrections are absent. This is automatically satisfied in the SUSY theory, but these corrections are present in the SM and its non-SUSY extensions.

Note that the D5 operator corrections are due to the gauge interactions and self interactions of the Higgs boson, which are by themselves flavor blind. However, they influence the flavor structure of the light neutrino mass matrix due to difference of masses of the RH neutrinos and therefore different threshold effects.

We apply the results obtained in this section to several phenomenologically interesting structures of M_{SS}. We study effects of the radiative corrections on the light neutrino mass matrix. The matrix M_{SS} will be defined in the basis where the equality of the Yukawa couplings Eq. (4.5) is fulfilled. We discuss m_ν^f - the neutrino mass matrix in the flavor basis where the charge lepton mass matrix Y_e is diagonal. It is related to m_ν as

$$m_\nu^f = U_e^T m_\nu U_e, \tag{5.43}$$

where U_e is the transformation of left-handed charged lepton components which diagonalizes the matrix Y_e at the electroweak scale. The radiative corrections to Y_e are in general small due to the strong mass hierarchy, as it was already mentioned in Sec. 5.1. In the following three subsections, we explore the Dirac screening case. In Secs. 5.3.4 and 5.3.5, we discuss the two realizations of the cancellation mechanism by a flavor symmetry.

5.3.1 Singular M_{SS}

Let us consider the effect of radiative corrections in the singular case. As long as all contributions to the Majorana mass matrix m_ν receive the same quantum corrections, the RG evolution does not generate non-zero masses from vanishing masses [226]. However, between the mass thresholds of the RH neutrinos, there are two contributions from the decoupling of the RH neutrinos which are renormalized differently. One contribution is due to the D5 operator of already decoupled RH neutrinos and the other is due to the contribution of the RH neutrinos which are not decoupled yet $(Y_\nu^T M_{NN}^{-1} Y_\nu)$ in the intervals $M_2 - M_3$ and $M_1 - M_2$. Hence, the generated mass is proportional to the additional renormalization factor δZ_κ from the D5 operator between the thresholds and the mismatch between the two mass contributions, *i.e.* the deviation of the unitary matrix transforming

from the eigenbasis of the D5 operator to the eigenbasis of $-Y_\nu^T M_{NN}^{-1} Y_\nu$ between the thresholds from the unit matrix (See Sec. 4 in [69].). In the SUSY version, all contributions to the Majorana mass matrix receive the same quantum corrections, and hence zero mass eigenvalues remain zero.

5.3.2 Quasi-Degenerate Neutrino Spectrum

Let us first consider M_{SS} which is proportional to the unit matrix I at Λ, *i.e.*,

$$M_{SS} = M_{SS}^0 I \ . \tag{5.44}$$

This choice is apparently basis independent and therefore we can take $Y_\nu = Y_{SN} = \mathrm{diag}(y_1, y_2, y_3)$. The RH neutrino mass matrix is diagonal and strongly hierarchical:

$$M_{NN} = -Y_{SN}^T M_{SS}^{-1} Y_{SN} \langle\Delta\rangle_N^2 = \frac{\langle\Delta\rangle_N^2}{M_{SS}} \mathrm{diag}\left(y_1^2,\, y_2^2,\, y_3^2\right) \ . \tag{5.45}$$

Therefore $V_N = I$ and we find

$$m_\nu^f = \frac{\langle H_u\rangle^2}{\langle\Delta\rangle_N^2} M_{SS}^0 U_e^T Z_{\rm ext}^T \left[I + \delta Z_\kappa\right] Z_{\rm ext} U_e. \tag{5.46}$$

The corrections are also diagonal[3]

$$\delta Z_\kappa = \overset{(0)}{Z_\kappa} \left[\exp\left(-\mathcal{A}\ \mathrm{diag}\left(0,\, \ln\frac{y_1^2}{y_2^2},\, \ln\frac{y_1^2}{y_3^2}\right)\right) - I\right] \sim \mathcal{O}(0.1) \ , \tag{5.47}$$

where

$$\mathcal{A} \equiv \frac{1}{16\pi^2}\left(\lambda + \frac{9}{10} g_1^2 + \frac{3}{2} g_2^2\right). \tag{5.48}$$

This leads to splittings of the light neutrino masses which would be degenerate otherwise.
Note that the external corrections (due to wave function renormalization of the left-handed leptons, Eq. (C.2), and the vertex corrections to the neutrino Yukawa couplings, Eq. (C.4)), are described in general by off-diagonal matrices due to the mismatch of the structures of Y_e and Y_ν. As the charged lepton Yukawa couplings are also strongly hierarchical, the largest flavor dependent correction is the one to the 3-3 element. Neglecting the off-diagonal entries, it can be estimated as

$$-2\frac{y_\tau^2}{16\pi^2} \ln\frac{\langle H_u\rangle}{\Lambda} - 4\frac{y_3^2}{16\pi^2} \ln\frac{M_3}{\Lambda} \sim \mathcal{O}(0.1), \tag{5.49}$$

where the second term (due to the neutrino Yukawa coupling) dominates. It has the same order of magnitude as the correction due to the D5 operator renormalization in Eq. (5.47).
Let us now comment on a possibility to explain the neutrino data. In the non-SUSY version, the mass split, δm, generated by the D5 operator corrections, $\delta m = m_0 \delta Z$, leads to $\Delta m_{32}^2 = 2 m_0 \delta m = 2 m_0^2 \delta Z = (2-8)\cdot 10^{-3}$ eV^2 for the overall scale $m_0 = (0.1 - 0.2)$ eV. This can reproduce the atmospheric mass split, but it is too large for the solar mass split. The ratio of solar and atmospheric mass squared differences for quasi-degenerate neutrinos,

$$\zeta \ \approx \ \frac{m_2 - m_1}{m_3 - m_2} \sim \mathcal{O}(1) \ , \tag{5.50}$$

[3]We assume a strong hierarchy in Y_ν and use $Y_\nu \sim Y_u$ for numerical estimates.

does not fit the observations. The external corrections do not improve the situation either. Therefore some other (non-radiative) contribution is required to compensate the 1-2 mass split. Mixings can also be generated by small (non-radiative) corrections.
In the SUSY version we have $\delta Z_\kappa = 0$ and $Z_{Y_\nu} = I$, so that the mass splitting is produced by the external renormalization only:

$$m_\nu^f = \frac{\langle H_u \rangle^2}{\langle \Delta \rangle_N^2} M_{SS}^0 U_e^T Z_{\rm ext}^T Z_{\rm ext} U_e \ . \tag{5.51}$$

In the flavor basis we obtain the mass split due to Yukawa couplings coming from the external renormalization:

$$\exp\left[-\frac{1}{8\pi^2} {\rm diag}(y_e^2,\ y_\mu^2,\ y_\tau^2) \ln \frac{\langle H_u \rangle}{\Lambda} \right] \ , \tag{5.52}$$

where the neutrino Yukawa couplings are neglected. This can provide the atmospheric mass split and the mixings should be generated again by corrections to the zero order structure.
Next, we consider for M_{SS} the "triangle" structure

$$M_{SS} = M_{SS}^0 \begin{pmatrix} 1 & 0 & 0 \\ 0 & 0 & 1 \\ 0 & 1 & 0 \end{pmatrix} \tag{5.53}$$

in the basis where the neutrino Yukawa matrix is diagonal. In lowest order it produces a degenerate mass spectrum and maximal 2-3 mixing of the light neutrinos. This matrix leads to a spectrum of RH neutrinos with two heavy degenerate states and one relatively light state:

$$M_1 = \frac{\langle \Delta \rangle_N^2 \, y_1^2}{M_{SS}^0}, \qquad M_2 = -M_3 = \frac{\langle \Delta \rangle_N^2 \, y_2 y_3}{M_{SS}^0}. \tag{5.54}$$

The renormalization interval (2) (See Fig. 2.1.) is therefore absent and the matrix of D5 operator corrections can be written as

$$\delta Z_\kappa = \left[\exp\left(\delta \overset{(1)}{Z_\kappa} \right) - 1 \right] {\rm diag}(0,1,1) \ , \qquad \delta \overset{(1)}{Z_\kappa} = \mathcal{A} \ln \frac{y_1^2}{y_2 y_3} \ , \tag{5.55}$$

where $\mathcal{A}$ is defined in Eq. (5.48). The state N_1 decouples and maximal mixing is realized in the 2-3 block of V_N. Using this feature and Eq. (5.55) we find from Eq. (5.42)

$$m_\nu^f = Z_{\rm ext}^T \frac{\langle H_u \rangle^2}{\langle \Delta \rangle_N^2} M_{SS}^0 U_e^T \overset{(0)}{Z_\kappa} \begin{pmatrix} 1 & 0 & 0 \\ 0 & 0 & 1 - \delta \overset{(1)}{Z_\kappa} \\ 0 & 1 - \delta \overset{(1)}{Z_\kappa} & 0 \end{pmatrix} Z_{\rm ext} U_e \ . \tag{5.56}$$

Therefore the D5 operator corrections do not destroy the triangular structure, but they lead to a mass splitting between the degenerate pair and the isolated state:

$$\frac{\Delta m}{m} = \delta \overset{(1)}{Z_\kappa} \ . \tag{5.57}$$

In the SUSY version $\delta \overset{(1)}{Z_\kappa} = 0$, so that the original "triangle" structure is renormalized by the external corrections only. In this case, one also needs perturbations of the original screening structure in order to obtain phenomenologically viable mixings and mass splittings.

Note, that the stability of the structure in (non-)SUSY theories can be easily understood. The seesaw formula leads to the same mass texture. Therefore m_ν as well as M_{NN} have the same structure. Furthermore, as it has been mentioned in Sec. 3.3.1, $L_\mu - L_\tau$ which also results in a triangular structure is anomaly-free which explains the stability of the structure.
As a third possibility we consider for M_{SS} the "triangle" structure which leads to a degenerate spectrum and maximal 1-2 mixing:

$$M_{SS} = M^0_{SS} \begin{pmatrix} 0 & 1 & 0 \\ 1 & 0 & 0 \\ 0 & 0 & 1 \end{pmatrix} . \tag{5.58}$$

Similar considerations as above results in the mass spectrum of RH neutrinos with two light degenerate states and an isolated heavier state:

$$M_{1N} = -M_{2N} = \frac{\langle\Delta\rangle^2_N\, y_1 y_2}{M^0_{SS}}, \qquad M_{3N} = \frac{\langle\Delta\rangle^2_N\, y_3^2}{M^0_{SS}} . \tag{5.59}$$

For the light neutrinos we find

$$m_\nu \equiv Z^T_{\rm ext} \frac{\langle H_u\rangle^2}{\langle\Delta\rangle^2_N} M^0_{SS} U_e^T \overset{(0)}{Z}_\kappa \begin{pmatrix} 0 & 1 & 0 \\ 1 & 0 & 0 \\ 0 & 0 & 1-\delta \overset{(2)}{Z}_\kappa \end{pmatrix} Z_{\rm ext} U_e , \tag{5.60}$$

where

$$\delta \overset{(2)}{Z}_\kappa = \exp\left(\mathcal{A} \ln \frac{y_1 y_2}{y_3^2}\right) - 1 . \tag{5.61}$$

The corrections due to running of the D5 operator are of the same order as in the previous case. The mass split

$$\Delta m^2_{32} = 2 m_0 \delta m_{32} = -2 m_0^2 \delta \overset{(2)}{Z}_\kappa = (2-8)\cdot 10^{-3}\,\mathrm{eV}^2 , \tag{5.62}$$

for $m_0 = (0.08 - 0.16)$ eV can explain the atmospheric neutrino data. The external renormalization contributes in the same way as for $M_{SS} \propto I$.
The original matrix M_{SS} as given in Eq. (5.58) has to be perturbed in order to produce phenomenologically acceptable mixings.

5.3.3 Perturbations of M_{SS}

Next, we consider perturbations of the structure of M_{SS} which (can be required by phenomenology and) effect radiative corrections on these perturbed structures.
As an example we take the matrix

$$M_{SS} = M^0_{SS} \begin{pmatrix} 1 & 0 & 0 \\ 0 & x & 1 \\ 0 & 1 & 0 \end{pmatrix} \tag{5.63}$$

with x being a small parameter. Now the second and third neutrinos are no longer degenerate and the renormalization factor $\overset{(2)}{Z}_\kappa$ in the interval (2) between their masses appears. Approximating $\overset{(n)}{Z}_\kappa$ by $1 + \mathcal{A}\ln(M_n/M_{n+1})$ we obtain for the light neutrinos

$$m^f_\nu = \frac{\langle H_u\rangle^2}{\langle\Delta\rangle^2_N} M^0_{SS} U_e^T \overset{(0)}{Z}_\kappa Z^T_{\rm ext} \begin{pmatrix} 1 & 0 & 0 \\ \dots & x\,(1+\mathcal{A})\, m^{\rm th}_{22} & 1 + \mathcal{A} m^{\rm th}_{23} \\ \dots & \dots & \mathcal{A} m^{\rm th}_{33} \end{pmatrix} Z_{\rm ext} U_e , \tag{5.64}$$

where the threshold dependent corrections, $m_{fg}^{\rm th}$, equal

$$\begin{aligned} m_{22}^{\rm th} =& -3\ln\lambda + \left(\frac{1}{2} - \frac{\lambda^2}{x^2 y}\right)\ln\frac{y-1}{y+1}\ , \\ m_{23}^{\rm th} =& -3\ln\lambda + \frac{1}{2y}\ln\frac{y-1}{y+1}\ , \\ m_{33}^{\rm th} =& \frac{1}{xy}\ln\frac{y-1}{y+1}\ . \end{aligned} \tag{5.65}$$

Here $y \equiv \sqrt{1+4\left(\frac{\lambda}{x}\right)^2}$ and $\lambda \equiv y_2/y_3$. (The logarithms depend on the ratios of the RH neutrino masses M_2/M_3.)
The nonzero 3-3 element is generated in Eq. (5.64) by radiative corrections. Furthermore, this element can be enhanced by the small parameter x in the denominator, provided that λ is also small enough. Indeed, from Eq. (5.65) we find explicitly

$$(m_\nu)_{33} = \begin{cases} \dfrac{2\mathcal{A}}{x}\ln\dfrac{\lambda}{x}, & x \gg \lambda \\ -\dfrac{1.26\mathcal{A}}{x}, & x = 2\lambda \\ -\dfrac{\mathcal{A}x}{2\lambda^2}, & x \ll \lambda \end{cases} \tag{5.66}$$

As $\mathcal{A} \sim 10^{-2}$, the 3-3 element can be of the order $\mathcal{O}(1)$ or even more if, *e.g.*, $\lambda \ll x < 10^{-2}$. Thus, a quasi-degenerate M_{SS} with nearly maximal 2-3 mixing leads after (non-SUSY) RG corrections to the hierarchical mass matrix m_ν with small mixing. The texture Eq. (5.63) is not stable against quantum corrections, since the structure of m_ν strongly differs from the original structure of M_{SS}. This example shows that radiative corrections can substantially modify the original texture of M_{SS} in the light neutrino mass matrix for a particular M_{SS}. In other words, radiative corrections may destroy Dirac screening.
Apparently the corrections are small if $\lambda \ll x \sim 1$. This corresponds to the phenomenologically important case of a dominant 2-3 block:

$$M_{SS} = M_{SS}^0 \begin{pmatrix} \epsilon & 0 & 0 \\ 0 & x & 1 \\ 0 & 1 & x \end{pmatrix} \tag{5.67}$$

with $x \sim 1$ and $\epsilon \ll 1$.
In the SUSY version of the model screening is stable.

5.3.4 T_7 Realization

As the realization is SUSY, thresholds, as they are discussed in Sec. 5.1, do not lead to corrections. Hence the structure is stable and RG running is entirely given by the external renormalization and it can be described by the formulas given in Sec. 6.1 after the singlets have been integrated out. Since the RH neutrinos are heavier than the singlets, the RG evolution has to be considered only in the effective theory. Therefore, the running strongly depends on $\tan\beta$ as well as the absolute neutrino mass scale. In case of small $\tan\beta$ and a strong normal hierarchy which is produced by the DS term alone, there is only a weak RG evolution. After the inclusion of the LS term, the hierarchy does not necessarily have to be strong. It can be as well quasi-degenerate, which leads to large RG corrections, especially for large $\tan\beta$.

5.3.5 Σ(81) Realization

The RG evolution is described by Eq. (5.41). Hence, the singlet masses as well as the RH neutrino masses are rescaled by the threshold corrections. The corrections due to the singlet mass thresholds can be included by rescaling A and B. In the following, we concentrate on the corrections due to the RH neutrino mass thresholds. Since there is a large hierarchy in the RH neutrino masses

$$M_1 = \frac{1}{|\tilde{A}+2\tilde{B}|}\epsilon^4 \qquad M_2 = \left|\frac{\tilde{A}+2\tilde{B}}{3\tilde{B}\left(2\tilde{A}+\tilde{B}\right)}\right|\epsilon^2 \qquad M_3 = \left|\frac{2\tilde{A}+\tilde{B}}{9\tilde{A}\tilde{B}}\right| , \tag{5.68}$$

large corrections can be expected. The RG effect due to thresholds can be estimated to

$$\delta Z_\kappa = \overset{(0)}{Z}_\kappa \left[\exp\left(\mathcal{A}\,\mathrm{diag}\left(0,\, \ln\left|3\tilde{B}\left(2\tilde{A}+\tilde{B}\right)\right|\epsilon^2,\, \ln 9\left|\frac{\tilde{A}\tilde{B}}{\left(2\tilde{A}+\tilde{B}\right)\left(9\tilde{A}+2\tilde{B}\right)}\right|\epsilon^4\right)\right) - 1\right] . \tag{5.69}$$

This leads to a correction to the 2-3 block of the neutrino mass matrix $m_\nu = m_\nu^0 + \delta m_\nu$

$$\delta m_\nu = 3\mathcal{A}\left(\frac{\alpha\,\langle H\rangle}{\langle\Delta\rangle_N}\right)^2 \begin{pmatrix} 0 & 0 & 0 \\ \cdot & \frac{\tilde{B}\left(2\tilde{A}+\tilde{B}\right)}{\tilde{A}+2\tilde{B}}\ln\left(\frac{M_1}{M_2}\right) & \frac{\tilde{B}\left(\tilde{A}-\tilde{B}\right)}{\tilde{A}+2\tilde{B}}\ln\left(\frac{M_1}{M_2}\right) \\ \cdot & \cdot & \frac{\tilde{B}\left(\tilde{A}-\tilde{B}\right)^2}{\left(\tilde{A}+2\tilde{B}\right)\left(2\tilde{A}+\tilde{B}\right)}\ln\left(\frac{M_1}{M_2}\right) + \frac{\tilde{A}}{2\tilde{A}+\tilde{B}}\ln\left(\frac{M_1}{M_3}\right) \end{pmatrix} , \tag{5.70}$$

which generates a split between the 2-2 and 3-3 element. Therefore the degeneracy of m_2 and m_3 is lifted. However, the resulting atmospheric mass squared difference and mixing angle

$$\Delta m^2_{32} \approx 18\mathcal{A}\,\tilde{B}^2\left(\frac{\alpha\,\langle H\rangle}{\langle\Delta\rangle_N}\right)^4 \ln\frac{4}{3\epsilon^2} \quad \text{for } \tilde{A}\to 0 \tag{5.71}$$

$$\tan 2\theta_{23} \approx \frac{2\tilde{B}}{9\mathcal{A}\,\tilde{A}\ln\left(6\tilde{A}\epsilon^2/\tilde{B}\right)} . \tag{5.72}$$

cannot explain the data, since the RG corrections can be estimated

$$\left|\mathcal{A}\ln\epsilon^2\right| \sim \mathcal{O}(0.1) . \tag{5.73}$$

This results in the ratio of mass squared differences

$$\zeta \sim 5\left(1-\frac{|\tilde{A}|^2}{|\tilde{B}|^2}\right) , \tag{5.74}$$

i.e. $|\tilde{A}| \approx |\tilde{B}|$ which leads to a large correction to the atmospheric mixing angle $\theta_{23} \approx 34^\circ$ which is incompatible with the experimental data. Hence, the atmospheric mass squared difference has to be generated by multi-flavon insertions. In this case, quantum corrections can be absorbed in the additional couplings.

Beyond LL Approximation

Let us briefly comment on RG effects beyond the LL approximation. For certain structures of M_{SS} which are discussed in the following subsections, the additional two loop diagrams lead to corrections to the renormalization of the effective neutrino mass operator which could be comparable to the

one loop corrections. However, assuming the same hierarchy in the neutrino Yukawa couplings as in the up-type quark Yukawa couplings, these contribution are further suppressed since the heaviest right-handed neutrino is already integrated out. Therefore all two loop contributions in the effective theory are suppressed by $y_2^2/16\pi^2 \leq 10^{-6}$, where y_2 is the second to largest singular value of Y_ν compared to the one loop contributions. Altogether higher loop contributions are less than 10% of the one loop corrections and can be neglected.

Chapter 6

RG Effects in Neutrino Mass Models

In this chapter, we apply RG techniques to several models. Firstly, Sec. 6.1 summarizes the structure of RG equations in matrix form in the effective theory, standard, triplet as well as the type I+II seesaw scenario. Furthermore, the derivation of the RG equations of the mixing parameters is outlined. The RG effect in the case of the flavor symmetry $L_\mu - L_\tau$ is discussed in Sec. 6.2 numerically and analytically and Sec. 6.3 treats the QLC relations in the scenario given in Sec. 3.4. Finally, RG equations of leptonic mixing parameters in the triplet seesaw scenario are derived in Sec. 6.4.

6.1 General Structure of RG Equations in Seesaw Models

In summary, the running of the effective neutrino mass matrix m_ν is given by the running of the different contributions to the neutrino mass matrix $m_\nu^{(i)}$ which have been shown in Sec. 3.1.
The one-loop β-function for $m_\nu^{(i)}$ in the various effective theories can be summarized as

$$16\pi^2\,\dot{m}_\nu^{(i)} = P^{(i)\,T} m_\nu^{(i)} + m_\nu^{(i)}\,P^{(i)} + \alpha_\nu^{(i)}\,m_\nu^{(i)}\;, \tag{6.1}$$

where

$$P^{(i)} \equiv \left[C_e^{(i)} Y_e^\dagger Y_e + C_\nu^{(i)} Y_\nu^\dagger Y_\nu + C_\Delta^{(i)} Y_\Delta^\dagger Y_\Delta\right]\;. \tag{6.2}$$

and

$$\dot{m}_\nu^{(i)} \equiv \mu\,\frac{\mathrm{d}m_\nu^{(i)}}{\mathrm{d}\mu}\;, \tag{6.3}$$

$m_\nu^{(i)}$ stands for any of the contributions to the light neutrino mass matrix and α_ν includes the gauge interaction terms that can influence the flavor structure in the SM case between mass thresholds. The coefficients $C_{e,\nu,\Delta}^{(i)}$ and $\alpha_\nu^{(i)}$ are listed in Tab. 6.1, where $T = \mathrm{tr}\left(Y_\nu^\dagger Y_\nu + Y_e^\dagger Y_e + 3Y_u^\dagger Y_u + 3Y_d^\dagger Y_d\right)$.
Note, that they are the same for all mass contributions $m_\nu^{(i)}$ in the MSSM due to the non-renormalization theorem [227, 228]. As the running of the MNS matrix depends on the evolution of the charged lepton Yukawa matrix Y_e, we also present its RG equation,

$$16\pi^2 \dot{Y}_e = Y_e F + \alpha_e Y_e \tag{6.4}$$

where

$$F \equiv \left[D_e Y_e^\dagger Y_e + D_\nu Y_\nu^\dagger Y_\nu + D_\Delta Y_\Delta^\dagger Y_\Delta\right]\;. \tag{6.5}$$

The coefficients $D_{e,\nu,\Delta}$ and α_e are listed in Tab. 6.2. In the case that the renormalization of the

model	$m_\nu^{(i)}$	C_e	C_ν	C_Δ	flavor-trivial term α_ν
SM	κ	$-\frac{3}{2}$	$\frac{1}{2}$	$\frac{3}{2}$	$2T - 3g_2^2 + \lambda$
SM	$2\,Y_\nu^T M^{-1} Y_\nu$	$-\frac{3}{2}$	$\frac{1}{2}$	$\frac{3}{2}$	$2T - \frac{9}{10}g_1^2 - \frac{9}{2}g_2^2$
SM	$-2\,\Lambda_6 M_\Delta^{-2} Y_\Delta$	$\frac{1}{2}$	$\frac{1}{2}$	$\frac{3}{2}$	$T - 2\mathrm{tr}\left(Y_\Delta^\dagger Y_\Delta\right) - 3g_2^2 + \lambda - 8\Lambda_1 - 2\Lambda_2 - 4\Lambda_4 + 8\Lambda_5 - \left(4\Lambda_4 m^2 + \lvert\Lambda_6\rvert^2\right) M_\Delta^{-2} - 4\mathrm{tr}\left(Y_\Delta^\dagger Y_\nu^T M Y_\nu\right)\Lambda_6^{-1}$
MSSM	κ	1	3	$\frac{3}{2}$	$2\mathrm{tr}\left(Y_\nu^\dagger Y_\nu + 3Y_u^\dagger Y_u\right) + 3\lvert\Lambda_u\rvert^2 - 2\left(\frac{3}{5}g_1^2 + 3g_2^2\right)$
MSSM	$2\,Y_\nu^T M^{-1} Y_\nu$	1	3	$\frac{3}{2}$	$2\mathrm{tr}\left(Y_\nu^\dagger Y_\nu + 3Y_u^\dagger Y_u\right) + 3\lvert\Lambda_u\rvert^2 - 2\left(\frac{3}{5}g_1^2 + 3g_2^2\right)$
MSSM	$-2\,\Lambda_6 M_\Delta^{-2} Y_\Delta$	1	3	$\frac{3}{2}$	$2\mathrm{tr}\left(Y_\nu^\dagger Y_\nu + 3Y_u^\dagger Y_u\right) + 3\lvert\Lambda_u\rvert^2 - 2\left(\frac{3}{5}g_1^2 + 3g_2^2\right)$

Table 6.1: Coefficients of the β-functions of Eq. (6.1), which govern the running of the effective neutrino mass matrix in minimal type I+II seesaw models. In the MSSM, the coefficients coincide due to the non-renormalization theorem [227, 228] in supersymmetric theories.

model	D_e	D_ν	D_Δ	flavor-trivial term α_e
SM	$\frac{3}{2}$	$-\frac{3}{2}$	$\frac{3}{2}$	$T - \frac{9}{4}g_1^2 - \frac{9}{4}g_2^2$
MSSM	3	1	$\frac{3}{2}$	$\mathrm{tr}\left(Y_e^\dagger Y_e + 3Y_d^\dagger Y_d\right) + \frac{3}{2}\lvert\Lambda_d\rvert^2 - \frac{9}{5}g_1^2 - 3g_2^2$

Table 6.2: Coefficients of the β-functions of Eq. (6.4), which govern the running of the charged lepton Yukawa coupling in minimal type I+II seesaw models.

effective neutrino mass matrix $m_\nu = \sum_i m_\nu^{(i)}$ can be written in the form

$$16\pi^2 \dot{m}_\nu = P^T m_\nu + m_\nu P + \alpha_\nu m_\nu \,, \tag{6.6}$$

i.e. $P = P^{(i)}$ and $\alpha_\nu = \alpha_\nu^{(i)}$ $\forall i$, RG equations for masses, as well as mixing angles and phases can be derived by the method which is described in the Appendix of [69]. It is based on earlier works [55, 221, 226, 229]. It is always possible in supersymmetric theories and in the SM below all thresholds and above all thresholds, if there are only RH neutrinos or a Higgs triplet. Here, we just sketch the main steps and refer the interested reader to the stated references. The resulting RG equations in the standard seesaw framework are listed in App. C.1 which have been taken from [69].

- In an arbitrary basis, one can define unitary matrices U_ν and U_e by

$$U_\nu(t)^T\, m_\nu(t)\, U_\nu(t) = \mathrm{diag}\big(m_1(t), m_2(t), m_3(t)\big) \equiv D_\nu \,, \tag{6.7a}$$

$$U_e(t)^\dagger\, Y_e^\dagger Y_e(t)\, U_e(t) = \mathrm{diag}\big(y_e^2(t), y_\mu^2(t), y_\tau^2(t)\big) = \mathrm{diag}\left(\frac{m_e^2(t)}{v^2}, \frac{m_\mu^2(t)}{v^2}, \frac{m_\tau^2(t)}{v^2}\right) \equiv D_e \tag{6.7b}$$

  with v fixed.

  The MNS matrix is given by

$$U_{\mathrm{MNS}}(t) \;=\; U_e^\dagger(t)\, U_\nu(t) \,. \tag{6.8}$$

- The application of the RG operator $\delta_{RG} = \frac{\mathrm{d}}{\mathrm{d}t} = \mu\frac{\mathrm{d}}{\mathrm{d}\mu}$ on Eqs. (6.7a, 6.7b) results in

$$\dot{D}_\nu = \frac{1}{16\pi^2}\left(P'^T D_\nu + D_\nu P' + \alpha_\nu\right) + D_\nu X_\nu - X_\nu^* D_\nu \tag{6.9a}$$

$$\dot{D}_e = \frac{1}{16\pi^2}\left(F'^\dagger D_e + D_e F' + 2\mathrm{Re}\,\alpha_e\right) + D_e X_e - X_e D_e \tag{6.9b}$$

  after applying the chain rule, where the primed matrices are defined as $P' \equiv U_\nu^\dagger P U_\nu$, $F' \equiv U_e^\dagger F U_e$ and $X_{\nu,e} \equiv U_{\nu,e}^\dagger \dot{U}_{\nu,e}$ which is anti-Hermitian.

- The real and imaginary parts of those matrices yield the following set of equations for the running masses

$$16\pi^2 \dot{m}_f = \left(\mathrm{Re}\,\alpha_\nu + 2\,\mathrm{Re}\,P'_{ff}\right) m_f\,, \qquad f = 1,2,3 \tag{6.10a}$$

$$16\pi^2 \dot{m}_f = \left(\mathrm{Re}\,\alpha_e + \mathrm{Re}\,F'_{ff}\right) m_f\,, \qquad f = e,\mu,\tau \tag{6.10b}$$

  and the mixing parameters are implicitly given by

$$16\pi^2 \mathrm{Im}\,(X_\nu)_{fg} = -\frac{m_f - m_g}{m_f + m_g}\mathrm{Im}\,P'_{fg} \tag{6.11a}$$

$$16\pi^2 \mathrm{Re}\,(X_\nu)_{fg} = -\frac{m_f + m_g}{m_f - m_g}\mathrm{Re}\,P'_{fg} \tag{6.11b}$$

$$16\pi^2\,(X_e)_{fg} = \frac{y_g^2 + y_f^2}{y_g^2 - y_f^2} F'_{fg}\,, \tag{6.11c}$$

  where we used the hermiticity of P' and F'. The diagonal parts of X_e which determine the unphysical phases remain undetermined.

- In order to obtain the RG equations for the mixing parameters, we observe that the application of the RG operator to Eq. (6.8) yields

$$U_{\mathrm{MNS}}^\dagger \dot{U}_{\mathrm{MNS}} = U_e X_\nu U_e^\dagger - U_\nu^\dagger X_e U_\nu\,. \tag{6.12}$$

  Eq. (6.12) simplifies in the flavor basis where $U_e = \mathbb{1}$ and $U_\nu = U_{\mathrm{MNS}}$ to

$$U_{\mathrm{MNS}}^\dagger \dot{U}_{\mathrm{MNS}} = X_\nu - U_{\mathrm{MNS}}^\dagger X_e U_{\mathrm{MNS}}\,, \tag{6.13}$$

  which is a solvable linear system of equations in the β-functions of the mixing parameters. Although, a basis has been specified in the calculation, the resulting equations are basis-independent [1].

6.2 $L_\mu - L_\tau$ Flavor Symmetry

The flavor symmetry $L_\mu - L_\tau$ which has been introduced in Sec. 3.4 leads to quasi-degenerate neutrino masses. Therefore, strong running of the mixing angles is expected [52–59]. The running of the mixing angles θ_{ij} in a quasi-degenerate mass scheme with a common mass scale m_0 is typically proportional to $m_0^2/\Delta m_{ij}^2$ and therefore particularly strong for θ_{12} above and below the seesaw scales.

[1] If P and F are not expressed in terms of basis-independent quantities as it is done in the formulas of the standard seesaw case, the resulting equations still depend on the chosen basis.

This behavior also turns out to hold when the running between the seesaw scales [9, 62, 63, 69, 230, 231] is taken into account. In general this leads to quite involved expressions for the β-functions. However, in our case the structure of the Dirac and charged lepton mass matrices (i.e., the fact that they are diagonal and hence P is diagonal) simplifies matters considerably and allows for some analytic understanding of the numerical results

$$\begin{aligned}
16\pi^2\,\dot{\theta}_{12} =& \frac{m_0^2}{\Delta m_{21}^2}\,(1+\cos(\varphi_2-\varphi_1))\,\sin 2\theta_{12}\,\left[P_{11}-\left(P_{22}\,\cos^2\theta_{23}+P_{33}\,\sin^2\theta_{23}\right)\right]\,,\\
32\pi^2\,\dot{\theta}_{13} =& \frac{m_0^2}{\Delta m_{32}^2}\,(\cos(\delta-\varphi_1)-\cos(\delta-\varphi_2))\,\sin 2\theta_{12}\,\sin 2\theta_{23}\,(P_{22}-P_{33})\,,\\
16\pi^2\,\dot{\theta}_{23} =& \frac{m_0^2}{\Delta m_{32}^2}\,\left[(1+\cos\varphi_2)\,\cos^2\theta_{12}+(1+\cos\varphi_1)\,\sin^2\theta_{12}\right]\,\sin 2\theta_{23}\,(P_{22}-P_{33})\,.
\end{aligned} \tag{6.14}$$

Note, since the masses have the same CP parity, i.e. $\varphi_1 \approx \varphi_2 \approx \pi$ [196], there is no cancellation in the first relation for $\dot{\theta}_{12}$. We can safely neglect P_{11} with the values of the parameters in m_D as given in Sec. 3.3.1 (i.e., $a \ll b \sim d = \mathcal{O}(0.1)$). This leads in particular to a negative β-function for θ_{12}. Hence, it will increase when evolved from high to low scales. Furthermore, neglecting the charged lepton Yukawas in Y_e above the seesaw scales and noting that $P_{22} \approx b^2/2$ and $P_{33} \approx d^2/2$ for the SM and twice those values for the MSSM, we see that the running of θ_{13} and θ_{23} is suppressed with respect to the running of θ_{12} due to two reasons: firstly, it is inversely proportional to Δm_{32}^2 and secondly, it is proportional to $P_{22} - P_{33} \propto b^2 - d^2$, which is smaller than $P_{22} + P_{33}$, which the running of θ_{12} (approximately) depends on. Hence, the running of θ_{13} and θ_{23} is suppressed by $\zeta\ (b^2-d^2)/b^2$ above the seesaw scales.

Below the seesaw scales only the τ-lepton Yukawa coupling y_τ governs the RG corrections. In this regime the evolution is described by [59]

$$16\,\pi^2\,\dot{\theta}_{12} \approx -y_\tau^2\,\sin 2\theta_{12}\,\sin^2\theta_{23}\,\frac{m_0^2}{\Delta m_{21}^2}\,(1+\cos(\varphi_2-\varphi_1))\,, \tag{6.15}$$

in the MSSM, which is again negative and leads to sizable running. The formulas for the running of $\theta_{13,23}$ are suppressed by roughly a factor ζ.

The phases stay almost constant in the whole range, because it can be shown, that $\dot{\varphi}_1$ and $\dot{\varphi}_2$ are mainly proportional to $\sin\varphi_1$ and $\sin\varphi_2$, respectively. Roughly the same behavior is found below M_1. Finally, the RG effects on the neutrino masses correspond predominantly to a rescaling, since the flavor-diagonal couplings, i.e., gauge couplings and the quartic Higgs coupling, dominate the evolution [54]. Hence, ζ is relatively stable with respect to the RG evolution.

We can analyze whether zero entries in the mass matrix Eq. (3.54) remain zero entries. Below the seesaw scale it is well-known that the RG corrections are multiplicative on the mass matrix, a fact which leaves zero entries zero. Taking the running in between the heavy Majorana masses into account, one can factorize the RG effects $Z_{\rm ext}$ from the tree-level neutrino mass matrix in the MSSM as it is shown in Sec. 5.1

$$m_\nu = Z_{\rm ext}^T\,m_\nu^0\,Z_{\rm ext}\,. \tag{6.16}$$

As the RG effects are flavor diagonal, i.e. P is diagonal, texture zeroes in the charged lepton basis remain zero, even above all see-saw scales. With the already mentioned simplifications, $Z_{\rm ext}$ is

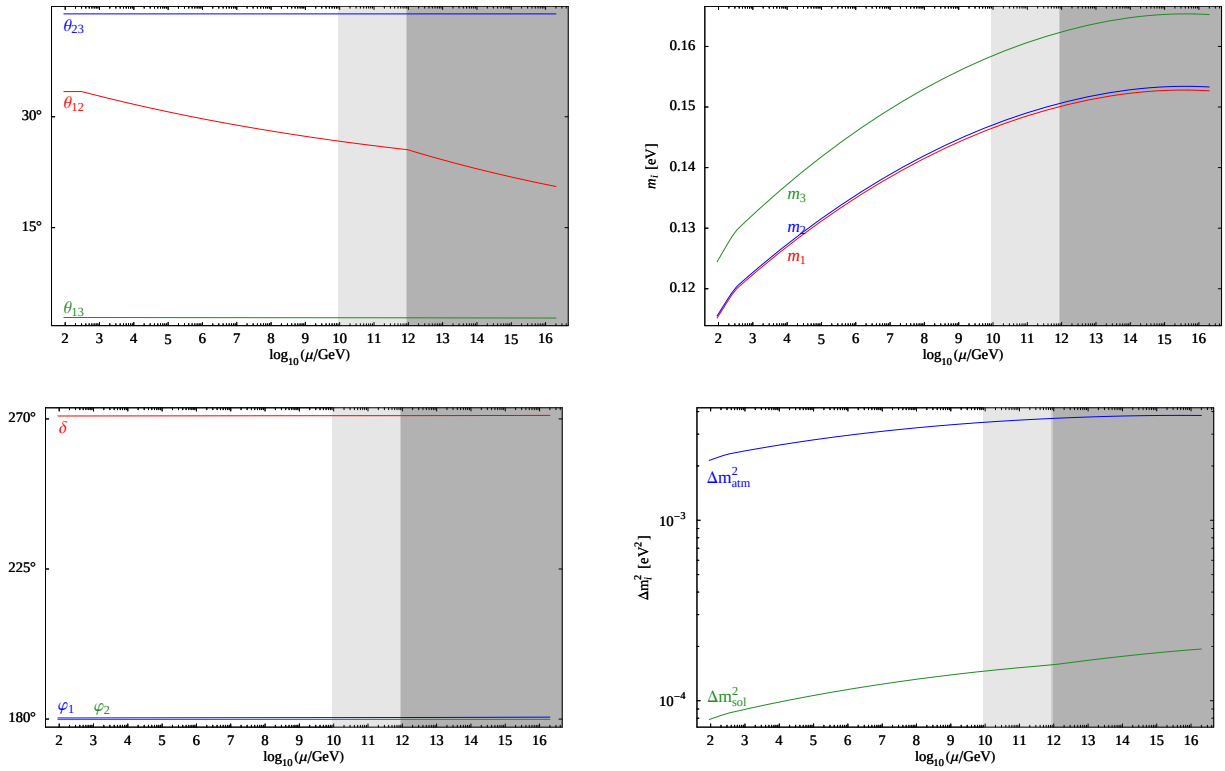

Figure 6.1: Typical plot for the evolution of the mixing angles and masses from $\Lambda_{\rm GUT}$ to the electroweak scale. In this example, we have $\tan\beta = 10$ and the parameters in the matrix Eq. (3.54) at the GUT scale are $a = 0.0066926$, $b = 0.0692883$, $c = 0.0697464$, $X = 0.0096528$, $Y = 1$, $\epsilon_1 = 0.0005595$, $\epsilon_2 = 0.0749098$, $\varphi = 2.45376$ and $M = 9.098937108 \cdot 10^{11}$ GeV. The software package REAP introduced in [69] has been used to produce those plots.

approximately[2] given by

$$16\pi^2 \left(Z_{\rm ext}^{\rm MSSM} - \mathbb{1}\right) = \mathrm{diag}\left(0,\, b^2 \ln\frac{MY}{\Lambda_{\rm GUT}},\, d^2 \ln\frac{MY}{\Lambda_{\rm GUT}} + y_\tau^2 \ln\frac{v}{\Lambda_{\rm GUT}}\right) + b^2 \ln\frac{MY}{\Lambda_{\rm GUT}} + d^2 \ln\frac{MY}{\Lambda_{\rm GUT}} + \left[-\frac{3}{5}g_1^2 - 3g_2^2 + 3y_t^2\right] \ln\frac{v}{\Lambda_{\rm GUT}}\,. \quad (6.17)$$

In the SM, however, there are additional corrections which cannot be factorized. They are responsible for the instability of texture zeroes under the RG which is shown in Sec. 5.1. We checked that for most observables the running behavior in the SM is similar to the running in case of the MSSM. The solar neutrino mixing angle receives more RG corrections in the SM, a fact which can be traced back to the appearance of an 1-2 entry in the mass matrix Eq. (3.54). One might wonder at this point if this filling of zero entries would allow to generate a successful phenomenology from a mass matrix obeying the flavor symmetry $L_\mu - L_\tau$ without any breaking, i.e., just from Eq. (3.50). Recall, however, that in the SM $L_\mu - L_\tau$ is anomaly free and therefore the texture of the mass matrix is stable.

We plot in Fig. 6.1 the running of the angles, phases and masses for a typical example in the MSSM with $\tan\beta = 10$. The neutrino parameters at the GUT scale are $\sin^2\theta_{12} = 0.123$, $\sin\theta_{13} = 0.0484$, $\delta = 4.73\,\mathrm{rad}$, $\sin^2\theta_{23} = 0.481$, $(m_1, m_2, m_3) = (0.1527, 0.1533, 0.1653)\,\mathrm{eV}$ with $\Delta m_{21}^2 = 1.9 \cdot$

[2] As the perturbations are small, the mass eigenvalues of the heavy RH neutrinos are approximately given by $(M_1, M_2, M_3) \approx M\,(X, Y(1-\epsilon_2/2), Y(1+\epsilon_2/2)) \approx (X, Y, Y)$.

$10^{-4}\,\mathrm{eV}^2$ and $\Delta m^2_{32} = 3.8 \cdot 10^{-3}\,\mathrm{eV}^2$. They are changed by the RG evolution to $\sin^2\theta_{12} = 0.303$, $\sin\theta_{13} = 0.0496$, $\delta = 4.73$, $\sin^2\theta_{23} = 0.481$, $(m_1, m_2, m_3) = (0.1152, 0.1155, 0.1245)\,\mathrm{eV}$ with $\Delta m^2_{21} = 7.9{\cdot}10^{-5}\,\mathrm{eV}^2$ and $\Delta m^2_{32} = 2.1{\cdot}10^{-3}\,\mathrm{eV}^2$. Note that the phases and $\theta_{13,23}$ remain practically constant, whereas $\sin^2\theta_{12}$, Δm^2_{21} and Δm^2_{31} are changed by factors of up to three, and that the running in between and above the seesaw scales is at least as important as the running below them. This implies that radiative corrections, in particular for θ_{12} and the mass squared differences, can be crucial especially for quasi-degenerate neutrinos like in this model.

6.3 Quark Lepton Complementarity

In this section, we mainly study the RG evolution of θ_{12}, since it receiver the largest RG corrections in the QLC relations. The RG effect on V_{CKM} is negligible due to the large hierarchy in the charged fermion mass matrices and the smallness of ϑ_{12} [232].

6.3.1 RG Effects: General Considerations

General Considerations

The quark-lepton symmetry implied by the QLC relations means that physics responsible for these relations should be realized at some scale Λ which is at the quark-lepton unification scale, Λ_{GUT}, or at an even higher scales. An alternative possibility would be the quark-lepton relation due to the PS symmetry [140] broken below the GUT scale. Consequently, there are, in principle, three different regions of RG running:

- below the seesaw scales, $\mu < M_1$, where M_1 is the lightest RH neutrino mass. In this region all three neutrinos decouple and the D5 operator Eq. (3.9) is formed;
- between the seesaw scales, $M_1 < \mu < M_3$, where M_3 is the heaviest RH neutrino mass;
- above the seesaw scales $M_3 < \mu < \Lambda$. If $\Lambda > \Lambda_{\mathrm{GUT}}$ new features of running can appear above Λ_{GUT}.

Above the seesaw scales the renormalization of the couplings of the full Lagrangian Eq. (3.11) has to be considered.
Below the seesaw scales, running is dominated by P_{33} in the flavor basis which results in an increase of θ_{12} in the MSSM and a slight decrease in the SM due to a different sign of C_e:

$$32\pi^2\dot{\theta}_{12} \approx -\mathcal{Q}^+_{12}\sin 2\theta_{12}s^2_{23}P_{33}\ . \tag{6.18}$$

Above the seesaw scales, the leading contribution is again given by P_{33}, and the next–to–leading contribution is due to P_{32}. This yields an increase of θ_{12} when running to low scales both in the MSSM and in the SM. Explicitly the corresponding evolution equation can be written as

$$32\pi^2\dot{\theta}_{12} = -\mathcal{Q}^+_{12}C_\nu \sin 2\theta_{12}\sin\theta_{23}\left[\sin\theta_{23} - V_{cb}\cos\theta_{23}\cos\left(\phi_2 - \phi_3\right)\right]\ , \tag{6.19}$$

where the phases ϕ_i are determined in Eqs. (3.71, 3.72).
The effect of running between the seesaw scales (about ten orders of magnitude in μ) is more complicated. In this range there are more contributions to the neutrino mass matrix which evolve differently as it is described in Sec. 5.1. So, in the MSSM, the RG equations are the same for both contributions and the RG equation for θ_{12} is applicable in contrast to the SM.

After the heaviest RH neutrino is integrated out, the RH neutrino mixing at the threshold influences the running of θ_{12}. In the second order of $\sin\vartheta_{12}$, the expression for $\dot{\theta}_{12}$ reads:

$$32\pi^2\dot{\theta}_{12} = -\frac{1}{4}\mathcal{Q}_{12}^{+}C_\nu\left(s_{23} - V_{cb}c_{23}\cos\left(\phi_2 - \phi_3\right)\right) \\ \left(3 - 2\cos 2\Theta_{23}\cos^2\Theta_{13} - \cos 2\Theta_{13}\right)\sin 2\theta_{12}s_{23}\ , \quad (6.20)$$

where Θ_{ij} are the RH neutrino mixing angles at the scale at which the heaviest neutrino is integrated out. The unitary rotation of the RH neutrino fields is done at the threshold of the heaviest RH neutrino, and the exact definitions of the angles are given in Eqs. (3.84, 3.85).

RG Evolution and Scales of Flavor Physics

We have performed the running from the scale Λ down to the electroweak scale and calculated $\Delta\theta_{12} \equiv \theta_{12}(M_Z) - \theta_{12}(\Lambda)$. For that we have numerically solved the complete set of RG equations including sub-leading effects due to non-zero 1-3 mixing. In most of our calculations we take for definiteness $\Lambda = \Lambda_{\rm GUT} = 2\cdot 10^{16}$ GeV. We separately consider the dependence of our results on Λ in Sec. 6.3.6.

The following free parameters determine the RG effects substantially: the absolute scale of light neutrino masses, the Majorana CP phase difference, $\Delta\varphi = \varphi_2 - \varphi_1$, and the phases α_i, which have been defined in Sec. 3.4, as well as $\tan\beta$ in the MSSM. The dependence on other parameters (e.g., other phases) is rather weak. Still we will explicitly use the phase φ_2 keeping everywhere $\varphi_1 = 0°$. We studied the dependence of the RG effects on these parameters. For each set of parameters we have calculated the RH mass matrix and the running effects. The angles are fixed by the QLC relation at Λ, and the mass squared differences are adjusted to lie in the experimentally allowed region at the electroweak scale. For the neutrino Yukawa couplings we take $y_1 : y_2 : y_3 = \epsilon^2 : \epsilon : 1$, $(\epsilon = \epsilon')$ and $\epsilon = 3\cdot 10^{-3}$.

In what follows we will describe the results of our numerical calculations. We give an interpretation of the results using the derived approximate formulas in this section and Sec. 3.4.

6.3.2 RG Effects: MSSM Case

MSSM and Normal Mass Hierarchy

We consider the RG evolution in the MSSM with a unique SUSY threshold at 1 TeV. In Fig. 6.2 we show some examples of the scale dependence of θ_{12} for various values of parameters. With increase of m_1 two factors enhance the RG effects:

- the largest mass M_3 decreases according to Eq. (3.81). Correspondingly, the region above the seesaw scale, $M_3 - \Lambda_{\rm GUT}$ increases where the running is especially strong due to the large neutrino Yukawa couplings;
- corrections to the mass matrix elements δm_{ij} are proportional to their values: $\delta m_{ij} \propto m_{ij}$ and since with the increase of m_1 the matrix elements m_{ij} generically increase, the corrections increase correspondingly.

For relatively small $\tan\beta \sim (3-10)$, the dominant contribution follows from the region above the seesaw scales due to large $(Y_\nu)_{33}$. The evolution below M_3 is mainly due to the Yukawa couplings Y_e which are relatively small. The effect increases fast with m_1:

$$\Delta\theta_{12} \propto \mathcal{Q}_{12}^{+}\log(\Lambda_{\rm GUT}/M_3). \quad (6.21)$$

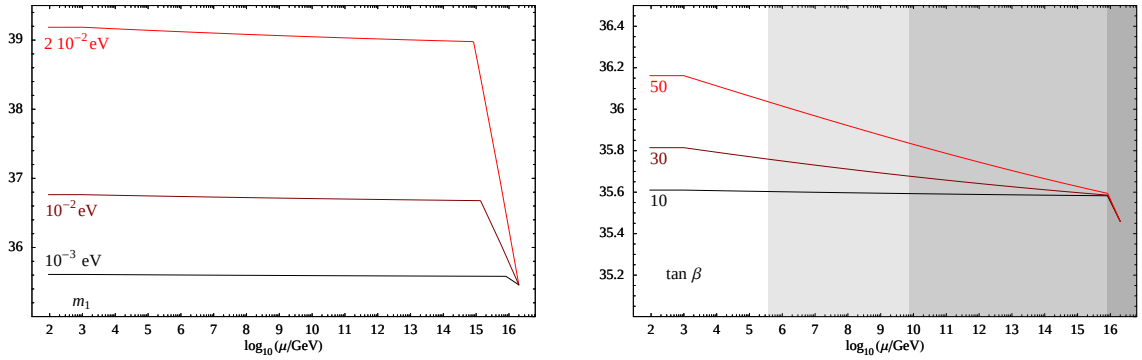

(a) (b)

Figure 6.2: Examples of running θ_{12} in the case of MSSM and normal mass hierarchy. The dependence of θ_{12} on μ (a) for different values of m_1, and $\tan\beta = 10$; (b) on $\tan\beta$ for $m_1 = 10^{-3}$ eV. All CP-phases are taken to be zero.

Note that the largest RH neutrino mass M_3 is proportional to the lightest left-handed neutrino mass: $M_3 \propto 1/m_1$. Therefore for $m_1 \sim 10^{-3}$ eV the running of θ_{12} is mainly related to an increase of the region above the seesaw scale. For $m_1 > 10^{-2}$ eV the spectrum of light neutrinos becomes degenerate and $\Delta\theta_{12} \propto \mathcal{Q}_{12}^{+} \propto m_1^2$ (Fig. 6.2(a)). For large $\tan\beta$ and small m_1 the dominant contribution to $\Delta\theta_{12}$ comes from the region below M_3 where $\Delta\theta_{12} \propto \tan^2\beta$ (see Fig. 6.2(b)).

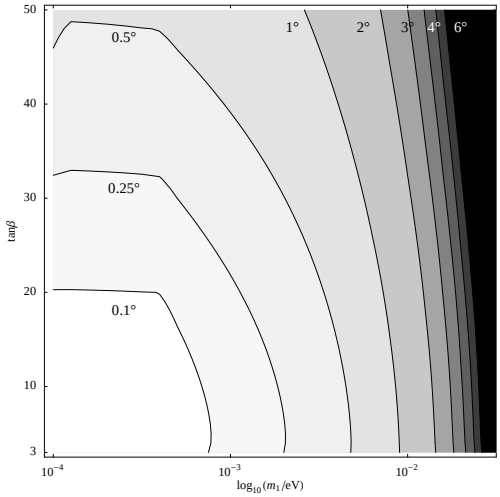

Figure 6.3: Contours of constant RG corrections, $\Delta\theta_{12}$, in the $\tan\beta - m_1$ plane in the case of MSSM and normal mass hierarchy. All the CP-phases are taken to be zero.

A combined dependence of the corrections, $\Delta\theta_{12}$, on m_1 and $\tan\beta$ is presented in Fig. 6.3 where we show contours of constant $\Delta\theta_{12}$ in the $(m_1 - \tan\beta)$ plane. The change of behavior of contours at $m_1 = 8 \cdot 10^{-4}$ eV is a consequence of our boundary condition: At $m_1 < 8 \cdot 10^{-4}$ eV we have $M_3 > \Lambda_{\rm GUT}$, and therefore the region above the seesaw scale disappears.
In Fig. 6.4 we show the correction $\Delta\theta_{12}$ as function of m_1 for different values of φ_2. The dependence of $\Delta\theta_{12}$ on φ_2, given essentially by the factor $\mathcal{Q}_{12}^{+}$, is weak for an hierarchical spectrum, $m_1 \ll 8{\cdot}10^{-3}$ eV, and very strong for a degenerate spectrum: $\Delta\theta_{12} \propto (1 + \cos\Delta\varphi)$. The corrections are strongly suppressed for opposite CP parities $\varphi_2 = 180°$ (Fig. 6.4). This agrees with the results of previous studies of corrections in the quasi-degenerate case [52–59].

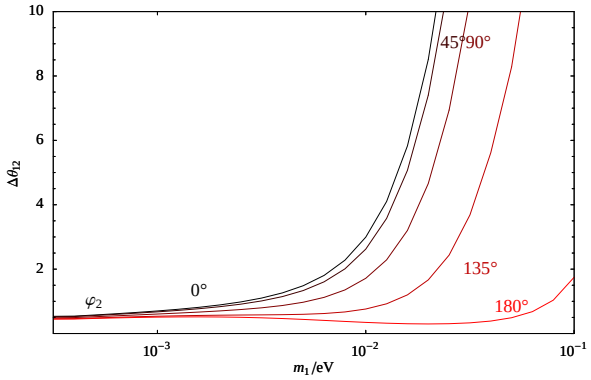

Figure 6.4: The dependence of the RG correction, $\Delta\theta_{12}$ (in degrees), on m_1 for different values of φ_2 (figures at the curves) in the MSSM and a normal mass hierarchy. The lines correspond to $\tan\beta = 10$ and $\varphi_1 = 0°$.

The corrections $\Delta\theta_{12}$ are positive. This fact is mainly a consequence of a strong hierarchy of the Yukawa couplings Y_ν and Y_e. The evolution is given approximately by the general RG equation for θ_{12}, where $P_{33} \propto (|(Y_e)_{33}|^2 + |(Y_\nu)_{33}|^2)/2 > 0$. The off-diagonal couplings P_{fg} are much smaller. Since $\mathcal{Q}_{12}^+ > 0$ we obtain $\dot{\theta}_{12} < 0$, that is, the angle θ_{12} increases with decreasing μ.
The condition of the QLC prediction for θ_{12} being within 1σ of the best fit experimental value requires $\Delta\theta_{12} < 0.5° - 1°$. This, in turn, leads to bounds on parameters of the neutrino spectrum and $\tan\beta$. In particular, according to Fig. 6.4 the degenerate neutrino spectrum is excluded for the same CP parities ($\varphi_2 = 0°$). In the case of large $\tan\beta$ it requires a strongly hierarchical spectrum: $m_1 < 10^{-3}$ eV that eliminates the running region above all seesaw scales. However, a degenerate spectrum is allowed for $\varphi_2 \sim 180°$.
Taking the $2\,\sigma$ upper bound $\Delta\theta_{12} < 2°$ we find that the quasi-degenerate spectrum with $m_1 \sim 10^{-2}$ eV is allowed even for the same CP parities. For a normal mass hierarchy with $m_1 < 10^{-3}$ eV and $\tan\beta \sim (3 - 10)$ the running effect is negligible: $\Delta\theta_{12} < 0.1°$.

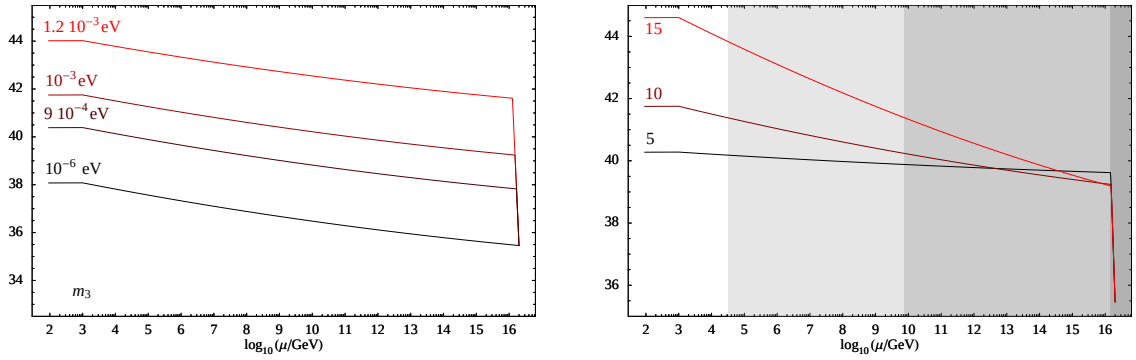

(a) (b)

Figure 6.5: Examples of running θ_{12} in the case of MSSM and inverted mass hierarchy. The dependence of θ_{12} on μ (a) for different values of m_1, and $\tan\beta = 10$, (b) on $\tan\beta$ for $m_1 = 10^{-3}$ eV. The value $\varphi_2 = 0°$ is taken.

MSSM and Inverted Mass Hierarchy

In the case of an inverted mass hierarchy, the states ν_1 and ν_2 associated to 1-2 mixing are strongly degenerate. Therefore, the RG effects are similar to those in the normal hierarchical case for

$m_1 = m_A \sim 5 \cdot 10^{-2}$ eV. The corrections $\Delta\theta_{12}$ are enhanced by the factor

$$\frac{(\Delta\theta_{12})^{IH}}{(\Delta\theta_{12})^{NH}} \approx \frac{(m_2^{IH})^2}{(m_2^{NH})^2} \approx \frac{(m_1^{IH})^2}{(m_1^{NH})^2}, \tag{6.22}$$

where the superscripts NH and IH stand for a normal and an inverted mass hierarchy, respectively. In Fig. 6.5 we show examples of the running of θ_{12} for different values of masses and phases. The dependences of θ_{12} are well-described by $\mathcal{Q}_{12}^+$, as in the case of a normal mass hierarchy. Notice that now the heaviest RH neutrino mass is determined by m_3, and the two others by m_A. With increase of m_3 which is the lightest neutrino mass (See Fig. 6.5(a).) the range above the seesaw scales, where the evolution of θ_{12} is strongest, increases. The change of θ_{12} below M_3 is smaller and it is of the same size for different values of m_3 as long as $m_3 \ll m_A$. In this range the evolution is mainly due to charged lepton Yukawa couplings Y_e, so that $\Delta\theta_{12} \propto \tan^2\beta$ (Fig. 6.5(b)). The correction can be strongly suppressed for opposite CP parities of ν_1 and ν_2: $\Delta\theta_{12} \propto (1 + \cos\Delta\varphi)$.

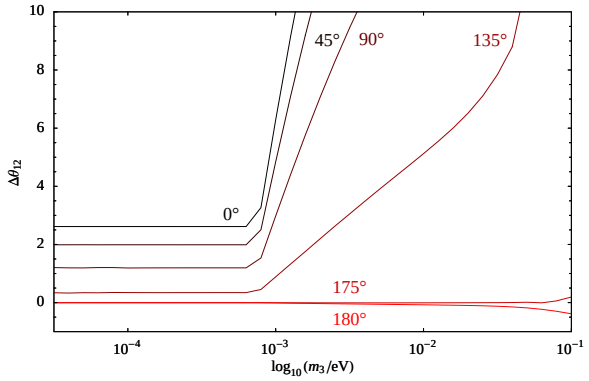

Figure 6.6: The dependence of the RG correction $\Delta\theta_{12}$ on m_1 for different values of φ_2 (figures at the curves) in the case of MSSM, inverted mass hierarchy and $\tan\beta = 10$.

As in the case of a normal hierarchy, in a large part of the parameter space the correction is positive, $\Delta\theta_{12} > 0°$, due to the dominant effect of P_{33}. For $\varphi_2 = 0°$, consistency of the QLC prediction with the experimental data, especially $\Delta\theta_{12} < 2°$, implies $\tan\beta < 10$ and $m_3 < 8 \cdot 10^{-4}$ eV. For $\varphi_2 \sim 180°$ corrections can be strongly suppressed, so that a larger region of the parameter space becomes allowed. The corrections become negative for $\varphi_2 = 180°$ (See Figs. 6.6 and 6.7.) when the leading RG effects are strongly suppressed and the running is mainly due to sub-leading effects related to non-zero 1-3 mixing. This possibility has been mentioned in [14]. The sign of the contribution due to non-zero θ_{13} to the RG running of θ_{12} depends on the parameter (masses, phases) region.
In general, for non-zero θ_{13}, the contribution to $\dot\theta_{12}$ is given by

$$\frac{C_\nu\theta_{13}}{32\pi^2}\sin 2\theta_{23}\Bigg[\left(\mathcal{Q}_{12}^+\cos 2\theta_{12} + \mathcal{Q}_{13}^+ s_{12}^2 + \mathcal{Q}_{23}^+ c_{12}^2\right)\cos\delta + 2\left(\frac{m_1 m_2}{\Delta m_{21}^2}\sin(\varphi_1-\varphi_2) + \frac{m_1 m_3}{\Delta m_{31}^2}\sin\varphi_1 s_{12}^2 + \frac{m_2 m_3}{\Delta m_{32}^2}\sin\varphi_2 c_{12}^2\right)\sin\delta\Bigg]. \tag{6.23}$$

According to this equation for $\varphi_2 = 180°$, $\varphi_1 = 0°$ and $\delta = 180°$, the dominant contribution is determined by the combination $-\frac{m_3+m_1}{m_3-m_1}\sin^2\theta_{12}\sin 2\theta_{23}$, that is positive in the inverted hierarchy case, and therefore θ_{12} decreases from high to low energies.

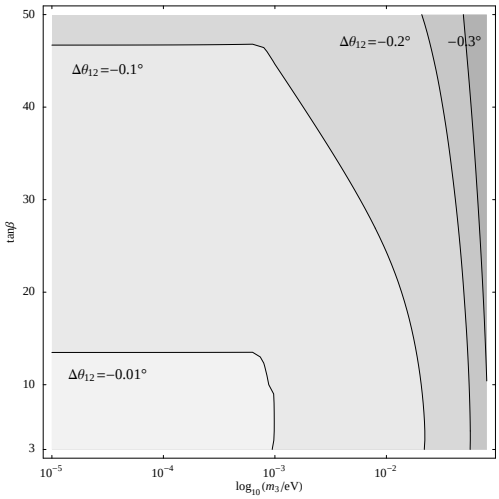

Figure 6.7: Contours of constant RG corrections, $\Delta\theta_{12}$, in the $\tan\beta - m_1$ plane in the case of MSSM, inverted mass hierarchy and $\Delta\varphi = \varphi_2 = 180°$.

6.3.3 RG Effects: SM Case

In the SM the evolution of θ_{12} is more complicated. As we have already mentioned, apart from the Yukawa coupling contributions, there are additional vertex diagrams [63]. Furthermore, the vertex diagrams with the gauge bosons become important: their contribution to the running between the seesaw scales influences the flavor structure of the mass matrix and therefore changes θ_{12}. Above the seesaw scales (where all RH neutrinos are operative) and below the seesaw scales (where all RH neutrinos decouple), flavor universality of the gauge interaction corrections is restored. There is no simple analytic formula for the RG evolution of θ_{12} in the SM.

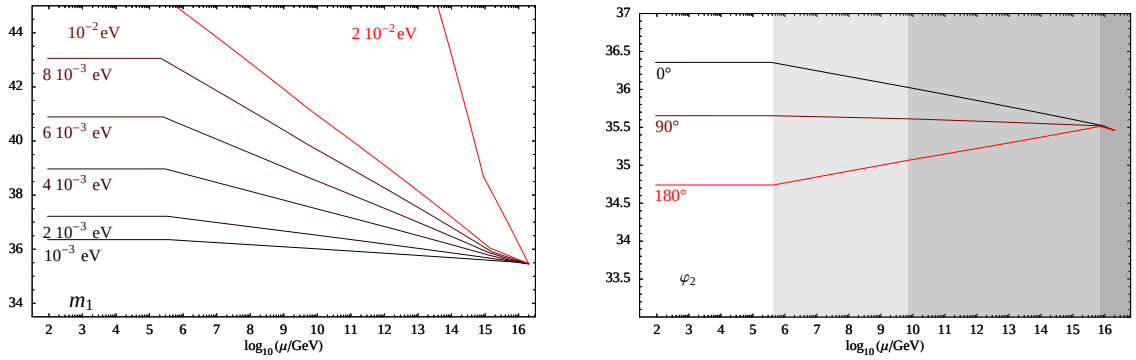

(a) (b)

Figure 6.8: Examples of running of θ_{12} in the case of SM and normal mass hierarchy. The dependence of θ_{12} on μ (a) for different values of m_1, and $\varphi_2 = 0°$, (b) on φ_2 for $m_1 = 10^{-3}$ eV.

In Fig. 6.8 we show examples of the RG running of the solar mixing angle θ_{12}. Above the seesaw scales the running is due to the Yukawa interactions, Y_ν, and the effect is well-described by the analytic formula for θ_{12}. Below the seesaw scales, $\mu < M_1$, the evolution is negligible: it is related to Y_e couplings that are small in the SM. The main effect arises between the seesaw scales. As we mentioned above, it is mainly due to the gauge vertex corrections since N_3 with the largest Yukawa coupling is decoupled and Y_e are small. The corrections increase with m_1.

The most interesting dependence of $\Delta\theta_{12}$ is the one on the CP-violation phase φ_2 (See Fig. 6.8(b).). The corrections are positive, $\Delta\theta_{12} > 0^\circ$, for $\varphi_2 \sim 0^\circ$. They are strongly suppressed for $\varphi_2 \sim 90^\circ$, in contrast to the SUSY case where the suppression is realized for $\varphi_2 \sim 180^\circ$. The corrections are negative for $\varphi_2 \sim 180^\circ$. The phase of zero corrections, $\varphi_2(\theta_{12} = 0^\circ)$, depends on m_1 and in general deviates from 90°. The deviation is due to the Yukawa interaction effects that produce the positive shift for a strong Yukawa coupling hierarchy as we discussed before. The shift occurs both above and between the seesaw scales (see Fig. 6.8(b)).
In Fig. 6.9 we show contours of constant corrections in the $m_1 - \varphi_2$ plane, and in Fig. 6.10, an explicit dependence of $\Delta\theta_{12}$ on m_1 for different values of φ_2. The line $\Delta\theta_{12} = 0^\circ$, is close to $\varphi_2 = 90^\circ$, 270° for $m_1 \to 0$, and it approaches 180° with increase of m_1 when the spectrum becomes strongly degenerate. The pattern is nearly symmetric with respect to $\varphi_2 = 180^\circ$ for small m_1, the asymmetry appears for $m_1 > 3 \cdot 10^{-3}$ eV.

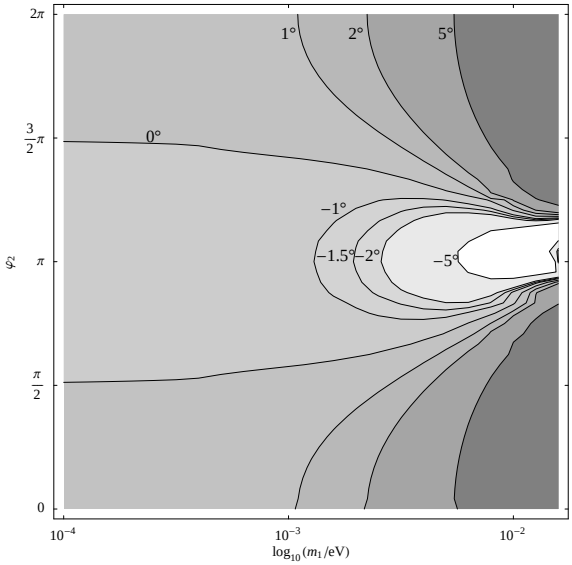

Figure 6.9: Contours of constant RG corrections to θ_{12} (figures at the curves) in the $\varphi_2 - m_1$ plane in the case of the SM and a normal mass hierarchy.

The line $\Delta\theta_{12} = 2^\circ$ restricts the region consistent with the QLC relations. Along the contours $\Delta\theta_{12} = -1.5^\circ$ the best fit experimental value for θ_{12} can be reproduced. This corresponds to $m_1 > 2{\cdot}10^{-3}$ eV and $\varphi_2 \sim 150^\circ - 210^\circ$. Large negative corrections appear in the region $m_1 > 5{\cdot}10^{-3}$ eV and $\varphi_2 \sim 180^\circ$.

6.3.4 Renormalization of 1-3 Mixing

In the scenario discussed in this thesis, the 1-3 mixing is non-zero and relatively large at the flavor-breaking scale

$$\sin^2\theta_{13} \approx 0.024\ . \tag{6.24}$$

Notice that θ_{13}

- interferes with the 1-2 mixing in the QLC relations as we discussed before;
- produces sub-leading effects in the renormalization of θ_{12};
- can provide further bounds on the considered scenario if RG corrections are positive and large.

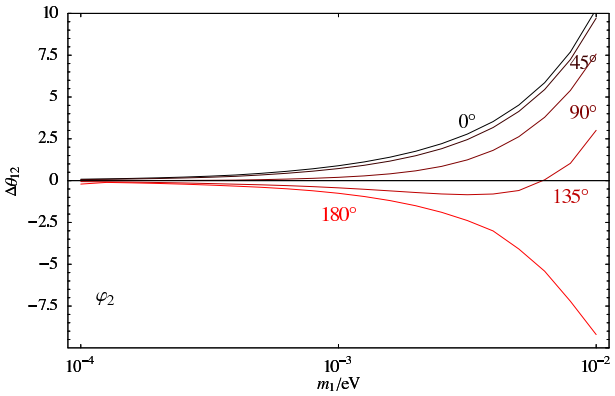

Figure 6.10: The dependence of the RG correction $\Delta\theta_{12}$ on m_1 for different values of φ_2 (figures at the curves) in the SM with a normal mass hierarchy.

The dominant contribution to the renormalization of θ_{13} is given by

$$64\pi^2\dot{\theta}_{13} = C_\nu \sin 2\theta_{12} \sin 2\theta_{23} (\mathcal{A}^+_{13} - \mathcal{A}^+_{23}), \tag{6.25}$$

where $\mathcal{A}^+_{i3}$ is given in App. C.1. In our case $\sin 2\theta_{12} > 0°$, $\sin 2\theta_{23} > 0°$, $\delta \approx 180°$ and for vanishing Majorana CP phases, $\varphi_i = 0°$, the dominant contribution can be approximated to

$$64\pi^2\dot{\theta}_{13} = C_\nu \sin 2\theta_{12} \sin 2\theta_{23} (\mathcal{Q}^+_{23} - \mathcal{Q}^+_{13}), \tag{6.26}$$

and the last factor in Eq. (6.26): $\mathcal{Q}^+_{23} - \mathcal{Q}^+_{13} = \mathcal{A}^+_{13} - \mathcal{A}^+_{23}$ is negative, irrespective of the mass hierarchy. Consequently θ_{13} increases when running to low energies. For non-vanishing phases φ_i this factor can be positive, thus leading to a decrease of θ_{13} when μ decreases.
In the case of a strong mass hierarchy Eq. (6.25) gives

$$64\pi^2\dot{\theta}_{13} = -2 \sin 2\theta_{12} \sin 2\theta_{23} \cos(\delta - \varphi_2) \sqrt{\zeta}. \tag{6.27}$$

The running is suppressed by a small mass ratio. Therefore only a small RG effect on the 1-3 mixing appears for the hierarchical (normal as well as inverted) case. For instance, we find that for the parameter sets used in Fig. 6.2 (MSSM), the correction $\Delta\theta_{13}$ is always smaller than 0.2°. In the SM, it is smaller than 0.3°.
For the degenerate spectrum, there can be a larger effect which strongly depends on the CP phases. From Eq. (6.25) we find

$$64\pi^2\dot{\theta}_{13} \approx 2 \sin 2\theta_{12} \sin 2\theta_{23} \frac{m_1^2}{\Delta m^2_{31}} [\cos(\delta - \varphi_1) - \cos(\delta - \varphi_2)]. \tag{6.28}$$

Notice that for zero CP phases the cancellation occurs again. In the MSSM for $m_1 = 0.03$ eV and $\tan\beta = 50$, we find $\Delta\theta_{13} \sim 0.5°$. In contrast, for $\delta = \varphi_1 = 180°$ and $\varphi_2 = 0°$ the two terms in Eq. (6.28) sum up and we obtain running towards larger values: $64\pi^2\dot{\theta}_{13} \approx 4 \sin 2\theta_{12} \sin 2\theta_{23}$. Consequently θ_{13} becomes smaller at low energies.

6.3.5 Level Crossing Points

As we have established in Sec. 3.4 the spectrum of the RH Majorana neutrinos is generically hierarchical. However, there are level crossing points, where two of the RH neutrino masses become equal [212]. When the two lighter RH neutrino states $M_1 \approx M_2$ are degenerate, it is of special

interest for the generation of the baryon asymmetry in the Universe, since in this case resonant leptogenesis [233] becomes possible which produces a large enough asymmetry in spite of the smallness of the masses and consequently, a large wash-out effect.
From Eq. (3.80) we find

$$M_1 = \frac{2m_t^2\epsilon'^4}{\tilde{m}_1+\tilde{m}_2}, \quad M_2 = \frac{2m_t^2\epsilon^2(\tilde{m}_1+\tilde{m}_2)}{(\tilde{m}_1+\tilde{m}_2)\tilde{m}_3+2\tilde{m}_1\tilde{m}_2}. \tag{6.29}$$

It is easy to see that due to the smallness of ϵ the condition $M_1 \approx M_2$ can be satisfied only in the case of strong mass degeneracy $|m_1| \approx |m_2| \approx m_0$ when

$$\tilde{m}_1+\tilde{m}_2 = \frac{\Delta m^2_{21}}{2m_0} \approx 0. \tag{6.30}$$

Then from the condition $M_1 \approx M_2$ we find

$$m_0 = \sqrt{\frac{\Delta m^2_{21}}{2\sqrt{2}\epsilon}} \sim 0.1 \text{ eV}. \tag{6.31}$$

In this special case the mass

$$M_1 \approx M_2 \frac{4m_t^2\epsilon'^4 m_0}{\Delta m^2_{21}} = M_1^{NH}\frac{2m_0}{\sqrt{\Delta m^2_{21}}} \tag{6.32}$$

is enhanced by a factor $2m_0/\sqrt{\Delta m^2_{21}} \sim 20$ and the third mass is much smaller than in the hierarchical case:

$$M_3 \approx \frac{m_t^2}{2m_3}, \tag{6.33}$$

that is, smaller by a factor $m_1^{NH}/m_3 < 10^{-3}$.
The level crossing condition Eq. (6.30) implies opposite Majorana CP phases and it coincides with the condition of strong suppression of RG effects. It also implies smallness of the 1-1 element of the matrix $m_{\rm bm}$. The condition for level crossing differs from that in [212] since here we require the neutrino Dirac matrix to be diagonal in the basis where the mass matrix of light neutrinos has exactly bimaximal form. If instead we use a generic matrix with non-maximal 1-2 mixing the level crossing condition can be realized for the hierarchical spectrum [212].

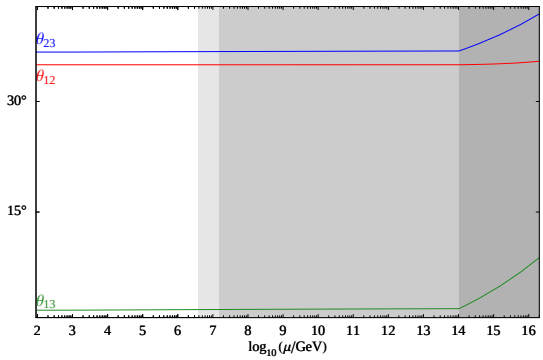

Figure 6.11: Examples of running of mixing angles in the case of $M_1 \approx M_2$ in MSSM and a normal mass ordering. We show the dependence of θ_{12}, θ_{13} θ_{23} on μ for $\tan\beta = 10$, $\varphi_1 = 0°$, $\varphi_2 = 180°$ and $m_1 = 0.13$ eV.

In Fig. 6.11 we show the RG evolution of the mixing angles for parameters that correspond to the level crossing point $M_1 = M_2$. In this point $M_1 = M_2 = 8 \cdot 10^6$ GeV, $M_3 = 8 \cdot 10^{13}$ GeV, $\varphi_1 = 0°$,

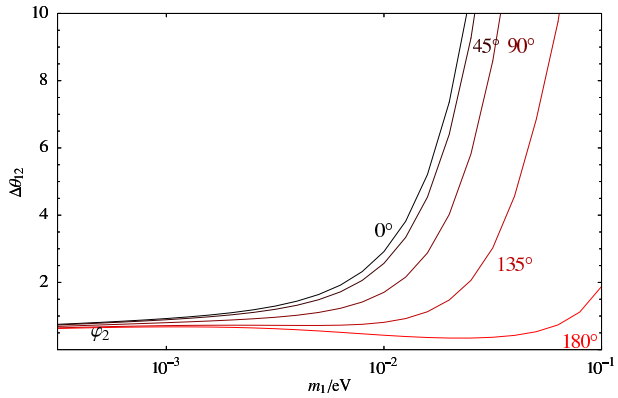

Figure 6.12: The dependence of the RG correction $\Delta\theta_{12}$ on m_1 for different values of φ_2 (figures at the curves) in the MSSM with a normal mass hierarchy and $\tan\beta = 10$. The boundary condition is at M_{Pl}.

$\varphi_2 = 180°$, $m_1 = 0.13$ eV. Note, that the equality of M_1 and M_2 is broken by RG effects. The angle θ_{12} evolves very weakly due to the cancellation $\mathcal{Q}_{12}^+ = \mathcal{S}_{12}^+ \approx 0$ related to Eq. (6.30). In contrast, the 1-3 mixing evolves substantially above the thresholds: $\Delta\theta_{13} = 7°$. The same holds for the 2-3 mixing which can influence the second QLC relation.
We find that in this crossing point the solar mass squared difference becomes large even if it is very small at the boundary. So, the solar mass squared difference has a radiative origin. The atmospheric mass squared difference decreases by a factor ~ 2.

6.3.6 Evolution above the GUT scale

For $\Lambda > \Lambda_{\rm GUT}$ the RG evolution should be also performed above the GUT scale. Restoration of the GUT symmetry and unification of the gauge couplings does not prevent from different running of the Yukawa couplings, and therefore, from a change of the mixing angles. Renormalization of mixing angles would stop after a possible unification of the Yukawa couplings which can be related, *e.g.*, to the restoration at Λ of a non-Abelian flavor symmetry. An alternative is the boundary at the string or Planck scale, where the Yukawa couplings are formed and their properties are determined immediately by some symmetry or/and string selection rules.
For illustration we performed the running in the MSSM up to the Planck scale (ignoring possible GUT effects, which are highly model-dependent). In Fig. 6.12 we show the dependence of $\Delta\theta_{12}$ on m_1 for the same (QLC) initial conditions at the Planck scale: $\Lambda = M_{Pl} = 1.2 \cdot 10^{19}$ GeV. The RG effect becomes much larger. In particular the contribution from the region above the seesaw scale due to large Yukawa coupling Y_ν increases substantially. It is enhanced in comparison to the case of running up to $\Lambda_{\rm GUT}$ by the factor

$$\frac{\log(M_{Pl}/M_3)}{\log(\Lambda_{\rm GUT}/M_3)} \tag{6.34}$$

that can be as large as 3 - 5 in some cases. Still for $\varphi_2 = 180°$ or for small m_1 the RG effects are suppressed and can be consistent with the QLC relations.
Similar RG effects are expected in SU(5) with RH neutrinos. In fact, no new diagrams with large Y_ν appear. The effect of charged lepton couplings Y_e is enhanced by a factor 4 above $\Lambda_{\rm GUT}$ due to the loop diagrams with down quarks (squarks) and $H^{1/3}$ charged Higgs bosons (Higgsinos).
The flavor-diagonal parts of the RG equations do influence the angles only indirectly through the change of the mass eigenvalues. Thus, the main effect of these interactions is due to the evolution of Δm^2_{12}.

6.4 Triplet (Type II) Seesaw Model

In this section, we derive the RG equations of the mixing parameters in the triplet (type II) seesaw model. Chao and Zhang [234] have derived the formulas in the approximation $|Y_e| \ll |Y_\Delta|$ which captures the dominant effects as long as there is a strong hierarchy. Here, we calculate the RG equations exactly [3] and compare them with their results. The evolution of the neutrino mass matrix and the charged lepton Yukawa couplings are given by Eqs. (6.1, 6.4) in Sec. 6.1. Since Y_Δ is directly proportional to the neutrino mass matrix, we can express P and F in terms of physical parameters.

$$P = C_e \mathrm{diag}(y_e^2, y_\mu^2, y_\tau^2) + C_\Delta U_{\mathrm{MNS}}^* \mathrm{diag}(y_1^2, y_2^2, y_3^2) U_{\mathrm{MNS}}^T \tag{6.35a}$$

$$F = D_e \mathrm{diag}(y_e^2, y_\mu^2, y_\tau^2) + D_\Delta U_{\mathrm{MNS}}^* \mathrm{diag}(y_1^2, y_2^2, y_3^2) U_{\mathrm{MNS}}^T \,, \tag{6.35b}$$

where $y_i = m_i / \langle\Delta\rangle$ and $\langle\Delta\rangle$ is the VEV of the Higgs triplet Δ. Note, that the Majorana phases drop out in the definition of P and F in flavor basis. Hence the RG equations of the angles and the Dirac CP phase are independent of the Majorana phases, as it can be seen below.
We derive the RG equations by using the technique outlined in Sec. 6.1. In all numerical examples, we set $M_\Delta(\Lambda_{\mathrm{GUT}}) = 10^{10}\,\mathrm{GeV}$. As we are only interested in showing the generic features of the RG evolution, we choose the Higgs self-couplings to be $\Lambda_{1,2,4,5} = 0.5$ for simplicity, since they only indirectly influence the RG evolution of the angles and the flavor-dependent part of the RG equations of the masses. In a realistic model, the parameters Λ_i have to satisfy certain relations to produce the desired VEV structure, e.g. see [235] for the RG effect in the Higgs sector.
In the following, we present all formulas in the approximation $y_e \ll y_\mu \ll y_\tau$ and $\theta_{13} \ll 1$. The exact formulas can be downloaded from `http://www.mpi-hd.mpg.de/~mschmidt/rgeTriplet`.

6.4.1 Running of Masses

The main contributions to the RG equations of the masses

$$16\pi^2 \frac{\dot{m}_1}{m_1} = \mathrm{Re}\,\alpha_\nu + 2\,C_\Delta \frac{m_1^2}{\langle\Delta\rangle^2} + 2 C_e y_\tau^2 \sin^2\theta_{12} \sin^2\theta_{23} + \mathcal{O}(\theta_{13}) \tag{6.36a}$$

$$16\pi^2 \frac{\dot{m}_2}{m_2} = \mathrm{Re}\,\alpha_\nu + 2\,C_\Delta \frac{m_2^2}{\langle\Delta\rangle^2} + 2 C_e y_\tau^2 \cos^2\theta_{12} \sin^2\theta_{23} + \mathcal{O}(\theta_{13}) \tag{6.36b}$$

$$16\pi^2 \frac{\dot{m}_3}{m_3} = \mathrm{Re}\,\alpha_\nu + 2\,C_\Delta \frac{m_3^2}{\langle\Delta\rangle^2} + 2 C_e y_\tau^2 \cos^2\theta_{23} + \mathcal{O}(\theta_{13}) \tag{6.36c}$$

are the flavor–independent term $\mathrm{Re}\,\alpha_\nu$ and the flavor–dependent term $2\,C_\Delta m_i^2 / \langle\Delta\rangle^2$. These equations agree well with the result by Chao and Zhang [234] in their approximation. As the smallness of neutrino masses is usually explained by a small VEV of the Higgs triplet $\langle\Delta\rangle$, the eigenvalues y_i of the Yukawa coupling Y_Δ can be of $\mathcal{O}(1)$. This in turn leads to sizable flavor-dependent RG effects. Furthermore, the evolution of the mass squared differences are mainly given by

$$16\pi^2 \frac{\Delta\dot{m}_{ji}^2}{\Delta m_{ji}^2} \approx 2\,\mathrm{Re}\,\alpha_\nu + 4\,C_\Delta \frac{m_j^2 + m_i^2}{\langle\Delta\rangle^2} \tag{6.37}$$

in the SM and MSSM with small $\tan\beta$. There can be a cancellation of the RG effect depending on the parameters Λ_i in the Higgs potential and the sign of C_Δ, but generically the RG effect in

[3] A Mathematica package with the exact formulas can be downloaded from `http://www.mpi-hd.mpg.de/~mschmidt/rgeTriplet/`.

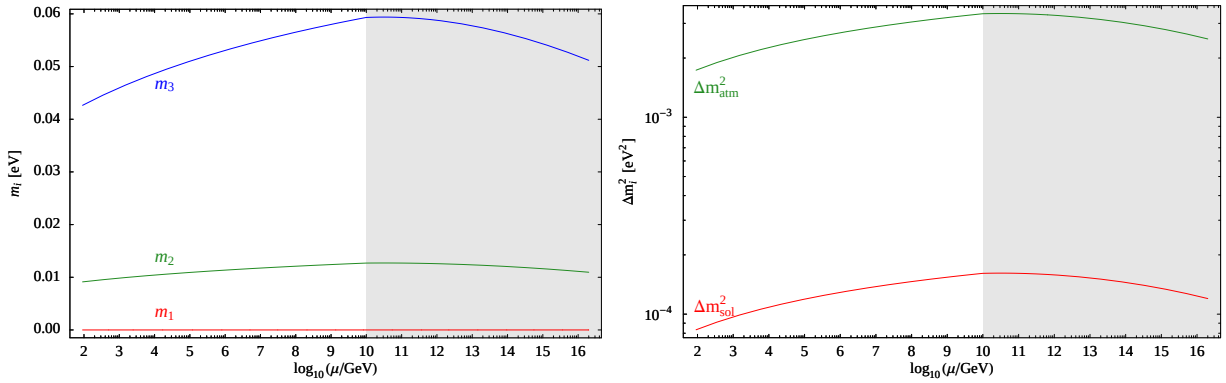

(a) Evolution of neutrino masses

(b) Evolution of the mass squared differences

Figure 6.13: As input values, we have chosen tri-bimaximal mixing at the GUT scale, $m_1 = 0\,\mathrm{eV}$, $\Delta m^2_{32} = 2.5 \cdot 10^{-3}\,\mathrm{eV}^2$, $\Delta m^2_{21} = 1.2 \cdot 10^{-4}\,\mathrm{eV}^2$, $M_\Delta = 10^{10}\,\mathrm{GeV}$ and $\Lambda_6 = 2.5\,10^{-5} M_\Delta$, corresponding to $\langle\Delta\rangle = 0.15\,\mathrm{eV}$. The shadowed area indicates the full theory including the Higgs triplet. It is integrated out at the energy scale between the shadowed and the white area.

the effective theory is large, as it can be seen in Fig. 6.13. This is just one possible example. The precise RG effect strongly depends on the parameters in the Higgs potential Λ_i. The charged lepton masses depend on the neutrino masses in a flavor non–diagonal way:

$$16\pi^2 \frac{\dot{m}_e}{m_e} = \mathrm{Re}\,\alpha_e + D_\Delta \left(\frac{m_1^2}{\langle\Delta\rangle^2} \cos^2\theta_{12} + \frac{m_2^2}{\langle\Delta\rangle^2} \sin^2\theta_{12} \right) + \mathcal{O}(\theta_{13}) \tag{6.38a}$$

$$16\pi^2 \frac{\dot{m}_\mu}{m_\mu} = \mathrm{Re}\,\alpha_e + D_\Delta \left[\frac{m_3^2}{\langle\Delta\rangle^2} \sin^2\theta_{23} + \left(\frac{m_2^2}{\langle\Delta\rangle^2} \cos^2\theta_{12} + \frac{m_1^2}{\langle\Delta\rangle^2} \sin^2\theta_{12} \right) \cos^2\theta_{23} \right] + \mathcal{O}(\theta_{13}) \tag{6.38b}$$

$$16\pi^2 \frac{\dot{m}_\tau}{m_\tau} = \mathrm{Re}\,\alpha_e + D_\Delta \left[\frac{m_3^2}{\langle\Delta\rangle^2} \cos^2\theta_{23} + \left(\frac{m_2^2}{\langle\Delta\rangle^2} \cos^2\theta_{12} + \frac{m_1^2}{\langle\Delta\rangle^2} \sin^2\theta_{12} \right) \sin^2\theta_{23} \right] + D_e y_\tau^2 + \mathcal{O}(\theta_{13})\,. \tag{6.38c}$$

6.4.2 Running of Mixing Angles

We present the equations for the mixing angles in the approximation of vanishing y_e, y_μ and θ_{13}:

$$16\pi^2 \dot{\theta}_{12} = -\frac{1}{2} \left[D_\Delta \frac{\Delta m^2_{21}}{\langle\Delta\rangle^2} + C_e y_\tau^2 \frac{(m_2 + m_1)^2}{\Delta m^2_{21}} \sin\theta_{23} \right] \sin 2\theta_{12} + \mathcal{O}(\theta_{13}) \tag{6.39a}$$

$$16\pi^2 \dot{\theta}_{13} = -\frac{C_e}{2} y_\tau^2 \frac{(m_2 - m_1) m_3}{(m_3 - m_1)(m_3 - m_2)} \cos\delta \sin 2\theta_{12} \sin 2\theta_{23} + \mathcal{O}(\theta_{13}) \tag{6.39b}$$

$$\begin{aligned} 16\pi^2 \dot{\theta}_{23} = -\frac{1}{2} \Bigg[& D_\Delta \left(\frac{m_3^2}{\langle\Delta\rangle^2} - \frac{m_1^2}{\langle\Delta\rangle^2} \sin^2\theta_{12} - \frac{m_2^2}{\langle\Delta\rangle^2} \cos^2\theta_{12} \right) \\ & + C_e y_\tau^2 \frac{m_3^2 - m_1 m_2 + (m_2 - m_1)\, m_3 \cos 2\theta_{12}}{(m_3 - m_2)\,(m_3 - m_1)} \Bigg] \sin 2\theta_{23} + \mathcal{O}(\theta_{13})\,. \end{aligned} \tag{6.39c}$$

The equations of θ_{12} and θ_{13} agree well with the result by Chao and Zhang [234] in their approximation, however, we disagree in the RG equation of θ_{23} by a factor of 2. In order to support our

result, let us note, that the evolution of θ_{23} in Fig. 6.14 agrees well with our result. It is obtained by running the mass matrices to the low-energy scale before they are diagonalized, which is different from the calculation of the RG equations of the mixing parameters. The two contributions to the running from charged leptons and neutrinos can be of the same order of magnitude and it strongly depends on the hierarchy of neutrino masses which of the two contributions is dominant. The contribution coming from the evolution of the neutrino mass matrix ($\propto C_e$) shows almost the same features as in the effective theory:

- there is an enhancement factor which is proportional to $\frac{m_0^2}{\Delta m_{ji}^2}$, where m_0 denotes the mass scale of neutrinos;
- the running strongly depends on $\tan\beta$ through the charged lepton Yukawa couplings;
- vanishing mixing is a fixed point.

In contrast to the effective theory, however, there is no dependence on Majorana phases. This still holds for the exact equations. The RG evolution of the mixing angles is only influenced by the Dirac CP phase. On the other hand, the contribution from the charged leptons shows a completely different dependence on the Yukawa couplings. It is mainly proportional to the corresponding mass squared difference divided by the square of the VEV of the Higgs triplet. Hence, there is no large enhancement factor and no dependence on $\tan\beta$ in the SUSY case. Thus the overall size of the RG effect mainly depends on $\langle\Delta\rangle$. The formula

$$\dot{\theta}_{ij} \sim \frac{\Delta m_{ji}^2}{\langle\Delta\rangle^2} \sin 2\theta_{ij} \; . \tag{6.40}$$

gives a good estimate for the running in the strongly hierarchical case. The sign of the RG effect is determined by the sign of the mass squared difference and the factor D_Δ. As D_Δ is positive in the SM and MSSM, θ_{23} is evolving to larger values coming from the high renormalization scale for a normal hierarchy. Furthermore, the β–function is approximately proportional to $\sin 2\theta_{ij}$ implying that a vanishing angle remains small. Taking into account these generic features, the RG effect from the charged leptons is largest on θ_{23} due to the combination of a large mass squared difference and a large mixing angle. Moreover, as it can be seen from equations, zero mixing is a fixed point. This is also obvious from the RG equation in matrix form, since in this configuration, P and F will be diagonal, if Y_e and Y_Δ are diagonal. In Fig. 6.14, we have plotted the evolution of mixing angles in the SM for a strongly hierarchical spectrum in order to suppress the effect coming from the effective D5 operator. The gross features of the running can be immediately seen: the only sizable effect is on θ_{23} due to the large angle and mass squared difference. As it can be seen from Fig. 6.14, the RG effect can be estimated by a LL approximation to

$$\Delta\theta_{ij} \approx -\frac{D_\Delta}{2} \frac{\Delta m_{ji}^2}{\langle\Delta\rangle^2} \sin 2\theta_{ij} \ln\left(\frac{\Lambda}{M_\Delta}\right) \; . \tag{6.41}$$

The contribution to θ_{13} coming from the charged leptons vanishes in our approximation. For non–vanishing θ_{13}, it is given by

$$-\frac{D_\Delta}{2}\left(\frac{m_3^2}{\langle\Delta\rangle^2} - \frac{m_1^2}{\langle\Delta\rangle^2}\cos^2\theta_{12} - \frac{m_2^2}{\langle\Delta\rangle^2}\sin^2\theta_{12}\right)\sin 2\theta_{13} \tag{6.42}$$

Let us comment on the configuration $\theta_{13} = m_3 = 0$, which is stable under the RG in the effective theory. Vanishing mass eigenvalues remain zero, as it can be seen from Eq. (6.36c), but θ_{13} receives

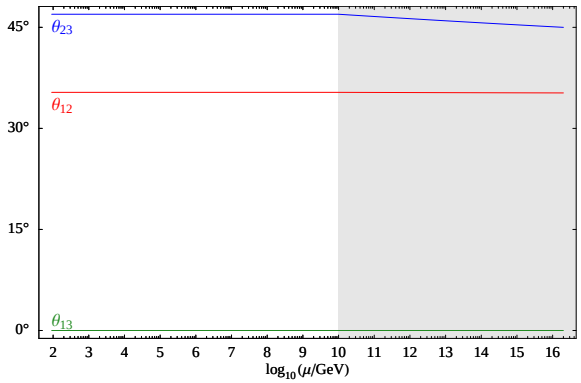

Figure 6.14: Plot showing the evolution of the leptonic mixing angles in the SM. As input values, we have chosen tri-bimaximal mixing at the GUT scale, $m_1 = 0\,\mathrm{eV}$, $\Delta m^2_{32} = 2.5 \cdot 10^{-3}\,\mathrm{eV}^2$, $\Delta m^2_{21} = 1.2 \cdot 10^{-4}\,\mathrm{eV}^2$, $M_\Delta = 10^{10}\,\mathrm{GeV}$ and $\Lambda_6 = 2.5\,10^{-5} M_\Delta$, corresponding to $\langle\Delta\rangle = 0.15\,\mathrm{eV}$. The shadowed area indicates the full theory including the Higgs triplet. It is integrated out at the energy scale between the shadowed and the white area.

corrections

$$16\pi^2\dot{\theta}_{13} = \frac{C_e}{2}\frac{\Delta m^2_{21}}{\langle\Delta\rangle^2}\frac{y_e^2\left(y_\tau^2 - y_\mu^2\right)}{\left(y_\tau^2 - y_e^2\right)\left(y_\mu^2 - y_e^2\right)}\cos\delta\sin 2\theta_{12}\sin 2\theta_{23} + \mathcal{O}(\theta_{13},\, y_3) \tag{6.43}$$

Thus $\theta_{13} = m_3 = 0$ is not stable under the RG. However, the effect is negligible, because $\left(\frac{y_e}{y_\mu}\right)^2 \frac{\Delta m^2_{21}}{\langle\Delta\rangle^2}$ is very small and $m_3 = 0$ is stable.

6.4.3 Running of Phases

The RG evolution of the phases is rather small and can be neglected in most cases:

$$16\pi^2\dot{\delta} = \frac{C_e}{2}\frac{(m_2 - m_1)m_3}{(m_3 - m_1)(m_3 - m_2)}y_\tau^2\sin\delta\sin 2\theta_{12}\sin 2\theta_{23}\,\theta_{13}^{-1} + \mathcal{O}(\theta_{13}) \tag{6.44a}$$

$$\begin{aligned}16\pi^2\dot{\varphi}_1 = -2\Bigg[&2C_e y_\tau^2\frac{(m_1^2 + m_3^2)m_2\sin^2\theta_{23} - ((m_1^2 + m_2^2)\sin^2\theta_{12} - m_1 m_2(\cos 2\theta_{12} - \cos 2\theta_{23}))m_3}{(m_3 - m_1)(m_3 - m_2)(m_2 - m_1)}\cot\theta_{12}\\ &+ D_\Delta\frac{\Delta m^2_{21}}{\langle\Delta\rangle^2}\sin 2\theta_{12}\Bigg]\cot\theta_{23}\sin\delta\,\theta_{13} + \mathcal{O}(\theta_{13}^2)\end{aligned} \tag{6.44b}$$

$$\begin{aligned}16\pi^2\dot{\varphi}_2 = -2\Bigg[&2C_e y_\tau^2\frac{-(m_1^2 + m_2^2)m_3\cos^2\theta_{12} + m_1((m_2^2 + m_3^2)\sin^2\theta_{23} + m_2 m_3(\cos 2\theta_{12} + \cos 2\theta_{23}))}{(m_3 - m_1)(m_3 - m_2)(m_2 - m_1)}\tan\theta_{12}\\ &+ D_\Delta\frac{\Delta m^2_{21}}{\langle\Delta\rangle^2}\sin 2\theta_{12}\Bigg]\cot\theta_{23}\sin\delta\,\theta_{13} + \mathcal{O}(\theta_{13}^2)\,,\end{aligned} \tag{6.44c}$$

because the leading order of the Majorana phases is of order θ_{13}. Only the Dirac CP phase δ involves a term which is inversely proportional to θ_{13}. Thus, there is a sizable effect for small θ_{13}. For vanishing θ_{13}, δ has to vanish (for realistic values of θ_{12} and θ_{23}) in order to ensure analyticity of $\delta(t)$ analogous to the effective theory [59]. The RG equation of the Dirac CP phase δ does like the angles not depend on the Majorana phases φ_i.
We agree with the result of Chao and Zhang [234] for the Dirac CP phase δ in their approximation. However, we completely disagree for the Majorana phases. Their result for the Majorana phases is not sensible, since the Majorana phases are physical parameters even in the limit of vanishing 1-3 mixing unlike δ. Therefore, the RG equations should not show a pole at vanishing 1-3 mixing.

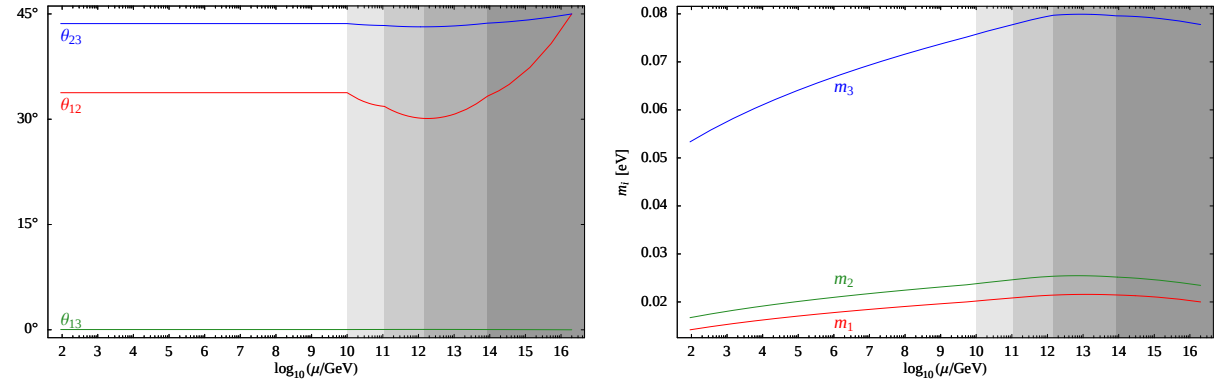

(a) Angles (b) Masses

Figure 6.15: In the type I+II seesaw case, there is a complicated interplay between the two contributions to the neutrino mass matrix. Here, we just plot an example for the following initial values at the GUT scale: $M_\Delta = 10^{10}\,\mathrm{GeV}$, $\Lambda_6 = 4.56\cdot 10^9\,\mathrm{GeV}$, $m_1 = 0.02\,\mathrm{eV}$, $\Delta m^2_{21} = 1.5\cdot 10^{-4}\,\mathrm{eV}^2$, $\Delta m^2_{32} = 5.5\cdot 10^{-3}\,\mathrm{eV}^2$, $\theta_{12} = \theta_{23} = \frac{\pi}{4}$, $\theta_{13} = 0$, $\delta = \varphi_1 = \varphi_2 = 0$, $Y_\nu = 0.37\,\mathrm{diag}\left(10^{-2},\ 10^{-1},\ 1\right)$, where Y_Δ is chosen diagonal $Y_\Delta = \mathrm{diag}\left(1.3\cdot 10^{-5},\ 1.5\cdot 10^{-5},\ 5.1\cdot 10^{-5}\right)$ and M is chosen appropriately to produce bimaximal mixing. The differently shaded areas indicate the different energy ranges of the various EFTs. At each border, a particle, either a RH neutrino or the Higgs triplet, is integrated out.

6.4.4 RG Evolution in Type I+II Model

In the type I+II case, it is not possible to express the RG equations in terms of mixing parameters. Therefore one has to resort to numerical calculations. For this purpose, we have extended the Mathematica package REAP, which is available on the webpage `http://www.ph.tum.de/~rge`, to include a left–handed triplet.
To illustrate the largeness of RG effects in the type I+II seesaw scenario, we show an example, where bimaximal mixing at high energy evolves to the large mixing angle (LMA) solution at low energy. In previous works [64, 66, 67, 69], this evolution was due to an inverted hierarchy in the neutrino Yukawa couplings Y_ν or large imaginary off-diagonal entries. Here, the relevant matrix $Y_\nu^\dagger Y_\nu$ is real and has a normal hierarchy. In addition, the singular values of the Yukawa coupling matrix Y_Δ are small ($\mathcal{O}(10^{-5})$). In spite of the small couplings, there is a sizable effect on θ_{12} which can be seen in Fig. 6.15. It is due to the different RG equations of the contributions to the neutrino mass matrix.

In our example, we have chosen Λ_6 to be relatively large $\Lambda_6 = \mathcal{O}(10^9)\,\mathrm{GeV}$, because it receives corrections of the order of $M_3\,(Y_\nu)^2_{33}\,(Y_\Delta)_{33}$. The evolution of the mixing angles θ_{12} and θ_{23} is highly non–linear above the threshold of the Higgs triplet. Hence, a LL approximation is not possible. In the MSSM, the equations for the mixing angles presented in [69] are valid at each renormalization scale μ. Hence, θ_{12} is increasing, as long as there there are no imaginary off-diagonal entries and there is a normal hierarchy in the neutrino Yukawa couplings.

Chapter 7

Summary & Conclusions

Despite of the great success of the SM, there are several hints to physics beyond the SM, like the quantization of charge and gauge coupling unification in the MSSM, as well as the already mentioned regularities in the flavor sector. In particular, neutrino masses might be related to physics at a high energy scale via the seesaw mechanism because of their smallness and different flavor structure.

Therefore, in Chapter 4, we have studied a mechanism which cancels the large hierarchies in the neutrino mass matrix and allows to have a special structure that is completely different from all charged fermions. It works within the cascade seesaw mechanism which can be viewed as an extension of the standard seesaw mechanism. We showed a possible connection of the cancellation mechanism and the QLC relations and argued that the cancellation mechanism allows to implement a special neutrino symmetry. The light neutrino mass matrix is given by the same formula Eq. (3.20) in the case of singular M_{SS}, which leads to a massless neutrino. As vanishing masses can only be generated between mass thresholds when there are several contributions to the neutrino mass matrix, the vanishing mass is protected in the MSSM and receives corrections proportional to the logarithmic hierarchy between the largest and smallest mass threshold in the SM. Otherwise the light neutrino mass matrix is just rescaled. The DS structure will dominate over the LS contribution if the additional singlets are heavier than the scale $\langle\Delta\rangle_N$.

We outlined several possibilities to obtain the DS structure and, additionally, we have presented three different realizations of the cancellation mechanism, one based on an extended gauge symmetry, more precisely the GU group E_6, and two realizations with non-Abelian discrete flavor symmetries in the context of SO(10). These two predict nearly maximal atmospheric mixing. The realization with the flavor symmetry T_7 is SUSY and achieves a partial cancellation of the hierarchy. The choice of scales requires to include the LS contribution which cancels the remaining hierarchy. Thus, the weak hierarchy in the neutrino mass matrix is explained by an interplay between the LS and DS contribution. The DS contribution alone cannot lead to a viable phenomenology. We studied corrections by higher-dimensional operators which can be controlled by an additional Z_7 symmetry. The realization with the discrete group $\Sigma(81)$ has to be non-SUSY due to the group structure. It leads to a complete cancellation of the hierarchy, while the additional singlet masses are close to the Planck scale. Hence, the DS contribution dominates. In the leading order, two masses are degenerate and the mass matrix is diagonalized by the tri-bimaximal mixing matrix. However, the atmospheric mixing angle is unphysical as long as the atmospheric mass squared difference vanishes. The study of higher-dimensional operators shows that their corrections are safe, since they are always smaller than the leading order. In general, they generate a non-vanishing atmospheric mass squared difference and a phenomenologically viable neutrino mass matrix can be obtained. An additional Z_N symmetry can further suppress these corrections. Finally, since the

VEV structure of the flavons is essential, we demonstrated how the leading order can be obtained. The next-to-leading order requires a more complicated flavon potential.
As threshold corrections turn out to be important in non-SUSY theories, we studied them in Chapter 5. The interplay of different contributions to the neutrino mass matrix does not allow to derive RG equations for the mixing parameters between the seesaw scales. Therefore, we calculated the RG effect in the LL approximation. Our main result, here, is that the quantum corrections can be summarized as a rescaling of the RH neutrino masses at leading order. We discussed the RG effects beyond LL approximation qualitatively. Furthermore we argued, that the results immediately apply, if the vertex corrections to the Yukawa couplings and the effective operator factorize and the mass term does not receive vertex corrections.
We applied our results to the cascade seesaw mechanism. The corrections can be described by a rescaling of the additional singlets as well as the RH neutrinos, i.e. all particles which have been integrated out. The rescaling of the RH neutrinos leads to an effective standard seesaw contribution besides the corrections to the DS and LS term, although the standard seesaw term exactly cancels without RG corrections.
Hence, the cancellation mechanism is stable with respect to the RG in the MSSM, i.e. its structure does not change, since RG corrections can be factorized in SUSY theories. Thus, in the T_7 realization, they strongly depend on $\tan\beta$ and the absolute neutrino mass scale which has not been specified. The RG effect in a concrete model is easily obtained by the usual formulas in the effective theory. In non-SUSY theories, the mass thresholds of the RH neutrinos are important, since they can change the structure of the DS formula and can neither be factorized like the wave function renormalization nor absorbed in parameters of the full theory like the threshold corrections from additional singlets. In the framework of the cancellation mechanism, they can be large, since there is a large hierarchy in the RH neutrino masses. The results have been analytically discussed in several examples where M_{SS} takes a particularly simple form. Small perturbations in vanishing elements can lead to large effects. However, in the $\Sigma(81)$ model, they can be absorbed in coefficients of higher-dimensional operators.
In Chapter 6, we have discussed quantum corrections to several models. The model based on the $L_\mu - L_\tau$ symmetry leads to a quasi-degenerate neutrino mass spectrum and equal CP parities of the masses. Therefore, there are large RG corrections to the solar mixing angle as well as the mass squared differences and it is crucial to take them into account.
Furthermore, we did a comprehensive study of RG corrections to the QLC relations under the assumption that they are realized with "lepton mixing = bi-maximal mixing$-$CKM". In the MSSM, RG corrections to θ_{12} are generically positive due to a dominant effect of the 3-3 element of Y_ν. So, they worsen the agreement of the predicted θ_{12} with the experimental data. Small negative corrections, $|\Delta\theta_{12}| < 0.5^\circ$, can appear for opposite CP parities and an inverted mass hierarchy, in which case the main terms in the RG equations are strongly suppressed and the running is due to sub-leading effects related to non-zero 1-3 mixing. The RG corrections increase with m_1 and strongly depend on the relative Majorana phase. For $\Delta\varphi \approx 0^\circ$ the consistency of the QLC prediction for θ_{12} with the experimental data implies a strong mass hierarchy of the light neutrinos and small $\tan\beta$. For $\Delta\varphi \approx 180^\circ$ the corrections are suppressed and even the degenerate spectrum becomes allowed. For an inverted mass hierarchy RG corrections are generically enhanced by larger neutrino masses $m_{1,2}$. The situation is qualitatively different in the SM. Here important contributions follow from the vertex corrections to the D5 operator in the range between the seesaw scales. The Yukawa couplings (especially for small m_1) give sub-leading contributions. The RG corrections are negative around $\Delta\varphi \approx 180^\circ$. The corrections depend substantially on the scale Λ. The value $\Delta\theta_{12}$ can be enhanced by a factor 2–5 if Λ increases from $\Lambda_{\rm GUT}$ to M_{Pl}. For the hierarchical mass spectrum the renormalization of the 1-3 mixing is, in general, small: $\Delta\theta_{13} \sim 0.2^\circ - 0.3^\circ$, although it can be large,

$\Delta\theta_{13} \sim \theta_{13}$, for a quasi-degenerate spectrum.
We derived exact RG equations in terms of the mixing parameters in the triplet seesaw scenario. The equations have a different structure compared to the ones in the standard seesaw case as well as in the effective theory. Majorana phases do not influence the evolution of the other parameters. Hence, there is no damping of the RG effect due to phases. The main difference is the proportionality of the β-functions to the mass squared difference in contrast to the inverse proportionality in the case of an hierarchical spectrum. Hence, there is no enhancement factor and the RG effect is small as long as Y_Δ is small. Furthermore, as the RG equations of the mixing angles θ_{ij} are proportional to sin $2\theta_{ij}$, there are sizable RG corrections to the atmospheric mixing angle for a strong normal hierarchy in contrast to the standard seesaw scenario. The RG equations in the full case can only be studied numerically. The interplay of the contributions from RH neutrinos and the Higgs triplet can lead to large RG effects even in the SM.

Concluding, it is essential to consider RG effects in model building to make predictions which can be compared to the experimental data, because they can lead to substantial corrections of the predicted values at an high energy scale. The largest RG effects show up for θ_{12} and the mass squared differences in the standard seesaw as well as θ_{23} in the triplet seesaw framework. In general, they are enhanced for large $\tan\beta$ due to charged lepton and down-type quark loops. If there are two contributions to the neutrino mass matrix or any mass matrix which have different RG equations, very large corrections can be expected from the interplay of both contributions. This has been demonstrated by the threshold corrections in the standard seesaw scenario and in the type I+II seesaw framework in non-SUSY theories. Furthermore, future experiments will improve the precision of leptonic mixing parameters and neutrino masses. Therefore, even small corrections like for a strongly hierarchical spectrum will become comparable to the experimental precision.
The discussion of RG effects in already existing GU models is an interesting task in order to be able to compare their predictions of masses and mixing angles to future precision data. Besides the RG evolution of masses and mixing angles, the quantum corrections to sfermion mass matrices in SUSY theories are interesting and help to constrain SUSY GUTs (See e.g. [153].), because non-diagonal sfermion matrices lead to lepton flavor violating processes. The Mathematica package REAP can be easily extended to include the running of sfermion mass matrices.
Otherwise, the cancellation mechanism in the cascade seesaw framework offers new possibilities to combine a flavor symmetry with a GU model, since neutrino masses are related to the additional singlet sector, which can explain the differences between neutral and charged fermions. As the hierarchy in the charged fermion sector depends on the generation of the VEV hierarchy, the explicit construction of the flavon potential is an important task. Moreover, it is interesting to extend one of the presented realizations to a complete GU model, which explains all fermions masses and mixings, and to discuss its predictions for the low-energy data. The used flavor groups are minimal [82]. This proof shows, in addition, that there are three alternative small groups which allow to implement the cancellation mechanism, but have not been discussed so far. As they might overcome some of the problems of the investigated flavor groups, a study of their predictions can lead to useful results.
Anyway, the coming years will be exiting, because there are many experiments further constraining the flavor sector and the LHC which will probe the TeV region directly to investigate the Higgs mechanism and test whether there is low-energy SUSY, i.e. the MSSM or one of its extensions.

Appendix A

Conventions

In this chapter, we collect conventions, which are used throughout the thesis.

- We use RL convention for SM Yukawa couplings, i.e.

$$\overline{e_R^f} Y_e^{fg} \ell^g H_d + \overline{N}^f Y_\nu^{fg} \ell^g H_u,$$

  where e_R and N denotes the RH charged and neutral leptons, respectively. The left-handed doublet is called ℓ.

- GUT charge normalization is used for the $\mathrm{U}(1)_Y$ hypercharge, i.e. the charge q_Y is related to the charge in GUT normalization by $q_Y^U = \sqrt{\frac{3}{5}} q_Y$ and the gauge coupling satisfies $g_1^2 = \frac{3}{5} \left(g_1^U\right)^2$.

- The Fourier transformation from position space to momentum space is defined by $\exp^{-\mathrm{i} p_\mu x^\mu}$. Therefore ∂_μ in position space corresponds to $-ip_\mu$ in momentum space.

A.1 Mixing Matrices

The connection between the flavor basis and the mass basis in the SM is described by two mixing matrices $V_{\mathrm{CKM}} = V_{\mathrm{CKM}}(\vartheta_{12}, \vartheta_{13}, \vartheta_{23}, \delta^q)$ in the quark and $U_{MNS} = U_{MNS}(\theta_{12}, \theta_{13}, \theta_{23}, \delta, \varphi_1, \varphi_2)$ in the leptonic sector. We use the standard parameterization which is defined in App. A.2 for both matrices. Mixing angles in the leptonic sector are denoted by θ_{ij}, the Dirac CP phase by δ and the Majorana phases are referred to as φ_i. The corresponding mixing angles and Dirac CP phase in the quark sector are denoted by ϑ_{ij} and δ^q. Sometimes, the quark mixing is expressed in terms of matrix elements of the CKM matrix which can be approximately described by the Wolfenstein parameterization [236]

$$V_{\mathrm{CKM}} = V_{u_L}^\dagger V_{d_L} = \begin{pmatrix} V_{ud} & V_{us} & V_{ub} \\ V_{cd} & V_{cs} & V_{cb} \\ V_{td} & V_{ts} & V_{tb} \end{pmatrix} = \begin{pmatrix} 1 - \frac{1}{2}\lambda^2 & \lambda & A\lambda^3 (\rho - \mathrm{i}\eta) \\ -\lambda & 1 - \frac{1}{2}\lambda^2 & A\lambda^2 \\ A\lambda^3 (1 - \rho - \mathrm{i}\eta) & -A\lambda^2 & 1 \end{pmatrix} . \quad \text{(A.1)}$$

As the QLC relation [12–14] suggests a relation between the quark and lepton sector, it is useful to use the Cabibbo angle $V_{us} = \lambda \approx \sin \vartheta_{12}$ as expansion parameter [237]

$$U_{e2} = \sqrt{\frac{1}{2}} (1 - \lambda) \ , \qquad U_{e3} = A\lambda^n \ , \qquad U_{\mu 3} = \sqrt{\frac{1}{2}} (1 - B\lambda^m) \, e^{\mathrm{i}\delta^q} \ . \quad \text{(A.2)}$$

The free parameters m and n account for the experimental uncertainty in the matrix elements. Unitarity determines the remaining elements. For definiteness, we show the case $m = n = 1$

$$U_{\rm MNS} = U_{e_L}^\dagger U_{\nu_L} = \begin{pmatrix} U_{e1} & U_{e2} & U_{e3} \\ U_{\mu 1} & U_{\mu 2} & U_{\mu 3} \\ U_{\tau 1} & U_{\tau 2} & U_{\tau 3} \end{pmatrix}$$
$$= \begin{pmatrix} \sqrt{\frac{1}{2}}\,(1+\lambda) & \sqrt{\frac{1}{2}}\,(1-\lambda) & A\lambda \\ -\frac{1}{2}\left(1-\left(1-B-Ae^{\mathrm{i}\delta}\right)\lambda\right) & \frac{1}{2}\left(1+\left(1+B-Ae^{\mathrm{i}\delta}\right)\lambda\right) & \sqrt{\frac{1}{2}}\,(1-B\lambda)\,e^{\mathrm{i}\delta^q} \\ \frac{1}{2}\left(1-\left(1+B+Ae^{\mathrm{i}\delta}\right)\lambda\right) & -\frac{1}{2}\left(1+\left(1-B+Ae^{\mathrm{i}\delta}\right)\lambda\right) & \sqrt{\frac{1}{2}}\,(1+B\lambda)\,e^{\mathrm{i}\delta^q} \end{pmatrix} + \mathcal{O}(\lambda^2)\,. \tag{A.3}$$

The CP violating phases can also be expressed in terms of weak-basis invariants like the Jarlskog invariant [238]

$$\begin{aligned} J_{CP}^q &= \mathrm{Im}\left\{V_{ud}\,V_{cs}\,V_{us}^*\,V_{cd}^*\right\} \\ J_{CP}^l &= \mathrm{Im}\left\{U_{e1}\,U_{\mu 2}\,U_{e2}^*\,U_{\mu 1}^*\right\} \end{aligned} \tag{A.4}$$

which is related to the Dirac CP phase. The rephasing invariant CP violation measures are

$$S_1 \equiv \mathrm{Im}\left\{U_{e1}U_{e3}^*\right\}\,, \qquad S_2 \equiv \mathrm{Im}\left\{U_{e2}U_{e3}^*\right\} \tag{A.5}$$

in the case of the Majorana phases [239].

A.2 Standard Parameterization

A unitary matrix can be described by three angles and six phases. Thus it can be written in the following way:

$$U \;=\; \mathrm{diag}(e^{\mathrm{i}\delta_e}, e^{\mathrm{i}\delta_\mu}, e^{\mathrm{i}\delta_\tau}) \cdot V(\theta_{12}, \theta_{13}, \theta_{23}, \delta) \cdot \mathrm{diag}(e^{-\mathrm{i}\varphi_1/2}, e^{-\mathrm{i}\varphi_2/2}, 1) \tag{A.6}$$

V is a special unitary matrix and is parameterized in standard parameterization like the CKM matrix in the quark sector with three angles (θ_{12}, θ_{13}, θ_{23}) and one CP phase (δ) [93].

$$V(\theta_{12}, \theta_{13}, \theta_{23}, \delta) = \begin{pmatrix} c_{12}c_{13} & s_{12}c_{13} & s_{13}\,e^{-\mathrm{i}\delta} \\ -c_{23}s_{12} - s_{23}s_{13}c_{12}\,e^{\mathrm{i}\delta} & c_{23}c_{12} - s_{23}s_{13}s_{12}\,e^{\mathrm{i}\delta} & s_{23}c_{13} \\ s_{23}s_{12} - c_{23}s_{13}c_{12}\,e^{\mathrm{i}\delta} & -s_{23}c_{12} - c_{23}s_{13}s_{12}\,e^{\mathrm{i}\delta} & c_{23}c_{13} \end{pmatrix} \tag{A.7}$$

where s_{ij} and c_{ij} are defined as $s_{ij} = \sin\theta_{ij}$ and $c_{ij} = \cos\theta_{ij}$, respectively. The Jarlskog invariant Eq. (A.4) is related to the mixing angles and the Dirac CP phase by

$$J_{CP}^l = \frac{1}{8}\,\sin 2\theta_{12}\,\sin 2\theta_{23}\,\sin 2\theta_{13}\,\cos\theta_{13}\,\sin\delta\,. \tag{A.8}$$

In addition, there are phase matrices multiplied from both sides. In the lepton sector, the matrix on the left-hand side is characterized by the unphysical phases δ_e, δ_μ and δ_τ which can be rotated away by a change of the phases in the left-handed charged leptons. The matrix on the right-hand side is described by the Majorana phases φ_1 and φ_2 which can only be rotated away by left-handed neutrinos, if they are Dirac particles. Analogous reasoning applies to the quark sector, where all additional phases can be rotated away.

Appendix B

Group Theory

In this chapter, we collect the relevant technical details which are needed for the calculations in the main part.

B.1 Lie Groups

Here, we present technical details about Lie groups, more precisely their Lie algebras, which are needed in the main chapters. A detailed discussion of Lie algebras is given in [240, 241], which includes the calculation of Clebsch-Gordan coefficients by the ladder operator technique and breaking to subgroups.
All semi-simple Lie algebras can be classified by Dynkin diagrams, e.g. the Dynkin diagram belonging to $\mathfrak{su}(5)$ is shown in Fig. B.1. It determines the Cartan matrix $A_{ij} = 2\frac{(\alpha_i,\alpha_j)}{(\alpha_j,\alpha_j)}$ which can be translated to the metric tensor $G_{ij} = \left(A^{-1}\right)_{ij} \frac{(\alpha_j,\alpha_j)}{2}$ of the weight space in terms of the simple root α_i which form a basis. Thus the non-orthogonality of simple roots is encoded in the Cartan matrix. The Lie algebra is uniquely given by the Dynkin diagram. There are 4 series of semi-simple Lie algebras $A_n \cong \mathfrak{su}(n+1)$, $B_n \cong \mathfrak{so}(2n+1)$, $C_n \cong \mathfrak{sp}(2n)$ and $D_n \cong \mathfrak{so}(2n)$ as well as 5 exceptional algebras G_2, F_4, E_6, E_7 and E_8.

Figure B.1: Dynkin diagram of $A_4 \cong \mathfrak{su}(5)$.

An irreducible representation of a Lie algebra is completely determined by its highest weight Λ. The Weyl formula determines the dimensionality

$$N(\Lambda) = \prod_{\alpha \in \text{positive roots}} \frac{(\Lambda + \delta, \alpha)}{(\delta, \alpha)} \tag{B.1}$$

of the representation, where $\delta = (1, 1, \ldots, 1, 1)^T$ in the Dynkin basis. Besides the dimensionality, there are further invariants of a given representation. The quadratic Casimir

$$C(\Lambda) = (\Lambda, \Lambda + 2\delta) \tag{B.2}$$

is directly related to the Dynkin index of a representation

$$l(\Lambda) = \frac{N(\Lambda)}{N(Ad)} C(\Lambda) \ . \tag{B.3}$$

This relation becomes obvious from the definitions in terms of generators in the given representation

$$C(\Lambda)\delta_{ab} = \sum_A \left(T^A T^A\right)_{ab} \tag{B.4a}$$

$$l(\Lambda)\delta^{AB} = \mathrm{tr}\left(T^A T^B\right) \ . \tag{B.4b}$$

In an Abelian group, the above formulas for the quadratic Casimir and the Dynkin index are replaced by the squared charge of the representation, i.e. $l(\Lambda) = C(\Lambda) = q_\Lambda^2$.

B.1.1 SO(10)

The Dynkin diagram of $\mathfrak{so}(10)$ is shown in Fig. B.2 and leads to the Cartan matrix

$$A = \begin{pmatrix} 2 & -1 & 0 & 0 & 0 \\ -1 & 2 & -1 & 0 & 0 \\ 0 & -1 & 2 & -1 & -1 \\ 0 & 0 & -1 & 2 & 0 \\ 0 & 0 & -1 & 0 & 2 \end{pmatrix} \tag{B.5}$$

and the metric tensor for the weight space

$$G = \begin{pmatrix} 1 & 1 & 1 & 1/2 & 1/2 \\ 1 & 2 & 2 & 1 & 1 \\ 1 & 2 & 3 & 3/2 & 3/2 \\ 1/2 & 1 & 3/2 & 5/4 & 3/4 \\ 1/2 & 1 & 3/2 & 3/4 & 5/4 \end{pmatrix} \ . \tag{B.6}$$

The relevant representations and their properties are collected in Tab. B.1. The decomposition of

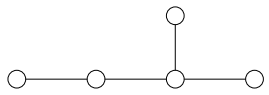

Figure B.2: Dynkin diagram of $D_5 \cong \mathfrak{so}(10)$.

representations in terms of their subgroups is shown in Tab. B.2.
In Tab. B.3, all tensor product which are used in the main part are summarized. There are two convenient ways to calculate the results which are presented in the tables besides the general one by ladder operators. Depending on the symmetry breaking chain, it is either more convenient to do the calculation in terms of the subgroup SU(5) [242] or in terms of the PS subgroup $\mathrm{SO}(4) \times \mathrm{SO}(6) \cong \mathrm{SU}(2) \times \mathrm{SU}(2) \times \mathrm{SU}(4)$ [243]. We used the decomposition in terms of SU(5) which is extensively discussed in [244, 245].

label	N	type	l
(10000)	10	r	2
(00001)	16	c	4
(01000)	45	r	16
(20000)	54	r	24
(00100)	120	r	56
(00002)	126	c	70

Table B.1: SO(10) representations. Real representations are denoted by "r" and complex ones by "c".

$$
\begin{aligned}
&\mathrm{SO}(10) \supset \mathrm{SU}(5) \times \mathrm{U}(1) \\
&\underline{\mathbf{10}} = \underline{\mathbf{5}}(2) \oplus \overline{\underline{\mathbf{5}}}(\overline{2}) \\
&\underline{\mathbf{16}} = \underline{\mathbf{1}}(\overline{5}) \oplus \overline{\underline{\mathbf{5}}}(\overline{3}) \oplus \underline{\mathbf{10}}(\overline{1}) \\
&\underline{\mathbf{45}} = \underline{\mathbf{1}}(0) \oplus \underline{\mathbf{10}}(4) \oplus \overline{\underline{\mathbf{10}}}(\overline{4}) \oplus \underline{\mathbf{24}}(0) \\
&\underline{\mathbf{54}} = \underline{\mathbf{15}}(4) \oplus \overline{\underline{\mathbf{15}}}(\overline{4}) \oplus \underline{\mathbf{24}}(0) \\
&\underline{\mathbf{120}} = \underline{\mathbf{5}}(2) \oplus \overline{\underline{\mathbf{5}}}(\overline{2}) \oplus \underline{\mathbf{10}}(\overline{6}) \oplus \overline{\underline{\mathbf{10}}}(6) \oplus \underline{\mathbf{45}}(2) \oplus \overline{\underline{\mathbf{45}}}(\overline{2}) \\
&\underline{\mathbf{126}} = \underline{\mathbf{1}}(\overline{10}) \oplus \overline{\underline{\mathbf{5}}}(\overline{2}) \oplus \underline{\mathbf{10}}(\overline{6}) \oplus \overline{\underline{\mathbf{15}}}(6) \oplus \underline{\mathbf{45}}(2) \oplus \overline{\underline{\mathbf{50}}}(\overline{2})
\end{aligned}
$$

$$
\begin{aligned}
&\mathrm{SO}(10) \supset \mathrm{SU}(2) \times \mathrm{SU}(2) \times \mathrm{SU}(4) \\
&\underline{\mathbf{10}} = (\underline{\mathbf{2}}, \underline{\mathbf{2}}, \underline{\mathbf{1}}) \oplus (\underline{\mathbf{1}}, \underline{\mathbf{1}}, \underline{\mathbf{6}}) \\
&\underline{\mathbf{16}} = (\underline{\mathbf{2}}, \underline{\mathbf{1}}, \underline{\mathbf{4}}) \oplus (\underline{\mathbf{1}}, \underline{\mathbf{1}}, \overline{\underline{\mathbf{4}}}) \\
&\underline{\mathbf{45}} = (\underline{\mathbf{3}}, \underline{\mathbf{1}}, \underline{\mathbf{1}}) \oplus (\underline{\mathbf{1}}, \underline{\mathbf{3}}, \underline{\mathbf{1}}) \oplus (\underline{\mathbf{1}}, \underline{\mathbf{1}}, \underline{\mathbf{15}}) \oplus (\underline{\mathbf{2}}, \underline{\mathbf{2}}, \underline{\mathbf{6}}) \\
&\underline{\mathbf{54}} = (\underline{\mathbf{1}}, \underline{\mathbf{1}}, \underline{\mathbf{1}}) \oplus (\underline{\mathbf{3}}, \underline{\mathbf{3}}, \underline{\mathbf{1}}) \oplus (\underline{\mathbf{1}}, \underline{\mathbf{1}}, \underline{\mathbf{20}}') \oplus (\underline{\mathbf{2}}, \underline{\mathbf{2}}, \underline{\mathbf{6}}) \\
&\underline{\mathbf{120}} = (\underline{\mathbf{2}}, \underline{\mathbf{2}}, \underline{\mathbf{1}}) \oplus (\underline{\mathbf{1}}, \underline{\mathbf{1}}, \underline{\mathbf{10}}) \oplus (\underline{\mathbf{1}}, \underline{\mathbf{1}}, \overline{\underline{\mathbf{10}}}) \oplus (\underline{\mathbf{3}}, \underline{\mathbf{1}}, \underline{\mathbf{6}}) \oplus (\underline{\mathbf{1}}, \underline{\mathbf{3}}, \underline{\mathbf{6}}) \oplus (\underline{\mathbf{2}}, \underline{\mathbf{2}}, \underline{\mathbf{15}}) \\
&\underline{\mathbf{126}} = (\underline{\mathbf{1}}, \underline{\mathbf{1}}, \underline{\mathbf{6}}) \oplus (\underline{\mathbf{3}}, \underline{\mathbf{1}}, \overline{\underline{\mathbf{10}}}) \oplus (\underline{\mathbf{1}}, \underline{\mathbf{3}}, \underline{\mathbf{10}}) \oplus (\underline{\mathbf{2}}, \underline{\mathbf{2}}, \underline{\mathbf{15}})
\end{aligned}
$$

Table B.2: Decomposition of some representations of SO(10) in terms of subgroups. Barred U(1) charges $\overline{q}$ are understood as $-q$.

B.1.2 E_6

The Dynkin diagram of E_6 is shown in Fig. B.3. The corresponding Cartan matrix is

$$
A = \begin{pmatrix}
2 & -1 & 0 & 0 & 0 & 0 \\
-1 & 2 & -1 & 0 & 0 & 0 \\
0 & -1 & 2 & -1 & 0 & -1 \\
0 & 0 & -1 & 2 & -1 & 0 \\
0 & 0 & 0 & -1 & 2 & 0 \\
0 & 0 & -1 & 0 & 0 & 2
\end{pmatrix} \tag{B.7}
$$

$$\underline{\mathbf{10}} \otimes \underline{\mathbf{10}} = \underline{\mathbf{1}}_s \oplus \underline{\mathbf{45}}_a \oplus \underline{\mathbf{54}}_s$$
$$\underline{\mathbf{10}} \otimes \underline{\mathbf{16}} = \overline{\underline{\mathbf{16}}} \oplus \overline{\underline{\mathbf{144}}}$$
$$\underline{\mathbf{16}} \otimes \underline{\mathbf{16}} = \underline{\mathbf{10}}_s \oplus \underline{\mathbf{120}}_a \oplus \underline{\mathbf{126}}_s$$
$$\underline{\mathbf{16}} \otimes \overline{\underline{\mathbf{16}}} = \underline{\mathbf{1}} \oplus \underline{\mathbf{45}} \oplus \underline{\mathbf{210}}$$

Table B.3: Tensor products of SO(10) representations which are used in the main text.

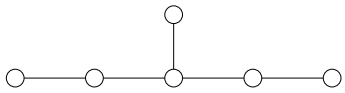

Figure B.3: Dynkin diagram of E_6.

which leads to the metric tensor

$$G = \begin{pmatrix} 4/3 & 5/3 & 2 & 4/3 & 2/3 & 1 \\ 5/3 & 10/3 & 4 & 8/3 & 4/3 & 2 \\ 2 & 4 & 6 & 4 & 2 & 3 \\ 4/3 & 8/3 & 4 & 10/3 & 5/3 & 2 \\ 2/3 & 4/3 & 2 & 5/3 & 4/3 & 1 \\ 1 & 2 & 3 & 2 & 1 & 2 \end{pmatrix} . \tag{B.8}$$

The relevant representations and their properties are collected in Tab. B.4. Note, that we do not follow the notation of Slansky [240] in the main text. In order to distinguish the symmetric and antisymmetric $\underline{\mathbf{351}}$-plets, we assign to the symmetric one the index S and to the antisymmetric one the index A. The decomposition of the representations in terms of their subgroups is shown in Tab. B.5. Besides the general method for group-theoretical calculations in E_6, tensor products of small representations are most easily performed in terms of maximal subgroups. In Sec. 4.4, we use the trinification subgroup $\mathrm{SU}(3)^3$: upper indices are $\mathrm{SU}(3)_L$ indices in the fundamental $\underline{\mathbf{3}}$ representation and the lower ones belong to $\mathrm{SU}(3)_R$. The irreducible representation $\underline{\mathbf{6}}$ of SU(3) is represented by symmetric 3×3 matrices and described by two symmetrized indices. Dotted indices belong to the complex conjugate representation $\overline{\underline{\mathbf{3}}}$.

label	N	type	l
(100000)	27	c	6
(000001)	78	r	24
(000100)	$351_A \cong 351$	c	150
(000020)	$351_S \cong 351'$	c	168

Table B.4: E_6 representations. Real representations are denoted by "r" and complex ones by "c".

In Tab. B.6, all tensor products which are used in the main part are summarized.

$$
\begin{aligned}
E_6 &\supset \mathrm{SO}(10) \times \mathrm{U}(1) \\
\underline{\mathbf{27}} &= \underline{\mathbf{1}}(4) \oplus \underline{\mathbf{10}}(\overline{2}) \oplus \underline{\mathbf{16}}(1) \\
\underline{\mathbf{78}} &= \underline{\mathbf{1}}(0) \oplus \underline{\mathbf{45}}(0) \oplus \underline{\mathbf{16}}(\overline{3}) \oplus \overline{\underline{\mathbf{16}}}(\overline{3}) \\
\underline{\mathbf{351}}_A \cong \underline{\mathbf{351}} &= \underline{\mathbf{10}}(\overline{2}) \oplus \overline{\underline{\mathbf{16}}}(\overline{5}) \oplus \underline{\mathbf{16}}(1) \oplus \underline{\mathbf{45}}(4) \oplus \underline{\mathbf{120}}(\overline{2}) \oplus \underline{\mathbf{144}}(1) \\
\underline{\mathbf{351}}_S \cong \underline{\mathbf{351}}' &= \underline{\mathbf{1}}(\overline{8}) \oplus \underline{\mathbf{10}}(\overline{2}) \oplus \overline{\underline{\mathbf{16}}}(\overline{5}) \oplus \underline{\mathbf{54}}(4) \oplus \overline{\underline{\mathbf{126}}}(\overline{2}) \oplus \underline{\mathbf{144}}(1)
\end{aligned}
$$

$$
\begin{aligned}
E_6 &\supset \mathrm{SU}(3) \times \mathrm{SU}(3) \times \mathrm{SU}(3) \\
\underline{\mathbf{27}} &= (\overline{\underline{\mathbf{3}}}, \underline{\mathbf{3}}, \underline{\mathbf{1}}) \oplus (\underline{\mathbf{3}}, \underline{\mathbf{1}}, \underline{\mathbf{3}}) \oplus (\underline{\mathbf{1}}, \overline{\underline{\mathbf{3}}}, \overline{\underline{\mathbf{3}}}) \\
\underline{\mathbf{78}} &= (\underline{\mathbf{8}}, \underline{\mathbf{1}}, \underline{\mathbf{1}}) \oplus (\underline{\mathbf{1}}, \underline{\mathbf{8}}, \underline{\mathbf{1}}) \oplus (\underline{\mathbf{1}}, \underline{\mathbf{1}}, \underline{\mathbf{8}}) \oplus (\underline{\mathbf{3}}, \underline{\mathbf{3}}, \overline{\underline{\mathbf{3}}}) \oplus (\overline{\underline{\mathbf{3}}}, \overline{\underline{\mathbf{3}}}, \underline{\mathbf{3}}) \\
\underline{\mathbf{351}}_A \cong \underline{\mathbf{351}} &= (\overline{\underline{\mathbf{3}}}, \underline{\mathbf{3}}, \underline{\mathbf{1}}) \oplus (\overline{\underline{\mathbf{3}}}, \overline{\underline{\mathbf{6}}}, \underline{\mathbf{1}}) \oplus (\underline{\mathbf{6}}, \underline{\mathbf{3}}, \underline{\mathbf{1}}) \oplus (\underline{\mathbf{3}}, \underline{\mathbf{1}}, \underline{\mathbf{3}}) \oplus (\overline{\underline{\mathbf{6}}}, \underline{\mathbf{1}}, \underline{\mathbf{3}}) \oplus (\underline{\mathbf{3}}, \underline{\mathbf{8}}, \underline{\mathbf{3}}) \oplus (\underline{\mathbf{1}}, \overline{\underline{\mathbf{3}}}, \overline{\underline{\mathbf{3}}}) \\
&\quad \oplus (\underline{\mathbf{1}}, \underline{\mathbf{6}}, \overline{\underline{\mathbf{3}}}) \oplus (\underline{\mathbf{8}}, \overline{\underline{\mathbf{3}}}, \overline{\underline{\mathbf{3}}}) \oplus (\underline{\mathbf{3}}, \underline{\mathbf{1}}, \overline{\underline{\mathbf{6}}}) \oplus (\underline{\mathbf{1}}, \overline{\underline{\mathbf{3}}}, \underline{\mathbf{6}}) \oplus (\underline{\mathbf{1}}, \overline{\underline{\mathbf{3}}}, \underline{\mathbf{6}}) \oplus (\overline{\underline{\mathbf{3}}}, \underline{\mathbf{3}}, \underline{\mathbf{8}}) \\
\underline{\mathbf{351}}_S \cong \underline{\mathbf{351}}' &= (\overline{\underline{\mathbf{3}}}, \underline{\mathbf{3}}, \underline{\mathbf{1}}) \oplus (\underline{\mathbf{6}}, \overline{\underline{\mathbf{6}}}, \underline{\mathbf{1}}) \oplus (\underline{\mathbf{3}}, \underline{\mathbf{1}}, \underline{\mathbf{3}}) \oplus (\underline{\mathbf{3}}, \underline{\mathbf{8}}, \underline{\mathbf{3}}) \oplus (\underline{\mathbf{1}}, \overline{\underline{\mathbf{3}}}, \overline{\underline{\mathbf{3}}}) \oplus (\underline{\mathbf{8}}, \overline{\underline{\mathbf{3}}}, \overline{\underline{\mathbf{3}}}) \oplus (\overline{\underline{\mathbf{6}}}, \underline{\mathbf{1}}, \overline{\underline{\mathbf{6}}}) \\
&\quad \oplus (\underline{\mathbf{1}}, \underline{\mathbf{6}}, \underline{\mathbf{6}}) \oplus (\overline{\underline{\mathbf{3}}}, \underline{\mathbf{3}}, \underline{\mathbf{8}})
\end{aligned}
$$

Table B.5: Decomposition of representations of E_6 in terms of their subgroups. Barred U(1) charges $\overline{q}$ stand for $-q$.

$$
\begin{aligned}
\underline{\mathbf{27}} \otimes \underline{\mathbf{27}} &= \overline{\underline{\mathbf{27}}} \oplus \overline{\underline{\mathbf{351}}}_A \oplus \overline{\underline{\mathbf{351}}}_S \\
\underline{\mathbf{27}} \otimes \overline{\underline{\mathbf{27}}} &= \underline{\mathbf{1}} \oplus \underline{\mathbf{78}} \oplus \underline{\mathbf{650}}
\end{aligned}
$$

Table B.6: Tensor products of E_6 representations.

	classes				
	$\mathcal{C}_1$	$\mathcal{C}_2$	$\mathcal{C}_3$	$\mathcal{C}_4$	$\mathcal{C}_5$
G	$\mathbb{1}$	B	B^2	A	A^3
$^\circ\mathcal{C}_i$	1	7	7	3	3
$^\circ\mathrm{h}\ _{\mathcal{C}_i}$	1	3	3	7	7
$\underline{\mathbf{1_1}}$	1	1	1	1	1
$\underline{\mathbf{1_2}}$	1	ω	ω^2	1	1
$\underline{\mathbf{1_3}}$	1	ω^2	ω	1	1
$\underline{\mathbf{3}}$	3	0	0	ξ	$\xi^\star$
$\underline{\mathbf{3}}^\star$	3	0	0	$\xi^\star$	ξ

Table B.7: Character table of T_7. $\omega = e^{\frac{2\pi \mathrm{i}}{3}} = -\frac{1}{2} + \mathrm{i}\frac{\sqrt{3}}{2}$ and $\xi = \frac{1}{2}(-1 + \mathrm{i}\sqrt{7})$. Furthermore $\xi = \rho + \rho^2 + \rho^4$ where $\rho = e^{\frac{2\pi \mathrm{i}}{7}}$. $\mathcal{C}_i$ denotes the different classes which make up the group. The elements of a class $\mathcal{C}_i$ are related by an inner group automorphism, i.e. $G_1 = T^{-1}G_2T$, where $G_1, G_2 \in \mathcal{C}_i$ and T is an element of the group. G is a representative of the corresponding class, $^\circ\mathcal{C}_i$ is the order of the class, i.e. the number of elements and $^\circ\mathrm{h}\ _{\mathcal{C}_i}$ is the order of the elements in the class, i.e. the smallest integer with $G^{\,^\circ\mathrm{h}\ _{\mathcal{C}_i}} = \mathbb{1}$. The characters χ of a group are defined as the trace over the matrix $D(G)$ which represents the group element G in representation D: $\chi \equiv \mathrm{tr}D(G)$.

B.2 Discrete Groups

Here, we collect the relevant group-theoretical details which are used in Sec. 4.5.

B.2.1 T_7

T_7 is group of order 21 which is very similar to A_4 with the crucial difference that A_4 contains one real three-dimensional representation and T_7 has two complex three-dimensional representations. T_7 as well as A_4 contain the subgroup Z_3. The character table is presented in Tab. B.7. The used generators for the three-dimensional representations are:

$$\underline{\mathbf{3}} : \mathrm{A} = \begin{pmatrix} e^{\frac{2\pi i}{7}} & 0 & 0 \\ 0 & e^{\frac{4\pi i}{7}} & 0 \\ 0 & 0 & e^{\frac{8\pi i}{7}} \end{pmatrix}\ ,\ \mathrm{B} = \begin{pmatrix} 0 & 1 & 0 \\ 0 & 0 & 1 \\ 1 & 0 & 0 \end{pmatrix}$$

and

$$\underline{\mathbf{3}}^\star : \mathrm{A} = \begin{pmatrix} e^{-\frac{2\pi i}{7}} & 0 & 0 \\ 0 & e^{-\frac{4\pi i}{7}} & 0 \\ 0 & 0 & e^{-\frac{8\pi i}{7}} \end{pmatrix}\ ,\ \mathrm{B} = \begin{pmatrix} 0 & 1 & 0 \\ 0 & 0 & 1 \\ 1 & 0 & 0 \end{pmatrix}\ .$$

They fulfill the generator relations:

$$\mathrm{A}^7 = \mathbb{1}\ ,\ \ \mathrm{B}^3 = \mathbb{1}\ ,\ \ \mathrm{AB} = \mathrm{BA}^4\ .$$

The Kronecker products are

$$\begin{aligned} &\underline{\mathbf{1_1}} \times \underline{\mathbf{1_i}} = \underline{\mathbf{1_i}}\ ,\ \ \underline{\mathbf{1_2}} \times \underline{\mathbf{1_3}} = \underline{\mathbf{1_1}}\ , && [\underline{\mathbf{3}} \times \underline{\mathbf{3}}] = \underline{\mathbf{3}} + \underline{\mathbf{3}}^\star\ ,\quad \{\underline{\mathbf{3}} \times \underline{\mathbf{3}}\} = \underline{\mathbf{3}}^\star \\ &\underline{\mathbf{1_2}} \times \underline{\mathbf{1_2}} = \underline{\mathbf{1_3}}\ ,\ \ \underline{\mathbf{1_3}} \times \underline{\mathbf{1_3}} = \underline{\mathbf{1_2}}\ , && [\underline{\mathbf{3}}^\star \times \underline{\mathbf{3}}^\star] = \underline{\mathbf{3}} + \underline{\mathbf{3}}^\star\ ,\quad \{\underline{\mathbf{3}}^\star \times \underline{\mathbf{3}}^\star\} = \underline{\mathbf{3}} \\ &\underline{\mathbf{1_i}} \times \underline{\mathbf{3}} = \underline{\mathbf{3}}\ ,\ \ \underline{\mathbf{1_i}} \times \underline{\mathbf{3}}^\star = \underline{\mathbf{3}}^\star && \underline{\mathbf{3}} \times \underline{\mathbf{3}}^\star = \underline{\mathbf{1_1}} + \underline{\mathbf{1_2}} + \underline{\mathbf{1_3}} + \underline{\mathbf{3}} + \underline{\mathbf{3}}^\star \end{aligned}$$

with $[\mu \times \mu]$ being the symmetric part of the product $\mu \times \mu$ and $\{\mu \times \mu\}$ being the anti-symmetric

part. The non-trivial Clebsch-Gordan coefficients are for $(a_1, a_2, a_3)^T \sim \underline{\mathbf{3}}$, $(b_1, b_2, b_3)^T \sim \underline{\mathbf{3}}^\star$ and $c \sim \underline{\mathbf{1_1}}$, $c' \sim \underline{\mathbf{1_2}}$, $c'' \sim \underline{\mathbf{1_3}}$:

$$\begin{aligned}
\underline{\mathbf{3}} \times \underline{\mathbf{1_1}} &: (a_1\, c, a_2\, c, a_3\, c) \sim \underline{\mathbf{3}} & \qquad \underline{\mathbf{3}}^\star \times \underline{\mathbf{1_1}} &: (b_1\, c, b_2\, c, b_3\, c) \sim \underline{\mathbf{3}}^\star \\
\underline{\mathbf{3}} \times \underline{\mathbf{1_2}} &: \left(a_1\, c', \omega\, a_2\, c', \omega^2\, a_3\, c'\right) \sim \underline{\mathbf{3}} & \qquad \underline{\mathbf{3}}^\star \times \underline{\mathbf{1_2}} &: \left(b_1\, c', \omega\, b_2\, c', \omega^2\, b_3\, c'\right) \sim \underline{\mathbf{3}}^\star \\
\underline{\mathbf{3}} \times \underline{\mathbf{1_3}} &: \left(a_1\, c'', \omega^2\, a_2\, c'', \omega\, a_3\, c''\right) \sim \underline{\mathbf{3}} & \qquad \underline{\mathbf{3}}^\star \times \underline{\mathbf{1_3}} &: \left(b_1\, c'', \omega^2\, b_2\, c'', \omega\, b_3\, c''\right) \sim \underline{\mathbf{3}}^\star
\end{aligned}$$

For $(a_1, a_2, a_3)^T, (a'_1, a'_2, a'_3)^T \sim \underline{\mathbf{3}}$:

$$(a_3\, a'_3, a_1\, a'_1, a_2\, a'_2)^T \sim \underline{\mathbf{3}}\,, \quad (a_2\, a'_3, a_3\, a'_1, a_1\, a'_2)^T \sim \underline{\mathbf{3}}^\star \text{ and } (a_3\, a'_2, a_1\, a'_3, a_2\, a'_1)^T \sim \underline{\mathbf{3}}^\star\,.$$

For $(b_1, b_2, b_3)^T, (b'_1, b'_2, b'_3)^T \sim \underline{\mathbf{3}}^\star$:

$$(b_2\, b'_3, b_3\, b'_1, b_1\, b'_2)^T \sim \underline{\mathbf{3}}\,, \quad (b_3\, b'_2, b_1\, b'_3, b_2\, b'_1)^T \sim \underline{\mathbf{3}} \text{ and } (b_3\, b'_3, b_1\, b'_1, b_2\, b'_2)^T \sim \underline{\mathbf{3}}^\star\,.$$

For $(a_1, a_2, a_3)^T \sim \underline{\mathbf{3}}$, $(b_1, b_2, b_3)^T \sim \underline{\mathbf{3}}^\star$ the T_7 covariant combinations are:

$$\begin{aligned}
&a_1\, b_1 + a_2\, b_2 + a_3\, b_3 \sim \underline{\mathbf{1_1}}\,, \quad a_1\, b_1 + \omega^2\, a_2\, b_2 + \omega\, a_3\, b_3 \sim \underline{\mathbf{1_2}}\,, \\
&a_1\, b_1 + \omega\, a_2\, b_2 + \omega^2\, a_3\, b_3 \sim \underline{\mathbf{1_3}}\,, \\
&(a_2\, b_1, a_3\, b_2, a_1\, b_3)^T \sim \underline{\mathbf{3}}\,, \quad (a_1\, b_2, a_2\, b_3, a_3\, b_1)^T \sim \underline{\mathbf{3}}^\star\,.
\end{aligned}$$

In Tab. B.8 the leading order contributions of the higher-dimensional operators are presented.

Order	Operators					
	$\mathcal{O}(1)$	$\mathcal{O}(\epsilon^2)$	$\mathcal{O}(\epsilon)$	$\mathcal{O}(\epsilon^3)$	$\mathcal{O}(\epsilon^2)$	$\mathcal{O}(\epsilon^3)$
	χ_1^n	$\chi_1^{n-1}\,\chi_2$	$\chi_1^{n-1}\,\chi_3$	$\chi_1^{n-2}\,\chi_2\,\chi_3$	$\chi_1^{n-2}\,\chi_3^2$	$\chi_1^{n-3}\,\chi_3^3$
$n=1$		$\begin{pmatrix}\chi_1\\ \chi_2\\ \chi_3\end{pmatrix} \sim \underline{\mathbf{3}}^\star$				
$n=2$	$\begin{pmatrix}\chi_3^2\\ \chi_1^2\end{pmatrix} \sim \underline{\mathbf{3}}^\star$	$\begin{pmatrix}\chi_2\,\chi_3\\ \chi_1\,\chi_3\\ \chi_1\,\chi_2\end{pmatrix} \sim \underline{\mathbf{3}}$			see χ_1^n	
$n=3$	$\begin{pmatrix}\chi_3^3\\ \chi_1^3\end{pmatrix} \sim \underline{\mathbf{3}}$	$\begin{pmatrix}\chi_1\,\chi_3^2\\ \chi_1^2\,\chi_2\end{pmatrix} \sim \underline{\mathbf{3}}^\star$	$\begin{pmatrix}\chi_1^2\,\chi_3\end{pmatrix} \sim \underline{\mathbf{3}}$	$\chi_1\,\chi_2\,\chi_3 \sim \underline{\mathbf{1}}_{\mathbf{1}}$	see $\chi_1^{n-1}\,\chi_2$	see χ_1^n
$n=4$	$\begin{pmatrix}\\ \chi_1^4\end{pmatrix} \sim \underline{\mathbf{3}}^\star$	$\begin{pmatrix}\chi_1\,\chi_3^3\\ \chi_1^3\,\chi_2\end{pmatrix} \sim \underline{\mathbf{3}}$	$\chi_1^3\,\chi_3 + \chi_1\,\chi_2^3 + \chi_2\,\chi_3^3 \sim \underline{\mathbf{1}}_{\mathbf{1}}$	$\begin{pmatrix}\chi_1^2\,\chi_2\,\chi_3\end{pmatrix} \sim \underline{\mathbf{3}}^\star$	$\begin{pmatrix}\\ \chi_1^2\,\chi_3^2\end{pmatrix} \sim \underline{\mathbf{3}}$	see $\chi_1^{n-1}\,\chi_2$
$n=5$	$\begin{pmatrix}\chi_1^5\end{pmatrix} \sim \underline{\mathbf{3}}$	$\begin{pmatrix}\chi_1^4\,\chi_2\\ \\ \end{pmatrix} \sim \underline{\mathbf{3}}$	$\begin{pmatrix}\chi_1^4\,\chi_3\\ \\ \end{pmatrix} \sim \underline{\mathbf{3}}^\star$	$\begin{pmatrix}\chi_1^3\,\chi_2\,\chi_3\end{pmatrix} \sim \underline{\mathbf{3}}^\star$	$\begin{pmatrix}\\ \chi_1^3\,\chi_3^2\end{pmatrix} \sim \underline{\mathbf{3}}^\star$	$\chi_1^2\,\chi_3^3 + \chi_1^3\,\chi_2^2 + \chi_2^3\,\chi_3^2 \sim \underline{\mathbf{1}}_{\mathbf{1}}$
$n=6$	$\begin{pmatrix}\chi_1^6\\ \\ \end{pmatrix} \sim \underline{\mathbf{3}}$	$\chi_1^5\,\chi_2 + \chi_2^5\,\chi_3 + \chi_1\,\chi_3^5 \sim \underline{\mathbf{1}}_{\mathbf{1}}$	$\begin{pmatrix}\chi_1^5\,\chi_3\end{pmatrix} \sim \underline{\mathbf{3}}^\star$	$\begin{pmatrix}\\ \chi_1^4\,\chi_2\,\chi_3\end{pmatrix} \sim \underline{\mathbf{3}}$	$\begin{pmatrix}\chi_1^4\,\chi_3^2\end{pmatrix} \sim \underline{\mathbf{3}}$	$\begin{pmatrix}\chi_1^3\,\chi_3^3\end{pmatrix} \sim \underline{\mathbf{3}}^\star$
$n=7$	$\chi_1^7 + \chi_2^7 + \chi_3^7 \sim \underline{\mathbf{1}}_{\mathbf{1}}$	$\begin{pmatrix}\chi_1^6\,\chi_2\\ \\ \end{pmatrix} \sim \underline{\mathbf{3}}^\star$	$\begin{pmatrix}\\ \chi_1^6\,\chi_3\end{pmatrix} \sim \underline{\mathbf{3}}$	$\begin{pmatrix}\\ \chi_1^5\,\chi_2\,\chi_3\end{pmatrix} \sim \underline{\mathbf{3}}^\star$	$\begin{pmatrix}\chi_1^5\,\chi_3^2\\ \\ \end{pmatrix} \sim \underline{\mathbf{3}}$	$\begin{pmatrix}\chi_1^4\,\chi_3^3\end{pmatrix} \sim \underline{\mathbf{3}}^\star$
$n=8$	$\begin{pmatrix}\chi_1^8\\ \\ \end{pmatrix} \sim \underline{\mathbf{3}}^\star$	$\begin{pmatrix}\chi_1^7\,\chi_2\end{pmatrix} \sim \underline{\mathbf{3}}^\star$	$\begin{pmatrix}\\ \chi_1^7\,\chi_3\end{pmatrix} \sim \underline{\mathbf{3}}^\star$	$\begin{pmatrix}\chi_1^6\,\chi_2\,\chi_3\end{pmatrix} \sim \underline{\mathbf{3}}$	$\chi_1^6\,\chi_3^2 + \chi_1^2\,\chi_2^6 + \chi_2^2\,\chi_3^6 \sim \underline{\mathbf{1}}_{\mathbf{1}}$	$\begin{pmatrix}\\ \chi_1^5\,\chi_3^3\end{pmatrix} \sim \underline{\mathbf{3}}$
$n=9$	$\begin{pmatrix}\chi_1^9\end{pmatrix} \sim \underline{\mathbf{3}}^\star$	$\begin{pmatrix}\\ \chi_1^8\,\chi_2\end{pmatrix} \sim \underline{\mathbf{3}}$	$\begin{pmatrix}\chi_1^8\,\chi_3\end{pmatrix} \sim \underline{\mathbf{3}}$	$\begin{pmatrix}\chi_1^7\,\chi_2\,\chi_3\end{pmatrix} \sim \underline{\mathbf{3}}$	$\begin{pmatrix}\chi_1^7\,\chi_3^2\end{pmatrix} \sim \underline{\mathbf{3}}^\star$	$\begin{pmatrix}\\ \chi_1^6\,\chi_3^3\end{pmatrix} \sim \underline{\mathbf{3}}^\star$
$n=10$	$\begin{pmatrix}\\ \chi_1^{10}\end{pmatrix} \sim \underline{\mathbf{3}}$	$\begin{pmatrix}\\ \chi_1^9\,\chi_2\end{pmatrix} \sim \underline{\mathbf{3}}^\star$	$\begin{pmatrix}\chi_1^9\,\chi_3\end{pmatrix} \sim \underline{\mathbf{3}}$	$\chi_1^8\,\chi_2\,\chi_3 + \chi_1\,\chi_2^8\,\chi_3 + \chi_1\,\chi_2\,\chi_3^8 \sim \underline{\mathbf{1}}_{\mathbf{1}}$	$\begin{pmatrix}\chi_1^8\,\chi_3^2\end{pmatrix} \sim \underline{\mathbf{3}}^\star$	$\begin{pmatrix}\chi_1^7\,\chi_3^3\end{pmatrix} \sim \underline{\mathbf{3}}$
$n=11$	$\begin{pmatrix}\\ \chi_1^{11}\end{pmatrix} \sim \underline{\mathbf{3}}^\star$	$\begin{pmatrix}\chi_1^{10}\,\chi_2\end{pmatrix} \sim \underline{\mathbf{3}}$	$\chi_1^{10}\,\chi_3 + \chi_1\,\chi_2^{10} + \chi_2\,\chi_3^{10} \sim \underline{\mathbf{1}}_{\mathbf{1}}$	$\begin{pmatrix}\chi_1^9\,\chi_2\,\chi_3\end{pmatrix} \sim \underline{\mathbf{3}}^\star$	$\begin{pmatrix}\\ \chi_1^9\,\chi_3^2\end{pmatrix} \sim \underline{\mathbf{3}}$	$\begin{pmatrix}\chi_1^8\,\chi_3^3\end{pmatrix} \sim \underline{\mathbf{3}}$

Table B.8: Higher-dimensional operators of T_7. Note that in the cases in which the one-dimensional representation $\underline{\mathbf{1}}_{\mathbf{1}}$ appears as a polynomial also the similar polynomials for the representations $\underline{\mathbf{1}}_{\mathbf{2,3}}$ exist which have the same order in ϵ as the representation $\underline{\mathbf{1}}_{\mathbf{1}}$.

B.2.2 $\Sigma(81)$

$\Sigma(81)$ is a group of order 81 which has nine one-dimensional representations and eight three-dimensional ones. The irreducible representations are $\underline{\mathbf{1_i}}$ with $\mathrm{i} = 1, ..., 9$ and $\underline{\mathbf{3_i}}$ with $\mathrm{i} = 1, ..., 8$. All representations are complex besides the trivial one $\underline{\mathbf{1_1}}$. The complex conjugate pairs are presented in Tab. B.9. Six of the eight three-dimensional representations are faithful, *i.e.* have as many distinct representation matrices as there are elements of the group.

Rep.	$\underline{\mathbf{1_1}}$	$\underline{\mathbf{1_2}}$	$\underline{\mathbf{1_4}}$	$\underline{\mathbf{1_5}}$	$\underline{\mathbf{1_6}}$	$\underline{\mathbf{3_1}}$	$\underline{\mathbf{3_3}}$	$\underline{\mathbf{3_5}}$	$\underline{\mathbf{3_7}}$
Rep.*	$\underline{\mathbf{1_1}}$	$\underline{\mathbf{1_3}}$	$\underline{\mathbf{1_7}}$	$\underline{\mathbf{1_8}}$	$\underline{\mathbf{1_9}}$	$\underline{\mathbf{3_2}}$	$\underline{\mathbf{3_4}}$	$\underline{\mathbf{3_6}}$	$\underline{\mathbf{3_8}}$

Table B.9: The representations of the group $\Sigma(81)$ and their complex conjugates.

The character table can be found in [214] together with a choice of representation matrices for the representation $\underline{\mathbf{3_1}}$ which has been called $\underline{\mathbf{3_A}}$ in the cited work. The generators are given in Tab. B.11.
Some of the Kronecker products are already shown in [215]. In Tab. B.10 we show the Kronecker products which we need to discuss the lowest order.

(a) Kronecker products with one dimensional representations

Rep.	$\underline{\mathbf{1_1}}$	$\underline{\mathbf{1_2}}$	$\underline{\mathbf{1_3}}$
$\underline{\mathbf{1_1}}$	$\underline{\mathbf{1_1}}$	$\underline{\mathbf{1_2}}$	$\underline{\mathbf{1_3}}$
$\underline{\mathbf{1_2}}$	$\underline{\mathbf{1_2}}$	$\underline{\mathbf{1_3}}$	$\underline{\mathbf{1_1}}$
$\underline{\mathbf{1_3}}$	$\underline{\mathbf{1_3}}$	$\underline{\mathbf{1_1}}$	$\underline{\mathbf{1_2}}$
$\underline{\mathbf{3_1}}$	$\underline{\mathbf{3_1}}$	$\underline{\mathbf{3_1}}$	$\underline{\mathbf{3_1}}$
$\underline{\mathbf{3_2}}$	$\underline{\mathbf{3_2}}$	$\underline{\mathbf{3_2}}$	$\underline{\mathbf{3_2}}$

(b) Kronecker products of three dimensional representations

Product $\underline{\mathbf{3_i}} \times \underline{\mathbf{3_j}}$:

$$[\underline{\mathbf{3_1}} \times \underline{\mathbf{3_1}}] = \underline{\mathbf{3_2}} + \underline{\mathbf{3_4}} \quad \text{and} \quad \{\underline{\mathbf{3_1}} \times \underline{\mathbf{3_1}}\} = \underline{\mathbf{3_4}}$$
$$[\underline{\mathbf{3_2}} \times \underline{\mathbf{3_2}}] = \underline{\mathbf{3_1}} + \underline{\mathbf{3_3}} \quad \text{and} \quad \{\underline{\mathbf{3_2}} \times \underline{\mathbf{3_2}}\} = \underline{\mathbf{3_3}}$$

$$\underline{\mathbf{3_1}} \times \underline{\mathbf{3_2}} = \underline{\mathbf{1_1}} + \underline{\mathbf{1_2}} + \underline{\mathbf{1_3}} + \underline{\mathbf{3_7}} + \underline{\mathbf{3_8}}$$

Table B.10: Relevant Kronecker products of $\Sigma(81)$.

The non-trivial Clebsch-Gordan coefficients[1] are for $(a_1, a_2, a_3)^T \sim \underline{\mathbf{3_i}}$ and $c \sim \underline{\mathbf{1_j}}$:

$$\begin{aligned}
\underline{\mathbf{3_i}} \times \underline{\mathbf{1_1}} &: (a_1\, c, a_2\, c, a_3\, c) \sim \underline{\mathbf{3_i}} \\
\underline{\mathbf{3_i}} \times \underline{\mathbf{1_2}} &: \left(a_1\, c, \omega\, a_2\, c, \omega^2\, a_3\, c\right) \sim \underline{\mathbf{3_i}} \quad \text{for} \quad \mathrm{i} = 1, ..., 6 \\
\underline{\mathbf{3_i}} \times \underline{\mathbf{1_3}} &: \left(a_1\, c, \omega^2\, a_2\, c, \omega\, a_3\, c\right) \sim \underline{\mathbf{3_i}} \quad \text{for} \quad \mathrm{i} = 1, ..., 6
\end{aligned}$$

For $(a_1, a_2, a_3)^T \sim \underline{\mathbf{3_1}}$ and $(b_1, b_2, b_3)^T \sim \underline{\mathbf{3_1}}$ the structure of the Clebsch-Gordan coefficients is:

$$(a_1\, b_1, a_2\, b_2, a_3\, b_3)^T \sim \underline{\mathbf{3_2}}\,, \quad (a_2\, b_3, a_3\, b_1, a_1\, b_2)^T \sim \underline{\mathbf{3_4}}\,, \quad (a_3\, b_2, a_1\, b_3, a_2\, b_1)^T \sim \underline{\mathbf{3_4}}$$

For $(a_1, a_2, a_3)^T \sim \underline{\mathbf{3_2}}$ and $(b_1, b_2, b_3)^T \sim \underline{\mathbf{3_2}}$ the structure of the Clebsch-Gordan coefficients is:

$$(a_1\, b_1, a_2\, b_2, a_3\, b_3)^T \sim \underline{\mathbf{3_1}}\,, \quad (a_2\, b_3, a_3\, b_1, a_1\, b_2)^T \sim \underline{\mathbf{3_3}}\,, \quad (a_3\, b_2, a_1\, b_3, a_2\, b_1)^T \sim \underline{\mathbf{3_3}}$$

[1] The remaining Clebsch-Gordan coefficients can be obtained via the formulas given in [246].

For $(a_1, a_2, a_3)^T \sim \underline{\mathbf{3_1}}$ and $(b_1, b_2, b_3)^T \sim \underline{\mathbf{3_2}}$ we arrive at the covariant combinations:

$$a_1\, b_1 + a_2\, b_2 + a_3\, b_3 \sim \underline{\mathbf{1_1}}\ , \quad a_1\, b_1 + \omega^2\, a_2\, b_2 + \omega\, a_3\, b_3 \sim \underline{\mathbf{1_2}}\ , a_1\, b_1 + \omega\, a_2\, b_2 + \omega^2\, a_3\, b_3 \sim \underline{\mathbf{1_3}}\ ,$$
$$(a_3\, b_2, a_2\, b_1, a_1\, b_3)^T \sim \underline{\mathbf{3_7}} \quad \text{and} \quad (a_2\, b_3, a_1\, b_2, a_3\, b_1)^T \sim \underline{\mathbf{3_8}}\ .$$

Rep.	A	B	C
$\underline{\mathbf{1}}_\mathbf{1}$	1	1	1
$\underline{\mathbf{1}}_\mathbf{2}$	ω	1	1
$\underline{\mathbf{1}}_\mathbf{3}$	ω^2	1	1
$\underline{\mathbf{1}}_\mathbf{4}$	1	1	ω^2
$\underline{\mathbf{1}}_\mathbf{5}$	ω^2	1	ω^2
$\underline{\mathbf{1}}_\mathbf{6}$	ω	1	ω^2
$\underline{\mathbf{1}}_\mathbf{7}$	1	1	ω
$\underline{\mathbf{1}}_\mathbf{8}$	ω	1	ω
$\underline{\mathbf{1}}_\mathbf{9}$	ω^2	1	ω
$\underline{\mathbf{3}}_\mathbf{1}$	$\begin{pmatrix} 0 & 1 & 0 \\ 0 & 0 & 1 \\ 1 & 0 & 0 \end{pmatrix}$	$\begin{pmatrix} 1 & 0 & 0 \\ 0 & \omega & 0 \\ 0 & 0 & \omega^2 \end{pmatrix}$	$\begin{pmatrix} 1 & 0 & 0 \\ 0 & 1 & 0 \\ 0 & 0 & \omega \end{pmatrix}$
$\underline{\mathbf{3}}_\mathbf{2}$	$\begin{pmatrix} 0 & 1 & 0 \\ 0 & 0 & 1 \\ 1 & 0 & 0 \end{pmatrix}$	$\begin{pmatrix} 1 & 0 & 0 \\ 0 & \omega^2 & 0 \\ 0 & 0 & \omega \end{pmatrix}$	$\begin{pmatrix} 1 & 0 & 0 \\ 0 & 1 & 0 \\ 0 & 0 & \omega^2 \end{pmatrix}$
$\underline{\mathbf{3}}_\mathbf{3}$	$\begin{pmatrix} 0 & 1 & 0 \\ 0 & 0 & 1 \\ 1 & 0 & 0 \end{pmatrix}$	$\begin{pmatrix} 1 & 0 & 0 \\ 0 & \omega & 0 \\ 0 & 0 & \omega^2 \end{pmatrix}$	$\begin{pmatrix} \omega^2 & 0 & 0 \\ 0 & \omega^2 & 0 \\ 0 & 0 & 1 \end{pmatrix}$
$\underline{\mathbf{3}}_\mathbf{4}$	$\begin{pmatrix} 0 & 1 & 0 \\ 0 & 0 & 1 \\ 1 & 0 & 0 \end{pmatrix}$	$\begin{pmatrix} 1 & 0 & 0 \\ 0 & \omega^2 & 0 \\ 0 & 0 & \omega \end{pmatrix}$	$\begin{pmatrix} \omega & 0 & 0 \\ 0 & \omega & 0 \\ 0 & 0 & 1 \end{pmatrix}$
$\underline{\mathbf{3}}_\mathbf{5}$	$\begin{pmatrix} 0 & 1 & 0 \\ 0 & 0 & 1 \\ 1 & 0 & 0 \end{pmatrix}$	$\begin{pmatrix} 1 & 0 & 0 \\ 0 & \omega & 0 \\ 0 & 0 & \omega^2 \end{pmatrix}$	$\begin{pmatrix} \omega & 0 & 0 \\ 0 & \omega & 0 \\ 0 & 0 & \omega^2 \end{pmatrix}$
$\underline{\mathbf{3}}_\mathbf{6}$	$\begin{pmatrix} 0 & 1 & 0 \\ 0 & 0 & 1 \\ 1 & 0 & 0 \end{pmatrix}$	$\begin{pmatrix} 1 & 0 & 0 \\ 0 & \omega^2 & 0 \\ 0 & 0 & \omega \end{pmatrix}$	$\begin{pmatrix} \omega^2 & 0 & 0 \\ 0 & \omega^2 & 0 \\ 0 & 0 & \omega \end{pmatrix}$
$\underline{\mathbf{3}}_\mathbf{7}$	$\begin{pmatrix} 0 & 0 & 1 \\ 1 & 0 & 0 \\ 0 & 1 & 0 \end{pmatrix}$	$\begin{pmatrix} \omega & 0 & 0 \\ 0 & \omega & 0 \\ 0 & 0 & \omega \end{pmatrix}$	$\begin{pmatrix} \omega & 0 & 0 \\ 0 & 1 & 0 \\ 0 & 0 & \omega^2 \end{pmatrix}$
$\underline{\mathbf{3}}_\mathbf{8}$	$\begin{pmatrix} 0 & 0 & 1 \\ 1 & 0 & 0 \\ 0 & 1 & 0 \end{pmatrix}$	$\begin{pmatrix} \omega^2 & 0 & 0 \\ 0 & \omega^2 & 0 \\ 0 & 0 & \omega^2 \end{pmatrix}$	$\begin{pmatrix} \omega^2 & 0 & 0 \\ 0 & 1 & 0 \\ 0 & 0 & \omega \end{pmatrix}$

Table B.11: Generators of $\Sigma(81)$. We show three generators A, B and C for the representation, although it is enough to take the generators A and C in order to reproduce the whole group. Note that $\omega = \mathrm{e}^{\frac{2\pi i}{3}}$

Order in ϵ	Operator Structure	Representation
$\mathcal{O}(1)$	$\chi_3^m\,(\chi_3^\star)^{n-m}\ (m=0,...,n)$	$\underline{\mathbf{1}}_{\mathbf{1,2,3}}$ for $(2\,m-n)\mod 3=0$ $3^{\rm rd}$ comp. of $\underline{\mathbf{3}}_{\mathbf{1}}$ for $(2\,m-n)\mod 3=1$ $3^{\rm rd}$ comp. of $\underline{\mathbf{3}}_{\mathbf{2}}$ for $(2\,m-n)\mod 3=2$
$\mathcal{O}(\epsilon^2)$	$\chi_3^m\,(\chi_3^\star)^{n-1-m}\,\chi_1\ (m=0,...,n-1)$	$1^{\rm st}$ comp. of $\underline{\mathbf{3}}_{\mathbf{2}}$ for $(2\,m+1-n)\mod 3=0$ $2^{\rm nd}$ comp. of $\underline{\mathbf{3}}_{\mathbf{3}}$ for $(2\,m+1-n)\mod 3=1$ $3^{\rm rd}$ comp. of $\underline{\mathbf{3}}_{\mathbf{8}}$ for $(2\,m+1-n)\mod 3=2$
	$\chi_3^m\,(\chi_3^\star)^{n-1-m}\,\chi_1^\star\ (m=0,...,n-1)$	$1^{\rm st}$ comp. of $\underline{\mathbf{3}}_{\mathbf{1}}$ for $(2\,m-n+1)\mod 3=0$ $3^{\rm rd}$ comp. of $\underline{\mathbf{3}}_{\mathbf{7}}$ for $(2\,m-n+1)\mod 3=1$ $2^{\rm nd}$ comp. of $\underline{\mathbf{3}}_{\mathbf{4}}$ for $(2\,m-n+1)\mod 3=2$
$\mathcal{O}(\epsilon)$	$\chi_3^m\,(\chi_3^\star)^{n-1-m}\,\chi_2\ (m=0,...,n-1)$	$2^{\rm nd}$ comp. of $\underline{\mathbf{3}}_{\mathbf{2}}$ for $(2\,m-n+1)\mod 3=0$ $1^{\rm st}$ comp. of $\underline{\mathbf{3}}_{\mathbf{3}}$ for $(2\,m-n+1)\mod 3=1$ $1^{\rm st}$ comp. of $\underline{\mathbf{3}}_{\mathbf{7}}$ for $(2\,m-n+1)\mod 3=2$
	$\chi_3^m\,(\chi_3^\star)^{n-1-m}\,\chi_2^\star\ (m=0,...,n-1)$	$2^{\rm nd}$ comp. of $\underline{\mathbf{3}}_{\mathbf{1}}$ for $(2\,m-n+1)\mod 3=0$ $1^{\rm st}$ comp. of $\underline{\mathbf{3}}_{\mathbf{8}}$ for $(2\,m-n+1)\mod 3=1$ $1^{\rm st}$ comp. of $\underline{\mathbf{3}}_{\mathbf{4}}$ for $(2\,m-n+1)\mod 3=2$
$\mathcal{O}(\epsilon^3)$	$\chi_3^m\,(\chi_3^\star)^{n-2-m}\,\chi_1\,\chi_2\ (m=0,...,n-2)$	$3^{\rm rd}$ comp. of $\underline{\mathbf{3}}_{\mathbf{3}}$ for $(2\,m-n+2)\mod 3=0$ $\underline{\mathbf{1}}_{\mathbf{4,5,6}}$ for $(2\,m-n+2)\mod 3=1$ $3^{\rm rd}$ comp. of $\underline{\mathbf{3}}_{\mathbf{6}}$ for $(2\,m-n+2)\mod 3=2$
	$\chi_3^m\,(\chi_3^\star)^{n-2-m}\,\chi_1^\star\,\chi_2\ (m=0,...,n-2)$	$2^{\rm nd}$ comp. of $\underline{\mathbf{3}}_{\mathbf{8}}$ for $(2\,m-n+2)\mod 3=0$ $1^{\rm st}$ comp. of $\underline{\mathbf{3}}_{\mathbf{6}}$ for $(2\,m-n+2)\mod 3=1$ $2^{\rm nd}$ comp. of $\underline{\mathbf{3}}_{\mathbf{5}}$ for $(2\,m-n+2)\mod 3=2$
	$\chi_3^m\,(\chi_3^\star)^{n-2-m}\,\chi_1\,\chi_2^\star\ (m=0,...,n-2)$	$2^{\rm nd}$ comp. of $\underline{\mathbf{3}}_{\mathbf{7}}$ for $(2\,m-n+2)\mod 3=0$ $2^{\rm nd}$ comp. of $\underline{\mathbf{3}}_{\mathbf{6}}$ for $(2\,m-n+2)\mod 3=1$ $1^{\rm st}$ comp. of $\underline{\mathbf{3}}_{\mathbf{5}}$ for $(2\,m-n+2)\mod 3=2$
	$\chi_3^m\,(\chi_3^\star)^{n-2-m}\,\chi_1^\star\,\chi_2^\star\ (m=0,...,n-2)$	$3^{\rm rd}$ comp. of $\underline{\mathbf{3}}_{\mathbf{4}}$ for $(2\,m-n+2)\mod 3=0$ $3^{\rm rd}$ comp. of $\underline{\mathbf{3}}_{\mathbf{5}}$ for $(2\,m-n+2)\mod 3=1$ $\underline{\mathbf{1}}_{\mathbf{7,8,9}}$ for $(2\,m-n+2)\mod 3=2$
$\mathcal{O}(\epsilon^2)$	$\chi_3^m\,(\chi_3^\star)^{n-2-m}\,\chi_2^2\ (m=0,...,n-2)$	$2^{\rm nd}$ comp. of $\underline{\mathbf{3}}_{\mathbf{1}}$ for $(2\,m-n+2)\mod 3=0$ $1^{\rm st}$ comp. of $\underline{\mathbf{3}}_{\mathbf{8}}$ for $(2\,m-n+2)\mod 3=1$ $1^{\rm st}$ comp. of $\underline{\mathbf{3}}_{\mathbf{4}}$ for $(2\,m-n+2)\mod 3=2$
	$\chi_3^m\,(\chi_3^\star)^{n-2-m}\,\chi_2\,\chi_2^\star\ (m=0,...,n-2)$	$\underline{\mathbf{1}}_{\mathbf{1,2,3}}$ for $(2\,m-n+2)\mod 3=0$ $3^{\rm rd}$ comp. of $\underline{\mathbf{3}}_{\mathbf{2}}$ for $(2\,m-n+2)\mod 3=1$ $3^{\rm rd}$ comp. of $\underline{\mathbf{3}}_{\mathbf{1}}$ for $(2\,m-n+2)\mod 3=2$
	$\chi_3^m\,(\chi_3^\star)^{n-2-m}\,(\chi_2^\star)^2\ (m=0,...,n-2)$	$2^{\rm nd}$ comp. of $\underline{\mathbf{3}}_{\mathbf{2}}$ for $(2\,m-n+2)\mod 3=0$ $1^{\rm st}$ comp. of $\underline{\mathbf{3}}_{\mathbf{3}}$ for $(2\,m-n+2)\mod 3=1$ $1^{\rm st}$ comp. of $\underline{\mathbf{3}}_{\mathbf{7}}$ for $(2\,m-n+2)\mod 3=2$
$\mathcal{O}(\epsilon^3)$	$\chi_3^m\,(\chi_3^\star)^{n-3-m}\,\chi_2^3\ (m=0,...,n-3)$	$\underline{\mathbf{1}}_{\mathbf{1,2,3}}$ for $(2\,m-n)\mod 3=0$ $3^{\rm rd}$ comp. of $\underline{\mathbf{3}}_{\mathbf{2}}$ for $(2\,m-n)\mod 3=1$ $3^{\rm rd}$ comp. of $\underline{\mathbf{3}}_{\mathbf{1}}$ for $(2\,m-n)\mod 3=2$
	$\chi_3^m\,(\chi_3^\star)^{n-3-m}\,\chi_2^2\,\chi_2^\star\ (m=0,...,n-3)$	$2^{\rm nd}$ comp. of $\underline{\mathbf{3}}_{\mathbf{2}}$ for $(2\,m-n)\mod 3=0$ $1^{\rm st}$ comp. of $\underline{\mathbf{3}}_{\mathbf{3}}$ for $(2\,m-n)\mod 3=1$ $1^{\rm st}$ comp. of $\underline{\mathbf{3}}_{\mathbf{7}}$ for $(2\,m-n)\mod 3=2$
	$\chi_3^m\,(\chi_3^\star)^{n-3-m}\,\chi_2\,(\chi_2^\star)^2\ (m=0,...,n-3)$	$2^{\rm nd}$ comp. of $\underline{\mathbf{3}}_{\mathbf{1}}$ for $(2\,m-n)\mod 3=0$ $1^{\rm st}$ comp. of $\underline{\mathbf{3}}_{\mathbf{8}}$ for $(2\,m-n)\mod 3=1$ $1^{\rm st}$ comp. of $\underline{\mathbf{3}}_{\mathbf{4}}$ for $(2\,m-n)\mod 3=2$
	$\chi_3^m\,(\chi_3^\star)^{n-3-m}\,(\chi_2^\star)^3\ (m=0,...,n-3)$	$\underline{\mathbf{1}}_{\mathbf{1,2,3}}$ for $(2\,m-n)\mod 3=0$ $3^{\rm rd}$ comp. of $\underline{\mathbf{3}}_{\mathbf{2}}$ for $(2\,m-n)\mod 3=1$ $3^{\rm rd}$ comp. of $\underline{\mathbf{3}}_{\mathbf{1}}$ for $(2\,m-n)\mod 3=2$

Table B.12: Higher-dimensional Operators of $\Sigma(81)$. Analogously to T_7, the higher-dimensional operators can be identified by three representation matrices $\mathrm{S}_1=\mathrm{C}^2$, $\mathrm{S}_2=\mathrm{A}^2\,\mathrm{C}^2\,\mathrm{A}$ and $\mathrm{S}_3=\mathrm{A}\,\mathrm{B}^2\,\mathrm{C}\,\mathrm{A}^2$ which are products of the three given generators A, B and C. The resulting relations are shown in the third column. The number of operators is about $[\frac{n}{3}]$ for larger values of n.

B.3 Anomalies

After the correct interpretation of the decay $\pi^0 \to \gamma\gamma$ by Adler [247] as well as Bell and Jackiw [248] in terms of a breakdown of the symmetry on the quantum level, which is denoted the Abelian anomaly. Many more anomalies in quantum field theory have been discovered [249], like the non-Abelian chiral anomaly, the gravitational anomaly, the conformal anomaly and the global anomaly. As we are especially interested in gauge theories and flavor symmetries, we summarize which gauge groups are safe and the main facts about discrete anomalies.

B.3.1 Anomalies of Gauge Theories

Any sensible gauge theory has to be anomaly-free. Here, we concentrate on chiral gauge anomalies which are given by

$$A_{abc} = \mathrm{tr}\left(\gamma_5 \left\{\Gamma_a, \Gamma_b\right\} \Gamma_c\right) \ , \tag{B.13}$$

where γ_5 denotes the chirality operator of the Lorentz γ-algebra and $\Gamma_a = P_L T_a^- + P_R T_A^+$, $P_{R,L} = \frac{1}{2}\left(1 \pm \gamma_5\right)$. $T_a^\pm$ is the generator of the gauge group in the given representation[2]. In an Abelian theory $T_a^\pm$ is replaced by the charge q of the particle. The anomaly constraints have been discussed in [250]. Vector representations are automatically free of anomalies, since the anomaly is related to γ_5. All other chiral representations have to fulfill the anomaly constraint

$$\mathrm{tr}\left(\left\{T_a^\pm, T_b^\pm\right\} T_c^\pm\right) = 0 \ . \tag{B.14}$$

All real representations are anomaly-free. Hence, Lie algebras which contain only real representations are safe. Those include A_1, $B_N, N \geq 2$, $C_N, N \geq 3$, $D_{2N}, N \geq 2$, G_2, F_4, E_7 and E_8. $A_N, N \geq 2$, $D_{2(N+1)}, N \geq 1$ and E_6 can have complex representations. However, it can be shown by an explicit calculation that the series $\mathfrak{so}(N), N \geq 7$ is also safe. Therefore models based on SO(10) are automatically anomaly-free. Models based on E_6 are also anomaly-free, independent of which representation is associated to the fermions, since the anomaly in Eq. (B.13) is an E_6 singlet and on the other hand Γ_a are in the adjoint representation. However, the tensor product

$$\left[\underline{\mathbf{78}} \otimes \underline{\mathbf{78}}\right]_{\mathrm{sym}} \otimes \underline{\mathbf{78}} = \left[\underline{\mathbf{1}} \oplus \underline{\mathbf{650}} \oplus \underline{\mathbf{2430}}\right] \otimes \underline{\mathbf{78}} \tag{B.15}$$

does not contain a singlet. Hence, all chiral anomalies have to vanish. The only semi-simple Lie algebras, which can lead to anomalies are $A_N, N \geq 2$, where every representation has to be checked. Let us note two important examples. In SU(5), $\underline{\mathbf{10}} \oplus \underline{\overline{\mathbf{5}}}$, which is assigned to fermions is anomaly-free. In the SM, the fundamental representations and its complex conjugate one as well as the adjoint representation of SU(3) are anomaly-free. However, Abelian anomalies from $\mathrm{U}(1)_Y$, as well as the mixed Abelian – non-Abelian anomalies have to be cancelled, which leads to the constraints

$$\sum_{i \in \text{SM particle}} Q_i = \sum_{i \in \text{SM particle}} Q_i^3 = 0 \ . \tag{B.16}$$

B.3.2 Discrete Anomalies

Discrete symmetries [251] can be broken by quantum effects like continuous symmetries. In the case of Abelian Z_N symmetries, it was argued [252, 253] that the discrete symmetries have to fulfill the anomaly constraints of U(1) "mod N", which can be understood when they are embedded into U(1).

[2] If there are more representations, there are also mixed anomalies which have to be cancelled. This can be seen if all particles are in one reducible representation.

Anomalies of non-Abelian symmetries have first been discussed in examples [254] and Araki [255] derived an anomaly constraint by the Fujikawa method, which was further extended in [256]. The main result of the work by Araki is that only the maximal Abelian subgroups of the non-Abelian group G are relevant for the anomaly. Therefore a non-Abelian discrete group is anomaly-free if it satisfies

$$\sum_{i \in \text{particles}} q_{iI} \equiv 0 \bmod N_I \ , \tag{B.17}$$

where the Abelian subgroups of G are $\prod_I Z_{N_I} \leq G$ and q_{iI} is the charge of particle i with respect to Z_{N_I}.

Appendix C

Renormalization Group

C.1 General RG Equations for Mixing Parameters

We show the RG equations for the lepton mixing parameters obtained from the derivation discussed above. We give the first order of the expansion in the small CHOOZ angle θ_{13}.
The results are presented in the form of tables which list the coefficients of

$$P_{fg} = (C_e\, Y_e^\dagger Y_e + C_\nu\, Y_\nu^\dagger Y_\nu)_{fg} \text{ or}$$
$$F_{fg} = (D_e\, Y_e^\dagger Y_e + D_\nu\, Y_\nu^\dagger Y_\nu)_{fg}$$

in the RG equations. Thus, if only a single element of P, is dominant, the derivatives of the mixing parameters are found from the corresponding rows in the tables. Of course, if several entries of P_{fg} are relevant, their contributions simply add up. While the complete RG equations are basis-independent, the entries of the table depend on the choice of the basis, since P is basis-dependent. We use the basis where Y_e is diagonal and where the unphysical phases in the MNS matrix are zero.

	$16\pi^2\, \dot{m}_1/m_1$	$16\pi^2\, \dot{m}_2/m_2$	$16\pi^2\, \dot{m}_3/m_3$
α_ν	1	1	1
P_{11}	$2c_{12}^2$	$2s_{12}^2$	0
P_{22}	$2s_{12}^2 c_{23}^2$	$2c_{12}^2 c_{23}^2$	$2s_{23}^2$
P_{33}	$2s_{12}^2 s_{23}^2$	$2c_{12}^2 s_{23}^2$	$2c_{23}^2$
$\mathrm{Re}P_{21}$	$-2\sin 2\theta_{12} c_{23}$	$2\sin 2\theta_{12} c_{23}$	0
$\mathrm{Re}P_{31}$	$2\sin 2\theta_{12} s_{23}$	$-2\sin 2\theta_{12} s_{23}$	0
$\mathrm{Re}P_{32}$	$-2\sin 2\theta_{23} s_{12}^2$	$-2\sin 2\theta_{23} c_{12}^2$	$2\sin 2\theta_{23}$
$\mathrm{Im}P_{21}$	0	0	0
$\mathrm{Im}P_{31}$	0	0	0
$\mathrm{Im}P_{32}$	0	0	0

$$16\pi^2\, \dot{m}_e/m_e = \mathrm{Re}\,\alpha_e + F_{11}$$
$$16\pi^2\, \dot{m}_\mu/m_\mu = \mathrm{Re}\,\alpha_e + F_{22}$$
$$16\pi^2\, \dot{m}_\tau/m_\tau = \mathrm{Re}\,\alpha_e + F_{33}$$

Table C.1: β-functions of neutrino and charged lepton masses for $\theta_{13} = 0$.

$$\begin{array}{|ll|ll|}
\hline
\mathcal{Q}_{13}^{\pm} &= \frac{|m_3 \pm m_1 e^{i\varphi_1}|^2}{\Delta m_{32}^2(1+\zeta)} & \mathcal{S}_{13} &= \frac{m_1 m_3 \sin\varphi_1}{\Delta m_{32}^2(1+\zeta)} \\
\mathcal{Q}_{23}^{\pm} &= \frac{|m_3 \pm m_2 e^{i\varphi_2}|^2}{\Delta m_{32}^2} & \mathcal{S}_{23} &= \frac{m_2 m_3 \sin\varphi_2}{\Delta m_{32}^2} \\
\mathcal{Q}_{12}^{\pm} &= \frac{|m_2 e^{i\varphi_2} \pm m_1 e^{i\varphi_1}|^2}{\Delta m_{21}^2} & \mathcal{S}_{12} &= \frac{m_1 m_2 \sin(\varphi_1-\varphi_2)}{\Delta m_{21}^2} \\
\hline
\mathcal{A}_{13}^{\pm} &= \frac{\left(m_1^2+m_3^2\right)\cos\delta \pm 2m_1 m_3 \cos(\delta-\varphi_1)}{\Delta m_{32}^2(1+\zeta)} & \mathcal{B}_{13}^{\pm} &= \frac{\left(m_1^2+m_3^2\right)\sin\delta \pm 2m_1 m_3 \sin(\delta-\varphi_1)}{\Delta m_{32}^2(1+\zeta)} \\
\mathcal{A}_{23}^{\pm} &= \frac{\left(m_2^2+m_3^2\right)\cos\delta \pm 2m_2 m_3 \cos(\delta-\varphi_2)}{\Delta m_{32}^2} & \mathcal{B}_{23}^{\pm} &= \frac{\left(m_2^2+m_3^2\right)\sin\delta \pm 2m_2 m_3 \sin(\delta-\varphi_2)}{\Delta m_{32}^2} \\
\hline
\end{array}$$

$$\begin{aligned}
\mathcal{C}_{13}^{12} &= \tfrac{m_1}{\Delta m_{21}^2(1+\zeta)}\left[(1+\zeta)\, m_2 \sin\left(\varphi_1-\varphi_2\right) - \zeta m_3 \sin\left(2\delta-\varphi_1\right)\right] \\
\mathcal{C}_{13}^{23} &= \tfrac{m_3}{\Delta m_{32}^2(1+\zeta)}\left[m_1 \sin\left(2\delta-\varphi_1\right) + (1+\zeta)\, m_2 \sin\varphi_2\right] \\
\mathcal{C}_{23}^{12} &= \tfrac{m_2}{\Delta m_{21}^2}\left[m_1 \sin\left(\varphi_1-\varphi_2\right) - \zeta m_3 \sin\left(2\delta-\varphi_2\right)\right] \\
\mathcal{C}_{23}^{13} &= \tfrac{m_3}{\Delta m_{32}^2(1+\zeta)}\left[m_1 \sin\varphi_1 + (1+\zeta)\, m_2 \sin\left(2\delta-\varphi_2\right)\right]
\end{aligned}$$

$$\begin{aligned}
\mathcal{D}_1 &= \tfrac{m_3}{\Delta m_{32}^2(1+\zeta)}\left[m_1 \cos\left(\delta-\varphi_1\right) - (1+\zeta)\, m_2 \cos\left(\delta-\varphi_2\right)\right]\sin\delta \\
\mathcal{D}_2 &= \tfrac{m_3}{\Delta m_{32}^2(1+\zeta)}\left[m_1 \cos\left(2\delta-\varphi_1\right) - (1+\zeta)\, m_2 \cos\left(2\delta-\varphi_2\right) + \zeta m_3\right]
\end{aligned}$$

Table C.2: Definition of the abbreviations used in Tab. C.3–Tab. C.5.

	$32\pi^2\,\dot\theta_{12}$	$64\pi^2\,\dot\theta_{13}$	$32\pi^2\,\dot\theta_{23}$
P_{11}	$\mathcal{Q}_{12}^{+}\sin 2\theta_{12}$	0	0
P_{22}	$-\mathcal{Q}_{12}^{+}\sin 2\theta_{12}c_{23}^2$	$\left(\mathcal{A}_{23}^{+}-\mathcal{A}_{13}^{+}\right)\sin 2\theta_{12}\sin 2\theta_{23}$	$\left(\mathcal{Q}_{23}^{+}c_{12}^2+\mathcal{Q}_{13}^{+}s_{12}^2\right)\sin 2\theta_{23}$
P_{33}	$-\mathcal{Q}_{12}^{+}\sin 2\theta_{12}s_{23}^2$	$-\left(\mathcal{A}_{23}^{+}-\mathcal{A}_{13}^{+}\right)\sin 2\theta_{12}\sin 2\theta_{23}$	$-\left(\mathcal{Q}_{23}^{+}c_{12}^2+\mathcal{Q}_{13}^{+}s_{12}^2\right)\sin 2\theta_{23}$
$\mathrm{Re}P_{21}$	$2\mathcal{Q}_{12}^{+}\cos 2\theta_{12}c_{23}$	$4\left(\mathcal{A}_{13}^{+}c_{12}^2+\mathcal{A}_{23}^{+}s_{12}^2\right)s_{23}$	$\left(\mathcal{Q}_{23}^{+}-\mathcal{Q}_{13}^{+}\right)\sin 2\theta_{12}s_{23}$
$\mathrm{Re}P_{31}$	$-2\mathcal{Q}_{12}^{+}\cos 2\theta_{12}s_{23}$	$4\left(\mathcal{A}_{13}^{+}c_{12}^2+\mathcal{A}_{23}^{+}s_{12}^2\right)c_{23}$	$\left(\mathcal{Q}_{23}^{+}-\mathcal{Q}_{13}^{+}\right)\sin 2\theta_{12}c_{23}$
$\mathrm{Re}P_{32}$	$\mathcal{Q}_{12}^{+}\sin 2\theta_{12}\sin 2\theta_{23}$	$2\left(\mathcal{A}_{23}^{+}-\mathcal{A}_{13}^{+}\right)\sin 2\theta_{12}\cos 2\theta_{23}$	$2\left(\mathcal{Q}_{23}^{+}c_{12}^2+\mathcal{Q}_{13}^{+}s_{12}^2\right)\cos 2\theta_{23}$
$\mathrm{Im}P_{21}$	$4\mathcal{S}_{12}c_{23}$	$4\left(\mathcal{B}_{13}^{-}c_{12}^2+\mathcal{B}_{23}^{-}s_{12}^2\right)s_{23}$	$2\left(\mathcal{S}_{23}-\mathcal{S}_{13}\right)\sin 2\theta_{12}s_{23}$
$\mathrm{Im}P_{31}$	$-4\mathcal{S}_{12}s_{23}$	$4\left(\mathcal{B}_{13}^{-}c_{12}^2+\mathcal{B}_{23}^{-}s_{12}^2\right)c_{23}$	$2\left(\mathcal{S}_{23}-\mathcal{S}_{13}\right)\sin 2\theta_{12}c_{23}$
$\mathrm{Im}P_{32}$	0	$2\left(\mathcal{B}_{23}^{-}-\mathcal{B}_{13}^{-}\right)\sin 2\theta_{12}$	$4\left(\mathcal{S}_{23}c_{12}^2+\mathcal{S}_{13}s_{12}^2\right)$

Table C.3: Coefficients of P_{fg} in the RG equation of the mixing angles θ_{ij} in the limit $\theta_{13}\to 0$. The abbreviations $\mathcal{A}_{ij}^{\pm}$, $\mathcal{B}_{ij}^{\pm}$, $\mathcal{S}_{ij}$ and $\mathcal{Q}_{ij}^{\pm}$ depend on the mass eigenvalues and phases only, and enhance the running for a degenerate mass spectrum, since they are of the form $f_{ij}(m_i, m_j, \text{phases})/(m_j^2-m_i^2)$. They are listed in Tab. C.2.

	$64\pi^2\dot{\delta}^{(-1)}$
P_{11}	0
P_{22}	$-\left(\mathcal{B}_{23}^{+}-\mathcal{B}_{13}^{+}\right)\sin 2\theta_{12}\sin 2\theta_{23}$
P_{33}	$\left(\mathcal{B}_{23}^{+}-\mathcal{B}_{13}^{+}\right)\sin 2\theta_{12}\sin 2\theta_{23}$
$\mathrm{Re}P_{21}$	$-4\left(\mathcal{B}_{13}^{+}c_{12}^{2}+\mathcal{B}_{23}^{+}s_{12}^{2}\right)s_{23}$
$\mathrm{Re}P_{31}$	$-4\left(\mathcal{B}_{13}^{+}c_{12}^{2}+\mathcal{B}_{23}^{+}s_{12}^{2}\right)c_{23}$
$\mathrm{Re}P_{32}$	$-2\left(\mathcal{B}_{23}^{+}-\mathcal{B}_{13}^{+}\right)\sin 2\theta_{12}\cos 2\theta_{23}$
$\mathrm{Im}P_{21}$	$4\left(\mathcal{A}_{13}^{-}c_{12}^{2}+\mathcal{A}_{23}^{-}s_{12}^{2}\right)s_{23}$
$\mathrm{Im}P_{31}$	$4\left(\mathcal{A}_{13}^{-}c_{12}^{2}+\mathcal{A}_{23}^{-}s_{12}^{2}\right)c_{23}$
$\mathrm{Im}P_{32}$	$2\left(\mathcal{A}_{23}^{-}-\mathcal{A}_{13}^{-}\right)\sin 2\theta_{12}$

	$64\pi^2\dot{\delta}^{(0)}$
P_{11}	$-8\left(\left(\mathcal{C}_{13}^{23}+\mathcal{S}_{12}-\mathcal{S}_{23}\right)c_{12}^{2}+\left(\mathcal{C}_{23}^{13}+\mathcal{S}_{12}-\mathcal{S}_{13}\right)s_{12}^{2}\right)$
P_{22}	$8\left(\left(\left(\mathcal{S}_{12}-\mathcal{S}_{23}\right)c_{23}^{2}+\mathcal{C}_{13}^{23}s_{23}^{2}\right)c_{12}^{2}+\left(\left(\mathcal{S}_{12}-\mathcal{S}_{13}\right)c_{23}^{2}+\mathcal{C}_{23}^{13}s_{23}^{2}\right)s_{12}^{2}\right)$
P_{33}	$8\left(\left(\mathcal{C}_{13}^{23}c_{23}^{2}+\left(\mathcal{S}_{12}-\mathcal{S}_{23}\right)s_{23}^{2}\right)c_{12}^{2}+\left(\mathcal{C}_{23}^{13}c_{23}^{2}+\left(\mathcal{S}_{12}-\mathcal{S}_{13}\right)s_{23}^{2}\right)s_{12}^{2}\right)$
$\mathrm{Re}P_{21}$	$-16\mathcal{S}_{12}c_{23}\cot 2\theta_{12}+4\left(2\mathcal{D}_1c_{23}+\left(\mathcal{S}_{23}-\mathcal{S}_{13}\right)s_{23}\tan\theta_{23}\right)\sin 2\theta_{12}$
$\mathrm{Re}P_{31}$	$16\mathcal{S}_{12}s_{23}\cot 2\theta_{12}-4\left(2\mathcal{D}_1s_{23}+\left(\mathcal{S}_{23}-\mathcal{S}_{13}\right)c_{23}\cot\theta_{23}\right)\sin 2\theta_{12}$
$\mathrm{Re}P_{32}$	$-16\left(\mathcal{S}_{23}c_{12}^{2}+\mathcal{S}_{13}s_{12}^{2}\right)\cos 2\theta_{23}\cot 2\theta_{23}-8\left(\mathcal{C}_{13}^{12}c_{12}^{2}+\mathcal{C}_{23}^{12}s_{12}^{2}\right)\sin 2\theta_{23}$
$\mathrm{Im}P_{21}$	$-8\mathcal{Q}_{12}^{-}c_{23}\csc 2\theta_{12}-2\left(2\mathcal{D}_2c_{23}+\left(\mathcal{Q}_{23}^{-}-\mathcal{Q}_{13}^{-}\right)\cos 2\theta_{23}\sec\theta_{23}\right)\sin 2\theta_{12}$
$\mathrm{Im}P_{31}$	$8\mathcal{Q}_{12}^{-}s_{23}\csc 2\theta_{12}+2\left(2\mathcal{D}_2s_{23}-\left(\mathcal{Q}_{23}^{-}-\mathcal{Q}_{13}^{-}\right)\cos 2\theta_{23}\csc\theta_{23}\right)\sin 2\theta_{12}$
$\mathrm{Im}P_{32}$	$-8\left(\mathcal{Q}_{23}^{-}c_{12}^{2}+\mathcal{Q}_{13}^{-}s_{12}^{2}\right)\cot 2\theta_{23}$

Table C.4: Coefficients of P_{fg} in the derivative of the Dirac CP phase. The complete RG equation is given by $\dot{\delta}=\theta_{13}^{-1}\dot{\delta}^{(-1)}+\dot{\delta}^{(0)}+\mathcal{O}(\theta_{13})$. The abbreviations $\mathcal{A}_{ij}^{\pm}$, $\mathcal{B}_{ij}^{\pm}$, $\mathcal{Q}_{ij}^{\pm}$, $\mathcal{C}_{ij}^{kl}$ and $\mathcal{D}_i$ depend on the mass eigenvalues and phases only, and are listed in Tab. C.2.

	$16\pi^2\dot{\varphi}_1$
P_{11}	$-4\mathcal{S}_{12}c_{12}^2$
P_{22}	$4\mathcal{S}_{12}c_{12}^2c_{23}^2 - 4\left(\mathcal{S}_{23}c_{12}^2 + \mathcal{S}_{13}s_{12}^2\right)\cos 2\theta_{23}$
P_{33}	$4\mathcal{S}_{12}c_{12}^2s_{23}^2 + 4\left(\mathcal{S}_{23}c_{12}^2 + \mathcal{S}_{13}s_{12}^2\right)\cos 2\theta_{23}$
$\mathrm{Re}P_{21}$	$-4\mathcal{S}_{12}c_{23}\cos 2\theta_{12}\cot\theta_{12} - 2\left(\mathcal{S}_{23} - \mathcal{S}_{13}\right)\cos 2\theta_{23}\sec\theta_{23}\sin 2\theta_{12}$
$\mathrm{Re}P_{31}$	$4\mathcal{S}_{12}s_{23}\cos 2\theta_{12}\cot\theta_{12} - 2\left(\mathcal{S}_{23} - \mathcal{S}_{13}\right)\cos 2\theta_{23}\csc\theta_{23}\sin 2\theta_{12}$
$\mathrm{Re}P_{32}$	$-8\left(\mathcal{S}_{23}c_{12}^2 + \mathcal{S}_{13}s_{12}^2\right)\cos 2\theta_{23}\cot 2\theta_{23} - 4\mathcal{S}_{12}c_{12}^2\sin 2\theta_{23}$
$\mathrm{Im}P_{21}$	$-2\mathcal{Q}_{12}^-c_{23}\cot\theta_{12} - \left(\mathcal{Q}_{23}^- - \mathcal{Q}_{13}^-\right)\cos 2\theta_{23}\sec\theta_{23}\sin 2\theta_{12}$
$\mathrm{Im}P_{31}$	$2\mathcal{Q}_{12}^-s_{23}\cot\theta_{12} - \left(\mathcal{Q}_{23}^- - \mathcal{Q}_{13}^-\right)\cos 2\theta_{23}\csc\theta_{23}\sin 2\theta_{12}$
$\mathrm{Im}P_{32}$	$-4\left(\mathcal{Q}_{23}^-c_{12}^2 + \mathcal{Q}_{13}^-s_{12}^2\right)\cot 2\theta_{23}$

	$16\pi^2\dot{\varphi}_2$
P_{11}	$-4\mathcal{S}_{12}s_{12}^2$
P_{22}	$4\mathcal{S}_{12}c_{23}^2s_{12}^2 - 4\left(\mathcal{S}_{23}c_{12}^2 + \mathcal{S}_{13}s_{12}^2\right)\cos 2\theta_{23}$
P_{33}	$4\mathcal{S}_{12}s_{23}^2s_{12}^2 + 4\left(\mathcal{S}_{23}c_{12}^2 + \mathcal{S}_{13}s_{12}^2\right)\cos 2\theta_{23}$
$\mathrm{Re}P_{21}$	$-4\mathcal{S}_{12}c_{23}\cos 2\theta_{12}\tan\theta_{12} - 2\left(\mathcal{S}_{23} - \mathcal{S}_{13}\right)\cos 2\theta_{23}\sec\theta_{23}\sin 2\theta_{12}$
$\mathrm{Re}P_{31}$	$4\mathcal{S}_{12}s_{23}\cos 2\theta_{12}\tan\theta_{12} - 2\left(\mathcal{S}_{23} - \mathcal{S}_{13}\right)\cos 2\theta_{23}\csc\theta_{23}\sin 2\theta_{12}$
$\mathrm{Re}P_{32}$	$-8\left(\mathcal{S}_{23}c_{12}^2 + \mathcal{S}_{13}s_{12}^2\right)\cos 2\theta_{23}\cot 2\theta_{23} - 4\mathcal{S}_{12}s_{12}^2\sin 2\theta_{23}$
$\mathrm{Im}P_{21}$	$-2\mathcal{Q}_{12}^-c_{23}\tan\theta_{12} - \left(\mathcal{Q}_{23}^- - \mathcal{Q}_{13}^-\right)\cos 2\theta_{23}\sec\theta_{23}\sin 2\theta_{12}$
$\mathrm{Im}P_{31}$	$2\mathcal{Q}_{12}^-s_{23}\tan\theta_{12} - \left(\mathcal{Q}_{23}^- - \mathcal{Q}_{13}^-\right)\cos 2\theta_{23}\csc\theta_{23}\sin 2\theta_{12}$
$\mathrm{Im}P_{32}$	$-4\left(\mathcal{Q}_{23}^-c_{12}^2 + \mathcal{Q}_{13}^-s_{12}^2\right)\cot 2\theta_{23}$

Table C.5: Coefficients of P_{fg} in the RG equation of the Majorana phases for $\theta_{13} = 0$.

	$16\pi^2\,\dot{\theta}_{12}$	$16\pi^2\,\dot{\theta}_{13}$	$16\pi^2\,\dot{\theta}_{23}$
F_{11}	0	0	0
F_{22}	0	0	0
F_{33}	0	0	0
$\mathrm{Re}F_{21}$	$-c_{23}$	$-s_{23}\cos\delta$	0
$\mathrm{Re}F_{31}$	s_{23}	$-c_{23}\cos\delta$	0
$\mathrm{Re}F_{32}$	0	0	-1
$\mathrm{Im}F_{21}$	0	$-s_{23}\sin\delta$	0
$\mathrm{Im}F_{31}$	0	$-c_{23}\sin\delta$	0
$\mathrm{Im}F_{32}$	0	0	0

Table C.6: Coefficients of F_{fg} in the U_e contribution to the slope of the mixing angles for $\theta_{13} = 0$ and $y_e, y_\mu \ll y_\tau$.

C.2 RG Factors in the Standard Seesaw Model

The Z factors describing the LL approximation are obtained from the counterterms in [63]. The notation is described in Sec. 5.1.

C.2.1 SM

In the SM extended by RH neutrinos, the wave function renormalization of the RH neutrinos is given by

$$\overset{(n)}{Z}_N = \exp\left(\frac{1}{16\pi^2}\overset{(n)}{Y}_\nu\overset{(n)}{Y}_\nu^\dagger \ln\frac{M_n}{M_{n+1}}\right) \tag{C.1}$$

and collecting the contributions from the renormalization of the left-handed doublets

$$\beta^L_{Y_\nu} = \frac{1}{32\pi^2}\left(\overset{(n)}{Y}_\nu^\dagger\overset{(n)}{Y}_\nu + Y_e^\dagger Y_e\right) , \tag{C.2}$$

the Higgs doublet

$$\beta^\phi_{Y_\nu} = \frac{1}{32\pi^2}\left(2\mathrm{tr}\left(\overset{(n)}{Y}_\nu^\dagger\overset{(n)}{Y}_\nu + Y_e^\dagger Y_e + 3Y_u^\dagger Y_u + 3Y_d^\dagger Y_d\right) - \frac{9}{10}g_1^2 - \frac{9}{2}g_2^2\right) , \tag{C.3}$$

and the vertex correction to Y_ν

$$\beta^{Y_\nu}_{Y_\nu} = -\frac{1}{8\pi^2}Y_e^\dagger Y_e , \tag{C.4}$$

the external renormalization in the effective theory with n RH neutrinos yields

$$\begin{aligned}\overset{(n)}{Z}_{\mathrm{ext}} = \exp\Bigg(\frac{1}{32\pi^2}\Bigg(&\overset{(n)}{Y}_\nu^\dagger\overset{(n)}{Y}_\nu - 3Y_e^\dagger Y_e + 2\mathrm{tr}\left(\overset{(n)}{Y}_\nu^\dagger\overset{(n)}{Y}_\nu + Y_e^\dagger Y_e + 3Y_u^\dagger Y_u + 3Y_d^\dagger Y_d\right)\\ &- \frac{9}{10}g_1^2 - \frac{9}{2}g_2^2\Bigg)\ln\frac{M_n}{M_{n+1}}\Bigg) .\end{aligned} \tag{C.5}$$

Neglecting the thresholds in the charged lepton sector and the quark sector, the expression for the external renormalization factor $Z^{\mathrm{SM}}_{\mathrm{ext}}$ describing the total external renormalization can be further approximated to

$$\begin{aligned}Z^{\mathrm{SM}}_{\mathrm{ext}} = \exp\Bigg(&\frac{1}{32\pi^2}\sum_{n=0}^{3}\left[\overset{(n)}{Y}_\nu^\dagger\overset{(n)}{Y}_\nu + 2\mathrm{tr}\left(\overset{(n)}{Y}_\nu^\dagger\overset{(n)}{Y}_\nu\right)\right]\ln\frac{M_n}{M_{n+1}}\\ &+\frac{1}{32\pi^2}\left[-3Y_e^\dagger Y_e + 2\mathrm{tr}\left(Y_e^\dagger Y_e + 3Y_u^\dagger Y_u + 3Y_d^\dagger Y_d\right) - \frac{9}{10}g_1^2 - \frac{9}{2}g_2^2\right]\ln\frac{\langle\phi\rangle}{\Lambda}\Bigg) .\end{aligned} \tag{C.6}$$

Here, we have denoted

$$M_0 \equiv \langle\phi\rangle , \qquad M_4 \equiv \Lambda$$

for uniformity of the presentation. The renormalization effect due to the additional vertex corrections to the D5 operator is given by

$$\overset{(n)}{Z}_\kappa = \exp\left(\frac{1}{16\pi^2}\left(\lambda + \frac{9}{10}g_1^2 + \frac{3}{2}g_2^2\right)\ln\frac{M_n}{M_{n+1}}\right) . \tag{C.7}$$

The mass of RH neutrinos receives only corrections from the wave function renormalization to arbitrary loop order.

C.2.2 MSSM

In the MSSM extended by RH neutrinos, there are no vertex corrections due to the non-renormalization theorem and the wave function renormalization yields

$$\overset{(n)}{Z}_L = \exp\left(\frac{1}{32\pi^2}\left(2Y_e^\dagger Y_e + 2\,\overset{(n)}{Y}{}_\nu^\dagger \overset{(n)}{Y}_\nu - \frac{3}{5}g_1^2 - 3g_2^2\right)\ln\frac{M_n}{M_{n+1}}\right) \tag{C.8}$$

$$\overset{(n)}{Z}_N = \exp\left(\frac{1}{8\pi^2}\,\overset{(n)}{Y}_\nu \overset{(n)}{Y}{}_\nu^\dagger \ln\frac{M_n}{M_{n+1}}\right) \tag{C.9}$$

$$\overset{(n)}{Z}_\phi = \exp\left(\frac{1}{32\pi^2}\left(\mathrm{tr}\left(6Y_u^\dagger Y_u + 2\,\overset{(n)}{Y}{}_\nu^\dagger \overset{(n)}{Y}_\nu\right) - \frac{3}{5}g_1^2 - 3g_2^2\right)\ln\frac{M_n}{M_{n+1}}\right)\,. \tag{C.10}$$

The external renormalization factor $Z_{\mathrm{ext}}^{\mathrm{MSSM}}$ is given by the product of the wave function renormalization of the left-handed doublet with the Higgs doublet

$$\overset{(n)}{Z}_{\mathrm{ext}} = \overset{(n)}{Z}_L \overset{(n)}{Z}_\phi \tag{C.11}$$

because the two wave function renormalization factors commute. As the neutrino Yukawa couplings only change at the thresholds (up to 1 loop order), the external renormalization factor can be further approximated by

$$\begin{aligned} Z_{\mathrm{ext}}^{\mathrm{MSSM}} = \exp\Bigg(&\frac{1}{16\pi^2}\sum_{n=0}^{3}\left(\overset{(n)}{Y}{}_\nu^\dagger \overset{(n)}{Y}_\nu + \mathrm{tr}\left(\overset{(n)}{Y}{}_\nu^\dagger \overset{(n)}{Y}_\nu\right)\right)\ln\frac{M_n}{M_{n+1}} \\ &+\frac{1}{16\pi^2}\left(Y_e^\dagger Y_e - \frac{3}{5}g_1^2 - 3g_2^2 + 3\mathrm{tr}\left(Y_u^\dagger Y_u\right)\right)\ln\frac{\langle\phi\rangle}{\Lambda}\Bigg)\,. \end{aligned} \tag{C.12}$$

Acknowledgments

At the end of my PhD studies, I want to take the opportunity to thank everybody who supported me during the completion of my thesis. In particular, I would like to thank

- my supervisor Manfred Lindner for an interesting topic, the possibility to attend several summer schools and conferences, interesting discussions as well as the excellent working environment;
- Stefan Antusch, Claudia Hagedorn, Martin Holthausen, Jörn Kersten, Manfred Lindner, Michael Ratz, Werner Rodejohann and Alexei Smirnov for interesting and fruitful collaborations;
- Claudia Hagedorn for proofreading the whole manuscript and many useful comments;
- my flat mate Andreas Hohenegger for proofreading parts of my thesis, cooking together, ...;
- Mathias Garny and Alexander Kartavtsev, my office mates in München and Heidelberg, respectively, for many interesting and useful discussions about physics and other topics;
- Martin Holthausen for being patient when I was writing up;
- Markus Michael Müller "MMM" for a perfectly running computer system;
- our secretary Karin Ramm in München and Anja Bernheiser in Heidelberg for taking care of all administrational tasks;
- all people for the nice and comfortable atmosphere in the group: Adisorn Adulpra, Evgeny Akhmedov, Florian Bauer, Alexander Blum, Marc-Thomas Eisele, Mathias Garny, Sruba Goswami, Naoyuki Haba, Claudia Hagedorn, Andreas Hohenegger, Martin Holthausen, Alexander Kartavtsev, Hendrik Kienert, Joachim Kopp, Manfred Lindner, Alexander Merle, Markus Michael Müller, Viviana Niro, Toshi Ota, Mark Rolinec, Joe Sato, Tom Underwood and the whole division "particle & astro-particle physics" at the MPI-K.

Finally, I want to especially thank my family (my parents as well as my brothers Martin and Johannes) for supporting me in every possible way during my PhD studies and before.

Bibliography

[1] J. C. Pati and A. Salam, *Unified lepton-hadron symmetry and a gauge theory of the basic interactions*, Phys. Rev. **D8** (1973), 1240–1251.

[2] H. Georgi and S. L. Glashow, *Unity of all elementary particle forces*, Phys. Rev. Lett. **32** (1974), 438–441.

[3] H. Georgi, *The state of the art - gauge theories. (talk)*, AIP Conf. Proc. **23** (1975), 575–582.

[4] H. Fritzsch and P. Minkowski, *Unified interactions of leptons and hadrons*, Ann. Phys. **93** (1975), 193–266.

[5] F. Gursey, P. Ramond, and P. Sikivie, *A universal gauge theory model based on E_6*, Phys. Lett. **B60** (1976), 177.

[6] Y. Achiman and B. Stech, *Quark lepton symmetry and mass scales in an E_6 unified gauge model*, Phys. Lett. **B77** (1978), 389.

[7] Q. Shafi, *E_6 as a unifying gauge symmetry*, Phys. Lett. **B79** (1978), 301.

[8] R. Barbieri, D. V. Nanopoulos, and A. Masiero, *Hierarchical fermion masses in E_6*, Phys. Lett. **B104** (1981), 194.

[9] B. Stech and Z. Tavartkiladze, *Fermion masses and coupling unification in E_6: Life in the desert*, Phys. Rev. **D70** (2004), 035002, hep-ph/0311161 .

[10] F. Wilczek and A. Zee, *Horizontal interaction and weak mixing angles*, Phys. Rev. Lett. **42** (1979), 421.

[11] R. Gatto, G. Sartori, and M. Tonin, *Weak selfmasses, Cabibbo angle, and broken $SU(2)\times SU(2)$*, Phys. Lett. **B28** (1968), 128–130.

[12] A. Y. Smirnov, *Neutrinos: '...Annus mirabilis'*, (2004), hep-ph/0402264 .

[13] M. Raidal, *Prediction $\theta_c + \theta_{\rm sol} = \pi/4$ from flavor physics: A new evidence for grand unification?*, Phys. Rev. Lett. **93** (2004), 161801, hep-ph/0404046 .

[14] H. Minakata and A. Y. Smirnov, *Neutrino mixing and quark lepton complementarity*, Phys. Rev. **D70** (2004), 073009, hep-ph/0405088 .

[15] Y. Koide, *Charged lepton mass sum rule from $U(3)$ family higgs potential model*, Mod. Phys. Lett. **A5** (1990), 2319–2324.

[16] R. Barbieri, L. J. Hall, D. R. Smith, A. Strumia, and N. Weiner, *Oscillations of solar and atmospheric neutrinos*, JHEP **12** (1998), 017, hep-ph/9807235 .

[17] W. Buchmüller and T. Yanagida, *Quark lepton mass hierarchies and the baryon asymmetry*, Phys. Lett. **B445** (1999), 399–402, hep-ph/9810308 .

[18] F. Vissani, *Large mixing, family structure, and dominant block in the neutrino mass matrix*, JHEP **11** (1998), 025, hep-ph/9810435 .

[19] S. T. Petcov, *On pseudo-Dirac neutrinos, neutrino oscillations and neutrinoless double beta decay*, Phys. Lett. **B110** (1982), 245–249.

[20] P. Binetruy, S. Lavignac, S. T. Petcov, and P. Ramond, *Quasi-degenerate neutrinos from an Abelian family symmetry*, Nucl. Phys. **B496** (1997), 3–23, hep-ph/9610481 .

[21] N. F. Bell and R. R. Volkas, *Bottom-up model for maximal $\nu_\mu - \nu_\tau$ mixing*, Phys. Rev. **D63** (2001), 013006, hep-ph/0008177 .

[22] K. S. Babu, E. Ma, and J. W. F. Valle, *Underlying A_4 symmetry for the neutrino mass matrix and the quark mixing matrix*, Phys. Lett. **B552** (2003), 207–213, hep-ph/0206292 .

[23] M. Hirsch, J. C. Romao, S. Skadhauge, J. W. F. Valle, and A. Villanova del Moral, *Phenomenological tests of supersymmetric A_4 family symmetry model of neutrino mass*, Phys. Rev. **D69** (2004), 093006, hep-ph/0312265 .

[24] S. Choubey and W. Rodejohann, *A flavor symmetry for quasi-degenerate neutrinos: $L_\mu - L_\tau$*, Eur. Phys. J. **C40** (2005), 259–268, hep-ph/0411190 .

[25] R. Barbieri, L. J. Hall, S. Raby, and A. Romanino, *Unified theories with $U(2)$ flavor symmetry*, Nucl. Phys. **B493** (1997), 3–26, hep-ph/9610449 .

[26] R. Barbieri, L. Giusti, L. J. Hall, and A. Romanino, *Fermion masses and symmetry breaking of a $U(2)$ flavour symmetry*, Nucl. Phys. **B550** (1999), 32–40, hep-ph/9812239 .

[27] S. F. King, *Predicting neutrino parameters from $SO(3)$ family symmetry and quark-lepton unification*, JHEP **08** (2005), 105, hep-ph/0506297 .

[28] S. F. King and G. G. Ross, *Fermion masses and mixing angles from $SU(3)$ family symmetry*, Phys. Lett. **B520** (2001), 243–253, hep-ph/0108112 .

[29] S. F. King and G. G. Ross, *Fermion masses and mixing angles from $SU(3)$ family symmetry and unification*, Phys. Lett. **B574** (2003), 239–252, hep-ph/0307190 .

[30] E. Ma and G. Rajasekaran, *Softly broken A_4 symmetry for nearly degenerate neutrino masses*, Phys. Rev. **D64** (2001), 113012, hep-ph/0106291 .

[31] S. Morisi, M. Picariello, and E. Torrente-Lujan, *A model for fermion masses and lepton mixing in $SO(10) \times A_4$*, Phys. Rev. **D75** (2007), 075015, hep-ph/0702034 .

[32] G. Altarelli, F. Feruglio, and C. Hagedorn, *A SUSY SU(5) Grand Unified Model of Tri-Bimaximal Mixing from A4*, JHEP **03** (2008), 052–052, 0802.0090 .

[33] B. Stech and Z. Tavartkiladze, *Generation Symmetry and E_6 Unification*, Phys. Rev. **D77** (2008), 076009, 0802.0894 .

[34] P. Minkowski, *$\mu \to e\gamma$ at a rate of one out of 1-billion muon decays?*, Phys. Lett. **B67** (1977), 421.

[35] M. Gell-Mann, P. Ramond, and R. Slansky, *Complex spinors and unified theories*, in *Supergravity* (P. van Nieuwenhuizen and D. Z. Freedman, eds.), North Holland, Amsterdam, 1979, p. 315.

[36] T. Yanagida, *Horizontal gauge symmetry and masses of neutrinos*, in *Proceedings of the Workshop on The Unified Theory and the Baryon Number in the Universe* (O. Sawada and A. Sugamoto, eds.), KEK, Tsukuba, Japan, 1979, p. 95.

[37] R. N. Mohapatra and G. Senjanović, *Neutrino mass and spontaneous parity violation*, Phys. Rev. Lett. **44** (1980), 912.

[38] S. L. Glashow, *The future of elementary particle physics*, in *Proceedings of the 1979 Cargèse Summer Institute on Quarks and Leptons* (M. L. vy, J.-L. Basdevant, D. Speiser, J. Weyers, R. Gastmans, and M. Jacob, eds.), Plenum Press, New York, 1980, pp. 687–713.

[39] M. Magg and C. Wetterich, *Neutrino mass problem and gauge hierarchy*, Phys. Lett. **B94** (1980), 61.

[40] R. N. Mohapatra and G. Senjanovic, *Neutrino mass and spontaneous parity nonconservation*, Phys. Rev. Lett. **44** (1980), 912.

[41] G. Lazarides, Q. Shafi, and C. Wetterich, *Proton lifetime and fermion masses in an $SO(10)$ model*, Nucl. Phys. **B181** (1981), 287.

[42] R. Foot, H. Lew, X. G. He, and G. C. Joshi, *Seesaw neutrino masses induced by a triplet of leptons*, Z. Phys. **C44** (1989), 441.

[43] E. Ma, *Pathways to naturally small neutrino masses*, Phys. Rev. Lett. **81** (1998), 1171–1174, hep-ph/9805219 .

[44] R. N. Mohapatra and J. W. F. Valle, *Neutrino mass and baryon-number nonconservation in superstring models*, Phys. Rev. **D34** (1986), 1642.

[45] R. N. Mohapatra, *Mechanism for understanding small neutrino mass in superstring theories*, Phys. Rev. Lett. **56** (1986), 561–563.

[46] A. Y. Smirnov, *Seesaw enhancement of lepton mixing*, Phys. Rev. **D48** (1993), 3264–3270, hep-ph/9304205 .

[47] A. Y. Smirnov, *Alternatives to the seesaw mechanism*, (2004), hep-ph/0411194 .

[48] T. Fukuyama and H. Nishiura, *Mass matrix of Majorana neutrinos*, (1997), hep-ph/9702253 .

[49] R. N. Mohapatra and S. Nussinov, *Bimaximal neutrino mixing and neutrino mass matrix*, Phys. Rev. **D60** (1999), 013002, hep-ph/9809415 .

[50] E. Ma and M. Raidal, *Neutrino mass, muon anomalous magnetic moment, and lepton flavor nonconservation*, Phys. Rev. Lett. **87** (2001), 011802, hep-ph/0102255 .

[51] C. S. Lam, *A 2-3 symmetry in neutrino oscillations*, Phys. Lett. **B507** (2001), 214–218, hep-ph/0104116 .

[52] M. Tanimoto, *Renormalization effect on large neutrino flavor mixing in the minimal supersymmetric standard model*, Phys. Lett. **B360** (1995), 41–46, hep-ph/9508247 .

[53] J. R. Ellis and S. Lola, *Can neutrinos be degenerate in mass?*, Phys. Lett. **B458** (1999), 310–321, hep-ph/9904279 .

[54] P. H. Chankowski, W. Krolikowski, and S. Pokorski, *Fixed points in the evolution of neutrino mixings*, Phys. Lett. **B473** (2000), 109–117, hep-ph/9910231 .

[55] J. A. Casas, J. R. Espinosa, A. Ibarra, and I. Navarro, *General RG equations for physical neutrino parameters and their phenomenological implications*, Nucl. Phys. **B573** (2000), 652, hep-ph/9910420 .

[56] N. Haba, Y. Matsui, and N. Okamura, *The effects of majorana phases in three-generation neutrinos*, Eur. Phys. J. **C17** (2000), 513–520, hep-ph/0005075 .

[57] K. R. S. Balaji, R. N. Mohapatra, M. K. Parida, and E. A. Paschos, *Large neutrino mixing from renormalization group evolution*, Phys. Rev. **D63** (2001), 113002, hep-ph/0011263 .

[58] M. Frigerio and A. Y. Smirnov, *Radiative corrections to neutrino mass matrix in the standard model and beyond*, JHEP **02** (2003), 004, hep-ph/0212263 .

[59] S. Antusch, J. Kersten, M. Lindner, and M. Ratz, *Running neutrino masses, mixings and CP phases: Analytical results and phenomenological consequences*, Nucl. Phys. **B674** (2003), 401–433, hep-ph/0305273 .

[60] J. A. Casas, J. R. Espinosa, A. Ibarra, and I. Navarro, *Naturalness of nearly degenerate neutrinos*, Nucl. Phys. **B556** (1999), 3–22, hep-ph/9904395 .

[61] J. A. Casas, J. R. Espinosa, A. Ibarra, and I. Navarro, *Nearly degenerate neutrinos, supersymmetry and radiative corrections*, Nucl. Phys. **B569** (2000), 82–106, hep-ph/9905381 .

[62] S. F. King and N. N. Singh, *Renormalisation group analysis of single right-handed neutrino dominance*, Nucl. Phys. **B591** (2000), 3–25, hep-ph/0006229 .

[63] S. Antusch, J. Kersten, M. Lindner, and M. Ratz, *Neutrino mass matrix running for non-degenerate see-saw scales*, Phys. Lett. **B538** (2002), 87–95, hep-ph/0203233 .

[64] S. Antusch, J. Kersten, M. Lindner, and M. Ratz, *The LMA solution from bimaximal lepton mixing at the GUT scale by renormalization group running*, Phys. Lett. **B544** (2002), 1–10, hep-ph/0206078 .

[65] S. Antusch and M. Ratz, *Radiative generation of the LMA solution from small solar neutrino mixing at the GUT scale*, JHEP **11** (2002), 010, hep-ph/0208136 .

[66] T. Miura, T. Shindou, and E. Takasugi, *The renormalization group effect to the bi-maximal mixing*, Phys. Rev. **D68** (2003), 093009, hep-ph/0308109 .

[67] T. Shindou and E. Takasugi, *The role of Majorana CP phases in the bi-maximal mixing scheme: Hierarchical Dirac mass case*, Phys. Rev. **D70** (2004), 013005, hep-ph/0402106 .

[68] J. wei Mei and Z. zhong Xing, *Radiative generation of θ_{13} with the seesaw threshold effect*, Phys. Rev. **D70** (2004), 053002, hep-ph/0404081 .

[69] S. Antusch, J. Kersten, M. Lindner, M. Ratz, and M. A. Schmidt, *Running neutrino mass parameters in see-saw scenarios*, JHEP **03** (2005), 024, hep-ph/0501272 .

[70] Super-K amiokande Collaboration, Y. Fukuda et al., *Evidence for oscillation of atmospheric neutrinos*, Phys. Rev. Lett. **81** (1998), 1562–1567, hep-ex/9807003 .

[71] CHOOZ, M. Apollonio et al., *Limits on neutrino oscillations from the CHOOZ experiment*, Phys. Lett. **B466** (1999), 415–430, hep-ex/9907037 .

[72] SNO Collaboration, Q. R. Ahmad et al., *Direct evidence for neutrino flavor transformation from neutral-current interactions in the Sudbury Neutrino Observatory*, Phys. Rev. Lett. **89** (2002), 011301, nucl-ex/0204008 .

[73] K2K, M. H. Ahn et al., *Indications of neutrino oscillation in a 250-km long-baseline experiment*, Phys. Rev. Lett. **90** (2003), 041801, hep-ex/0212007 .

[74] KamLAND Collaboration, K. Eguchi et al., *First results from KamLAND : Evidence for reactor anti- neutrino disappearance*, Phys. Rev. Lett. **90** (2003), 021802, hep-ex/0212021 .

[75] MINOS, *Preliminary results from minos on muon neutrino disappearance based on an exposure of* $2.5 \cdot 10^{20}$ 120*-gev protons on the numi target*, (2007), 0708.1495 .

[76] Borexino, C. Arpesella et al., *First real time detection of Be7 solar neutrinos by Borexino*, Phys. Lett. **B658** (2008), 101–108, 0708.2251 .

[77] P. Huber, M. Lindner, M. Rolinec, T. Schwetz, and W. Winter, *Prospects of accelerator and reactor neutrino oscillation experiments for the coming ten years*, Phys. Rev. **D70** (2004), 073014, hep-ph/0403068 .

[78] M. Lindner, M. A. Schmidt, and A. Y. Smirnov, *Screening of Dirac flavor structure in the seesaw and neutrino mixing*, JHEP **07** (2005), 048, hep-ph/0505067 .

[79] W. Rodejohann and M. A. Schmidt, *Flavor symmetry* $L_\mu - L_\tau$ *and quasi-degenerate neutrinos*, Phys. Atom. Nucl. **69** (2006), 1833–1841, hep-ph/0507300 .

[80] M. A. Schmidt and A. Y. Smirnov, *Quark lepton complementarity and renormalization group effects*, Phys. Rev. **D74** (2006), 113003, hep-ph/0607232 .

[81] M. A. Schmidt, *Renormalization group evolution in the type I+II seesaw model*, Phys. Rev. **D76** (2007), 073010, 0705.3841 .

[82] C. Hagedorn, M. A. Schmidt, and A. Y. Smirnov, *Lepton mixing and cancellation of the Dirac mass hierarchy in* $SO(10)$ *GUT with discrete flavor symmetries (in preparation)*, 2008.

[83] M. E. Peskin and D. V. Schroeder, *An Introduction to quantum field theory*, Reading, USA: Addison-Wesley (1995) 842 p.

[84] G. 't Hooft, *Renormalization of massless Yang-Mills fields*, Nucl. Phys. **B33** (1971), 173–199.

[85] G. 't Hooft, *Renormalizable Lagrangians for massive Yang-Mills fields*, Nucl. Phys. **B35** (1971), 167–188.

[86] G. 't Hooft and M. J. G. Veltman, *Regularization and renormalization of gauge fields*, Nucl. Phys. **B44** (1972), 189–213.

[87] C. G. J. Callan, *Broken scale invariance in scalar field theory*, Phys. Rev. **D2** (1970), 1541–1547.

[88] K. Symanzik, *Small distance behavior in field theory and power counting*, Commun. Math. Phys. **18** (1970), 227–246.

[89] J. Kersten, *Renormalization group evolution of neutrino masses*, Diploma thesis, TU München, 2001.

[90] S. Antusch, *The running of neutrino masses, lepton mixings and CP phases*, Ph.D. thesis, TU München, 2003.

[91] M. Ratz, *Running neutrino masses*, Ph.D. thesis, TU München, 2002.

[92] The OPAL Collaboration, G. Abbiendi et al., *Tests of the Standard Model and constraints on new physics from measurements of fermion pair production at 189 GeV at LEP*, Eur. Phys. J. **C13** (2000), 553–572, hep-ex/9908008 .

[93] Particle Data Group, W. M. Yao et al., *Review of particle physics*, J. Phys. **G33** (2006), 1–1232.

[94] *Nobel laureates in physics 2004*, http://nobelprize.org/physics/laureates/2004/index.html.

[95] M. Bando, T. Kugo, N. Maekawa, and H. Nakano, *Improving the effective potential*, Phys. Lett. **B301** (1993), 83–89, hep-ph/9210228 .

[96] M. Bando, T. Kugo, N. Maekawa, and H. Nakano, *Improving the effective potential: Multimass scale case*, Prog. Theor. Phys. **90** (1993), 405–418, hep-ph/9210229 .

[97] K. Symanzik, *Infrared singularities and small distance behavior analysis*, Commun. Math. Phys. **34** (1973), 7–36.

[98] T. Appelquist and J. Carazzone, *Infrared singularities and massive fields*, Phys. Rev. **D11** (1975), 2856.

[99] S. Chang and T.-K. Kuo, *Renormalization invariants of the neutrino mass matrix*, Phys. Rev. **D66** (2002), 111302, hep-ph/0205147 .

[100] R. J. Davis, D. S. Harmer, and K. C. Hoffman, *Search for neutrinos from the sun*, Phys. Rev. Lett. **20** (1968), 1205–1209.

[101] KamLAND, S. Abe et al., *Precision measurement of neutrino oscillation parameters with KamLAND*, (2008), 0801.4589 .

[102] B. P. Roe, *Recent results from MiniBooNE*, (2008), 0805.2863 .

[103] LSND, C. Athanassopoulos et al., *Evidence for $\nu_\mu \to \nu_e$ neutrino oscillations from LSND*, Phys. Rev. Lett. **81** (1998), 1774–1777, nucl-ex/9709006 .

[104] C. Kraus et al., *Final results from phase II of the Mainz neutrino mass search in tritium beta decay*, Eur. Phys. J. **C40** (2005), 447–468, hep-ex/0412056 .

[105] H. V. Klapdor-Kleingrothaus et al., *Latest results from the Heidelberg-Moscow double-beta-decay experiment*, Eur. Phys. J. **A12** (2001), 147–154, hep-ph/0103062 .

[106] H. V. Klapdor-Kleingrothaus, A. Dietz, H. L. Harney, and I. V. Krivosheina, *Evidence for neutrinoless double beta decay*, Mod. Phys. Lett. **A16** (2001), 2409–2420, hep-ph/0201231 .

[107] WMAP, E. Komatsu et al., *Five-Year Wilkinson Microwave Anisotropy Probe (WMAP) Observations:Cosmological Interpretation*, (2008), 0803.0547 .

[108] Double Chooz, F. Ardellier et al., *Double Chooz: A search for the neutrino mixing angle theta(13)*, (2006), hep-ex/0606025 .

[109] KATRIN, A. Osipowicz et al., *KATRIN: A next generation tritium beta decay experiment with sub-eV sensitivity for the electron neutrino mass*, (2001), hep-ex/0109033 .

[110] I. Abt et al., *A new Ge-76 double beta decay experiment at LNGS*, (2004), hep-ex/0404039 .

[111] Planck, *Planck: The scientific programme*, (2006), astro-ph/0604069 .

[112] M. Maltoni, T. Schwetz, M. A. Tortola, and J. W. F. Valle, *Status of global fits to neutrino oscillations.*

[113] F. Vissani, *A study of the scenario with nearly degenerate Majorana neutrinos*, (1997), hep-ph/9708483 .

[114] V. D. Barger, S. Pakvasa, T. J. Weiler, and K. Whisnant, *Bi-maximal mixing of three neutrinos*, Phys. Lett. **B437** (1998), 107–116, hep-ph/9806387 .

[115] A. J. Baltz, A. S. Goldhaber, and M. Goldhaber, *The solar neutrino puzzle: An oscillation solution with maximal neutrino mixing*, Phys. Rev. Lett. **81** (1998), 5730–5733, hep-ph/9806540 .

[116] H. Georgi and S. L. Glashow, *Neutrinos on earth and in the heavens*, Phys. Rev. **D61** (2000), 097301, hep-ph/9808293 .

[117] I. Stancu and D. V. Ahluwalia, *L/E-flatness of the electron-like event ratio in Super-Kamiokande and a degeneracy in neutrino masses*, Phys. Lett. **B460** (1999), 431–436, hep-ph/9903408 .

[118] P. F. Harrison, D. H. Perkins, and W. G. Scott, *Tri-bimaximal mixing and the neutrino oscillation data*, Phys. Lett. **B530** (2002), 167, hep-ph/0202074 .

[119] P. F. Harrison and W. G. Scott, *Symmetries and generalisations of tri-bimaximal neutrino mixing*, Phys. Lett. **B535** (2002), 163–169, hep-ph/0203209 .

[120] Z. zhong Xing, *Nearly tri-bimaximal neutrino mixing and CP violation*, Phys. Lett. **B533** (2002), 85–93, hep-ph/0204049 .

[121] P. F. Harrison and W. G. Scott, *Permutation symmetry, tri-bimaximal neutrino mixing and the S3 group characters*, Phys. Lett. **B557** (2003), 76, hep-ph/0302025 .

[122] R. Kitano, *Small Dirac neutrino masses in supersymmetric grand unified theories*, Phys. Lett. **B539** (2002), 102–106, hep-ph/0204164 .

[123] S. Abel, A. Dedes, and K. Tamvakis, *Naturally small Dirac neutrino masses in supergravity*, Phys. Rev. **D71** (2005), 033003, hep-ph/0402287 .

[124] S. J. Huber and Q. Shafi, *Fermion masses, mixings and proton decay in a Randall- Sundrum model*, Phys. Lett. **B498** (2001), 256–262, hep-ph/0010195 .

[125] A. Zee, *A theory of lepton number violation, neutrino Majorana mass, and oscillation*, Phys. Lett. **B93** (1980), 389.

[126] K. S. Babu, *Model of 'calculable' Majorana neutrino masses*, Phys. Lett. **B203** (1988), 132.

[127] C. Wetterich, *Neutrino masses and the scale of $B - L$ violation*, Nucl. Phys. **B187** (1981), 343.

[128] H. Murayama, *Alternatives to seesaw*, Nucl. Phys. Proc. Suppl. **137** (2004), 206–219, hep-ph/0410140 .

[129] R. N. Mohapatra et al., *Theory of neutrinos*, (2004), hep-ph/0412099 .

[130] S. Weinberg, *Phenomenological lagrangians*, Physica **A96** (1979), 327.

[131] O. Lebedev et al., *A mini-landscape of exact MSSM spectra in heterotic orbifolds*, Phys. Lett. **B645** (2007), 88–94, hep-th/0611095 .

[132] S. M. Barr, *A different see-saw formula for neutrino masses*, Phys. Rev. Lett. **92** (2004), 101601, hep-ph/0309152 .

[133] G. 't Hooft, *Naturalness, chiral symmetry, and spontaneous chiral symmetry breaking*, in *Recent Developments in Gauge Theories* (G. 't Hooft, ed.), 1979.

[134] S. Antusch and M. Ratz, *Supergraph techniques and two-loop beta-functions for renormalizable and non-renormalizable operators*, JHEP **07** (2002), 059, hep-ph/0203027 .

[135] S. L. Glashow, *Trinification of all elementary particle forces*, Providence Grand Unif. (1984), Print-84-0577 (BOSTON).

[136] K. S. Babu, X.-G. He, and S. Pakvasa, *Neutrino masses and proton decay modes in $SU(3)\times SU(3)\times SU(3)$ trinification*, Phys. Rev. **D33** (1986), 763.

[137] G. Senjanović and R. N. Mohapatra, *Exact left-right symmetry and spontaneous violation of parity*, Phys. Rev. **D12** (1975), 1502.

[138] R. N. Mohapatra, F. E. Paige, and D. P. Sidhu, *Symmetry breaking and naturalness of parity conservation in weak neutral currents in left-right symmetric gauge theories*, Phys. Rev. D **17** (1978), 2462.

[139] R. N. Mohapatra and G. Senjanovic, *Neutrino masses and mixings in gauge models with spontaneous parity violation*, Phys. Rev. **D23** (1981), 165.

[140] J. C. Pati and A. Salam, *Lepton number as the fourth color*, Phys. Rev. **D10** (1974), 275–289.

[141] H. Murayama and A. Pierce, *Not even decoupling can save minimal supersymmetric SU(5)*, Phys. Rev. **D65** (2002), 055009, hep-ph/0108104 .

[142] B. Bajc, P. Fileviez Perez, and G. Senjanovic, *Proton decay in minimal supersymmetric SU(5)*, Phys. Rev. **D66** (2002), 075005, hep-ph/0204311 .

[143] D. Emmanuel-Costa and S. Wiesenfeldt, *Proton decay in a consistent supersymmetric SU(5) GUT model*, Nucl. Phys. **B661** (2003), 62–82, hep-ph/0302272 .

[144] A. De Rujula, H. Georgi, and S. L. Glashow, *Flavor goniometry by proton decay*, Phys. Rev. Lett. **45** (1980), 413.

[145] S. M. Barr, *A new symmetry breaking pattern for $SO(10)$ and proton decay*, Phys. Lett. **B112** (1982), 219.

[146] I. Antoniadis, J. R. Ellis, J. S. Hagelin, and D. V. Nanopoulos, *Supersymmetric flipped $SU(5)$ revitalized*, Phys. Lett. **B194** (1987), 231.

[147] E. Witten, *Mass Hierarchies in Supersymmetric Theories*, Phys. Lett. **B105** (1981), 267.

[148] S. Dimopoulos and H. Georgi, *Solution of the gauge hierarchy problem*, Phys. Lett. **B117** (1982), 287.

[149] L. E. Ibanez and G. G. Ross, *$SU(2)_L \times U(1)$ symmetry breaking as a radiative effect of supersymmetry breaking in guts*, Phys. Lett. **B110** (1982), 215–220.

[150] D. V. Nanopoulos and K. Tamvakis, *SUSY GUTS:* 4 - *GUTS:* 3, Phys. Lett. **B113** (1982), 151.

[151] MEG, C. Bemporad, *The MEG experiment at PSI*, (2007), Prepared for 12th International Workshop on Neutrinos Telescopes: Twenty Years after the Supernova 1987A Neutrino Bursts Discovery, Venice, Italy, 6-9 Mar 2007.

[152] MEGA, M. L. Brooks et al., *New limit for the family-number non-conserving decay $\mu^+ \to e^+\gamma$*, Phys. Rev. Lett. **83** (1999), 1521–1524, hep-ex/9905013 .

[153] C. H. Albright and M.-C. Chen, *Lepton Flavor Violation in Predictive SUSY-GUT Models*, (2008), 0802.4228 .

[154] M. Albrecht, W. Altmannshofer, A. J. Buras, D. Guadagnoli, and D. M. Straub, *Challenging SO(10) SUSY GUTs with family symmetries through FCNC processes*, JHEP **10** (2007), 055, 0707.3954 .

[155] M. Baldo-Ceolin et al., *A New experimental limit on neutron - anti-neutron oscillations*, Z. Phys. **C63** (1994), 409–416.

[156] H. Georgi and C. Jarlskog, *A new lepton-quark mass relation in a unified theory*, Phys. Lett. **B86** (1979), 297–300.

[157] H. Georgi and D. V. Nanopoulos, *Masses and mixing in unified theories*, Nucl. Phys. **B159** (1979), 16.

[158] C. S. Aulakh, B. Bajc, A. Melfo, A. Rasin, and G. Senjanovic, *Intermediate scales in supersymmetric GUTs: The survival of the fittest*, Phys. Lett. **B460** (1999), 325–332, hep-ph/9904352 .

[159] C. S. Aulakh, B. Bajc, A. Melfo, A. Rasin, and G. Senjanovic, *$SO(10)$ theory of R-parity and neutrino mass*, Nucl. Phys. **B597** (2001), 89–109, hep-ph/0004031 .

[160] J. P. Derendinger, J. E. Kim, and D. V. Nanopoulos, *Anti-SU(5)*, Phys. Lett. **B139** (1984), 170.

[161] N. Maekawa and T. Yamashita, *Flipped $SO(10)$ model*, Phys. Lett. **B567** (2003), 330–338, hep-ph/0304293 .

[162] M. Yasue, *Symmetry breaking of $SO(10)$ and constraints on higgs potential. 1. adjoint (45) and spinorial (16)*, Phys. Rev. **D24** (1981), 1005.

[163] V. A. Kuzmin and M. E. Shaposhnikov, *Higgs potential and symmetry breaking patterns in $SO(10)$ model*, (1981), IYaI-P-0201.

[164] K. S. Babu and E. Ma, *Symmetry breaking in $SO(10)$: Higgs boson structure*, Phys. Rev. **D31** (1985), 2316.

[165] D. Chang and A. Kumar, *No go theorems for the minimization of potentials*, Phys. Rev. **D31** (1985), 2698–2700.

[166] D. Chang and A. Kumar, *Symmetry breaking of $SO(10)$ by 210-dimensional Higgs boson and the Michel's conjecture*, Phys. Rev. **D33** (1986), 2695.

[167] R. W. Robinett and J. L. Rosner, *Mass scales in grand unified theories*, Phys. Rev. **D26** (1982), 2396.

[168] D.-G. Lee and R. N. Mohapatra, *Automatically R conserving supersymmetric SO(10) models and mixed light Higgs doublets*, Phys. Rev. **D51** (1995), 1353–1361, hep-ph/9406328 .

[169] D.-G. Lee and R. N. Mohapatra, *Intermediate scales in SUSY $SO(10)$, $b-\tau$ unification, and hot dark matter neutrinos*, Phys. Rev. **D52** (1995), 4125–4132, hep-ph/9502210 .

[170] M.-C. Chen and K. T. Mahanthappa, *From ckm matrix to mns matrix: A model based on supersymmetric $SO(10)\times U(2)_F$ symmetry*, Phys. Rev. **D62** (2000), 113007, hep-ph/0005292 .

[171] L. Lavoura, H. Kuhbock, and W. Grimus, *Charged-fermion masses in SO(10): Analysis with scalars in 10+120*, Nucl. Phys. **B754** (2006), 1–16, hep-ph/0603259 .

[172] S. Bertolini, T. Schwetz, and M. Malinsky, *Fermion masses and mixings in SO(10) models and the neutrino challenge to SUSY GUTs*, Phys. Rev. **D73** (2006), 115012, hep-ph/0605006 .

[173] K. R. Dienes, *New constraints on SO(10) model-building from string theory*, Nucl. Phys. **B488** (1997), 141–158, hep-ph/9606467 .

[174] K. S. Babu, J. C. Pati, and F. Wilczek, *Fermion masses, neutrino oscillations, and proton decay in the light of SuperKamiokande*, Nucl. Phys. **B566** (2000), 33–91, hep-ph/9812538 .

[175] C. H. Albright and S. M. Barr, *Explicit SO(10) supersymmetric grand unified model for the Higgs and Yukawa sectors*, Phys. Rev. Lett. **85** (2000), 244–247, hep-ph/0002155 .

[176] C. H. Albright and S. M. Barr, *Construction of a minimal Higgs SO(10) SUSY GUT model*, Phys. Rev. **D62** (2000), 093008, hep-ph/0003251 .

[177] C. H. Albright and S. M. Barr, *Realization of the large mixing angle solar neutrino solution in an SO(10) supersymmetric grand unified model*, Phys. Rev. **D64** (2001), 073010, hep-ph/0104294 .

[178] Q. Shafi and Z. Tavartkiladze, *Anomalous flavor U(1): Predictive texture for bi-maximal neutrino mixing*, Phys. Lett. **B482** (2000), 145–149, hep-ph/0002150 .

[179] N. Maekawa, *Gauge coupling unification with anomalous $U(1)_A$ gauge symmetry*, Prog. Theor. Phys. **107** (2002), 597–619, hep-ph/0111205 .

[180] T. Blazek, S. Raby, and K. Tobe, *Neutrino oscillations in a predictive SUSY GUT*, Phys. Rev. **D60** (1999), 113001, hep-ph/9903340 .

[181] S. Raby, *A natural framework for bi-large neutrino mixing*, Phys. Lett. **B561** (2003), 119–124, hep-ph/0302027 .

[182] Z. Berezhiani and A. Rossi, *Grand unified textures for neutrino and quark mixings*, JHEP **03** (1999), 002, hep-ph/9811447 .

[183] R. Kitano and Y. Mimura, *Large angle MSW solution in grand unified theories with SU(3) x U(1) horizontal symmetry*, Phys. Rev. **D63** (2001), 016008, hep-ph/0008269 .

[184] G. G. Ross and L. Velasco-Sevilla, *Symmetries and fermion masses*, Nucl. Phys. **B653** (2003), 3–26, hep-ph/0208218 .

[185] S. Dimopoulos and F. Wilczek, *Incomplete multiplets in supersymmetric unified models*, Print-81-0600 (SANTA BARBARA).

[186] Z. Chacko and R. N. Mohapatra, *A new doublet-triplet splitting mechanism for supersymmetric SO(10) and implications for fermion masses*, Phys. Rev. Lett. **82** (1999), 2836–2839, hep-ph/9810315 .

[187] J. Sayre, S. Wiesenfeldt, and S. Willenbrock, *Dimension-five operators in grand unified theories*, Phys. Rev. **D75** (2007), 037702, hep-ph/0605293 .

[188] S. F. King, S. Moretti, and R. Nevzorov, *Theory and phenomenology of an exceptional supersymmetric standard model*, Phys. Rev. **D73** (2006), 035009, hep-ph/0510419 .

[189] Y. Hosotani, *Dynamical mass generation by compact extra dimensions*, Phys. Lett. **B126** (1983), 309.

[190] F. Caravaglios and S. Morisi, *Gauge boson families in grand unified theories of fermion masses: $E_6^4 \times S_4$*, Int. J. Mod. Phys. **A22** (2007), 2469–2492, hep-ph/0611078 .

[191] C. D. Froggatt and H. B. Nielsen, *Hierarchy of quark masses, cabibbo angles and cp violation*, Nucl. Phys. **B147** (1979), 277.

[192] M. B. Green and J. H. Schwarz, *Anomaly Cancellation in Supersymmetric D=10 Gauge Theory and Superstring Theory*, Phys. Lett. **B149** (1984), 117–122.

[193] X. G. He, G. C. Joshi, H. Lew, and R. R. Volkas, *New Z-prime phenomenology*, Phys. Rev. **D43** (1991), 22–24.

[194] X.-G. He, G. C. Joshi, H. Lew, and R. R. Volkas, *Simplest Z-prime model*, Phys. Rev. **D44** (1991), 2118–2132.

[195] P. H. Frampton, S. L. Glashow, and D. Marfatia, *Zeroes of the neutrino mass matrix*, Phys. Lett. **B536** (2002), 79–82, hep-ph/0201008 .

[196] Z. zhong Xing, *Texture zeros and Majorana phases of the neutrino mass matrix*, Phys. Lett. **B530** (2002), 159–166, hep-ph/0201151 .

[197] Z. zhong Xing, *A full determination of the neutrino mass spectrum from two-zero textures of the neutrino mass matrix*, Phys. Lett. **B539** (2002), 85–90, hep-ph/0205032 .

[198] B. R. Desai, D. P. Roy, and A. R. Vaucher, *Three-neutrino mass matrices with two texture zeros*, Mod. Phys. Lett. **A18** (2003), 1355–1366, hep-ph/0209035 .

[199] E. Ma, *A_4 origin of the neutrino mass matrix*, Phys. Rev. **D70** (2004), 031901, hep-ph/0404199 .

[200] G. Altarelli and F. Feruglio, *Tri-bimaximal neutrino mixing from discrete symmetry in extra dimensions*, Nucl. Phys. **B720** (2005), 64–88, hep-ph/0504165 .

[201] P. H. Frampton and R. N. Mohapatra, *Possible gauge theoretic origin for quark-lepton complementarity*, JHEP **01** (2005), 025, hep-ph/0407139 .

[202] J. Ferrandis and S. Pakvasa, *QLC relation and neutrino mass hierarchy*, Phys. Rev. **D71** (2005), 033004, hep-ph/0412038 .

[203] S. Antusch, S. F. King, and R. N. Mohapatra, *Quark lepton complementarity in unified theories*, Phys. Lett. **B618** (2005), 150–161, hep-ph/0504007 .

[204] D. Falcone, *Quark lepton symmetry and complementarity*, Mod. Phys. Lett. **A21** (2006), 1815–1820, hep-ph/0509028 .

[205] F. Gonzalez Canales and A. Mondragon, *On quark-lepton complementarity*, AIP Conf. Proc. **857** (2006), 287–292, hep-ph/0606175 .

[206] T. Ohlsson and G. Seidl, *A flavor symmetry model for bilarge leptonic mixing and the lepton masses*, Nucl. Phys. **B643** (2002), 247–279, hep-ph/0206087 .

[207] I. Masina, *A maximal atmospheric mixing from a maximal CP violating phase*, Phys. Lett. **B633** (2006), 134–140, hep-ph/0508031 .

[208] S. Antusch and S. F. King, *Charged lepton corrections to neutrino mixing angles and CP phases revisited*, Phys. Lett. **B631** (2005), 42–47, hep-ph/0508044 .

[209] J. Harada, *Neutrino mixing and CP violation from Dirac-Majorana bimaximal mixture and quark-lepton unification*, Europhys. Lett. **75** (2006), 248–253, hep-ph/0512294 .

[210] B. C. Chauhan, M. Picariello, J. Pulido, and E. Torrente-Lujan, *Quark-lepton complementarity, neutrino and standard model data predict* $(\theta_{13}^{PMNS} = 9^{+1}_{-2})^\circ$, Eur. Phys. J. **C50** (2007), 573–578, hep-ph/0605032 .

[211] K. A. Hochmuth and W. Rodejohann, *Low and high energy phenomenology of quark-lepton complementarity scenarios*, Phys. Rev. **D75** (2007), 073001, hep-ph/0607103 .

[212] E. K. Akhmedov, M. Frigerio, and A. Y. Smirnov, *Probing the seesaw mechanism with neutrino data and leptogenesis*, JHEP **09** (2003), 021, hep-ph/0305322 .

[213] C. Luhn, S. Nasri, and P. Ramond, *Tri-bimaximal neutrino mixing and the family symmetry $Z_7 \rtimes Z_3$*, Phys. Lett. **B652** (2007), 27–33, 0706.2341 .

[214] E. Ma, *Lepton family symmetry and possible application to the Koide mass formula*, Phys. Lett. **B649** (2007), 287–291, hep-ph/0612022 .

[215] E. Ma, *New lepton family symmetry and neutrino tribimaximal mixing*, Europhys. Lett. **79** (2007), 61001, hep-ph/0701016 .

[216] S. F. King and M. Malinsky, *Towards a complete theory of fermion masses and mixings with $SO(3)$ family symmetry and 5d $SO(10)$ unification*, JHEP **11** (2006), 071, hep-ph/0608021 .

[217] S. F. King and M. Malinsky, *A_4 family symmetry and quark-lepton unification*, Phys. Lett. **B645** (2007), 351–357, hep-ph/0610250 .

[218] G. Altarelli and F. Feruglio, *Models of neutrino masses and mixings*, New J. Phys. **6** (2004), 106, hep-ph/0405048 .

[219] C.-Y. Chen and L. Wolfenstein, *Consequences of approximate S_3 symmetry of the neutrino mass matrix*, (2007), 0709.3767 .

[220] M. Maltoni, T. Schwetz, M. A. Tortola, and J. W. F. Valle, *Status of global fits to neutrino oscillations*, New J. Phys. **6** (2004), 122, hep-ph/0405172 .

[221] B. Grzadkowski and M. Lindner, *Nonlinear evolution of Yukawa couplings*, Phys. Lett. **B193** (1987), 71.

[222] B. Grzadkowski, M. Lindner, and S. Theisen, *Nonlinear evolution of Yukawa couplings in the double Higgs and supersymmetric extensions of the Standard Model*, Phys. Lett. **B198** (1987), 64.

[223] S. F. King and N. N. Singh, *Inverted hierarchy models of neutrino masses*, Nucl. Phys. **B596** (2001), 81–98, hep-ph/0007243 .

[224] M. T. Grisaru, W. Siegel, and M. Rocek, *Improved methods for supergraphs*, Nucl. Phys. **B159** (1979), 429.

[225] N. Seiberg, *Naturalness versus supersymmetric nonrenormalization theorems*, Phys. Lett. **B318** (1993), 469–475, hep-ph/9309335 .

[226] P. H. Chankowski and S. Pokorski, *Quantum corrections to neutrino masses and mixing angles*, Int. J. Mod. Phys. **A17** (2002), 575–614, hep-ph/0110249 .

[227] J. Wess and B. Zumino, *A Lagrangian model invariant under supergauge transformations*, Phys. Lett. **B49** (1974), 52.

[228] J. Iliopoulos and B. Zumino, *Broken supergauge symmetry and renormalization*, Nucl. Phys. **B76** (1974), 310.

[229] K. S. Babu, *Renormalization-Group analysis of the Kobayashi-Maskawa matrix*, Z. Phys. **C35** (1987), 69.

[230] J.-W. Mei, *Running neutrino masses, leptonic mixing angles and CP-violating phases: From M(Z) to Lambda(GUT)*, Phys. Rev. **D71** (2005), 073012, hep-ph/0502015 .

[231] J. Ellis, A. Hektor, M. Kadastik, K. Kannike, and M. Raidal, *Running of low-energy neutrino masses, mixing angles and CP violation*, Phys. Lett. **B631** (2005), 32–41, hep-ph/0506122 .

[232] M. Lindner, M. Ratz, and M. A. Schmidt, *Renormalization group evolution of dirac neutrino masses*, JHEP **09** (2005), 081, hep-ph/0506280 .

[233] A. Pilaftsis and T. E. J. Underwood, *Resonant leptogenesis*, Nucl. Phys. **B692** (2004), 303–345, hep-ph/0309342 .

[234] W. Chao and H. Zhang, *One-loop renormalization group equations of the neutrino mass matrix in the triplet seesaw model*, Phys. Rev. **D75** (2007), 033003, hep-ph/0611323 .

[235] I. Gogoladze, N. Okada, and Q. Shafi, *Higgs mass bounds, type II seesaw and LHC*, (2008), 0802.3257 .

[236] L. Wolfenstein, *Parametrization of the Kobayashi-Maskawa Matrix*, Phys. Rev. Lett. **51** (1983), 1945.

[237] W. Rodejohann, *A parametrization for the neutrino mixing matrix*, Phys. Rev. **D69** (2004), 033005, hep-ph/0309249 .

[238] C. Jarlskog, *Commutator of the quark mass matrices in the standard electroweak model and a measure of maximal CP violation*, Phys. Rev. Lett. **55** (1985), 1039.

[239] J. F. Nieves and P. B. Pal, *Minimal rephasing invariant CP violating parameters with Dirac and Majorana fermions*, Phys. Rev. **D36** (1987), 315.

[240] R. Slansky, *Group theory for unified model building*, Phys. Rept. **79** (1981), 1–128.

[241] R. N. Cahn, *Semisimple Lie algebras and their representations*, 1985, Menlo Park, Usa: Benjamin/cummings (1984) 158 P. (Frontiers In Physics, 59).

[242] R. N. Mohapatra and B. Sakita, $SO(2N)$ *grand unification in an* $SU(N)$ *basis*, Phys. Rev. **D21** (1980), 1062.

[243] C. S. Aulakh and A. Girdhar, $SO(10)$ *a la Pati-Salam*, Int. J. Mod. Phys. **A20** (2005), 865–894, hep-ph/0204097 .

[244] R. N. Mohapatra, *Unification and supersymmetry. the frontiers of quark - lepton physics*, 1986, Berlin, Germany: Springer (1986) 309 P. (Contemporary Physics).

[245] R. M. Syed, *Couplings in SO(10) grand unification*, (2005), hep-ph/0508153 .

[246] P. M. van den Broek and J. Cornwell, *Clebsch-Gordan coefficients of symmetry groups*, Phys.Stat.SolB **90**, 211.

[247] S. L. Adler, *Axial vector vertex in spinor electrodynamics*, Phys. Rev. **177** (1969), 2426–2438.

[248] J. S. Bell and R. Jackiw, *A PCAC puzzle:* $\pi^0 \to \gamma\gamma$ *in the sigma model*, Nuovo Cim. **A60** (1969), 47–61.

[249] S. Weinberg, *The quantum theory of fields. vol. 2: Modern applications*, Cambridge University Press, Cambridge, UK.

[250] H. Georgi and S. L. Glashow, *Gauge theories without anomalies*, Phys. Rev. **D6** (1972), 429.

[251] L. M. Krauss and F. Wilczek, *Discrete gauge symmetry in continuum theories*, Phys. Rev. Lett. **62** (1989), 1221.

[252] L. E. Ibanez and G. G. Ross, *Discrete gauge symmetry anomalies*, Phys. Lett. **B260** (1991), 291–295.

[253] T. Banks and M. Dine, *Note on discrete gauge anomalies*, Phys. Rev. **D45** (1992), 1424–1427, hep-th/9109045 .

[254] P. H. Frampton and T. W. Kephart, *Simple non-Abelian finite flavor groups and fermion masses*, Int. J. Mod. Phys. **A10** (1995), 4689–4704, hep-ph/9409330 .

[255] T. Araki, *Anomalies of discrete symmetries and gauge coupling unification*, Prog. Theor. Phys. **117** (2007), 1119–1138, hep-ph/0612306 .

[256] T. Araki et al., *(non-)Abelian discrete anomalies*, (2008), 0805.0207 .